

Activity Measurements with Ionization Chambers

1st

edition 1997



**Bureau International
des Poids et Mesures**

1st edition 1997

Copyright statement

This document is distributed under the terms of the Creative Commons Attribution 4.0 International License (<http://creativecommons.org/licenses/by/4.0/>), which permits unrestricted use, distribution, and reproduction in any medium, provided you give appropriate credit to the original author(s) and the source, provide a link to the Creative Commons license, and indicate if changes were made.

Édité par le BIPM
Pavillon de Breteuil
F-92312 Sèvres Cedex
FRANCE

Foreword

This monograph is one of several to be published by the Bureau International des Poids et Mesures (BIPM) on behalf of the Comité Consultatif pour les Étalons de Mesure des Rayonnements Ionisants (CCEMRI). The aim of this series of publications is to review various topics which are of importance for the measurement of ionizing radiation and radioactivity, in particular those techniques normally used by participants in international comparisons. It is hoped that these publications will prove to be useful reference volumes both to those who are already engaged in this field and to those who are approaching such measurements for the first time.

This volume, the fourth in the series of BIPM monographs, is devoted to ionization chambers used for activity measurements. The BIPM is most grateful to Dr. H. Schrader, of the Physikalisch-Technische Bundesanstalt (PTB) at Braunschweig (Germany), for having assembled in his meticulous way so much information on this important measuring instrument which, even after nearly a century of existence, still plays a basic role in nuclear metrology. The monograph is also an excellent introduction to relative activity measurements; it describes historical developments in some detail and guides the reader to the abundant scientific literature.

The success of the existing International Reference System (SIR) and its expected relevance for establishing equivalence between the activity measurements of the various national laboratories ensure that ionization chambers will continue to be of importance in radiation physics.

May this text inspire potential authors to treat in monographic form other subjects pertaining to the metrology of ionizing radiation.



G. Moscati
Chairman of the CCEMRI



T.J. Quinn
Director of the BIPM

A calibrated re-entrant ionization chamber, often also called a well-type or $4\pi\gamma$ ionization chamber, is commonly used to measure activity. On an international level, this is a powerful tool which allows the International Reference System (SIR) to measure γ -ray emitters to establish and maintain world-wide uniformity of radioactivity measurements [376]. Ionization

chambers serve in many national standards laboratories as secondary standard measuring systems and are used to maintain the results of activity measurements from primary standardization. They are also used for half-life measurements and, combined with weighing, for the quality assurance of dilutions which are disseminated to users as activity standards. Last but not least, simplified versions are commonly employed as radionuclide calibrators to measure the activity of solutions, mainly in the field of nuclear medicine.

For these reasons it was agreed that the Bureau International des Poids et Mesures (BIPM) would publish a monograph on the subject on behalf of Section II (Radionuclide measurements) of the Comité Consultatif pour les Étalons de Mesure des Rayonnements Ionisants (CCEMRI).

Ionization chambers have been used for about ninety years to measure radioactivity, and most of the basic studies are now more than forty years old, so several publications from the very beginning of radioactivity measurements are also included in the list of references. Among these a certain incompleteness of information and some subjectivity on the author's part could not be avoided. In preparing the text and selecting the references, emphasis has been placed both on experimental techniques and on the relevant theory. New references were included to some extent until 1994.

This monograph is intended for use as a practical guide to activity measurement with ionization chambers and is addressed to all those interested in the metrology of radioactivity. My intention has been to make the text appropriate for beginners in the field of radionuclide metrology who wish to learn how to make activity measurements using ionization chambers. The level of presentation assumes an elementary knowledge of nuclear physics and radioactivity, so any explanations in the text cover material familiar to the experienced metrologist. Nevertheless, it is hoped that these readers may also find items of interest or useful references. To make the text more accessible each chapter is self-contained and can be read as an individual unit.

The author is indebted to D. A. Blackburn, K. Debertin, D. and J. W. Müller, G. Ratel, D. F. G. Reher, A. Rytz and G. Siegert for their careful reading of the manuscript, as well as to many colleagues for their critical remarks which were integrated in the text. He also thanks R. Defèr for preparation of many of the drawings and B. Kuchenbuch for the composition of portions of the text. The constant help and technical support of many others during the realization of this monograph should also be acknowledged.

Braunschweig, January 1997

H. Schrader

Activity Measurements with Ionization Chambers

Contents

1. Introduction	9
2. Principles of measurement for re-entrant (or 4π) ionization chambers	12
2.1. Measurement geometry of the source and the ionization chamber	12
2.2. Ionization process and charge collection	13
2.3. Ionization current	15
2.4. Ionization chamber calibration for activity measurements	16
2.5. Relative activity measurements and reference sources	17
2.6. ^{226}Ra sources	19
3. Construction of ionization chambers	22
3.1. $4\pi\gamma$ ionization chambers	22
3.2. Special types of ionization chambers and their applications	23
4. Techniques of measurement for ionization current	29
4.1. Electrometer picoammeters	30
4.2. Feedback circuits and current integrators	32
4.3. Measurements by voltage drop across a high value resistor	33
4.4. Townsend induction balances with compensation	34
5. Systematic effects in ionization-current measurements	37
5.1. Fluctuations from ionization and charge collection	37
5.2. Variation of electronic parameters	38
5.3. Saturation-loss effects	38
5.4. Linearity in response to activity	39
6. Corrections to ionization-current values	42
6.1. Background	42
6.2. Decay correction	43
6.3. Variations of sample dimensions and materials	44
6.4. Variation of the sample position	46
6.5. Filling correction for sources of varying solution volume	47
6.6. Radionuclidic impurities	47
7. Calibration of re-entrant ionization chambers	53
7.1. Calibration factors for particular radionuclides	53
7.2. Efficiency as a function of photon energy	54
7.3. Efficiency of detection of bremsstrahlung from β -particle emitters	55
7.4. Representation and fitting of efficiency functions	56

7.5. Calculation of efficiency values from fundamental quantities of the interaction processes	57
7.6. Calculation of radionuclide efficiencies from energy-dependent photon efficiencies and photon-emission probabilities per decay	59
8. Uncertainties of activity measurements obtained using ionization chambers	61
8.1. Uncertainty components of an activity measurement	61
8.2. Combined uncertainty from uncertainty components	63
9. Applications of ionization-chamber measurements	64
9.1. Quality control in national standards laboratories	64
9.2. Quality control for activity measurements and intercomparisons in nuclear medicine and industry	65
9.3. Half-life measurements	66
10. Intercomparisons and the International Reference System (SIR)	69
10.1. Intercomparisons of activity standards and traceability	69
10.2. Measuring equipment and procedures of the SIR	71
10.3. Results of measurements with the SIR	72
10.4. Extension of the SIR	73
11. Conclusion	74
12. Tables	75
13. Figures	83
References	165

1. Introduction

The measuring instrument described here takes the form of an ionization chamber with a well in which is placed a radiation source. The chamber is connected to an electronic current-measuring device which, in more recent designs, is computer-controlled to permit data storage and on-line calculations. Pulse ionization chambers are not considered in this monograph. Some authors, for example Carmichael [64], Taylor and Sharpe [442], Tapp [441], adopt the convention that the term “ion chamber” denotes an ionization chamber operating in current mode, whereas “pulse chamber” denotes a chamber and electronic circuitry with which individual pulses are counted. Many other authors, however, do not make this distinction.

A calibrated re-entrant ionization chamber working in current mode is suitable for measuring the activity of a radioactive source which contains a single photon-emitting radionuclide. The physical quantity “activity” describing the phenomenon “radioactivity” has been defined as follows [226]: “The activity of an amount of a radioactive nuclide in a particular energy state at a given time is the expectation value, at that time, of the number of spontaneous nuclear transitions in unit time from that energy state”. The “particular energy state” is the ground state of the nuclide unless otherwise specified. The derived SI unit (Système International d’Unités) [26] for the quantity “activity” is “one per second” (s^{-1}) and is named the “becquerel” (Bq) [125], [226], [74], [294], [111], Part 4, [447]. For reasons of a long tradition and its general use in the field of nuclear medicine, the older unit, the “curie” (Ci), is still tolerated by the Conférence Générale des Poids et Mesures (CGPM), with the definition of $1\text{ Ci} = 3.7 \cdot 10^{10}\text{ Bq}$. This value was established in 1930 by the International Radium-Standards Commission, following the reorganization of the International Union of Chemistry and the International Atomic Weight Commission. Several other “radioactive constants” and decay constants (or half-lives, see Section 9.3, see p. 66) of radionuclides in the natural decay chains were recommended by the Commission [88] and its report includes an extended list of references. Some of the recommended values are still in use.

A re-entrant or 4π ionization chamber can be calibrated in terms of activity by appropriate radioactive standard sources, also called activity standards (see Chapter 7, see p. 53). Here, the terminology used to describe them is that given in the International Vocabulary of Basic and General Terms in Metrology (VIM) in its newly revised version [232]. Radioactivity standards are prepared and calibrated mainly in national standards laboratories that are responsible for radionuclide metrology. Other radioactivity standards are traceable to national standards which have been the subject of international comparisons or have been compared with the International Reference System (SIR) (see Chapter 10, see p. 69). The SIR is maintained at the BIPM and takes the form of an ionization chamber measuring system for comparing the activity values of radioactive solutions.

The activity of a radioactivity standard is measured by “direct” (or “absolute”) methods [316], [294], [99], [98]. Most direct methods depend on detailed knowledge of correlations between coincident events in the decay of the measured radionuclide and other decay parameters, such as half-life, decay mode, etc. Coincidence or anticoincidence measurements, correlation counting, modulo-2 counting or selective sampling [312] are typical examples of direct methods. In these methods the radiations emitted are counted in detectors with or without energy discrimination. The activity is calculated, using the count rates within relations from which, at the end, detector efficiencies must be eliminated. To measure the activity of most radionuclides, the efficiency-dependent parameters are varied and the calculated ratios of the count rates are extrapolated, for example, to 100% detection efficiency. Details of the methods

can be found in specialized textbooks [316], [294] or in publications on activity measurements for particular radionuclides, see for example [173], [421], [393], [305], [80], [161], [242].

The ionization chamber, once calibrated against sources of known activity by direct measurements, serves to maintain the unit of activity. This is especially important for rapidly decaying radionuclides since the ionization chamber can be recalibrated by individual activity standards at intervals much longer than many half-lives of the radionuclide and therefore, retains the validity of the value of an activity standard far beyond its lifetime.

The activity concentration of a radioactive standard solution of a particular radionuclide is derived from the activities of several measured sources prepared from the same mother solution by gravimetric procedures. Such a radioactive standard solution can be called a “standard reference material” when both the activity concentration (e.g. in Bq per gram of material) and the chemical parameters are expected to remain constant. From such a standard solution, other standards of the same concentration can be prepared. Similarly, dilutions are obtained by carefully weighing and dispensing into ampoules (see Chapter 6, see p. 42). These liquid samples are stored as aqueous solutions in flame-sealed glass ampoules. In national standards laboratories special care is taken to ensure that the ampoules are as uniform as possible with respect to geometry and material. Several thousands of ampoules are therefore bought from the same manufacturing batch, and are systematically checked for possible variations in dimensions [376]. In the wall thickness of the cylinder, for example, only variations of a few hundredths of a millimetre are acceptable.

Ionization-chamber measurements on series of ampoules are useful in the quality control of weighing procedures if the activity concentration of the master solution and the aliquot size are selected in such a way that the filled ampoules provide a suitable ionization chamber response (see Chapter 9, see p. 64).

To achieve the necessary level of accuracy in ionization-chamber measurements, certain precautions must be taken: radionuclide solutions with no, or only small and well-known, radionuclidic impurities, are used (see Chapter 6, see p. 42), and the measurement conditions are made as reproducible as possible. The geometry of sample and chamber should be kept constant to allow comparison of measurement results. Radionuclidic impurities in the solution should be detected by energy-selective measuring systems, for example with Ge detectors, or using other selective methods. Once the activity ratios and the calibration factors of the corresponding radionuclides are known, a correction factor must be applied to the ionization-chamber reading to give the result in terms of the activity of the dominant radionuclide (Section 6.6, see p. 47).

The stability of an ionization-chamber measuring system is usually verified by repeated measurements of a reference source of a long-lived radionuclide such as ^{226}Ra in equilibrium with its daughters (Section 2.6, see p. 19). Sample, background and reference source measurements are alternated in a cycle which checks the stability of the equipment and the reproducibility of the measurement conditions. Taking into account the radioactive decays of contributing radionuclides, the ratios of the related currents at a given reference time should remain constant for all measurements. Correctly designed and manufactured ionization chambers show good linearity with varying activity over a large dynamic range. They are relatively simple to operate and the required quality checks are inexpensive yet give measurement results with good reproducibility and accuracy. Ionization-chamber systems with a direct reading in units of activity, the so-called radionuclide calibrators (see Section 3.2.4, see p. 25), have therefore become favoured instruments for performing quantitative

assays of radiopharmaceuticals. Other applications of ionization-chamber measurements are described in Chapter 9.

Besides describing the many useful applications which may or may not require a high accuracy level, this monograph is also written to summarize the basic concepts of re-entrant ionization-chamber systems, their working principles and the art of measurement which leads to activity values with a minimum of uncertainty (Chapter 8, see p. 61).

2. Principles of measurement for re-entrant (or 4π) ionization chambers

Ionizing devices have been used since the discovery of x rays by Röntgen in 1895 and of “radio-activity” by Becquerel in 1896, the latter having observed the discharging effects of an electrometer by radiation from uranium [17], [18], [19]. The pioneers in developing devices for radiation measurements similar to ionization chambers were Thomson and Rutherford ([446], see p. 193) and Rutherford ([360], [361], see p. 187). Elster and Geitel ([127], see p. 173) and Owens ([329], see p. 185) also employed quantitative methods with ionizing devices before 1900. A cylindrical vessel, much resembling a re-entrant ionization chamber, is first described by Elster and Geitel ([128], [129], see p. 173) and in improved versions in 1904 and 1905 (see Figure 1-1-Figure 1-2, see p. 84). It mainly served to measure the radioactivity of “emanation” in air, but also to detect the radioactivity from uranium ore [Elster and Geitel (1899, 1904)]. A similar construction by Wilson ([474], see p. 194) was reported in one of the first textbooks on radioactivity by Rutherford ([363], see p. 187). Two of these early ionization chambers are shown in Figure 2-1-Figure 2-2. Another early re-entrant ionization chamber of cylindrical form, with about a 10 l volume, for the measurement of sources of radium minerals is described by Bothe ([40], see p. 167), and an improved version with an open well was constructed in 1921 (Figure 3-1, see p. 85), published by Fränz and Weiss ([153], see p. 174). Comparable constructions are described by Dorsey ([117], see p. 172) (Figure 3-2, see p. 86), Hess and Damon ([205], [206], see p. 177) and Bothe ([41], see p. 167). To measure ionization currents from those times and until the early 1950s, electrometers or electroscopes of various types were used, see preceding figures and the articles of Curie ([87], see p. 170), Meyer and Hess ([308], see p. 184), Hess ([204], see p. 177), Curtiss ([89], see p. 170), Lauritsen and Lauritsen ([273], see p. 182), Staub ([425], see p. 191), Lindemann and Keely ([279], see p. 182), Geiger and Campion ([167], see p. 175), Price ([341], see p. 186). Quadrant electrometers permit measurements over larger ionization current ranges, see [115], [363], [364], [432]. Many facts about the design and the working principles of current ionization chambers appear also in the context of measurements in the fields of dosimetry and radioprotection. Several models of such current ionization chambers can be found as examples in Figure 4-1-Figure 4-7, but only the type shown in Figure 4-7 is used for activity measurements in the sense of this review.

For a basic understanding of charge collection and ionization current characteristics, see [361], [366], [362], [363] and [364]. More sophisticated descriptions of the ionization process can be found for instance in [144], [145], [146], [116], [309], [357], [471], [425], [29], [30], [160], [203], [341], [257], [473], [258].

2.1. Measurement geometry of the source and the ionization chamber

Most re-entrant ionization chamber designs for activity measurements show a cylindrical symmetry as in Figure 4-7: the radioactive source, a solution in a cylindrical ampoule, is positioned at the centre of a cylindrical vessel having cylindrical electrodes. The symmetry of these structures is only interrupted by the entrance hole of the well, the electrical connections and the mountings of the electrodes covering a few percent of the total solid angle of 4π sr. Earlier constructions of spherical ionization chambers, as shown in Figure 2-1 [308] copied in [309] and [260], Figure 21 [403] and Figure 20 [53], or chambers without a well, but with

a lead entrance window (Figure 5 [264], [265], see p. 181), are no longer in use for activity measurements of photon emitting radionuclides.

In the ideal case the radioactivity is homogeneously distributed in an aqueous solution of a density of about 1 g cm^{-3} forming a cylindrical volume. Any point inside such a geometry could represent the origin of a trajectory of radiation from a decaying nucleus. In a few cases such as reference sources of ^{226}Ra or ^{137}Cs solid sources are measured in ionization chambers. The volume distribution of the radioactivity should be homogeneous to render theoretical considerations about attenuation effects possible. Thin point sources with low amounts of material are almost never used in calibrations of re-entrant ionization chambers.

To visualize the operating principle of an ionization chamber, as for example would be required in a Monte-Carlo calculation, the development of the interactions of the emitted radiations and their trajectories can be followed in the manner of a flow chart. Only photon radiation (α and γ rays) and the very small number of β particles with energies above a few MeV can reach the sensitive volume of the ionization chamber. However, high-energy β particles are detected with low probability by bremsstrahlung photons. All photons from the source and those from secondary effects transfer energy to the surrounding matter by three principal interaction processes: photoelectric effect, Compton effect and electron-positron pair production, the latter having an energy threshold of 1.022 MeV. Detailed descriptions of these effects may be found in books on nuclear physics or detector theory, such as [357], [425], [143], [316], [99] and [294]. Before the photons reach the sensitive volume of the chamber, their intensities undergo considerable attenuation in the material of the source, the containers and the sample holders, and in the ionization chamber walls. The photons that contribute to the ionization current are those that have transferred energy to electrons by direct interactions in the gas of the chamber, or in the matter around the gas from which electrons still reach the sensitive gas volume (Figure 6, see p. 90). All these electrons produce positive ions and electrons in the counting gas, usually referred to as ion pairs, with an average energy of about 30 eV per ion pair. When an electric field is applied to the chamber electrodes, the charges created move, are collected from the gas and measured as the ionization current of the chamber. A simple model of the processes is shown for a plane-parallel ionization chamber placed in a homogeneous photon radiation field in Figure 7 [31]. This may be extended to the more complicated cylindrical geometry with a radioactive source in the form of a solution, as shown in Figure 4-7.

2.2. Ionization process and charge collection

Let us now consider the interaction of “fast” electrons with gases. “Fast” in this context means the ability to create ion pairs that contribute to the ionization current. Fast-moving electrons in matter lose energy by Coulomb interaction and by radiative processes. The first leads to the formation of excited electronic states or to ionization in the atoms which were hit. The second produces bremsstrahlung or electromagnetic radiation. The knowledge we have of the processes involving fast electrons can be considered as reliable, and average data of the phenomena are available [29], [30], [160] in the Encyclopedia of Physics (Flügge S., Ed.), [341], [257], [473], [258] and many others]. However, in the slowing down of electrons by multiple scattering to the velocities of atomic electrons and the transport of slow electrons in an electric field, there are still “several points on which the picture is slightly hazy” [160]. A theoretical hypothesis or experimental generalities concerning averaged experimental data must be introduced to complete the picture of a charge collection, as described, for example, by

Grosswendt and Waibel ([189], see p. 176). This is understandable given the large numbers involved. For example, an incident 1 MeV β particle, fully stopped in pure argon creates nearly $4 \cdot 10^4$ ion pairs, the detailed path history of which cannot be followed individually. Our understanding of ionization chamber characteristics is therefore mainly based on empirical studies of averaged quantities or parameters.

During slow-down, energy straggling, range straggling and angular straggling occur. In addition, not all primary energy can be transferred to the final signal. Not only does the mean number of ion pairs formed vary from gas to gas, but fluctuations in their number occur in the same gas and for identical incident-particle energies. This imposes a fundamental limit on the accuracy of the detector response [147], [148], which applies not only to detectors with energy resolution, but also to integrating detectors among them current ionization chambers. In practice, these effects are superposed on stronger disturbing effects such as noise and fluctuations from the current-measuring electronics. All the available experimental information can be summarized in the essential fact that, for current ionization chambers, the ionization (number of ion pairs formed) is proportional to the energy of the electrons stopped in the gas, where the proportionality constant is the average energy lost by forming an ion pair: this constant is often referred to as the W value (Table 1, see p. 75). Because of the effects already noted, the W value is higher than the ionization energy, that is the energy needed to eject an electron from an individual atom.

Within less than a microsecond of the slowing-down process, an electron cloud is created along the track of ionization. In this time the energy of the electrons not influenced by other external forces is reduced to thermal velocity values with energies of order 0.04 eV. Very few free electrons may be expected to appear later by the depletion of metastable atomic states created along the track. If electric fields are weak or non-existent, the movement of electrons and ions can be described by theories of diffusion as a tendency to move away from zones of higher charge density. Charge transfer collisions occur, and electrons may be captured by positive ions in a process called recombination, or by neutral atoms (or molecules), a process called attachment [160]. There are two kinds of recombination effect. The first is called columnar recombination and takes place in the original ionization channel immediately after the creation of the ion pairs as a result of their high density in the tracks. The second is volume recombination and results from encounters between ions and electrons after they have left the immediate vicinity of the track.

When an external electric field is applied to the gas volume in the detector, the drift velocities are superposed on the random thermal motion of the ions and free electrons. In moving along the electric field, the ions and electrons gain kinetic energy, but lose it again through energy-loss processes. In the resulting steady state the average drift velocity v of the ions is given by

$$v = \mu E/p, \quad (1)$$

where

μ = mobility of ion,

E = electric field strength,

p = gas pressure.

Applying a voltage of 500 V to the electrodes, separated by 1 cm in a chamber with an argon pressure of 2 MPa results in ion velocities of about 20 cms^{-1} , so charge collection from the ion component takes about 50 ms. This is a rather long time and imposes a lower limit on the charge integration time for the ionization current measurement, usually chosen to be several seconds. Fortunately, the electron-drift velocity is typically about 1000 times that for

ions. An expression analogous to the equation for ions can be defined only for low-energy electrons moving in pure noble gases like argon. Generally, however, the behavior of the electrons cannot be predicted in detail. In a typical ionization chamber gas, such as pure argon or nitrogen, the excitation level of the outer shell is about 15 eV. The electrons can be accelerated up to this energy, limited only by elastic scattering. They then establish an average drift velocity which depends on the constituents of the gas in a very sensitive manner, and in some cases it does not even increase monotonically with the strength of the applied electric field [160], [341]. It has sometimes been reported that the current collected from an ionization chamber exposed to constant radiation intensity changes in magnitude when the polarity of the collecting potential is reversed [30]. This may be caused by

- contact, thermal or electrolytic potentials of materials,
- “selective operating” electrode geometries with respect to the direction of the photon flux,
- low-energy secondary electron emission in chamber walls,
- space charge effects or distortions of the electric field.

The various effects of electrode geometry on charge collection are discussed by Boag ([30], [31], see p. 167) and Colmenares ([76], see p. 169).

2.3. Ionization current

In activity measurements the photon flux of a radioactive source inside a current ionization chamber remains reasonably constant during the time of one measurement. In fact, for measuring times that are not short in comparison with the half-life of the radionuclide, a correction factor for radioactive decay has to be applied, see Equation (14). If the number of ion pairs created in the gas volume remains constant under well-defined measuring conditions, the charge collection as a function of the external polarizing voltage across the electrodes can be measured (Figure 8-1-Figure 8-2, see p. 91). This current-voltage characteristic curve is used to select the optimum working point of the ionization chamber. The measured current is proportional to the number of ion pairs collected. At low voltages, the current in the current-voltage characteristic curve increases strongly with increasing polarizing voltage. After this first increase, the slope of the curve decreases continuously to reach an almost constant current value, the so-called region of “ion saturation” (Figure 8-2, see p. 91). It serves no purpose to increase the voltage of the chamber to a value higher than this saturation region, because at very high voltages strongly ionizing processes occur and these may damage insulators and supports inside the chamber. In the region of saturation all charges due to ionization in the active chamber volume are collected and measured by the external current-measuring electronics. The result is an ionization current for chambers of the type under discussion in the range from about 10^{-13} A to 10^{-8} A for sources with activities ranging from a few hundred kBq up to about 10 GBq and radionuclides like ^{226}Ra or ^{60}Co , which have a high exposure rate constant because of their strong photon radiation components. The upper limit can be pushed to even higher activities if, in the construction of the ionization chamber, particular care is taken to avoid saturation losses.

For complete saturation, the maximum sustainable number of ion pairs in the chamber volume has been reached by irradiation with a source of very high activity. Apart from this, several factors may result in incomplete charge collection with the consequence of saturation loss [35]. The main reason for saturation loss is recombination (Section 5.3, see p. 38).

Recombination may be caused by:

- high local densities of ion pairs from strong local irradiation,
- displacement of charge into a reduced volume under the action of the collecting field (radial effect in a cylindrical volume),
- slow movement of ion pairs to the collection electrodes (time of transit comparable with that of recombination),
- long or complicated trajectories in the electric field.

For these reasons complicated structures at the end of the cylindrical electrodes and regions of weak electric field strength should be avoided.

The ion optics of the electric field between the cylindrical electrodes is important. The inner diameter should not be too small. The field should have good cylindrical symmetry near the centre and the sensitive region of the chamber should have a proper cutoff. This makes it possible to avoid high field gradients at sharp edges and the creation of “screened” zones from which an ion pair can be collected after following a long trajectory.

Also to be avoided are filling gases which form negative ions during ionization, as a result either of their electro-chemical properties or because of their high attachment coefficients (as in the case of oxygen). In most cases these show higher recombination effects, and hence should be avoided in ionization chambers used for activity measurements. The older open-air ionization chambers [29] are now rarely used for activity measurements as they require gas density corrections, as a function of temperature and air pressure, to relate measurement values to the calibration obtained under standard conditions (Section 3.2.1, see p. 23). A more detailed description of ionization chamber constructions and ionization-current measurement techniques is given in Chapter 3 and Chapter 4.

2.4. Ionization chamber calibration for activity measurements

It may be helpful for the understanding of the following text to begin with some definitions and to discuss a few simple relations which are valid provided that all measuring conditions of the ionization-chamber measuring system, including source parameters, remain uniform or stable during the measurements. The desired measurand is the activity A as defined in the Chapter 1 which decreases exponentially in time according to the well-known law of radioactive decay

$$A = A(t) = A_0 e^{-\lambda \Delta t}. \quad (2)$$

The activity A_0 is always referred to a fixed reference time $t = t_0$. For a source used as a radioactivity standard this value is certified. Using Equation (2), the activity $A(t)$ at the time of measurement can be calculated in terms of the time difference $\Delta t = t - t_0$ and the relation $\lambda = \ln 2 / T_{1/2}$, where $T_{1/2}$ is the half-life of the radionuclide. The half-life can be found in appropriate tables [272], [316], [51], [394], [225], [324].

Since the studies of Rutherford and Soddy ([367], [368], see p. 188), the half-life is taken to be a fundamental parameter of a radionuclide characterizing the decay. Its value may be influenced by chemical effects or interactions, for example in the case of electron capture nuclides (section 8.3). To convert time units in Equation (2) from years (a) to days (d), e.g. for $T_{1/2}$, a factor of 365.25 d/a is usually applied for time intervals of less than a few hundred years. For intervals of up to 100 a this correctly averages over leap years and therefore, follows the calendar scale in days. Precise time differences in days used for decay corrections are

calculated from the corresponding Julian dates given, for example, in a computer algorithm by Fliegel and Flandern ([152], see p. 174).

The ionization chamber current I , originating from a source with a single radionuclide N under the same measuring conditions, is proportional to its activity, i.e.

$$I = \varepsilon_N A. \quad (3)$$

The proportionality factor is called the radionuclide efficiency ε_N . The values for various radionuclides are expressed in units of ampere per becquerel (ABq^{-1}). In the equation given above, the measured current I_m must be corrected for background current I_b , with $I = I_m - I_b$, determined under identical measuring conditions. In what follows it is always assumed that the ionization current is already corrected for background.

With most of the current-measuring instruments it is possible to adjust the instrument reading R by an internal (or external) instrument setting. In modern current-measuring electronics this is done by adjusting the instrument amplification. This property can be described by an instrument constant g in the formula

$$R = gI = g\varepsilon_N A. \quad (4)$$

An instrument can be adjusted to show the activity reading $R_N = A$ for a defined radionuclide N directly in units of becquerel or its multiples (kBq, MBq, etc.). The adjustment condition is $g_N \varepsilon_N = 1$ and it follows that

$$A = R_N = (1/\varepsilon_N)I. \quad (5)$$

This technique is commonly applied to instruments such as radionuclide calibrators for performing quantitative assays of radiopharmaceuticals (Section 3.2.4, see p. 25) [398]. These instruments take the form of an ionization chamber coupled to current-measuring electronics with adjustments for particular radionuclides by fixed instrument settings chosen in advance. The settings are determined with the help of activity standards or transferred from a calibrated reference instrument by the manufacturer.

2.5. Relative activity measurements and reference sources

Ionization chambers working under reproducible measuring conditions are very effective for relative (or indirect) measurements by comparison with an activity standard. For many applications it is useful to compare current ratios, i.e.

$$\frac{I_i}{I} = \frac{\varepsilon_{N_i} A_i}{\varepsilon_N A}, \quad (6)$$

where i is an index specifying a particular sample. In quality assurance for standard source production, comparisons are made between samples of the same radionuclide, the same geometry, and almost the same activity. Alternatively, dilution factors are verified using samples with different ranges of activity. In each case, the terms expressing the radionuclide efficiencies in the formula cancel, and the unknown activity values are calculated from that of an activity standard.

In other cases, geometry correction factors are determined for radioactive solutions of various masses m_i in standard ampoules or in ampoules of different materials and forms. For this purpose the sources are dispensed from the same mother solution (index S, the activity being measured in a standard geometry), this having a constant activity concentration

$a = a_S = a_i = A_i/m_i$, the masses being determined by careful weighing. Dispensing procedures are described in the literature by Merritt and Taylor ([307], see p. 184), Eijk and Vaninbroukx ([126], see p. 173) and Campion in a monograph of BIPM ([63], see p. 168). The related ratios of the currents per mass (or instrument readings per mass) are deduced from the preceding equations:

$$\frac{I_i/m_i}{I_S/m_S} = \frac{R_i/m_i}{R_S/m_S} = \frac{\varepsilon_i a_i}{\varepsilon_S a_S} = \frac{\varepsilon_i}{\varepsilon_S}. \quad (7)$$

These ratios are independent of time only for radioactive solutions containing a single radionuclide, because in a mixed solution the ratios of the compositions change following the decay of the various radionuclides. Because the radiation mixtures change, variable radiation attenuation and detection effects are also involved in the ratios of Equation (7). For a solution with a single radionuclide measured in a non-standard geometry, the measurand is multiplied by the ratio $\varepsilon_S/\varepsilon_i$ to obtain the corresponding quantity in the standard calibration geometry. Several authors have studied filling correction factors or correction factors for displacements from a standard source position in the ionization chamber [95], [469], [372], [373]. Examples of this are presented in Chapter 6.

Perhaps the most important of relative measurements made with an ionization chamber are calibrations relative to a long-lived reference source of the type in general use in most national standards laboratories. Here, the activity of the sample to be determined is taken to be proportional to the quotient of the response to the radionuclide sample to the response to the reference source. In this way instrument instabilities are eliminated so long as they affect the responses to both sources equally. The preferred reference source is an old ^{226}Ra source. In such a source the radium should be in equilibrium with its daughter nuclides which have shorter half-lives. The half-life of ^{226}Ra is (1600 ± 7) a [449], [85], [86] or $(584\,400 \pm 2600)$ d, corresponding to a decay correction of 0.043% per year. The longest-living radium daughter, ^{210}Pb , has a half-life of (22.3 ± 0.2) a and the photon radiation from the decay consists mainly of bremsstrahlung from the ^{210}Bi daughter ($T_{1/2} = 5.0$ d). The \pm terms represent one standard deviation. Many of the nuclear properties, including the half-lives of the nuclides in the uranium-radium decay chain, were given by Weigel ([465], see p. 194) in the handbook of Gmelin. For ionization chamber measurements changes in time of the current ratios for mother and daughter nuclides of the radium decay chain are in most cases negligible if the reference sources are older than about 50 a and are kept in a sealed container. Equilibrium conditions are referred to in the literature (see Section 2.6, see p. 19) and the influence of the reference source on relative measurements of the half-lives of other long-lived radionuclides are reported, e.g. by Martin and Taylor ([299], see p. 183).

The basic equations for indirect calibration of an ionization chamber for a radionuclide N against a reference source (index r) are derived hereafter. The ratio of the instrument readings of the source to be measured R to that of the reference source R_r is related to the ratio of the corresponding activities A and A_r by

$$\frac{R}{R_r} = \frac{\varepsilon_N}{\varepsilon_r} \frac{A}{A_r}. \quad (8)$$

If the decay correction factor for the reference source is written explicitly, resolving the equation for the activity of the radionuclide gives

$$A = \left[\frac{\varepsilon_r}{\varepsilon_N} A_r \right] \frac{R}{R_r} = \left[\frac{\varepsilon_r}{\varepsilon_N} A_{ro} \right] e^{-\lambda_r(t_m - t_{ro})} \frac{R}{R_r} = A_e \frac{R}{R_{ro}}, \quad (9)$$

with

$$A_e = \left[\frac{\varepsilon_r}{\varepsilon_N} A_{ro} \right], \quad (10)$$

$$R_r = R_{ro} e^{-\lambda_r(t_m - t_{ro})}, \quad (11)$$

where A_{ro} is the activity of the reference source at t_{ro} , the reference time. The term A_e is referred to as the “equivalent activity.” It refers to an individual radionuclide under reference measuring conditions related to the individual reference source at a certain, but fixed, instrument setting g . By definition, a source of a radionuclide with an activity value equal to the equivalent activity ($A = A_e$) produces the same instrument reading as that of the reference source used for the calibration ($R = R_{ro}$). Because this is valid for each instrument setting when both sources are measured under these conditions, they must also produce the same current ($I = I_{ro}$).

The equivalent activity A_e is also sometimes called the “relative K factor” [294], and a quantity equal or proportional to it is called the “calibration factor” k_N , or less precisely the “calibration constant”, of the ionization chamber for that particular radionuclide (Section 7.1, see p. 53). More briefly, in laboratory jargon, this is called the “chamber constant”. The reciprocal of this quantity represents the relative efficiency of the ionization chamber for a particular radionuclide ($k_N = 1/\varepsilon_{N,rel}$, or $A_e \sim 1/\varepsilon_{N,rel}$).

The given relations can be used to adjust an activity meter (radionuclide calibrator) using the reference source belonging to the instrument. This source is placed in the instrument under reference conditions and the amplification of the current-measuring electronics is adjusted, for example by a potentiometer, until the instrument reading shows the equivalent activity value. With a series of instruments of common construction, this procedure can be used to transfer the values of calibration factors from a reference instrument to a new instrument or to one being recalibrated after repair. The procedure is also useful for an instrument already calibrated since it is only necessary to adjust the current-measuring electronics, for example after changes of the electronics, if the properties of the ionization chamber itself have not changed.

A further possibility for relative measurements is to use a simulated standard, or mock standard, as a reference source for a particular radionuclide. This is discussed in the literature with some more details on calibration constants: Examples include the simulation of $^{99}\text{Tc}^m$ with ^{141}Ce [303], [163] or with ^{57}Co [22]. The simulated standards should have radiation characteristics similar to those of the radionuclide to be measured and, clearly, care must be taken to apply a correct conversion factor related to the corresponding calibration factors (Section 7.1, see p. 53).

2.6. ^{226}Ra sources

From earliest radioactivity standardizations by Mme Marie Curie ([87], see p. 170), who prepared the first radium standard, to the 1950s, calibrated ^{226}Ra sources were used as activity standards and were compared with the primary activity standard at the BIPM or with the Hönigschmid standards [88], [365], [467], [97], [79], [283], [295], [296], [316]. Some of the last Hönigschmid standards, dating from 1934, are still available (Figure 9, see p. 92). They are accurate to about 1%. Nowadays ^{226}Ra sources are mainly used by national standards laboratories as reference sources for ionization chamber measuring systems. The measurement conditions and equilibrium problems of ^{226}Ra reference sources are similar to those experienced with the older measurements of radium standards using

ionization chambers. These are described by Meyer and Schweidler ([309], see p. 184), by several editions of Kohlrausch's handbook of [261], [260] and [264], or by Davenport et al. ([97], see p. 171), Loftus et al. ([283], see p. 182) and Mann et al. ([296], see p. 183), when solution standards of radium were prepared at the NBS. In 1982, under the auspices of the BIPM, the PTB and a producer of radioactive sources (Amersham Buchler, Braunschweig [6], see p. 165) jointly produced a set of about twenty ^{226}Ra reference sources made from old British radium prepared in 1912.

The small fraction of decay per year for a reference source of ^{226}Ra , with a half-life of $T_{1/2} = (1600 \pm 7)$ a [449], sets a lower limit to the uncertainty component from decay corrections for this reference source for measurement periods of up to several decades [376]. A ^{226}Ra reference source consists of purified ^{226}Ra , free from radioactive contaminations, such as ^{228}Ra . It has the chemical form of crystalline salt as chloride or sulphate, which may be mixed with inactive Ba sulphate. The confinement is a Pt-Ir or stainless steel (V2A) tube carefully sealed. For older sources, glass was frequently used. The seals must be checked for tightness at regular intervals to detect any possible escape of radon gas ^{222}Rn , one of the short-lived daughters, with a half-life of $T_{1/2} = (3.823 \pm 0.003)$ d. The ^{226}Ra should be in equilibrium with its daughters. This is reached in a few weeks for the short-lived daughters, but equilibrium with the long-lived ^{210}Pb ($T_{1/2} = 22.3$ a) is reached only a long time after preparation. The nuclide ^{210}Pb emits L-x rays of about 12 keV and γ rays of 46.5 keV with an emission probability per decay of about 4%. The low-energy photons are strongly attenuated in the source and the confinement layers, but the bremsstrahlung photons from the β decay of the following daughter ^{210}Bi are detected with high efficiency. To estimate the contribution of ^{210}Pb and its daughters to the ionization current of a ^{226}Ra source and its degree of disequilibrium, the exact date of the separation of the Pb from the Ra must be known.

According to [469], the contribution of ^{210}Pb and its daughters is of the order of 0.2% of the total ionization current of the decay chain of ^{226}Ra , and this is also the maximum error made in the course of time if the increase of ^{210}Pb in a newly-prepared radium source is not taken into account. Similar values are given by Rytz ([373], see p. 188). Although small, this error may still have a strong effect on half-life measurements. Christmas et al. ([70], see p. 169) have shown that for a sealed ^{226}Ra sample, observed with an ionization chamber for which the chamber response to ^{210}Bi is 0.25% of the ^{226}Ra response, the apparent half-life would vary from 1900 a, for a recently purified sample, to 1620 a, for preparations made at the time when the radium was discovered. A discussion of the effect on the half-life measurement of the longlived ^{137}Cs is given by Martin and Taylor ([299], see p. 183), who attributed an uncertainty component of 0.22% to the $^{210}\text{Pb}/^{226}\text{Ra}$ disequilibrium. The formulae for the change of activity ratios in decay chains are described in textbooks on radioactivity, for example by Evans ([143], see p. 174). Numerical expressions for the uranium-radium chain are given in detail by Weiss in Kohlrausch ([266], see p. 181), vol. III (1986). Fränz, in Kohlrausch ([264], see p. 181) gives a formula and a diagram describing the influence on activity measurements of the $^{222}\text{Rn}/^{226}\text{Ra}$ disequilibrium in freshly prepared samples. A summary on the measurements of ^{226}Ra and related problems can be found in a section by Weigel ([465], see p. 194) on Radium, suppl. vol. 2, in the handbook of Gmelin.

In standards laboratories a set of about five ^{226}Ra reference sources is usually available. These contain different amounts of radioactive substance covering an activity range of the order of 100. They are of similar construction and have the same attenuation properties. They are carefully compared at regular intervals to check the stability and linearity of the chamber. This makes it possible to measure samples of different activities, by choosing an appropriate reference source, in such a way that the current ratios fall within a range of about

five, an arrangement which improves the accuracy. Results of current measurements from five reference sources covering a range of about 100 in activity (with a maximum of 308 µg of radium element) were published by Rytz ([376], see p. 188) showing relative standard deviations of about $2 \cdot 10^{-4}$ over a period of about 7 a (Figure 10-1-Figure 10-2, see p. 93). The repeatability for a single source for a series of 50 measurements was about 0.09% (1σ).

3. Construction of ionization chambers

3.1. $4\pi\gamma$ ionization chambers

The optimum design of a re-entrant (or 4π) ionization chamber for activity measurements of photon-emitting radionuclides is nowadays a pressurized cylindrical construction. The earliest pressurized ionization chambers for capturing high-energy events can be found in the field of cosmic-ray measurements [136], [237], [260], [310], [77], [78], [428]. A detailed study on argon as filling gas is given by Hopfield ([214], see p. 178). A review article with references by Steinke ([426], see p. 191) can be found in the Handbook of Physics ([167], see p. 175).

Another branch in the development of pressurized devices came from the field of dosimetry measurements, in earlier times associated with the names of Gray ([182], [183], see p. 176) and Sievert ([411], [412], see p. 190) who studied fundamental properties of ionization by radiation in gases as functions of pressure and other parameters. A short review of dosimetry and activity measurements is given by Allen ([4], see p. 165). Many other references and details, mainly applied to dosimetry, can also be found in the review article on ionization chambers by Boag ([30], see p. 166) and in Kment and Kuhn ([257], see p. 181). The first practical designs of pressurized devices for dosimetry and radioprotection are given by Carmichael ([64], [65], see p. 169) and by his co-workers Smith et al. ([417], see p. 191), Steljes ([427], see p. 191), Peabody ([338], see p. 186), see Figure 11, which led to the development of ionization chambers for activity measurements of the form used today. These publications explain many technical details of the manufacturing of electrodes, insulators and gas fillings, etc. for these chambers. The working principles of the cylindrical ionization chambers filled with pressurized gases are more generally described by Siri ([416], see p. 191), Taylor and Sharpe ([442], see p. 192) and Sharpe ([407], see p. 190).

Wade ([458], see p. 193) constructed an ionization chamber (T.P.A. Mk IV), filled with argon at a pressure of 1 atmosphere (Figure 12, see p. 94), in which he added an inner aluminium tube for the reentrant well. This chamber is optimized for sources with β -particle emitting radionuclides.

In the same way, one of the first pressurized ionization chambers (T.P.A. Mk II) was constructed with modified electrodes, a steel well and filled with argon at a pressure of 20 atmospheres by Sharpe and Wade ([405], [406], see p. 190), Figure 13. More details of the design of this reentrant ionization chamber for activity measurements and calibration figures for some radionuclides can be found in Sharpe and Wade ([406], see p. 190). This model is still in use today and, with minor modifications, it is available on the market from Centronic ([69], see p. 169). Since then, Centronic ionization chambers have been installed in many national standards laboratories where they are used as secondary standard measuring systems for activity [307], [372], [376], [437], [395], [58], [441], [177]. A schematic drawing of this chamber is shown in Figure 14.

At about the same time as the work by Sharpe and Wade ([405], see p. 190), other aspects of the design of a “high precision”, high-pressure ionization chamber, among them the location and construction of the insulators, guard rings and guard-ring connectors were developed by Shonka and Stephenson ([408], see p. 190), Figure 15, and published by O’Kelley ([326], see p. 185). This chamber was filled with 40 atmospheres of dry argon. The high sensitivity

of such a chamber necessitates enclosure in a lead housing with walls some 10 cm thick to reduce environmental background effects [316].

Examples of other designs may still exist in standards laboratories [187], Figure 16, [45], [190] [27], Figure 17-1-Figure 17-2, [286]. Several pressurized chambers for activity measurements of photon-emitting radionuclides in the field of applications, especially in nuclear medicine, have been designed by manufacturers, such as Capintec, Merlin-Gerin, Meßelektronik Dresden (former Robotron) [402], ORIS, Philips, Physikalisch-Technische Werkstätten (PTW) Freiburg, Picker, Radcal, Siel (Nuclear Data), Veenstra, NE Technology (former Vinten), Zinsser Analytic. These have been or are still on the market (Section 3.2.4, see p. 25). Examples are shown in Figure 23-1-Figure 23-4. Among these the Vinten chamber, now manufactured by Nuclear Enterprises Technology Ltd. [319], should be emphasized. This was developed and tested at the NPL [476], [482], [479]. This system is delivered with a complete set of calibration figures measured at the NPL and the chamber can be delivered with a certificate from the NPL. It is thus traceable to NPL primary activity standards. It is in use in several national standards laboratories.

All these ionization chamber designs take the form of an external vessel of steel or aluminium with a thimble or well for introducing the sample (Figure 14, see p. 94). The vessel must be carefully welded or sealed to maintain a pressure of about 2 MPa (in old units about 20 atmospheres) over many years. The thickness of the walls should be about 3 mm to 4 mm to prevent deformation by pressure. One of the critical points in the design is the connectors (or insulators), which must be screwed and gas tight. For more details, see [442], [29], [160], [257]. The fabrication of ionization chambers is today an area which depends on the special know-how and competence of the manufacturing firms. The inner electrodes are nearly always made of aluminium foil. The copper or brass found in older constructions is no longer in use because of their larger content of α -particle emitting impurities which increase the background current, and because they have other unfavourable electrochemical and mechanical properties. A special chamber-electrode design has been suggested by Kostyleva et al. ([269], see p. 181): this uses materials which optimize the attenuation effects of photons and electrons. An electrode coating with high-Z materials has been studied by Kleeven and Wijnhoven ([256], see p. 181) with a view to increasing the chamber response.

At present, the most common filling gases are purified argon or nitrogen. Argon has a higher sensitivity, at least at photon energies below 100 keV, but the response of nitrogen is more nearly linear with photon energy (Chapter 7, see p. 53).

3.2. Special types of ionization chambers and their applications

3.2.1. Unsealed chambers at atmospheric pressure

Most of the earlier designs of re-entrant ionization chambers for activity measurements, but also some current ones used in simple applications, use unsealed vessels at atmospheric pressure. Examples are given by Wade ([458], see p. 193) (Figure 14, see p. 94), Smith and Seliger ([418], see p. 191), Seliger and Schwebel ([403], see p. 190) (Figure 21, see p. 99), Muth ([315], see p. 184), Mann and Seliger ([295], see p. 183), Engelmann ([133], [134], see p. 173), Geiger and Campion ([167], see p. 175), Robinson ([355], see p. 187), Dale et al. ([91], see p. 170) (Figure 18, see p. 97), Weiss ([468], see p. 194), Cohen et al. ([75], see p. 169), Dalmazzone ([93], see p. 170), Ramanuja Rao

([342], see p. 186), Sankaran and Gokarn ([386], see p. 189) (Figure 19, see p. 98). An unsealed chamber is cheaper than a pressurized one, and some manipulations are easier and can be carried out with less effort inside the chamber. It has the disadvantage, however, that measurement data have to be corrected for differences in pressure and temperature with respect to standard conditions. This correction is similar to that applied to air-equivalent ionization chambers for dosimetry measurements. It can be kept small by measuring against a reference source such as ^{226}Ra , but it cannot be completely neglected. A simplified formula by Knoll ([258], see p. 181), which is valid at higher photon energies, takes the air-density effect into account. Low-energy photons to about 50 keV, originating either directly from the source or resulting from secondary effects, produce relatively more electrons than high-energy photons. The electrons come to rest within the sensitive chamber volume so their ionization current is less density dependent. Corrections at these energies are therefore determined experimentally by measuring the chamber response for low-energy photons at different air densities. For radionuclides with low-energy photons measured relative to a ^{226}Ra reference source, the corrections remain below 0.5% [459]. A special spherical design for an unsealed 4π ionization chamber presented by Bucina et al. ([53], see p. 168) (Figure 20, see p. 98) was studied in detail so as to determine position dependence of the source on the calibration. Erdélyváry and Fehér ([135], see p. 173) describe an ionization chamber with a very thin entrance window in the well, in the form of a plastic tube, for measurement of the activity of a ^{125}I solution. Loftus ([282], see p. 182) describes a spherical re-entrant ionization chamber at the NBS for the standardization of ^{192}Ir sources in form of seeds in terms of the dosimetry quantity: exposure, the chamber having an outer aluminium electrode. For this standardization, data on photon-emission probabilities and mass-energy attenuation coefficients for the individual photon energies of ^{192}Ir were used to calculate the exposure rate constant as a function of activity. For the definition of the exposure rate constant, see [226] and [316].

3.2.2. β -particle ionization chambers

This section concerns β -particle ionization chambers in which β particles of low energies, of around 10 keV, are detected directly. Measuring methods for high-energy β -particle emitters in high-activity sources have already been described in the discussion of the detection mechanism for bremsstrahlung photons (see also Section 7.3, see p. 55). If activity measurements of low-energy β -particle emitters are to be made without dismounting the chamber, thin entrance windows between source and chamber must be used, only thin sources can be measured and absorption effects must be taken into account. Technical details on filling gases, pressure variations and wall materials for ionization chambers used to detect β particles may be found in [39], [357], [425], [160], [257]. A review article on the standardization of pure β emitters by Lowenthal ([284], see p. 182) includes a section on ionization chamber applications. Some chamber designs and more details on source preparation can be found in NCRP ([316], see p. 184). The designs given have a 2π geometry for the source and a spherical construction for the chamber, see Figure 21 [403], [295]. For a supplementary “parallel plate” chamber for β particles integrated in a cylindrical photon chamber, see Figure 18 [355], [91]. This kind of chamber has been used for many applications in the field of nuclear medicine and in general nuclear physics studies, for example for neutron activation analysis [212]. For β emitters such as ^{35}S or ^{204}Tl , uncertainties down to 1% (1σ) are obtained [284]. Lowenthal also suggested the use of proportional counters with very thin sources for activity measurements of β emitters to obtain an uncertainties of order 0.5% and liquid scintillation counting (LSC) for ^3H or ^{14}C .

To assay gases of ^3H or ^{14}C (in the form of CO_2) ionization chambers have been used with the gas directly filled in the chamber volume. Their advantage is that activities are measured under well-known sample conditions among them gas temperature, pressure, and chemical and radionuclide purity [52], [76], [105]. More literature on this is given in NCRP ([316], see p. 184). Another spherical ionization chamber design used for environmental radiation studies is reported by Shamos and Liboff ([404], see p. 190). This chamber discriminates almost completely against α particles originating in the walls without affecting the collection of β particles and against γ -ray-induced ionization by using highly electro-negative filling gases.

3.2.3. α -particle ionization chambers

Ionization chambers for radioactive gases of α -particle emitting radionuclides like radon, especially ^{222}Rn [139], were developed for the assay of ^{226}Ra samples in a period when ^{226}Ra was an important radiation source [196], [140], [141], [271]. Other references on measurement techniques are given by Kment and Kuhn ([257], see p. 181), and in NCRP ([316], see p. 184), (these references also include gas-handling and purification systems). Measurements of radium standards using α -particle ionization chambers are reported by Mann et al. ([296], see p. 183). Actually, ionization chambers with internal radioactive gases are used only for special applications [339], [213], such as radon monitoring in gases from the soil in the course of uranium prospecting or earthquake prediction research [156], [157].

3.2.4. Radionuclide calibrators

Radionuclide calibrators or “activity calibrators”, see [316], formerly called “dose calibrators”, in continental European countries also called “activity meters” or “activimeters”, are instruments used for the assay of radiopharmaceuticals to determine the activity of a specified radionuclide. They consist of a re-entrant ionization chamber with current-measuring electronics permitting a direct reading in units of activity (multiples of the SI unit becquerel or submultiples of the formerly used curie). This is done using a predefined, fixed instrument setting such as a push-button, plug-in, potentiometer adjustment or an electronically set multiplication factor (e.g. by a keyboard entrance to a microprocessor) for each particular radionuclide.

One of the first radionuclide calibrators in nuclear medicine applications was described and tested by Sinclair and Newbery ([414], see p. 190) (Figure 22-1-Figure 22-2, see p. 100), Bullen ([55], see p. 168) and Sinclair et al. ([415], see p. 191). They give calibration figures for solutions of ^{131}I , ^{24}Na , ^{198}Au , ^{59}Fe and ^{60}Co and other radionuclides, and many details of the instruments used at that time together with contemporary references. Simple instrument tests, such as linearity checks and the variation of response with source volume at constant activity concentration of the source, are described. More details on radionuclide calibrators may be found in Dale et al. ([91], see p. 170), Suzuki et al. ([431], see p. 192), Merritt and Gibson ([303], see p. 183), Broj and Gregor ([47], see p. 168), Husak and Kleinbauer ([224], see p. 179), Sankaran and Gokarn ([386], see p. 189), NCRP ([316], see p. 184), Schrader ([398], see p. 190). In this monograph, the topic is treated in Section 8.2 on quality assurance in nuclear medicine. A few examples of such instruments are shown in Figure 23-1-Figure 23-4. Technical details of the instruments may also be found in the manuals of the manufacturers, among them Capintec, Merlin-Gerin, Meßelektronik Dresden (former Robotron) [402], NE Technology (former Vinten), ORIS, Philips, Physikalisch-Technische Werkstätten (PTW) Freiburg, Picker, Radcal, Siel (Nuclear Data), Veenstra, Zinsser Analytic.

Instruments are usually calibrated by the manufacturer using standard solutions of the radionuclide (direct calibration) from a national standards laboratory (or traceable to it), or alternatively by comparison with a reference instrument (indirect calibration). In the indirect calibration, the reading of the instrument to be calibrated and that of the directly calibrated reference instrument are compared by introducing a reference source under identical measuring conditions into the well of each chamber. The instrument setting for the particular radionuclide is applied, and the reading of the first instrument is adjusted.

In order to transfer and apply the calibration factors determined, detailed information on the chamber and the measuring conditions must be given by the manufacturer (Chapter 6, see p. 42). This applies in particular to the description of the measurement geometry, which should include the dimensions and the material of the source, and its position in the chamber well. The use of identical ampoules, vials or syringes with defined volumes in a stable source holder with a fixed mounting of the chamber shielding is recommended. Care must also be taken that the radioactive solutions remain chemically stable in a homogeneous volume distribution, with no more than low and well-defined fractions of radionuclidic impurities for which a correction factor can be applied.

Measuring conditions with radionuclide calibrators are the subject of several national standards, guides for quality assurance and national and international recommendations for measuring the activity of a radiopharmaceutical. The purpose is to ensure good radiation protection practice, the end results being to reduce the integrated dose received by the persons affected [8], [10], [60], [110], [12], [323], [230], [231], [28], [333]. The European Pharmacopeia ([137], see p. 173), for example, prescribes accuracy limits of 10% for the activity of many radionuclides used in radiopharmaceuticals. Similar measurement and quality assurance conditions can be found in the US Pharmacopeia ([454], see p. 193). The practice of measurement accuracy has been checked by round-robin comparisons which show that these limits are not always achieved. More details on quality control and intercomparisons are given in Chapter 9.

Most of today's radionuclide calibrators have ten or more fixed instrument settings for the most commonly used radionuclides in the field of nuclear medicine, and it is possible to adjust the instrument settings to measure other radionuclides. When this is done, the calibration factor and the corresponding setting must be taken from a data file provided by the manufacturer. In other cases they are established by the user from decay data on the radionuclide in question, but this can be done only if the photon efficiency of the chamber is known as a function of energy. Several authors have reported methods for the determination of efficiency curves, including examples of data for particular types of ionization chamber (Chapter 7, see p. 53). These efficiency curves are especially useful for calculating the calibration factors of rare nuclides for which no calibration standards are available, e.g. radionuclidic impurities (Chapter 6, see p. 42).

As a supplement to correct instrument settings and stable measuring conditions, regular instrument checks are mandatory and are prescribed by relevant standards on the quality control of activity measurements. The regulations require a calibration check in the particular radionuclide setting to be used with the reference source, and a background check on each work shift, a check for the energy dependence of the instrument response with at least three reference sources, which cover a useful instrument range from low to high photon energy, roughly at daily intervals, and a linearity check (see Section 5.4, see p. 39) covering the activity range used at intervals not exceeding three months. A complete calibration check

against standards, or by a comparison with a calibrated reference instrument, is required at intervals of one year, and obviously after every repair.

3.2.5. Ionization chamber accessories: shielding, sample holders, sample changer, system control, data acquisition and data analysis

- **Shielding.** An ionization chamber meeting metrological requirements must be shielded by lead (at least 5 cm thick), shaped like a box or cylinder, around its sensitive volume (Figure 24-1-Figure 24-2 and Figure 25-1-Figure 25-3, see p. 107). The lead should contain a minimum of radionuclidian impurities. Lead which is several decades, or even centuries, old is most suitable for this purpose because one contaminant, ^{210}Pb with a half-life of 22.3 a (from the uranium-radium decay chain), then has sufficiently decayed. Other contaminants may originate from the alloy composition of the lead, among them antimony and thorium daughters (not eliminated in the production process) or, in more recently refined lead, from radionuclides in atmospheric fallout, see p. 726. Other aspects of shielding are discussed in Section 6.1. A design for the lay-out of a measurement cabinet for radionuclide calibrators in a radiopharmaceutical production line is described by Dye and Reece ([124], see p. 172) This provides optimized working conditions with low radiation exposure.
- **Sample holders** serve to maintain the ampoule being measured in a reproducible position in relation to the sensitive chamber volume. In most cases they take the form of a very thin cylindrical tube adapted to the diameter of the ampoule, with a thin bottom, a conical head and a cylindrical ring on top. This head allows samples to be positioned in the chamber well with a reproducibility better than a few tenths of a millimetre. The sample holder is manufactured from light materials containing elements with low Z-values, for example from plastic material such as Perspex. With cylinder walls about 0.5 mm thick, attenuation factors are typically about 0.2%. When the same type of holder is used for all relevant measurements, attenuation effects can be included in the calibration factors.
- **Automated sample changers** are connected to ionization chamber measuring systems in some national standards laboratories. Apart from a report by Lowenthal ([285], see p. 182) and a few publications on related subjects in which they are mentioned, including [443], [395] (Figure 24-1-Figure 24-2, see p. 104), [316], [441], [299], [300] (Figure 25-1-Figure 25-3, see p. 107) and [420], no detailed literature is available on sample changers. An automated sample changer makes it possible to make very efficient use of a measuring system by keeping it in continuous operation and reducing the manpower needed to operate the equipment.
The elements of a sample changer are a shielded reservoir which contains 10 or 20 samples, a transport rail and a chain or wheel with a gripper which allows the measuring instrument to be charged with a sample. The sample changer is controlled by a microprocessor or a small computer to run measuring cycles with several samples. In ionization chamber applications, measurements follow a cycle in which the samples alternate with a reference source and background.
- **System control** is required for automated ionization chamber measuring systems with sample changers running repeated cycles of measurement series (as described above). The cycles are computer-controlled and, generally, one cycle consist of a measurement part, in which the current measurement for one sample is recorded, and a part in which the measuring conditions, parameters or samples are changed. The time taken for a particular current measurement thus represents only a part of the total time required for the measurement series. In addition to the control of the cycles, the computer program

may also control the steps necessary for a current measurement. This may be the case if individual clock times are used to measure the time during current integration, a technique applied in some of the current-measuring systems (see Chapter 4, see p. 29). The status of a running charge-integration process is detected by sensors giving binary values, or by counting (or surveying) digitized values of the measured quantities from this process, for example an analogue-digital converter may transmit them to the control processor. Generally speaking, the processor transmits and receives signals, via an interface, to and from switches, relays, digital-analogue converters or analogue-digital converters which, in turn, are connected to motors, magnets or other electronic devices. The processor itself handles a program in machine code, assembler or a higher programming language to run logical and numerical operations.

- **Data acquisition and analysis** is much simplified if the measurand, here the ionization current, is directly linked to the corresponding clock time and date of the measurement and the values stored in static computer memory (on-board RAM) and on disc. Data evaluation programs can then be applied on-line (see Chapter 2, see p. 12) invoking parameters stored in permanent files, for example half-lives, calibration factors and geometry correction factors. Once stored on file the data are also accessible by commercial programs for record keeping and data representation.

4. Techniques of measurement for ionization current

Measurements of small ionization currents in ionization chambers have been used for activity determinations since the early days of the discovery of radioactivity, as noted in Chapter 2. The currents to be expected range from about 10^{-8} A to 10^{-13} A, with instrument leakage currents down to a few 10^{-15} A. The description of the physical processes (see Section 2.3, see p. 15) shows that the ionization current in a chamber with a fixed source is produced in a continuous or “stable” manner. The relevant time parameters for a single measurement are usually short in comparison with the half-life of the radionuclide being measured. The occurrence of interactions and charge production is “constant”, apart from small fluctuations due to the statistics of the detection process. The ionization current can therefore be regarded as almost constant during a measurement, apart from the small fluctuations caused by electronic noise and background variations. Particularly stable current sources have been produced by Dalmazzzone ([94], see p. 170) and Böhm ([36], see p. 167) (Figure 26, see p. 108) using radioactive sources such as $^{90}\text{Sr}/^{90}\text{Y}$ in ionizing devices as reference sources for currents from about 10^{-10} A to 10^{-14} A. The stability of ionization currents permits the application of quasi-static electronic methods, such as charge integration with large capacitors (up to 100 nF), or compensation procedures continuously following the current production. This keeps the duration of an individual measurement in a range from several tenths of a second to a few hundred seconds, depending on the activity of the source. During a current measurement of the order of magnitude described, leakage and instrument offset currents must be held as low as possible. This completely excludes galvanometric methods, and calls for electrometric methods with insulator resistances above $100\text{ T}\Omega$ [251].

The essential part of a current-measuring system is the electrometer. Today four classes of electrometer are known: electrostatic electrometers (with a mechanical part or indicator driven by electrostatic forces), electronic vacuum-tube electrometers, dynamic condenser electrometers, also called vibrating-reed electrometers (VRE), and solid-state device electrometers. From the early days of radioactivity measurements until the 1950s, the classical electrostatic electrometers were used almost exclusively (see introduction to Chapter 2, see p. 12). Some of the first instruments with electronic tubes appeared in the 1930s [235], [274], and were available until the 1960s with rather sophisticated circuit designs for measurements of high accuracy [276], [221], [222]. Starting from the 1940s, electrostatic electrometers were replaced by vibrating reed electrometers [330], [149]. Some of these are still in use today [193], [376], but they are no longer on the market. At present, most electrometers use solid-state device entry stages of high resistance [317], [251], [250]. Keithley’s commercial electrometers provide current ranges down to 10^{-17} A. Some electrometer properties are explained briefly in Section 4.1.

Early reviews of low current-measuring systems can be found in [363], [309], in several editions of Kohlrausch ([261] and [260] and later), and in [236], [442], [154], [155], [357], [425] and [203]. These articles describe the principles of low-current measurements and list the precautions to be taken. More recent reviews by Weiss ([469], see p. 194), Zsdanszky ([491], see p. 195), Keithley ([247], see p. 180), Keithley et al. ([251], see p. 180), Böhm ([34], [37], see p. 167), Mann et al. ([294], see p. 183) and Keithley ([250], see p. 180) cover the equipment used in national standards laboratories. Very little has been published in the last ten years on the application of modern electronic circuits for low current measurements in standards laboratories, but interesting articles include [390], [441], [288], [397] and [56].

The accompanying techniques for current measurement, such as insulator applications, noise and leakage current reduction by guard-ring techniques, are described in [73], [14] and [336]. Techniques using special cables (triax type) as well as disturbing low-current phenomena (piezoelectric, space charge, electrochemical, switching charge effects, etc.) can be found in [471], [30], [251], [258] and [250].

4.1. Electrometer picoammeters

An electrometer picoammeter usually has an input resistance of more than $100\text{ T}\Omega$ ($10^{14}\Omega$) and / or, depending on the connected voltage, an instrument leakage current (including offset contribution) of less than a few times 10^{-15} A . These characteristics define a device that can measure extremely low currents, charges or voltages, the choice of any particular one depending on the way in which the feedback at the high-resistance entry stage is connected. Operational amplifier theory can be applied to explain the behaviour of various feedback types. A short summary is given in the next section.

To measure such low input currents, special care must be taken in the choice of insulating materials and in the cleanliness of the surfaces, and the path lengths on insulators should be long [251], [250]. The best material for use around the input point is sapphire, the next choice being teflon of high quality. For the capacitors, the models made from styroflex give good results, for example from Siemens ([410], see p. 190). The input stage must be electromagnetically shielded in a metallic Faraday box against electromagnetic stray fields, and an optimum grounding of the components must be performed by direct connections in the housing: ground loops must be avoided in the circuitry. Radiation shielding of the entrance stage is recommended because ionizing effects in insulating materials may result in an undesirable increase of the low conductance. For all these reasons high-quality instruments have the preamplifier entry stage in a specially designed independent housing.

Of the four classes of electrometers referred to, only the dynamic condenser electrometer or vibrating-reed electrometer (VRE), and the solid-state device electrometer are still of practical interest. Their working principles are quite different.

- **Vibrating-reed electrometers** have one plate of their entrance capacitor charged by the current to be measured. This plate (the reed) vibrates with a stable frequency, modulating the electrostatic field of the capacitor and producing an AC signal which is capacitively coupled to an indicator stage, usually a vacuum tube, and amplified (Figure 27, see p. 108). Sophisticated nullindication or feedback methods with phase shift and rectification are used to transform the AC signal into a measure of the charge at the entrance stage. Such systems and their parameters are described by Palevsky et al. ([330], see p. 185), Friedlander and Kennedy ([154], [155], see p. 174), Staub ([425], see p. 191), Fassbender ([149], see p. 174), Loevinger ([280], see p. 182), Frieseke and Hoepfner ([159], see p. 174), Cary ([66], see p. 169), Gühne and Rodloff ([191], see p. 176), Guiho et al. ([193], see p. 177) and Böhm ([34], see p. 167). Provided that the working conditions (frequency, amplification, etc.) are stable, the transformed signal, or a compensation signal, can be used and subsequently displayed by a voltage-measuring instrument [245]. The impedance of such a system lies in practice close to infinity and measurements are limited only by the resistivity of the construction materials used for the entry stage.
- **Solid-state electrometers** possess the high input resistance of highly purified material in the entry stage. Today, metal-oxide-silicon field effect transistor (MOSFET) stages

give the best results. A particular solid-state electrometer is characterized by the design of its entry stage and the stage in which the function and range adjustment occurs, it may display in analogue or digital form. In modern low-current-measuring systems, microcomputer-controlled digital electrometers are mainly used [248], [249], [250]. The entry stage of such an instrument is a high-resistance preamplifier with a MOSFET, a main amplifier with the range and function switching connected to an analogue-digital converter which in turn, is connected to a display and a standard interface (Figure 28, see p. 109), for example an IEEE-488 bus. All the components are surveyed or controlled by a microprocessor or small computer which may also serve as the interface between instrument and user.

The advantages of the MOSFET entry stage are [251]:

- good high-input impedance operating as a voltage amplifier,
- good low-current characteristics, down to several 10^{-17} A,
- good stability under normal working conditions,
- easy realisation of input protection circuitry,
- commercial availability.

Other entry stage circuits are realized with junction-field-effect transistors (JFET). A JFET generally has lower input resistance, lower voltage noise and offset, but higher input current offset and noise than a MOSFET. Recent electrometer-input circuits go down to offset currents as low as a few 10^{-15} A. Commercial Keithley instruments are practical realizations of such electrometers. Other industrial models are connected to instrument systems with ionization chambers for radiation protection and nuclear medicine (Section 3.2.4, see p. 25). A portable, “intelligent” electrometer for applications with ionization chambers in the field of radioprotection is presented by Halbig and Caine ([195], see p. 177). Another field of low-current measurements is that of dosimetry where many helpful suggestions relating to electrometer techniques can be found, for examples, see [34], [37] and [266]. A study of the quality of a current integrator for dosimetry measurements realized with a commercial Keithley instrument with digital filter techniques is described by Brose ([49], see p. 168).

The varactor bridge [251] which operates at a frequency of several hundred kilohertz works on quite a different principle. One of the capacitors in the bridge is a varactor diode, the capacitance of which changes if a DC voltage is applied to the bridge. This unbalances the bridge and creates an AC output signal which is proportional to the DC input being measured. Varactor bridge circuits are rarely used in electrometers as they:

- require extensive associated circuitry,
- take an excessive time to recover from overload,
- have high susceptibility to high frequency interferences,
- show high sensitivity to environmental changes or working conditions.

A comparison of various electrometer types with notes on the concepts required for the design of femtoampere circuits is given by Patstone ([336], see p. 186), together with some suggestions for guard ring configurations and the necessary specifications for resistors and capacitors for low-current applications.

For other electrometer components, like main amplifier, analogue-digital converter, etc., integrated electronic circuits or components of high quality, taken from modern standard data acquisition systems, are used [444].

4.2. Feedback circuits and current integrators

General amplifier theory distinguishes between current and voltage feedback [103], [291], [448] and shows that the choice depends on the quantity to which the feedback signal is proportional; in the latter case the feedback voltage may be connected in series or in parallel with the input signal. The parallel arrangement is commonly called an operational amplifier [103], but this term may be extended to any linear amplifier [448] used for metrological applications or in analogue computers [268]. Electrometer circuit design can easily be understood by applying basic amplifier theory [103], [280], [178], [448], and is relevant for the design of solid-state device electrometers.

In the general sense, an operational amplifier is an electronic circuit with a positive and a negative input having very high input resistances, low offset currents and a linear response. The output voltage is given by the difference between the input potential and earth, multiplied by an amplification factor which is typically of the order of 10^5 . To this circuit a feedback network is taken directly from the output, or from a voltage divider at the output, to one of the inputs (normally to that of negative polarity) via a resistor, a capacitor or a shunt (Figure 29-1-Figure 29-4 [491], see p. 195). In the latter case the active signal is fed into the input of opposite polarity (series feedback). To derive the relations between the input and output signals, Kirchhoff's laws are applied either to the sum of the currents in a connecting knot or to the voltages on a closed loop of the network.

Four such types of feedback circuit are described by Zsdanszky ([491], see p. 195) (Figure 29-1-Figure 29-4, see p. 111), and Mann et al. ([294], see p. 183). Praglin ([340], see p. 186) compares a number of electrometer constructions using electrometer tubes, vibrating reed and FETs in terms of noise, offset current and drift. More recent reviews from Keithley et al. ([251], see p. 180) and Keithley ([250], see p. 180) distinguish between the various circuits in terms of their applications, such as electrometer voltmeters, picoammeters and coulombmeters, but reach with equivalent formulae and parameters: see also [266]. Böhm ([34], [37], see p. 167) describes the dynamic behavior of an integrator circuit so as to include impedance and stray components. An equivalent-circuit diagram of the current integrator is shown in Figure 30. In modern applications with high accuracy requirements the feedback-type current integrator is used [280], [193], [38], [390]. The measurement system installed by Santry et al. ([390], see p. 189) corresponds to the working principle of a feedback coulombmeter, (Figure 28 [249], [251], see p. 180).

In the current integrator (or coulombmeter) a feedback capacitor C_F is charged, and the charge is integrated during the measuring time Δt [491]. As for any inverting amplifier, the current summing point is held at virtual ground level ($V_i = 0$) by the very high gain of the amplifier and its feedback network. This produces an output voltage V_o , Kirchhoff's law for the feedback loop leads to a relation for the input current I_i , i.e.

$$I_i = -C_F \Delta V_o / \Delta t, \quad (12)$$

where the current I_i should be constant. The sensitivity of such a device is determined by the capacitor C_F which gives an input capacitance $\alpha \cdot C_F$, where α is an amplification factor of

order 10^5 . In comparison with the capacitance C_F , the capacitances of the operational amplifier input and the connecting cables are negligible.

Sophisticated current-measuring systems register several output voltage values as a function of time to pick up the optimum working condition of the electronics. Assuming that the ionization current to be measured is nearly constant, this makes it possible to carry out a linearity check in each individual time interval during integration. An RC filter at the integrator input is recommended with a time constant of order 10^{-3} s to reduce instabilities from noise or hum at the entrance stage.

Practical conditions [251] for running the operational amplifier in this way are that

- the insulation resistances around the input are very high,
- the leakage currents during the time Δt are negligible,
- high quality capacitors are used, without residual charges retained by dielectric absorption during the time of shorting.

Such a current integrator (or coulombmeter) system may be controlled either by preset timing [307], [441] or by voltage level discrimination [491], [372], which can be chosen to suit different orders of ionization current values. Alternatively, range switching can be done by changing the capacitor C_F . Some authors [169], [491] describe current integrators with voltage discrimination where the discriminator generates a reset pulse that removes a fixed charge from the integrating capacitor: The number of pulses per time is proportional to the current to be measured. [169] report on currents of 10 pA measured by this method with an accuracy of 1%.

A similar method of charge sampling is described by Yair [489]. In this method the charge generated by a current source is collected on a capacitor during a fixed time interval in which the capacitor is isolated from the amplifier. Discharging the capacitor produces an AC pulse which is then amplified. Since a direct current is converted into an AC pulse, there is no requirement for DC feedback over the entire system and the need for high performance feedback resistors is eliminated. The output display is obtained either by a peak-value measurement of the amplified AC pulse, employing sample-and-hold techniques and direct meter indication, or by integration of the amplified output pulses connected to an analogue-digital converter with a digital indication. The method is claimed to give good noise reduction with AC currents of order 5 fA. The need for a special construction with a reed-relay to switch the input capacitor is a disadvantage. The system is considered to be reliable for photon measurements in exposure monitoring.

Similar systems are described by other authors [5], [385], but in most cases they are not particularly adapted for use in ionization current measurements for activity determinations with high accuracy.

4.3. Measurements by voltage drop across a high value resistor

Measurements of ionization current in terms of the voltage drop across a high value resistor have their origin in the method of constant instrument deflection [48], [290], [309], [236] in which the voltage drop is measured directly by an electrometer. A technical difficulty is the realization of high performance, “high-megohm” resistors of order 10^{10} Ω or higher with minimal size and mass. In earlier times, air resistors with ionizing radiation from radioactivity

were used [48]. Later on, these were replaced by liquid column resistors or thin layer resistors of platinum on amber [263]. Today, modern industrial constructions [457] of a carbon-coated glass rod with silver contacts are available, the resistors being vacuum-sealed in a glass envelope and surface-treated with a special silicon product to eliminate the effects of moisture. It is evident that any contamination, and especially fingerprints, must be avoided on such a device. Resistance values of $10^{12} \Omega$ to $10^{14} \Omega$ can be obtained with these techniques.

A technical realization of the voltage drop method with compensation was published by Jaeger ([235], see p. 179) and applied to ionization-current measurements in the range 10^{-9} A to 10^{-12} A in x-ray dosimetry. As a current source for the compensation, a Bronson resistance [48] is used, with ionizing radiation from a U_3O_8 layer inside an air capacitor running at saturation current. A compensation current, ranging from almost zero to $5 \cdot 10^{-10} \text{ A}$, is controlled by a variable diaphragm. Similar uranium cells have been used in compensation methods since the beginning of radioactivity measurements: see also the Townsend induction balance (Section 4.4, see p. 34).

A more recent current-measuring system is described by Walz and Weiss ([459], see p. 193) using the voltage-drop method with compensation on the other side of a resistor of $10^{10} \Omega$ to $10^{12} \Omega$ (Figure 31, see p. 112). The system is directly connected to the ionization chamber together with a null instrument of very high input resistance, for example a vibrating-reed electrometer (VRE); the other side of the resistor is connected to a variable, but highly stable, voltage source realized by an electronic compensator. The input voltage at the VRE is compensated up to a small residual voltage of less than 10 mV by means of a variable voltage divider of high accuracy (relative adjustment of 0.001%). This residual voltage shows fluctuations caused by the statistical processes of radioactive decay, current detection and electronic noise. To record and average the voltage values, a voltage-frequency converter is connected to the output of the VRE. The pulses generated are fed to a scaler and integrated over a preselected time (typically 100 s). The number of counts in the scaler divided by the integration time is a measure of the mean value of the residual voltage. The residual voltage, added to the voltage reading of the compensator, gives the total “voltage drop across the high-ohmic resistor”. The ionization current can be calculated from the known value of the calibrated resistor. With such a measuring system, however, the current equivalent of a ^{226}Ra reference source can also be measured, and a calibration in terms of equivalent activity can be carried out (Section 2.5, see p. 17). This avoids uncertainty components from the resistor calibration.

4.4. Townsend induction balances with compensation

A Townsend induction balance [450] uses a current-integrating capacitor similar to the coulombmeter with an external capacitor as described in Section 4.2. The current source, here the ionization chamber, is connected to one side of the capacitor and a compensation voltage source to the other side; the electric charges on the two sides are balanced. The control signal is taken from that side of the capacitor to which the ionization chamber is connected, using an instrument or electronic circuit of very high resistance or very low leakage current. Uncertainties from current losses must be minimized. The correct compensation voltage is adjusted by “feedback” from the control signal, either continuously or in steps, a process which is comparable with the feedback in a coulombmeter with an external capacitor. More generally, an induction balance can be defined as a device where the charges related to the measured current are balanced on both sides of a capacitor during the short time interval of

the control or “feedback” step. This permits the time behaviour of the control or feedback circuit to be described and takes into account the fact that the charges are not exactly balanced all the time.

Several types of compensation circuits have been constructed starting with Townsend ([450], see p. 193) (Figure 32, see p. 112), who studied the theory of “Genesis of Ions by the Motion of Positive Ions in a Gas”. Different components for the compensation (Figure 33-1-Figure 33-3, see p. 114) were used, among them a cylinder capacitor charged by manual control [44], variable capacitors (Figure 33-2 [200], see p. 177), supplementary current sources (Figure 33-3 [235], see p. 179), a second ionization chamber as current source [234], [252], [253] and a uranium source with a second collector electrode inside the chamber [428]. For further details of compensation-system components, see the articles in [263] and [30].

Many devices for ionization current measurements have used a stable capacitor in combination with different control loops [30]. Photocell compensators were developed by Jacobsen [234] using two coupled ionization chambers of opposite polarity, by Leo and Hübner ([276], see p. 182) and by Hübner ([221], [222], see p. 178) with an electrostatic electrometer (Figure 34, see p. 114), and by Rothe and Willuhn ([358], see p. 187) with a quadrant electrometer. These compensators are rather sensitive to deviations from the adjustment and to mechanical shocks. Lea ([274], see p. 182) obtained automatic balance by a direct coupling in which he charged up the highly insulated grid of the first valve of an amplifier, its output being fed to one plate of the condenser. A motor-driven potentiometer, controlled by a Lindemann-Ryerson electrometer, was designed by Garfinkel ([164], see p. 175) using stepwise compensation (Figure 35-1, see p. 115). Similarly, a vibrating-reed electrometer connected to a servomotor-driven compensation device worked almost continuously (Figure 35-2 [175], see p. 175). A null balancing circuit was described by Geiger and Campion ([167], see p. 175). Cloos and Heigwer ([71], see p. 169) proposed an automatic compensation instrument with an electronic control circuit for the induction balance.

In other designs developed in national standards institutes for activity measurements with ionization chambers, vibrating reed electrometers have usually been used to control the compensation. Vibrating-reed electrometers with compensation by relay switching at well-defined time intervals have been described by Merritt and Taylor ([307], see p. 184) (Figure 36-1-Figure 36-2, see p. 117), by Tapp ([441], see p. 192) and by Guiho et al. ([193], see p. 177). A vibrating-reed electrometer with compensation at a very stable voltage level and counting the compensation steps was used by Rytz ([372], [376], see p. 188) (Figure 37-2, see p. 119). A digital feedback circuit with a vibrating-reed electrometer, a voltage-frequency converter with a pulse counter, and a digital-analogue converter of good accuracy as a compensation voltage source was developed by Deike and Walz ([104], see p. 171) (Figure 38-1-Figure 38-2, see p. 120). A feedback circuit with fast, programmable analogue-digital and digital-analogue converters was described by Schrader ([397], see p. 189) (Figure 39-1-Figure 39-3, see p. 122); the information from the control signal at the capacitor input is digitized by an analogue-digital converter at well-defined time intervals. The digitized signal is introduced into a fast computer, permitting an optimum compensation voltage value to be calculated in less than a millisecond. This value is fed to the capacitor by a digital-analogue converter of high accuracy [444]. A timing diagram for the compensation process is shown in Figure 39-3.

Common to all the compensation circuits with a fixed capacity value C is the measurement of the change in voltage ΔU_c across the integrating capacitor (including the capacitance of the

ionization chamber itself, the cables, etc.)—or of a quantity proportional to ΔU_c —during a time interval Δt_m . This leads for the current to the formula

$$I = C\Delta U_c / \Delta t_m, \quad (13)$$

This equation looks very similar to that for a feedback-type current integrator at Equation (12).

All these compensation methods require stable capacitors, e.g. the styroflex capacitors manufactured by Siemens ([410], see p. 190). Another possibility is to construct a mechanical parallel plate capacitor [358], [350], [353] as used in national standards laboratories for calibration of capacitances [263]. A recent example of such a capacitor by Reher et al. ([353], see p. 187) is shown in Figure 40. The capacitors of a measuring system should be mounted in a special box to protect them from moisture and contamination (Figure 36-2, see p. 117), and like other preamplifier components, they also must be shielded against external electromagnetic fields and protected from radiation (Section 4.2, see p. 32). To connect the capacitors at the beginning and end of a measurement or to switch ranges reed relays mounted near the capacitor should be used [254], [422], [50], [441]. Precautions must be taken against stray fields and protection measures comparable with those for the entry stages of low-current devices are required.

An advantage of compensation methods, like the Townsend induction balance, is that the voltage level at the ionization chamber output is maintained near zero. This reduces leakage currents from the electronic components coupled to the ionization chamber output, so the offset and leakage currents of the control instrument remain small in comparison with the current to be measured. Furthermore, this method does not increase the voltage in the ionization chamber and so avoids changes in the field strength applied in the collection of charge.

5. Systematic effects in ionization-current measurements

Radiation interactions and charge collection in ionization chambers are dominated by statistical processes [147], [148] which are described more generally in Section 2.2. The operation of the current-measuring electronics connected to the chamber can be understood in terms of the general theory of integrating ratemeter electronics which was first described by Schiff and Evans ([392], see p. 189) for a charge-integrating device. An analogous expression derived for a counting experiment gives a standard deviation of $\sigma_N = N^{-1/2}$, where N is the number of counts measured by a radiation-detector counter chain. A standard deviation of the instrument reading of $\sigma = (2x \cdot RC)^{-1/2}$ was deduced, where x is the average (or expected) number of pulses received per time unit in the device and RC is the time constant of the integrating capacitor and discharging resistor. Similar descriptions or expressions for integrating devices can be found in Evans ([143], see p. 174), Maier-Leibnitz ([289], see p. 183), Weber ([464], see p. 194), Andresen ([7], see p. 165), Dörfel ([114], see p. 172) and Weise ([466], see p. 194). An ionization chamber with current measurement corresponds to the special case of a device having a very large time constant RC .

5.1. Fluctuations from ionization and charge collection

This section details particular features of charge collection studied by current measurements with re-entrant ionization chambers. Few publications are available on the subject, but measurements of a minimum standard deviation with an ionization chamber are reported by Garfinkel ([164], see p. 175), Merritt and Taylor ([307], see p. 184) and Weiss ([469], see p. 194) (Figure 41-1–Figure 41-4, see p. 124).

The first study of fluctuations in activity measurements with ionization chambers as a function of source activity A was reported by Garfinkel ([164], see p. 175). He measured the ionization currents produced by four radium sources, the activities A of which ranged from $3 \mu\text{Ci}$ to $200 \mu\text{Ci}$, repeating each measurement several times during individual time intervals of duration t . The standard deviation σ_I of the measured individual current values was calculated and plotted versus $(At)^{-1/2}$ or, assuming a proportionality between A and I , versus $(It)^{-1/2} = Q^{-1/2}$. This is analogous to plotting σ_N versus $N^{-1/2}$ for a counting experiment. In the experiment of Garfinkel the curve (Figure 41-1, see p. 123) takes the form of a straight line which may be extrapolated to $(At)^{-1/2} = 0$, i.e. to the condition for a source of very large activity, giving a limit in “ultimate precision” of about 0.02%. This value represents the uncertainty of the complete ionization-chamber measuring system. Garfinkel used an unsealed chamber which, therefore, was at atmospheric air pressure, and interpreted his value as due to fluctuations in the density of the air in the chamber.

A similar plot of measured relative standard deviation versus the total charge collected in a single measurement is reported by Merritt and Taylor ([307], see p. 184) (Figure 41-3, see p. 124). Since the data can be fitted with a straight line passing through the origin with a smallest relative standard deviation of 0.016%, they interpreted the value as arising predominantly from the statistical nature of radioactive decay rather than from instrumental effects. An argument was also given which relates the relative standard deviation to the photon energies of various radionuclides.

Weiss ([469], see p. 194) made repeated measurements of sources having different activities, and plotted the relative standard deviations s of the single measurements against $Q^{-1/2}$, where Q is the charge collected during the time of a single measurement (Figure 41-2, see p. 123) and is proportional to the At of Garfinkel. To a first approximation, s was assumed to be the sum of the internal standard deviation s_i of the measuring system and the standard deviation s_R of the radiation. By linear extrapolation of the plot to $Q^{-1/2} = 0$ a minimum value of s_i was found: this was close to zero. Weiss ([469], see p. 194) gives a value of 0.005%. Recent measurement results from the secondary standard measuring system of the PTB are given in Figure 41-4 with a minimum relative standard deviation near to 0.01%.

The total uncertainty of current measurements with ionization chambers is further discussed by Guiho et al. ([193], see p. 177). The values reported on the curves shown range from about 0.07% at 10^{-9} A to about 3% at 10^{-15} A and were obtained with a Townsend induction balance system (Section 4.4, see p. 34). The uncertainties of the electronic parameters of the current-measuring system are also discussed.

5.2. Variation of electronic parameters

Apart from the statistical fluctuations, systematic variations may be caused, for example, by drifts of temperature or long-term changes in the electronic components. To minimize these influences, cyclic measurements of background, reference source and unknown source should not take more than one hour. Data evaluation with calibration against a reference source is recommended (Section 2.5, see p. 17) because this eliminates the long-term instabilities which produce similar effects during measurements of the sample and the reference source, but may change over periods longer than one hour.

Other variations may be caused by unstable power supplies or by electromagnetic fields which disturb the entry stage of the current-measuring electronics. These are mostly short-term effects which may be detected by statistical analysis of a series of measurements, and if necessary, eliminated.

Special care must be taken to use a stable power supply for the polarizing voltage of the chamber. In older measuring systems, large accumulators connected in series to give a potential of several hundred volts were often used. Most of these have been replaced by electronic power supplies which provide low hum and low noise for the polarizing voltage of the ionization chamber. They are decoupled from the supply for the current-measuring electronics. This avoids disturbance of the very sensitive entry stage of the current-measuring electronics.

5.3. Saturation-loss effects

When the ionization-chamber current from a high-activity sample is measured, the effects of saturation losses caused by incomplete ion collection and recombination effects [214], [30], [31], [160], [76], [35] must be considered, see Figure 42 from Colmenares ([76], see p. 169). Much more intense radiation fields may be applied to cylindrical re-entrant ionization chambers before saturation losses become important than to the smaller plane-parallel plate chambers used for dosimetry applications, however, volume (general) recombination, initial recombination and diffusion losses during charge collection appear with the same

characteristics in both. According to Boag ([30], see p. 166), Böhm ([35], see p. 167) and others, only volume recombination varies with the radiation field. The charge-collection defect due to volume recombination, depends on I/U^2 , where I is the measured ionization current and U the collecting potential and occupies a certain region of an (I , U) diagram. Charge-collection defects due to initial recombination and diffusion loss depend on the reciprocal value $1/U$ of the collection potential. Measurements of these effects are mainly carried out on chambers for dosimetry applications [160], [223], [423], [30], [31], [35], [314].

Measurements of saturation-loss effects in a re-entrant cylindrical ionization chamber for activity determinations are described by Weiss ([469], see p. 194) (Figure 43-2, see p. 126). The saturation loss is obtained by measuring the ionization current I at increasing collecting potentials U for a source of several hundred MBq. By plotting the measured currents against $1/U$ a nearly straight line is obtained which, extrapolated to $1/U = 0$, yields the saturation current I_∞ . The saturation loss is defined as $(I_\infty - I)/I$, where I is the current measured with the collecting voltage applied usually. The diagram of Weiss (Figure 43-2, see p. 126) shows saturation loss as a function of the ionization current I . The values for a chamber filled with air at atmospheric pressure and normally operated at a collecting voltage of 400 V were determined by this method which, it should be noted, can be applied only if the effective chamber volume does not change with the collecting voltage. An alternative diagram is shown by Merritt and Taylor ([307], see p. 184) who plot the chamber response versus the operating voltage (Figure 43-1, see p. 125).

A similar method has been used at the PTB to observe the saturation effects in different ionization chambers: in this, the ionization current I is measured as a function of the collecting voltage U for several sources covering a range of at least fifty in units of activity (or current). The collecting voltage is varied by about a factor of three and a relative quantity, the ratio I/I_0 of the ionization current to the current at 500 V (at the commonly used voltage), is plotted as a function of the voltage U (Figure 44-1-Figure 44-2, see p. 127). Necessarily, the curves for all sources cross at the normalization point ($U = 500$ V). For a chamber with good saturation qualities, the diagram shows straight lines with nearly the same values at the measured points for all sources. The slope of the straight line is about 0.05% in relative current change for a potential change of 100 V (Figure 44-1, see p. 126), which is comparable with the result of Merritt and Taylor ([307], see p. 184) (Figure 43-2, see p. 126). For a chamber of low quality (Figure 44-2, see p. 127), the steepest slope was obtained at low collecting voltages (from 300 V to 400 V) about 0.5% relative current change for a potential change of 100 V using the strongest source (this had about 40 MBq of ^{226}Ra equivalent activity). This value changed by about 0.05% per 100 V for the weakest source of about 1 MBq of ^{226}Ra equivalent activity. The variation of the slope is used as an empirical criterion for the charge-collection quality of the chamber. Woods et al. ([482], see p. 195) give values of the saturation-loss characteristics for the radionuclide calibrator (Figure 45, see p. 127), developed at the NPL, with important saturation losses for currents only above 10^{-8} A.

5.4. Linearity in response to activity

Good linearity in the response of an ionization chamber as a function of the source activity is one of its most essential qualities since the required range of measured activity values may cover more than five orders of magnitude. The linearity of an ionization-chamber measuring system is influenced mainly by saturation effects and by the linearity of the current-measuring electronics. In the latter, one important non-linearity effect is range switching. Generally,

all the disturbing effects discussed in the preceding chapters may cause non-linearity in the activity response, but some may be eliminated by measurements relative to a reference source producing about the same ionization current as the sample to be measured. In this case, the activity ratios of the various reference sources must be known with good accuracy (Figure 10-1-Figure 10-2 [376], see p. 188).

Linearity checks are often discussed in the literature on radionuclide calibrator measurements for nuclear medicine applications [270], [238], [3], [390], [389], and in the related standards for radionuclide calibrators or in regulations [8], [10], [476], [110], [230], [231]. The procedures described for these linearity checks apply to any measuring system with an ionization chamber.

Instrument linearity should be checked by measuring the ionization current from the maximum activity likely to be used down to the minimum reading possible with the instrument, following the decay of a radioactive source. This defines the activity range for which the instrument is properly calibrated and allows correction factors to be deduced for the radionuclide under test. A suitable radionuclide for this purpose is $^{99}\text{Tc}^m$. The measured raw data are corrected for background and decay, applying the relevant half-life; $T_{1/2}(^{99}\text{Tc}^m) = 0.25025(8)$ d [220]. Examples for two different radionuclide calibrators are given in Figure 46-1-Figure 46-2, the first shows a continuous deterioration of linearity as the activity (or current) increases, and the second a sudden breakdown of linearity at a certain limiting level at high activity. From Equation (2) the activity values can be calculated as a function of measurement time and compared with the measured activity values. If the cause of a deviation can be explained and continuous measurements show reproducible effects, a correction factor can be deduced. In the case of electronic switching effects with adjustable electronic components, direct adjustment of the relevant electronics is preferable. After each adjustment a linearity check or a check against the reference source is required. A more sophisticated form of evaluation is to perform a linear regression analysis of the logarithm of the measurand as a function of time. This allows the residuals of the individual measuring points to be studied in detail and helps to show up trends (Figure 47-1-Figure 47-2, see p. 130). For example, decade switching of the time-measuring electronics exhibits a step function characteristic at the corresponding measurement value (Figure 47-2, see p. 130).

For high-quality instruments residuals of the order of 0.1% can be expected over an activity range of at least three orders of magnitude. At the extreme upper end of the range, the current value usually shows a continuous decrease relative to the activity because of saturation-loss effects. An abrupt cutoff of the current above a certain level may indicate a failure of the instrument electronics caused by subjecting particular components to excessive amplitudes or frequencies of signal. At the low activity end of the range, the statistics of the current-measuring process (see preceding section) increase the differences with respect to a linear curve (Figure 48-1-Figure 48-2, see p. 131). This effect may be superimposed on contributions from radionuclidic impurities with half-lives which differ from that of the radionuclide used as a check source. In the case of $^{99}\text{Tc}^m$, for example, contamination with ^{99}Mo ($T_{1/2} = 2.748$ d) may increase the current causing deviations from the expected values of the measurand in a logarithmic scale (Figure 48-1, see p. 131).

Regulations for radionuclide calibrators require that relative deviations from the calculated values be smaller than 5%. Today's instruments, if correctly adjusted, are quite capable of achieving this, as is confirmed by Bullen [55], Kowalsky et al. [270], Jain and Rehman [238], Woods et al. [482], Ahluwalia [3], NCRP [316], Santry et al. [390], Santry and Bowes [389].

An alternative to the decaying source method is a linearity check using a set of sources having known activity values covering the range of interest. The sources are prepared by dividing a single strong source into parts and measuring these successively, or by preparing different quantitative dilutions to give a set of sources with suitable activity values. For both procedures careful weighing is essential, and care must be taken to use the same measurement geometry (containers, volumes, etc.) for all measurements. These procedures introduce supplementary uncertainty components, which may be small, but are avoided when using the decaying source method.

6. Corrections to ionization-current values

6.1. Background

The background in ionization-chamber measurements, as in many other radiation measurements, is composed of radiation from

- materials of the chamber itself,
- radioactive gases inside the chamber well and nearby, such as radon and its daughters,
- materials around the chamber, such as sample holders, supports, shielding, any of which may experience unintentional contamination,
- natural radioactivity in the materials of the environment, such as the walls of the building and soil,
- external sources, especially near accelerators or reactors,
- cosmic-ray events, which produce secondary interactions in the earth's atmosphere.

Inside the ionization chambers the background is due mainly to ionizing events following photon emission, but a small fraction comes from α or β particles emitted from the chamber materials in such a way that they reach the sensitive chamber volume. The fundamental characteristics of background and shielding are described in publications on the background of low-level radioactivity measurement laboratories [188], [267], low-background Ge detector systems [61], [207], [13], [208], [209] and studies on environmental radioactivity with ionization chambers [404], [151], [171] including those on the background from decay products of radon [325], [334]. A typical background spectrum from a Ge detector is shown in Figure 49. All this can also be applied to the shielding of ionization-chamber measuring systems. For a general review of background and detector shielding, see [258], which contains a list and classification of the relevant radionuclides, for a discussion of effects arising in the detectors themselves: see also [316].

The radioactivity from materials commonly used in and around the chamber is due to low concentrations of naturally radioactive elements contained as impurities. Its components are radiation from potassium (^{40}K) and from the thorium- and the uranium-radium decay series [151], [258]. Other contaminating nuclides in materials are ^7Be and ^{22}Na , produced by cosmic-ray reactions, and fission products from nuclear weapons and reactor accident fallout, among them the well known ^{137}Cs (or ^{95}Zr and ^{144}Ce , with shorter half-lives than ^{137}Cs) which may be picked up during the material production process. Recently produced steel may also contain impurities of ^{60}Co , ^{103}Ru and ^{106}Ru from the furnaces. These radionuclides were frequently used in the 1950s to check for erosion of furnace liners in steel production. On the other hand, steel is a better construction material for the chamber than copper or brass because it has a low level of natural radioactivity, its origin being the thorium and uranium decay series [61]. Special care must be taken when aluminium is used as a construction material inside the chamber, as it is highly contaminated with decay products from the uranium and thorium series, and so releases α particles [16], [404].

If properly shielded, the background reading for a pressurized re-entrant ionization chamber is typically about 50 fA for a sensitive volume of order of 10 l. This is equivalent to a ^{226}Ra activity of about 1 kBq to 3 kBq for a modern pressurized ionization chamber. In the activity determination of a sample, the measured current I_m must always be corrected for background

current I_b , the pure sample current being $I = I_m - I_b$ (Section 2.4, see p. 16), both measured with the same instrument settings and under identical measuring conditions.

One of the most important background components arises from the presence of radon and its decay products inside the ionization chamber well, in the space around the chamber and from a deposit on the wall materials inside the shielding. This component shows seasonal fluctuations with maximum values, for the northern hemisphere, in the months June, July and August and a minimum in January and February. This follows the general fluctuation in the release of radon from the soil by diffusion. Short-term fluctuations are also possible. It is therefore recommended that background measurements be taken close to the time of the actual sample measurement. To reduce the radon background, the room containing the measuring system should be well ventilated, a consideration which is of particular importance for measuring rooms below ground or at basement level.

Proper shielding reduces the background from external sources by about one order of magnitude. The usual shielding consists of a “castle” or “house”, made of lead bricks of about 5 cm thickness, around the cylindrical volume of the chamber and at a distance of several centimeters from it (Figure 24-1–Figure 24-2, see p. 104). Also cylindric lead rings may be used. The optimum thickness of the lead shielding is from 5 cm to 10 cm, the lower limit being defined by the need to attenuate photons with energies of about 2 MeV, the upper limit by the increase of radioactive contamination and cosmic-ray reactions in the lead volume and the need to avoid unnecessary weight. To reduce radiation from contaminations, a good quality lead should be chosen, one, for example, having an activity concentration of less than 30 mBq of ^{210}Pb per gram of lead. The studies on lead for low-level measurement systems [267], [335] also apply to the shielding of ionization chambers.

For any shielding, the scattering of photons and x-ray fluorescence effects increase the observed current component above the value caused by the source in the well. Modification of the shielding may thus change the values of calibration factors; for a measurement system of good accuracy, the same shielding should remain permanently around the ionization chamber.

The electronic background from instrument noise, leakage and offset currents, and electromagnetic field disturbances is usually an order of magnitude lower than the background from unwanted radioactivity. The electronic background depends on the quality of the current-measuring electronics and the cable installations (Chapter 4, see p. 29).

6.2. Decay correction

When a radioactive source is put in an ionization chamber, the measurand determined by the chamber, normally the activity (or, proportional to it, the ionization current), decreases with time following Equation (2): $A = A(t) = A_0 e^{-\lambda \Delta t}$, with $\Delta t = t - t_0$. The activity A_0 is the activity at the reference time t_0 . The decay constant is $\lambda = \ln 2 / T_{1/2}$. The half-life $T_{1/2}$ of the radionuclide can be found in data files or tables [272], [316], [51], [394], [324].

In this context, the duration of the measurement is regarded as a point on the time scale, which is not true in practice. The ionization-current measurement takes, for example, a time of 100 s which may cause a systematic bias of more than 1% for radionuclides with half-lives shorter than a few hours. To calculate the necessary correction term, the decreasing current is averaged in time over the duration of one measurement (here 100 s). The exponential decrease of the current is regarded as a function of time which is integrated over the interval and referred to a well-defined reference time, usually the beginning of the individual measurement

interval. It is also possible to refer to the midpoint of the measurement interval, but this has the effect that, for times of measurement which are not constant because of the particular current-measurement technique used, the interval between successive times on the scale is variable. For this reason the beginning of the measurement interval is preferred. This leads to a correction term $C(t_d, T_{1/2})$ which is the ratio of the charge collected with constant current to the charge collected with an exponential decrease of current in the same measurement interval t_d and to the equation

$$\begin{aligned} C(t_d, T_{1/2}) &= t_d / \int \exp(-\lambda t) dt \\ &= \lambda t_d / \{1 - \exp(-\lambda t_d)\}, \end{aligned} \quad (14)$$

hence

$$I_{\text{corrected}} = I_{\text{measured}} C(t_d, T_{1/2}). \quad (15)$$

For example, for $^{99}\text{Tc}^m$ ($T_{1/2} = 0.250\ 25\text{ d}$) and a measurement interval of 300 s, thus for $t_d/T_{1/2} = 0.0139$, the correction factor is 1.00563, it necessarily refers to the start of the measurement, as defined. It is 1.000347 for a ratio $t_d/T_{1/2} = 0.001$. For smaller ratios, the correction is negligible.

6.3. Variations of sample dimensions and materials

Solution standards, prepared and measured in national standards laboratories, consist of a radioactive solution of given mass defined by careful weighing, dispensed in a glass ampoule of standard geometry and flame sealed. Various types of ampoules are used for calibration purposes [91], [472], [58], NIST SP 250e1989. For international comparisons the BIPM ampoule [372] or the NBS (NIST) ampoule [60], [409] filled with 3.6 g of radioactive solution, is used (Figure 50-1, see p. 132). These ampoules are similar, the BIPM ampoule being standard for measurements with the International Reference System (SIR) at the BIPM (Chapter 10, see p. 69). The characteristic dimensions of this ampoule are given in Table 2, together with the results of an investigation on the influence of variations in these dimensions.

It is important that laboratories work with ampoules which are as uniform as possible in geometry and material. For this reason, ampoules are normally made in batches of several thousand and are checked for possible variations in the dimensions. For the BIPM ampoule, the following variations have been observed: 1% in the side-wall thickness of the cylinder, a few percent in the bottom thickness and 0.7% in the inner diameter of the cylinder [372]. In other laboratories similar standard ampoules are in use with filling masses of 1 g to 5 g. When very small amounts of solution mass are used, the relative uncertainty of the activity measurement is rather large, due to the spread in weighing and the related filling correction applied to an ionization chamber reading. When large solution masses are used, some radionuclides may present problems of cost and availability. As a compromise, at the PTB, a standard ampoule of 15.2 mm outer cylinder diameter, 0.47 mm side wall thickness and a mass of radioactive solution of 2 g has been adopted.

For practical applications, such as the distribution of radiopharmaceuticals, ampoules and vials of many shapes, dimensions and filling volumes are available (Figure 51, see p. 134). These are usually made of glass, but plastic materials are also used. In principle, the vials used for radioactivity measurements conform to the standard IEC 583 ([228], see p. 179), with a first supplement IEC 583A ([229], see p. 179), but the dimensions chosen are too large

for ionization chamber measurements. A more recent standard for glass ampoules (Figure 50-2, see p. 133) is given in ISO 9187-1, and in the corresponding ISO standard with the same number and title, and this seems suitable for metrological purposes. Plastic vials in particular, but also glass vials with wall thicknesses exceeding 1 mm or having large variations of the thickness, are not suitable for radioactivity measurements of metrological quality. If an ampoule from a standards laboratory cannot be used for a measurement or calibration, a cylindrical injection vial (also called a dose or penicillin vial) can be used, for example the vial P6 (Figure 51, see p. 134) from the Amersham ([6], see p. 165) catalogue. This ampoule is made of glass, has a cylindrical shape with an outer diameter of (20.0 ± 0.25) mm, a height of (54.5 ± 0.5) mm and 10 ml nominal filling volume; it is a good choice for routine measurements in the quality control of radiopharmaceuticals or for measurements with radionuclide calibrators. For the production and distribution of radiopharmaceuticals, standardized ampoules are recommended.

For non-standard ampoules, a sample-geometry correction factor must be determined by relative measurements with respect to the standard calibration geometry. With glass thicknesses exceeding 2 mm and radionuclides emitting photons with energies above 100 keV, the corrections range from 2% to 5%. For low-energy photon emitters, like ^{125}I , ^{123}I or for radionuclides with high emission probabilities for the emission of γ or x rays with energies of around 30 keV, relative corrections as large as 25% are not unusual [95], especially if the measurement is carried out using plastic vials or radiopharmaceutical syringes [477], [59], [60].

It is important that calibrations and measurements use solutions of the same density. When carrier solutions are used for a dilution with concentrations below 50 μg salt per gram of solution and have low acid concentration, the density of the radioactive solution remains close to 1 g ml^{-1} . This corresponds to standard calibration conditions so additional correction factors for attenuation of the photon radiation are not required.

Larger variations of the relative ionization-chamber response can be expected for β -emitting radionuclides such as ^{32}P or ^{90}Sr . These depend on variations in ampoule-wall thickness or on the spread of other dimensions in the particular type of ampoule used [95], [478]. The difference in response observed with different ampoule-wall thicknesses and with different chamber-well materials must be explained in terms not only of a simple spread in absorption, but also of changes in the location of bremsstrahlung creation by the β particles in the well materials with respect to the sensitive detector gas. Studies of radiation absorption with sources of ^{32}P and ^{90}Sr in glass have been described by Dalmazzone and Guiho ([95], see p. 171), and of ^{32}P and ^{204}Tl in various materials such as Al, Cu, Sn and Pb by Dhaliwal et al. ([106], see p. 171).

The measurement of noble gases like ^{41}Ar , ^{85}Kr or ^{133}Xe in sealed glass ampoules presents a particular problem of geometry (see vial P1A in Figure 51, see p. 134). These ampoules have roughly the same shape and dimensions as flame-sealed ampoules for solutions, but the radioactive substance fills the total volume with a uniform activity concentration. Variations of dimensions such as ampoule height and, especially, the size of the sealed part, therefore result in changes in response. The calibration of ionization chambers for these radionuclides can be carried out by comparison with activity measurements using Ge detectors at larger source-to-detector distances. This minimizes geometric effects as shown by Merritt et al. ([306], see p. 184) who carried out measurements using a thin-walled aluminium well chamber of the T.P.A. Mk IV type which has a dominant response peak at low photon energies.

Another extreme geometric correction factor is that which applies when solid sources are measured in an ionization chamber. An early calculation of attenuation effects in cylindrical solid sources of high-Z materials, like radium or uranium, was carried out by Evans and Evans ([142], see p. 173). Other studies of correction factors can be found in the literature, among them, in the field of brachytherapy, factors for radionuclides like ^{125}I and ^{192}Ir measured in a radionuclide calibrator. When used in the form of seeds or wires both these radionuclide sources show strong photon-attenuation effects in the source material, either because the energies of the emitted photons are low or because the material has a high density and a high Z value. Some details of measurement techniques are given in the publications referred to below. In these either special ionization chambers were used [283], [170], [83] or radionuclide calibrators with specific calibration factors were applied [391], [488], [54], [453], [481].

6.4. Variation of the sample position

A fundamental requirement for good relative activity measurements using ionization chambers is good reproducibility of the position of the samples to be compared. This reproducibility should be better than 0.1 mm for repeated measurements. The effect of variation in the source position and other sample-geometry effects have been studied by many authors [292], [75], [210], [469], [372], [440], [386], [482], [27]. Diagrams with deviations of response are shown in Figure 52-1-Figure 52-3. The effects may be understood by detailed study of the isodose zones inside the chamber well (Figure 17-2, see p. 97). In most chamber constructions the radial dependence of source displacement in the chamber well is one order of magnitude greater than the vertical dependence. The effects of displacement also depend on the photon energies. This can be understood qualitatively by noting that the photons may irradiate different material structures if the source is displaced. The strongest effects are observed if the source is placed near the bottom or top of the chamber well. Normally, the source to be measured should be positioned in the centre of the well and on its central axis in a source holder of thin plastic material. The holder should be symmetric in form, with its head fitting snugly into the upper part of the chamber well. A change of about 0.3% in chamber response is observed for a radial displacement of 3 mm from the centre of the well when using photon energies of about 1 MeV from radionuclides such as ^{54}Mn or ^{60}Co . Position dependence in a spherical 4π ionization chamber has been studied in detail by Bucina et al. ([53], see p. 168) and formulae are given for this geometry.

A special two-detector method for comparisons of source strength (activity) was proposed by Valkonen and Kantele ([455], see p. 193), and realized for two ionization chambers by Greupner and Groche ([186], see p. 176). A relatively strong source is measured at a distance of about 1 m from two almost identical, horizontal, cylindrical ionization chambers. By combining the measurements of the two chambers, the errors caused by source displacements can be reduced considerably. The results obtained are in good agreement with theoretical calculations.

Displacement of the radioactive parts inside the source confinement must also be considered as an aspect of ampoule or source manipulation. First, some of the solution may stick in the neck of an ampoule as a result of uncontrolled movements, temperature changes and condensation, or surface tension in the narrow glass tube. Such displacements can be undone by centrifuging the ampoule after careful manipulation at a stable temperature. After this, the ampoule must be kept permanently in a vertical position. A check to verify the absence of plate out is also necessary [8], at least by observation. Critical chemical elements are those whose compounds

have very low solubility, such as Ba and Ag. Finally, the volatility of the radioelement in particular chemical states or its passage through a gas phase by decay (noble gases like Kr, Xe, Rn) may lead to displacements within the source confinement and thus to changes in the measurement geometry.

6.5. Filling correction for sources of varying solution volume

Radioactivity standards for ionization-chamber measurements are realized by a radioactive solution in a standard glass ampoule with a well-defined cylinder diameter: they thus have a given mass and a corresponding well-defined filling height. As explained in the preceding section, the chamber response depends on the distribution of radioactivity within the ampoule. In addition, the standard calibration geometry corresponds to a defined configuration of attenuating materials or attenuation lengths within the source. A correction factor must therefore be applied to the ionization current if the filling level differs from the adopted standard.

These effects have been studied by many authors [403], [95], [469], [372], [440], [482]. The filling correction curve is determined empirically either by stepwise addition of weighed amounts of an inactive carrier solution to a concentrated defined radioactive solution in an ampoule, or by carefully weighing and placing different amounts of solution, taken from a mother solution, in ampoules of the same type. In the first method, the activity in the ampoule is constant, but the measurements are performed stepwise and, as evaporation occurs when the ampoule is not sealed, this introduces some uncertainty. In the second method, all ampoules can be sealed immediately after filling and the measurements can be repeated in various independent cycles, but minor variations in the ampoule dimensions resulting from the manufacturing process must be considered. Experience shows that the second effect is negligible in high-quality standard ampoules with glass walls less than 0.5 mm thick if the ampoules come from a single manufacturing batch, as is done in national standards laboratories. In both methods the ratio of the ionization current to the measured mass is compared with that obtained for a standard mass. When plotted as a function of solution mass interpolation of these relative currents in the curve at a desired mass value allows a correction to be made (Figure 53-1–Figure 53-3, see p. 138).

The shape of the filling correction function depends on the energies of the photons emitted by the radionuclides in the solution to be measured. With high energy-photons, the relative current per mass decreases continuously with increasing mass. This behavior may change for photon emitters at energies below about 100 keV, such as ^{109}Cd (88 keV), ^{241}Am (59.5 keV), ^{210}Pb (46.5 keV) or ^{125}I (about 30 keV), see Figure 53-3 or in the publication of Dalmazzzone and Guiho ([95], see p. 171). The activity of these radionuclides is usually measured in ionization chambers with Al walls since these have a high response at these energies. The shape of the filling correction function depends strongly on mass for radionuclides which emit β particles with endpoint energies above about 1 MeV, like $^{106}\text{Ru/Rh}$, $^{144}\text{Ce/Pr}$, $^{90}\text{Sr/Y}$ or ^{32}P [95], [478], which are accompanied by bremsstrahlung photons.

6.6. Radionuclidic impurities

An ionization chamber with a current-measurement system for activity determination is an integrating device which, in principle, picks up all the ionizing radiation which enters its

sensitive volume. One single measurement, therefore, does not suffice to distinguish the radiations from the different radionuclides present in the sample. In a radioactive source all radionuclides, except the nominal one and its daughter nuclides, are regarded as impurities. It is obviously very important to check for radionuclidic impurities in a sample and to correct for the contribution of impurity components to the ionization current. Well-known candidates for radionuclidic impurities are ^{56}Co and ^{58}Co in ^{57}Co , ^{99}Mo in $^{99}\text{Tc}^m$, ^{124}I in ^{123}I , ^{126}I in ^{125}I , ^{154}Eu in ^{152}Eu or ^{200}Tl and ^{202}Tl in ^{201}Tl . For example, if a ^{57}Co source containing only 0.1% of ^{56}Co is measured in an ionization chamber and no correction applied, an error of about 1.5% in the nominal activity value of the ^{57}Co will result [240]. Fairly complete lists of probable or possible impurities in standard sources for about fifty radionuclides are given by Jedlovszky and Szörenyi ([240], see p. 179), Rytz ([375], see p. 188) and Dryak et al. ([119], see p. 172), with the 2nd revised edition of Dryak et al. ([119], see p. 172).

Radionuclidic impurities can be avoided, or at least minimized, during the production of a radionuclide source by choosing an optimal nuclear reaction with a pure target material. In spite of this, chemical purification is sometimes essential after the production. In any case, the contribution to the activity from the the radionuclidic impurities must be measured carefully. Any standard or certified source used in a metrology or quality assurance programme should be accompanied by certified values for the activities of its impurity components in addition to its nominal activity.

For photon-emitting radionuclides, the problem can be solved by supplementary measurements which yield the activity of each contributing radionuclide. These values are obtained using semiconductor detectors of high energy resolution, e.g. Ge detectors, to identify and to assess, in a quantitative manner, the radionuclidic impurities in terms of their photon energies and emission probabilities.

For pure β emitters, like ^{32}P with an admixture of ^{33}P , more sophisticated methods must be applied, such as discrimination in terms of half-life, which requires a series of measurements covering at least one half-life of the nominal radionuclide [399], or discriminator-ratio or detector-response ratio methods which depend on photon-energy filters (absorbers, liners). A practical example of the latter method is to check on ^{99}Mo breakthrough by an ionization-chamber measurement using a solution from a $^{99}\text{Tc}^m$ generator with and without a lead filter in the chamber. Various techniques to determine impurity corrections for applications to ionization-chamber measurements are described in the following sections.

Corrections for radionuclidic impurities always take the same form; only the known and unknown parameters vary. The activity of each radionuclide in the source contributes to the ionization current. The basic equation is derived by adding the current components $I_i = \varepsilon_i A_i$ (Section 2.4, see p. 16), that is, the components of the nominal radionuclide (index N) and the impurities (indices k). The radionuclide efficiencies ε_N and ε_k are the weighting factors of the activities A_N and A_k . More generally, the current components I_i can be replaced by any other quantity proportional to them and added in the sum. The measurand R in the formula Equation (16) may be the instrument output, the ionization current itself or any other quantity proportional to it, such as the relative current related to the current of a ^{226}Ra reference source or the direct reading of an adjusted instrument in terms of activity of a particular radionuclide. In any case, these quantities must be corrected for the corresponding background. If a more general definition than in Equation (3) is applied for the efficiencies ε_i , which enter in $R_i = \varepsilon_i A_i$, the relevant values of these efficiencies must also be used in the expression for the impurity correction. In the case that the efficiencies ε_i are replaced by the reciprocal equivalent activities

$1/A_{ei}$, the equivalent activities A_{ei} defined in Section 2.5 should not be confused with the radionuclide activities A_N or A_k . With the general definition of the efficiencies, the equation

$$\begin{aligned} R &= \varepsilon_N A_N + \sum_k \varepsilon_k A_k = \\ &= \varepsilon_N A_N \left(1 + \sum_k \frac{\varepsilon_k A_k}{\varepsilon_N A_N} \right) \end{aligned} \quad (16)$$

is obtained. The activities A_i ($i = N, k$) must be corrected for decay each with its own half-life every time R is measured. To calculate A_N from R , the values of A_k (or A_k/A_N) and the corresponding ε_i ($i = N, k$) must be known. An efficiency ε_i or a quantity proportional to it, such as $\varepsilon_N \sim 1/k_N$ (Section 7.1, see p. 53), is determined by direct calibration against an activity standard or by calculation from the energy-dependent photon-efficiency curve of the chamber (Section 7.6, see p. 59).

6.6.1. Corrections using activity ratios from semiconductor detector measurements

Test measurements for radionuclidic impurities are carried out using spectrometers with semiconductor detectors of high energy resolution for which the total-absorption-peak efficiency is known over an energy range of about 20 keV to 3000 keV. This range does not necessarily have to be covered by a single detector. If it is suspected that impurities with photons in the low-energy range between 15 keV and 60 keV are present, silicon detectors may be preferable to germanium detectors. Typical high energy resolution values for a Ge detector are about 0.8 keV at 122 keV (^{57}Co) and about 1.8 keV at 1332 keV (^{60}Co), and about 0.2 keV at 5.9 keV (^{55}Fe) for a silicon detector. If the detector can be chosen specifically for the impurity measurements, a medium volume (about 30% efficiency for Ge), but with optimum energy resolution, should be used to obtain the best selectivity between neighbouring total-absorption peaks. A state-of-the-art measurement should use a Ge spectrometer calibrated in the relevant source geometry which is, in most cases, the geometry of a radioactive solution source in an ampoule.

Measurement procedures for Ge detectors are described in detail in [316], [99], [294], [258]. A pulse-height spectrum is taken in a well-defined measurement geometry and in a measuring time adapted to the level of the impurity. A total-absorption-peak analysis is then carried out to determine the activities of the radionuclides. With a strong source the measuring time should be carefully chosen, with a view to minimizing the influence of pile-up in the Ge spectrometer and possible channel overflows in the data-storage device. On the other hand, impurities present in small quantities (low activity ratios) require fairly long measuring times. The problems of strong sources may be avoided either by choosing a large source-detector distance or by preparing special samples from solution drops, an approach which is useful provided the activity ratios are not changed by the physicochemical procedures. A compromise must be found for the measurement of the strong activities while still detecting components of low-activity level.

An example for a Ge spectrometer measurement of ^{201}Tl , with ^{200}Tl , ^{202}Tl , ^{201}Pb and ^{203}Pb impurities is shown in Figure 54. Numerical values for a typical ^{201}Tl measurement are given in Table 3, which is taken from the book by Debertin and Helmer ([99], Section 5.2.1, see p. 171). Even if an over-all count rate as high as 10^4 s^{-1} can be accepted in the spectrometer chain, the counting time has to be at least a few hours in order to detect radionuclidic impurities

at an activity level of 0.001%. It is favourable for the detection of an impurity if the main radionuclide emits only photons with energies well below those of the impurities. On the other hand, this condition leads to less favourable current ratios in the ionization-chamber measurements and may increase the uncertainty of the corrected measurement value. This is the case for ^{201}Tl , with impurities of ^{200}Tl and ^{202}Tl , or for ^{125}I , with ^{124}I or ^{126}I , where low levels of contamination lead to large corrections due to the unfavourable ratios of $\varepsilon_k/\varepsilon_N$. For any radionuclidic impurity with a half-life longer than that of the main radionuclide, the detection sensitivity can be optimized by delaying the measurement by a few times the half-life of the main nuclide to increase the corresponding activity ratio A_k/A_N . If impurities with different half-lives are present, repeated measurements with delays corresponding to the relevant half-life values are required.

Once the activity ratios are measured and the corresponding efficiency ratios determined, the result of an ionization chamber measurement (measurand R) is corrected applying Equation (16), with the activity ratio calculated for each individual time t_m of the measurement, thus

$$R_{\text{corrected}} = R(t_m) / \left\{ 1 + \sum_k (\varepsilon_k / \varepsilon_N) A_k(t_m) / A_N(t_m) \right\}. \quad (17)$$

Numerical values for measurements with a typical ionization chamber are exemplified for a solution of ^{201}Tl with impurities ^{200}Tl , ^{202}Tl , ^{201}Pb and ^{203}Pb in Table 4. The corrections were calculated using a small computer program, with the half-lives and the efficiencies taken from permanent files.

6.6.2. Correction methods for radionuclide admixtures making use of the different half-lives

The activity of a particular radionuclide in a solution, in the presence of one or a few radionuclidic impurities, can be derived from repeated measurements at appropriate intervals with a detector, such as an ionization chamber, which has no energy discrimination. The method is described by Walz ([460], see p. 194), Johnston et al. ([241], see p. 180) and Schrader and Walz ([399], see p. 190). Applying the equation given above to a radionuclide N with a single impurity ($k=1$), the value of the time-dependent measurand $R(t)$ is the sum of two components,

$$R(t) = \varepsilon_N A_N(t_0) \exp\{-\lambda_N(t-t_0)\} + \varepsilon_k A_k(t_0) \exp\{-\lambda_k(t-t_0)\}, \quad (18)$$

where λ_N and λ_k are the decay constants ($\lambda = \ln 2/T_{1/2}$) of the nuclides and t_0 is an arbitrary, but fixed reference time. From this equation we obtain:

$$R(t) \exp\{\lambda_N(t-t_0)\} = \varepsilon_N A_N(t_0) + \varepsilon_k A_k(t_0) \exp\{(\lambda_N - \lambda_k)(t-t_0)\}. \quad (19)$$

This yields a linear equation of the form

$$y = y_0 + mx = y_0 (1 + (m/y_0)x), \quad (20)$$

with the two unknown terms

$$y_0 = \varepsilon_N A_N(t_0) \quad (21)$$

and

$$m = \varepsilon_k A_k(t_0), \quad (22)$$

and the terms to be calculated from the measured data and well-known decay constants are

$$y = R(t) \exp\{\lambda N(t - t_0)\} \quad (23)$$

and

$$x = \exp\{(\lambda_N - \lambda_k)(t - t_0)\}. \quad (24)$$

The ratio r of the activities, similar to Equation (17), is at the reference time

$$r = A_k/A_N = (\varepsilon_N/\varepsilon_k) (m/y_o). \quad (25)$$

If more than two measurements are performed at appropriate time intervals, the data can be evaluated by a linear regression analysis (Figure 55-1-Figure 55-2 [399], see p. 190). If systematic deviations from linearity are observed, further impurities with different half-lives should be suspected and must be analyzed. An extension of the method to more than one impurity is possible if the values of the decay constants are sufficiently different. Several terms of the type $m_k x_k(t) = \varepsilon_k A_k \exp\{(\lambda_N - \lambda_k)(t - t_0)\}$ for the impurities $k = 1, 2, \dots$ are included in $R(t)$, and Equation (20) has to be extended to

$$\begin{aligned} y &= y_o + m_1 x_1 + m_2 x_2 + \dots \\ &= y_o (1 + (m_1/y_o)x_1 + (m_2/y_o)x_2 + \dots) \end{aligned} \quad (26)$$

This equation can be solved easily if one impurity component (index i) dominates in a certain region of y . The parameter m_i is determined in this region, neglecting the other components, and the value of $m_i x_i$ is then subtracted from y . Thus, choosing appropriate regions of y with sufficient linearity for one impurity, all the other impurity components may be eliminated successively. If the components overlap in a region, iterations of the procedure may be necessary. An example of this is the successive determination of the impurities ^{202}Tl and ^{200}Tl in a ^{201}Tl source (Figure 55-2 [399], see p. 190). If the parameters ε_k and λ_k are well known, and a routine production process provides a radionuclide mixture which varies over a modest range of values, it is sufficient to measure a few data points that are properly positioned on the time scale to determine the activities of the mixture. Nevertheless, this method has the disadvantage that the total measurement time needed is roughly the half-life of the dominant radionuclide component, and this is usually that of the main nuclide. The method is therefore applied only in those cases where direct Ge detector measurements are not possible, for example, for radionuclides emitting β particles only.

6.6.3. Attenuation methods for radionuclidic impurity corrections

Another way of evaluating the current sum relation given in Equation (16) is to modify the ratios of the efficiencies $\varepsilon_k/\varepsilon_N$. This is done by inserting appropriate filters (liners, absorbers) into the chamber well around the source, a technique commonly used in an early stage of radioactivity measurements [41]. The analysis of the measurements is based on differences in transmission of the filters at different photon energies. The main radionuclide, and the radionuclidic impurities, must emit photons of different energies so that they modify the corresponding current components when the filters are put into the chamber well. The basic equation is then applied to each source-filter combination and yields a system of linear equations, with the efficiencies ε_i as coefficients and the activities as unknown parameters. This method works for simple mixtures of radionuclides if the components are known and if only a fairly quick and simple measurement is required to serve as a rough check of the amount of impurity. Mixtures having fairly large differences of emitted photon energy are

^{57}Co with ^{56}Co , ^{125}I with ^{124}I and ^{126}I or, very often used for a check of the Mo breakthrough in Tc generators [354], $^{99}\text{Tc}^m$ with ^{99}Mo .

The following simple example serves as an explanation of the measuring method. The nuclide $^{99}\text{Tc}^m$ emits photons with an energy of 140 keV, the photon flux of which can be considerably reduced by a lead filter about 5 mm thick. The nuclide ^{99}Mo emits photons with energies of the order of 750 keV, but only a small part of the flux is absorbed by the lead filter. In this case, measurements can be carried out in a few minutes without and with filter, so making corrections for the decay of the radionuclides negligible. The measurements are interpreted using two equations:

$$R = \varepsilon_{\text{Tc}} A_{\text{Tc}} + \varepsilon_{\text{Mo}} A_{\text{Mo}} \quad (27)$$

$$R_f = \varepsilon_{\text{Tc},f} A_{\text{Tc}} + \varepsilon_{\text{Mo},f} A_{\text{Mo}} \quad (28)$$

where f stands for filter.

When an ionization chamber with an aluminium well is used, typical values for the efficiency ratios of $^{99}\text{Tc}^m$ and ^{99}Mo are:

$$\varepsilon_{\text{Mo}}/\varepsilon_{\text{Tc}} = 0.63 ; \varepsilon_{\text{Tc},f}/\varepsilon_{\text{Tc}} = 1.5 \cdot 10^{-6} \text{ and } \varepsilon_{\text{Mo},f}/\varepsilon_{\text{Tc}} = 0.27.$$

Assuming that the background of the ionization chamber is known in terms of $^{99}\text{Tc}^m$ activity and has a value of about 4.5 kBq, the corresponding background value can be calculated in terms of the ^{99}Mo activity producing the same current in the ionization chamber with a filter, by using the value of the efficiency ratio $\varepsilon_{\text{Mo},f}/\varepsilon_{\text{Tc}}$. This results in a background reading of $4.5 \text{ kBq} \cdot \varepsilon_{\text{Tc}}/\varepsilon_{\text{Mo},f} = 4.5 \text{ kBq}/0.27 = 16.5 \text{ kBq}$ of ^{99}Mo . The data can be interpreted in such a way that, with this background level and an impurity limit of 0.1% of ^{99}Mo in $^{99}\text{Tc}^m$, as often required by regulations [109], $^{99}\text{Tc}^m$ solutions with activities above 16.5 MBq from a Tc generator can be checked for Mo breakthrough by the ionization-chamber filter system.

7. Calibration of re-entrant ionization chambers

7.1. Calibration factors for particular radionuclides

The term calibration refers to the relative (or indirect) measurement of a physical quantity [294], here the “activity”, in comparison with a standard that embodies this quantity, here an international or national “activity standard” or field standard, this last being traceable to the first ones. In our case, the comparison is made by a current measurement in an ionization chamber that represents, in a standards laboratory, a secondary standard measuring system to maintain the results of activity measurements from primary standardization. More generally, a re-entrant ionization chamber can be calibrated in terms of activity by comparison with an appropriate activity standard. For this type of measurement a calibration factor of the ionization chamber must be determined for the radionuclide of interest (see Section 2.4 and Section 2.5, see p. 17). The reciprocal of this calibration factor represents an efficiency of the ionization chamber for the particular radionuclide: $k_N = 1/\varepsilon_N$, with ε_N defined in Equation (3), or alternatively $k_{N'} = 1/\varepsilon_{N',\text{rel}}$, for a quantity which is proportional to the ionization current.

In fact, calibration is the key to any activity determination using an ionization-chamber measuring system. Nearly all the preceding chapters deal with procedures, questions and problems related to calibration. The calibration factors, for a particular radionuclide in a well-defined measurement geometry, are the essential parameters of the measuring system. Fairly complete tables or files of calibration factors have been developed in national standards or calibration laboratories by Engelmann ([134], see p. 173), Dale and Williams ([92], see p. 170), Dalmazzone ([93], see p. 170), Williams and Birdseye ([472], see p. 194), Goodier et al. ([174], see p. 175), Woods ([475], see p. 194), Lewis et al. ([278], see p. 182), Woods et al. ([483], see p. 195), Woods and Lucas ([484], see p. 195), Merritt and Gibson ([303], see p. 183), Dias ([107], see p. 171), Merritt and Gibson ([305], see p. 184), Kobayashi and Ishikawa ([259], see p. 181), Broda ([46], see p. 167), Szörényi and Zsinka ([437], see p. 192), Coursey et al. ([80], see p. 169), Woods et al. ([482], see p. 195), Szörényi et al. ([438], see p. 192), NIST (NIST SP 250e1989, see p. 185) and Vinten (now NE Technology ([319], see p. 184)). These values are frequently compared with the results of direct activity measurements, thereby maintaining the unit of activity over long time periods. After a measurement in a secondary-standard measuring system, such as a calibrated ionization chamber, the unit of activity is distributed to manufacturers and users of ionization-chamber measuring systems, for example, in the field of nuclear medicine. This can be done either by distributing suitable standards of activity for instrument calibrations, or by a rigorous quality-control programme for a particular type of instrument to which a file of published calibration factors, measured in a standards laboratory, is related. In both cases, the file of correctly determined calibration factors is the basis for all activity assays.

Sometimes a simulated standard, also called a mock standard, is used to estimate calibration figures. Such a standard is a radioactive source prepared from a long-lived radionuclide that approximates the radiation characteristics of the radionuclide to be simulated. A typical radionuclide simulation is $^{99}\text{Tc}^m$ by ^{57}Co or ^{139}Ce , but it is not recommended for realistic calibration of an ionization chamber [303], [22], [316]. Mock standards may serve as reference sources, but they should not be used for calibrations of other radionuclides, because the factors used do not usually take account of the energy-dependent photon-efficiency of the instrument and the emission probabilities per decay of the radionuclides under consideration.

Another way of determining the calibration factor of an ionization chamber for $^{99}\text{Tc}^m$ is described by Broda ([46], see p. 167). He measured activity ratios in the mother-daughter decay of the nuclides ^{99}Mo and $^{99}\text{Tc}^m$ by spectrometric and direct counting methods and used decay parameters to calculate a calibration factor. The method is a variation of that in which calibration factors are computed from energy-dependent efficiency curves and emission probabilities per decay (Section 7.6, see p. 59). It uses the balance condition to estimate the ratios of activities in a decay chain.

7.2. Efficiency as a function of photon energy

In an ionization chamber the current components from particular photons emitted in the decay of a radionuclide are detected and collected independently and their sum is the total ionization current measured. The nuclide efficiency ε_N can be expressed as the sum of these components (index i), i.e.

$$\varepsilon_N = \sum_i p_i(E_i) \varepsilon_i(E_i), \quad (29)$$

with $p_i(E_i)$ the emission probability per decay of photons of energy E_i , and $\varepsilon_i(E_i)$ the energy-dependent photon efficiency of the ionization chamber. Such an expression also applies to quantities which are proportional to the photon efficiencies $\varepsilon_i(E_i)$ and the related nuclide efficiency ε_N , such as the energy-dependent reciprocal photon-equivalent activities $1/A_{ei}(E_i)$ and the reciprocal equivalent activity $1/A_e$. Rytz ([376], see p. 188) preferred, for practical reasons, to write the equations for the SIR in terms of $10^6/A_e$.

Measurements undertaken with a view to establishing the energy-dependent efficiency curve should start by using radionuclides that emit practically monoenergetic photons in a region where the curve is nearly linear (Figure 57, see p. 142), for example at 835 keV (^{54}Mn) to 1253 keV (^{60}Co). The latter, emitting photons of two distinct energies (1173 keV and 1333 keV) in the linear region, can be considered as practically monoenergetic if the mean energy of the photons and the sum of their emission probabilities per decay are calculated. In further steps, radionuclides with more complex decay schemes can be used if the photons emitted have energies in the range of the efficiency curve already established with the exception of the one photon energy E_k for which $\varepsilon_k(E_k)$ should be calculated. Efficiency values for all the further photons can be interpolated, multiplied by the corresponding emission probability, and subtracted from the measured radionuclide efficiency ε_N . The difference represents the unknown component $p_k(E_k)\varepsilon_k(E_k)$. A list of calibration nuclides for the establishment of the energy-dependent efficiency curve is given in Table 5.

Thin-wall aluminium (Al) chambers show a strong peak in the efficiency at photon energies around 50 keV. This results from the rapid increase of the interaction cross section of the photoelectric effect in the sensitive chamber materials (mainly the filling gas) with decreasing energies, and the low energy cutoff with Al walls at about 20 keV. For iron (Fe) walls a similar cutoff occurs at about 40 keV. To establish the energy-dependent efficiency curve of an ionization chamber with aluminium walls, it is particularly useful to measure sources of relevant radionuclides both with and without a low-Z-material filter (liner). For an Fe liner, a thickness of 1 mm will suffice. The energy-dependent efficiency curve of an instrument fitted with such a liner is considerably displaced towards lower efficiency values at low photon energies. Current components from photons having energies below about 35 keV

vanish almost completely while components from photons having energies higher than about 150 keV are only slightly altered by the liner. From the difference of the results of these two measurements several efficiency points in the low-energy region can be deduced. This method was described by Schrader and Weiss ([401], see p. 190) in the case of a radionuclide calibrator with 3 mm thick aluminium walls and a 1 mm thick Fe liner (Figure 58-1-Figure 58-2, see p. 143). The fractional radionuclide calibrator response can also be derived using a copper filter and the properties of characteristic x rays. This is discussed by Dubuque et al. ([123], see p. 172) for the radionuclides ^{123}I and ^{129}Cs and by Harris et al. ([198], see p. 177) for ^{123}I .

The energy-dependent efficiency curve of an ionization chamber with Fe walls is similar in shape to that for a chamber with Al walls and an Fe liner with about the same wall thickness as the Fe wall chamber, see Figure 57 and Figure 59.

Several authors have published energy-dependent efficiency curves for different ionization chamber constructions; Mann and Seliger ([295], see p. 183) (Figure 60-1-Figure 60-2, see p. 145), Weiss ([468], see p. 194), Dale ([90], see p. 170) (Figure 61-1-Figure 61-2, see p. 146), Kohlrausch ([265], see p. 181), Oncescu and Rebigan ([327], see p. 185), Bensch and Ledermann ([21], see p. 166), Weiss ([469], see p. 194), Dubuque et al. ([123], see p. 172), Suzuki et al. ([431], see p. 192) (Figure 62, see p. 147), Merritt et al. ([306], see p. 184), Rytz ([376], see p. 188) (Figure 63-1, see p. 147), Rytz and Müller ([380], see p. 188), Dias ([108], see p. 171), Schrader and Weiss ([401], see p. 190) (Figure 58-1-Figure 58-2, see p. 143) and Blanchis ([27], see p. 166). Apart from a proportionality factor in the definition of the calibration (see above), the main differences in the values of the efficiency curves quoted result from differences in the attenuating materials between the source and the sensitive chamber gas, among them variations in the density and geometry of the radioactive solutions, the materials of the ampoules or confinements, the chamber walls inside the well, and the chamber electrodes. Details are given in Section 7.5.

A further parameter influencing the efficiency is the sensitivity of the filling gas. The efficiency curve of a chamber filled with argon at a pressure of 2 MPa is steeper, as a function of energy, than that of a chamber filled with nitrogen at the same pressure. On the other hand, the latter is more nearly a linear function of energy.

That the efficiency is strongly affected by the choice of material for the wall of the well has already been noted (Figure 58-1-Figure 58-2, see p. 143). Another important consideration is the geometry of the electrodes. Constructions with a single cylindrical tube for each electrode (high-voltage and collector electrode) should be distinguished from designs with multiple tubes, one inside the other, with varying electric potentials. With this construction the photon flux caused by the increase of total volume of attenuating materials inside the chamber is reduced, but secondary-electron production in the sensitive chamber gas is increased by the materials, as is the quality of the electron collection if the geometry of the electric fields is optimized.

7.3. Efficiency of detection of bremsstrahlung from β -particle emitters

Many radionuclides of interest for ionization-chamber measurements decay by the emission of β particles (electrons or positrons). By such a decay, excited states of the daughter nucleus (with one nuclear charge less or more) are populated, and they de-excite by electromagnetic

radiation, such as photon emission. However, some of the β -particle emitters decay directly to the ground state of a nucleus without photon emission. The consequent deceleration of the β particles by Coulomb interactions in matter is accompanied by the emission of bremsstrahlung photons with a continuous energy distribution. A β spectrum has a distribution function (shape) below its end-point energy E_0 that depends on the selection rules applicable to the β decay from the parent to the daughter nuclear states described by the spins, parities, etc. A short description can be found in the book of Evans ([143], see p. 174). An average β -particle energy can be calculated from this distribution. The complete energy spectrum of the bremsstrahlung photons emitted consists of the individual photon distribution folded with the shape of the β spectrum, and is limited by the maximum β end-point energy. In the energy region of interest for ionization chamber measurements, the bremsstrahlung photon spectrum is roughly the same shape as the β -particle energy distribution. The average β -particle energy is therefore a good parameter with which to characterize the ionization-chamber response to bremsstrahlung photons from β decay. The order of magnitude of the β -particle response may be characterized and estimated, because the probability of the Coulomb interaction creating the bremsstrahlung can be expected to be about three orders of magnitude smaller than the probability of the β -particle emission, and the response to the bremsstrahlung is fixed, in turn, by the photon efficiency of the ionization chamber used (Section 7.2, see p. 54).

An ionization chamber can be calibrated using sufficiently strong activity standards of pure β -particle emitting radionuclides like ^{90}Y (the daughter of ^{90}Sr) or ^{32}P [295], [134], [93], [384], [27], [478]. Other radionuclides, such as ^{106}Rh or ^{144}Pr (the daughters of ^{106}Ru or ^{144}Ce), decay by β -particle emission, the spectrum having a very high β -endpoint energy followed by the emission of photons from excited nuclear states. When the components of photon emission from the disintegration of excited states and the total radionuclide efficiency are known, a bremsstrahlung photon efficiency can be deduced by subtraction (Section 7.2, see p. 54). For these radionuclides a comparatively high bremsstrahlung-photon efficiency component results. In ionization chambers with an aluminium well only a few millimeters thick, the high β -energy emitters (E_0 above 2 MeV) may also produce small ionization current components from direct interactions of the β particles with the sensitive chamber gas and the wall materials.

In the way outlined above a list of calibration factors for β particle emitting radionuclides can be established in a range of average β -particle energies from about 60 keV to 1410 keV with the following radionuclides (with daughters): ^{35}S , ^{147}Pm , ^{204}Tl , ^{85}Kr , ^{210}Pb (^{210}Bi), ^{140}Ba (^{140}La), ^{89}Sr , ^{91}Y , ^{32}P , ^{90}Sr (^{90}Y), ^{144}Ce (^{144}Pr) and ^{106}Ru (^{106}Rh). At low energies a cutoff of the response occurs, its position depending on the entrance window of the chamber. A typical example of efficiency values for an ionization chamber (Centronic-IG12) is given in Figure 56-1-Figure 56-2 [69]. Few β -efficiency curves for $4\pi\gamma$ -ionization chambers and few detailed calibration factors for β -particle emitters have been published. It is evident that account must be taken of the bremsstrahlung component from a β -particle emitter with a high average β -particle energy in detailed calculations of the radionuclide efficiency for energy-dependent efficiency curves (Section 7.6, see p. 59).

7.4. Representation and fitting of efficiency functions

In many measurement systems, the values of the photon efficiency, determined by experimental methods as described in Section 7.2, increase almost linearly with energy E . Efficiency curves, therefore, used to be plotted in a reduced form (Figure 63-1 [376], [380] and Figure 64-1-Figure 64-2 [470], see p. 194). A linear function ($\varepsilon_0 = a + bE$) which gives

a good approximation to the experimental values in the range of interest is chosen and the ratio $f = \varepsilon/\varepsilon_0$ is plotted versus the photon energy E . The function of these plots was to allow easy interpolation of sufficient accuracy by reading directly from the diagram. Nowadays, these methods have been replaced by computer techniques which store the experimental values in a file and apply interpolation routines to calculate efficiency values at energies intermediate between the points of direct calibration. The difficulty of such calculations is to choose the best analytical function to be fitted to the experimental values. This is especially true in those energy regions where no or only few calibration values are available, for example in the energy range from 1332 keV (^{60}Co) to 1836 keV (^{88}Y).

One of the simplest ways to solve the problem is to plot the values on a large scale and to draw a smooth curve by eye through the calibration points [376], [380]. This method can be computerized using a polygon to represent the calibration points with linear interpolation between the points adding, if necessary, supplementary points, fitted by eye, to the polygon to improve the smooth interpolation of the curve (Figure 57, see p. 142).

A polynomial of the n^{th} order of the energy E is another useful representation of an efficiency curve. Thus Bensch and Ledermann ([21], see p. 166) proposed an equation with terms which were quadratic in the energy. Dryak and Dvorak ([122], see p. 172) used a higher-order polynomial, and a cubic-spline function was tested by Janszen ([239], see p. 179). Once determined, all these functions must be checked for consistency by efficiency calculations for radionuclides, such as ^{134}Cs or ^{152}Eu , which have several photon energies covering large regions of the curve, applying Equation (29) of Section 7.2.

Experimental efficiency measurements and consistency calculations have been published by Schrader and Weiss ([400], [395], see p. 189), Rytz ([376], see p. 188), Dryak and Dvorak ([122], see p. 172) and Reher and Sibbens ([352], see p. 187). Some of these results are given in Table 5 from Schrader and Weiss ([401], see p. 190) and Table 6 from Dryak and Dvorak ([122], see p. 172). The deviations of experimental calibration points from the curve of the International Reference System are plotted in Figure 63-1 [376].

The relative deviations from such curves are in the best cases a few parts per thousand and in critical cases as large as 3%. The origin of these deviations may be the form of the curve, but in some cases they may indicate an error in the direct calibration of a particular radionuclide, or at least a large uncertainty in the emission probabilities used in the calculations. Critical points to be checked are energy regions with two or several neighbouring photon energies from different radionuclides, such as ^{22}Na (511 keV) and ^{85}Sr (514 keV), ^{58}Co (810 keV) and ^{54}Mn (835 keV), and ^{59}Fe (1099 keV) and ^{46}Sc (1121 keV).

7.5. Calculation of efficiency values from fundamental quantities of the interaction processes

In several publications by Droste ([118], see p. 172), Bradt et al. ([43], see p. 167), Sinclair ([413], see p. 190), Staub ([425], see p. 191), Dale ([90], see p. 170), Oncescu and Rebigan ([327], see p. 185), Kleeven ([255], see p. 180) and Kleeven and Wijnhoven ([256], see p. 181) attempts have been made to explain the shape of an efficiency curve for ionizing detectors (including gas counters) by calculations involving the fundamental quantities of the interaction processes, like the cross section for the photoelectric effect, the Compton effect and pair production (Figure 65-1-Figure 65-2, see p. 151).

In the early days of the development of ionization chambers and gas counters attempts were made to estimate the number of electrons collected in terms of their range, and in terms of the variation with photon energy, taking into account the interactions in the detector walls, such as photon absorption, Compton scattering and electron pair production [118], [43]. Bradt et al. ([43], see p. 167) also studied the influence of various electrode materials, among them lead, aluminium and brass (Figure 65-2, see p. 151).

Another way of approaching the problem of the energy dependence of photon efficiencies and the calculation of radionuclide efficiencies from curves came from their use in dosimetry. An early study of the dependence of ionization currents on photon energy, using filtered x rays, was made by Behnken ([20], see p. 166) who found that the response of an ionization chamber increased linearly with the accelerating potential of the x-ray tube. Further literature from that period can also be found in his publication. It was later noted by Gray ([183], see p. 176), Dale ([90], see p. 170), Oncescu and Rebigan ([327], see p. 185), Bensch and Ledermann ([21], see p. 166) that the variation in response is fairly well related to the “k-value” or specific γ -ray emission constant of the radionuclide [316], at least in the ideal case of a chamber with walls of air-equivalent materials. Dale ([90], see p. 170) expected practical limitations for commercially produced chambers and he gave plots for experimental calibration factors relative to the k-value for several commonly used radionuclides. He also described practical adjustments of the response curves as a function of photon energy, taking into account secondary-electron production by Compton scattering and the photoelectric effect in the well (or liner) material of the chamber. Calibration factors expressed in terms of ionization current per activity have been calculated for several radionuclides and compared with experimental values. The agreement is at the level of 1% to 5%.

Kleeven and Wijnhoven ([256], see p. 181) proposed another way to explain the energy-dependent chamber response for different construction materials and included chambers in which the electrode was coated by a thin high-Z metal layer. The electrode coating considerably increases the chamber efficiency in the energy range from 100 keV to 500 keV. This is useful for most of the radionuclides used in nuclear medicine applications since the required photon energies are in this region. For the calculations, the chamber efficiency is defined as the mean number of electron-ion pairs formed in the sensitive gas per photon entering the chamber. In order to calculate the mean amount of energy per photon transferred to the gas, the photoelectric, Compton and pair production interactions are considered separately. A geometric model for the electrodes in the form of cylindrical elements is constructed, and the efficiency components are computed by numerical integration in the individual zones of the model. Various gas fillings and electrode coatings (tantalum, platinum or lead, 100 μm thick, for instance) are studied. The calculations help to understand the processes and the influence of various materials and dimensions in terms of relative efficiency. However, the model is not suitable for precise calculation of the efficiency values of actual radionuclide calibrators.

Another way of calculating efficiency values for various source geometries, in terms of parameters for a standard geometry, is to apply Monte-Carlo codes. In a study by Dryak ([120], see p. 172) correction coefficients for self-absorption were determined as the ratio of the ionization currents of a cylindrical source of aqueous ^{57}Co or ^{137}Cs solutions and a point source of very small mass. For this purpose, other modern Monte-Carlo codes also seem promising, among them the EGS4 code [318]: here EGS stands for electron-gamma shower. While this is a fairly complete system in computational physics, the authors of EGS4 consider the development of electron-photon Monte-Carlo transport techniques to be far from complete. As EGS4 is still not able to handle fluorescent x rays, Auger electrons, binding effects in Compton scattering or some types of multiple scattering, we cannot expect to

evaluate calibration factors in absolute terms of current for such a complex geometry as an ionization chamber.

An attempt to use EGS4 in relative terms of current ratios has been made by Büermann et al. ([54], see p. 168) in order to compute geometric correction factors for small cylindrical solid sources, for example ^{192}Ir brachytherapy sources. The attenuation-correction factor for the source was defined as the ratio of the efficiency of the radionuclide, in standard ampoule geometry, to the efficiency for the solid source, applying simple geometric models for the material layers and a homogeneous activity distribution in the solution and the solid radioactive material. Fluence spectra outside the sources were then calculated and the efficiency values for the different sources determined from the sum of photon components for the radionuclide, weighted with an experimental energy-dependent photon-efficiency curve in a point-source geometry. The results of calculation and experiment for several source assemblies, and also with various lead filters placed around the source, agree with each other to within 2%. In earlier studies the photon fluence from a solid ^{192}Ir source was measured with a radionuclide calibrator calibrated in terms of fluence [72].

Considerable effort will be required if Monte-Carlo calculations are to be used to penetrate to deeper layers of the chamber well and electrodes with a view to obtaining energy-dependent photon efficiencies. So far, no energy-dependent photon-efficiency curves for different chamber geometries and constructions have yet been calculated by Monte-Carlo methods and published. This is due to the complexity of the material distributions and geometric parameters in the practical realizations of re-entrant pressurized ionization chambers used for activity measurements.

7.6. Calculation of radionuclide efficiencies from energy-dependent photon efficiencies and photon-emission probabilities per decay

Radionuclide efficiencies ε_N are calculated from energy-dependent photon efficiencies $\varepsilon_i(E_i)$ (Figure 57, see p. 142) and photon-emission probabilities per decay $p_i(E_i)$ using Equation (29). An example can be found in Table 7 for Ir-192. The same form of equation is used for quantities proportional to the efficiencies $\varepsilon_i(E_i)$ and ε_N , such as the reciprocal equivalent activities $1/A_{ei}(E_i)$ and $1/A_e$. Methods for obtaining an analytical expression for, or a numerical representation of, the efficiency function are described in Section 7.2 together with the related interpolation procedures. An accurate calculation should include the bremsstrahlung components following high energy β decay in the sum of Equation (29), using an efficiency curve at average energy, as shown in Figure 56, and the corresponding β -particle emission probabilities per decay.

The emission probabilities per decay p_i entering into the calculation are taken from decay data compilations like [324], [272], [316], [51], [394]. Average β -particle energies and related probabilities needed for a determination of the bremsstrahlung component may be found in [51] or [316]. Several authors have published calculated efficiency values of this kind, indicating deviations between the measured and the calculated values, for example Merritt and Gibson ([304], see p. 183), Weiss ([470], see p. 194), Schrader and Weiss ([401], see p. 190) in Table 8, Dryak and Dvorak ([122], see p. 172) in Table 6. The results typically show a deviation of a few per cent.

Heydorn ([211], see p. 178) made critical comments on the use of these methods when low-energy x rays are neglected, for example in the case of ^{137}Cs . In contrast with Bensch and Ledermann ([21], see p. 166) he pointed out that it is not the average energy of the radionuclide which should be used in these calculations. Instead, the calculation should be carried out applying energy-dependent efficiencies in a straightforward way. It is evident nowadays, that all the components contributing to the ionization current must be included in the calculation. An efficiency curve must be established individually for each particular measuring system.

It should be noted that the parameter system for efficiency calculations is strongly correlated. On one hand, the emission probabilities per decay are determined from the activity of a radioactive source and from relative measurements with a Ge detector. On the other hand, the corresponding radionuclide efficiency of the chamber is calculated from the emission probabilities per decay and an efficiency curve (from a calibration with other activity standards): this then allows the activity to be determined. This correlation must be taken into account in any discussion of uncertainties in the results (Chapter 8, see p. 61) and introduced, if necessary, in an algorithm with covariance matrices. This consideration applies to the calculated efficiency for an individual radionuclide for which a calibration standard is not available and for which the activity is to be determined [197]. It also applies to the development of photon-efficiency values for measurement systems which use activity standards to check calibration consistency. In this sense, a photon-efficiency curve of high accuracy, i.e. one having only small deviations of the calibration points from the curve, confirms the consistency of the calibration. At the same time, it confirms the quality of the activity standards used. Such a smooth curve has been given for the International Reference System (SIR) at the BIPM by Rytz ([376], see p. 188), Rytz and Müller ([380], see p. 188) (Figure 63-1, see p. 147), and for the ionization chamber of the PTB by Weiss ([470], see p. 194) (Figure 57 and Figure 64-1-Figure 64-2, see p. 149). Figure 66 and Figure 67 show the relative deviations between the measured and the calculated efficiency values for the PTB curve and the BIPM curve, respectively, as a function of photon energy.

8. Uncertainties of activity measurements obtained using ionization chambers

8.1. Uncertainty components of an activity measurement

The conditions for obtaining high accuracy in activity measurements with ionization chambers have been discussed in the preceding chapters. In this section, these are summarized and the corresponding uncertainty components are listed. To do this, we take an equation similar to Equation (9) which is applied to the determination of an activity A_0 , at a certain reference time t_0 , with an ionization chamber measuring system. The activity is

$$A(t) = A_0 e^{-\lambda_N(t_m - t_0)} = A_e e^{-\lambda_r(t_{rm} - t_{r0})} C_g C_i \frac{I}{I_r}. \quad (30)$$

The expression Equation (30) describes an ionization chamber measurement in which most parameters and quantities are subject to some uncertainty. The chamber is calibrated in terms of the equivalent activity $A_e \sim 1/\varepsilon_N$ (or in terms proportional to it) for a radionuclide N with the half-life $T_{1/2} = \ln 2 / \lambda_N$. The current caused by the sample, $I = I_m - I_b$, is measured at a time t_m and that of the reference source I_r at time t_{rm} . For the present discussion, a reference source of ^{226}Ra is considered. The currents must be corrected for background (index b). The sample is measured in a particular geometry for which a correction factor C_g provides the transformation to a measurement in a standard geometry, and the sample contains radionuclidic impurities (index i), for which corrections are made through the factor C_i .

The components σ_j (written as $\sigma(Q_j)$ of the quantity Q_j) are discussed in the order in which they appear in Equation (30) from right to left. The first components originate from the current measurements. They contain the statistical uncertainty components $\sigma_{\text{stat}}(I)$ from fluctuations of the charge collection process (Section 2.3, see p. 15) similar to those of a counting experiment. The current measurements experience other systematic uncertainty components $\sigma_{\text{meas}}(I)$, arising from saturation-current losses (Section 2.3, see p. 15), leakage currents (Section 4.1, see p. 30) or instabilities in the current-measuring electronics (Section 5.1, see p. 37). To keep the values of these components as low as possible, good repeatability of the system is required, at least for times long enough to carry out several measurements in a series. Compensation for slow fluctuations or a slow shift is obtained by performing measurements relative to the reference source (Section 2.5, see p. 17), as both current values follow the same trend. Stability criteria are therefore required for the reference source seen as a source of stable current (Section 2.6, see p. 19). Other uncertainty components $\sigma(I_r)$ arise from the decay correction of the reference source (uncertainty of the half-life value), possible leaks of activity, deviations from equilibrium in the mother-daughter decay of ^{226}Ra (Section 2.6, see p. 19) or any change in the measuring conditions of the reference source (e.g. nonreproducible geometry). The reference source activity (or the related current) chosen should remain near the equivalent activity (or current) of the source to be measured [376]. Other uncertainty components $\sigma(I_b)$, for example from fluctuations in the radiation level of the environment or changes of shielding conditions (Section 3.2.5 or Section 6.1, see p. 42), are related to the background measurements.

The uncertainty components $\sigma(C_i)$ describe the quantities connected with the radionuclidic impurity correction factor C_i (Section 6.6, see p. 47), such as the activity ratio measured with a Ge detector, including uncertainties in its calibration, components from the decay corrections

$\sigma(T_{1/2} N)$ and $\sigma(T_{1/2} i)$, and the ratios of the chamber calibration factors $\sigma(A_e N)$ and $\sigma(A_e i)$ of the contributing radionuclides N and i.

Good reproducibility is required for measurements made under standard measuring conditions, so changes in sample geometry (Section 6.3, see p. 44) which can be quantitatively determined, must be taken into account using a correction factor and a corresponding uncertainty component. Changes in the sample geometry, related to vials, ampoules or filling are described by a factor C_g and an uncertainty $\sigma(C_g)$. In fact, the sample changes and the cyclic measurements (Section 3.2.5, see p. 27), involving reference source, background and sample, enter into such a component. Other components of this type result from the limited stability of the sample, among them leaks from the confinement and chemical instability of the solution (plate out of the source [8], see p. 165) with components $\sigma(C_s)$.

Measurements of time, such as t_m and t_{rm} in Equation (30), are usually based on quartz-oscillator computer clocks, giving the time of registration (usually day, hour, minute and second) of the measured current value. The accuracy of these data is in most cases sufficient if radionuclides with half-lives greater than several hours are studied. Care must be taken with older clocks which may show a time shift of several minutes per month. These remarks also apply to the accuracy of the duration of a current measurement because, for most current-measurement systems, an accurate time interval is needed (Chapter 4, see p. 29). Small errors in the duration of the current measurement may produce substantial errors in the resulting current values. This problem is related to the adjustment error of compact electronics of activity meters in the case of time interval changes for activity range switching (Section 5.4, see p. 39).

The uncertainty components $\sigma(t)$ of the time measurements are closely related to the decay corrections necessary for all radionuclides involved in a measurement procedure. They thus include the sample, the radionuclitic impurities, the reference source and any external background sources and are described by uncertainty components $\sigma(T_{1/2})$. A 0.1% relative error in the half-life produces a relative error in the corresponding activity value of 0.07% for each interval of one half-life between measurements, or 0.3% for four half-lives. Furthermore, the decay correction for the time elapsed during a current measurement (Section 6.2, see p. 43) has to be taken into account when dealing with very short half-lives and this also has an uncertainty component.

The last group of uncertainty components $\sigma(A_{\text{standard}})$, in some cases the dominant ones, result from the procedure used to calibrate the activity value of the standard, that is from the direct (or absolute) activity measurement. The related uncertainty components $\sigma(A_{\text{standard}})$ are transferred to the ionization chamber measuring system by the calibration, and the unit of activity is maintained there with the original quality of the direct measurement. With an optimized ionization chamber used as a secondary standard measuring system, a reproducibility of several 10^{-4} is normally obtained for relative activity measurements with sources of one radionuclide. This is usually one order of magnitude better than the uncertainty for the corresponding direct activity measurement.

Indirect calibrations, where a calibration factor (or efficiency) is calculated from the energy-dependent efficiency curve and the emission probability per decay (Section 7.6, see p. 59), transfer the uncertainty components of the related quantities $\sigma(\varepsilon_i(E_i))$ and $\sigma(p_i(E_i))$ to the uncertainty of the activity value. Usually, relative uncertainties of this type amount to a few percent. Typical values for direct and indirect measurements are quoted by Dalmazzone and

Guicho ([95], see p. 171) and, for the earlier NPL ionization chamber, by Woods ([475], see p. 194).

8.2. Combined uncertainty from uncertainty components

To exemplify the relative magnitudes of the uncertainties discussed, values from optimized measuring systems used in national standards laboratories are listed in Table 9. Some values are included which are based on estimates obtained with activity meters under rather unfavorable conditions. The uncertainty values quoted are standard deviations derived from a large number of observations. A Gaussian distribution of the measurement values is assumed. Student factors, applicable when the number of events is small, are therefore not taken into account nor are other distribution shapes. The numerical values in the table should be regarded as a guide, because individual cases vary considerably depending on the chamber construction.

To calculate the overall uncertainty value of an activity measurement, the law of uncertainty propagation must be applied: The combined standard uncertainty $\sigma(A)$ is the positive square root of the sum of the squares of the individual uncertainty components $\sigma(Q_j)$, weighted with the partial derivatives of the function $A(Q_j)$ of Equation (30). Thus

$$\sigma^2(A) = \sum_j \left\{ \frac{\partial A}{\partial Q_j} \right\}^2 \sigma^2(Q_j) \quad (31)$$

The individual components depend on the particular procedure used to evaluate the $A(Q_j)$ for which Equation (30) represents only one example. Another example is published by Rytz ([376], [378], see p. 188) for the efficiency curve of the SIR ionization chamber. The results are presented graphically in Figure 67. A similar presentation of uncertainties for various radionuclides is given in Figure 66 for an ionization chamber at the PTB. These pictures summarize the uncertainty in ionization chamber calibrations and show the individual contributions from various radionuclides.

If a calculated calibration factor (or efficiency) is used for an activity measurement, correlations are formed between parameters since they depend on the calibration points of the energy-dependent efficiency curve and the photon-emission probabilities, which are both related to other activity determinations. Correlations between the parameters must be taken into account by covariance terms in the sum for the combined uncertainty. The necessary theory of uncertainty propagation is beyond the scope of this review. Recommendations can be found in specialist papers and standards some of which include examples from metrological practice. Of particular interest is the “Guide to the Expression of Uncertainty in Measurement” ISO/IEC 98-3:1993.

9. Applications of ionization-chamber measurements

9.1. Quality control in national standards laboratories

Activity measurements with ionization chambers play an important role in the preparation of activity standards. The radioactive raw solution is quantitatively diluted by careful weighing, and the corresponding value of the activity concentration is checked after each dilution step by ionization-chamber measurements. Such dilution procedures have been described by Merritt and Taylor ([307], see p. 184), Eijk and Vaninbroukx ([126], see p. 173), in Campion's monograph [23], in the report [316] and by Mann et al. ([294], see p. 183). First, two or three ampoules of standard geometry are prepared gravimetrically from the raw solution and their activity concentration carefully compared. Other dilutions are then prepared gravimetrically and measured so as to produce a family of diluted solutions (Figure 68-1, see p. 153). The first stage may be the only one in the preparation of gravimetrically dripped solid point source standards, depending on the activity concentration needed to obtain an activity of several hundred kilobecquerels in the solid source, because the dispensed mass values are usually about 5 mg to 15 mg per drop. It is possible to dispense two or three drops onto the support and still obtain a fairly thin solid source with sufficiently low radiation attenuation. Another condition for diluting and preparing standards from a solution is a low salt concentration. For an inactive carrier solution, this is roughly 50 µg salt per gram of solution, a value which should not be exceeded for an aqueous radioactive solution. Many details of these procedures are given in Campion's monograph [23]. In one of the first dilution steps it is often useful to prepare solid samples so as to measure the activity ratio of the radionuclidian impurities in the solution with a Ge spectrometer (Section 6.6, see p. 47). Obviously, the activity ratios of the radionuclidian components must not change during the dilution steps.

In each dilution by a single factor, which should not exceed about 100, large numbers of ampoules are prepared together along with other types of source, and the activity concentration of the ampoules is checked by ionization-chamber measurements (Figure 68-1, see p. 153). This process may be continued to produce concentrations of quite a low activity. Such dilution factor measurements, or quantitative checks of ampoules after refilling the solution into other ampoules, also serve to confirm the chemical stability of a solution.

All solutions in a dilution family are usually interconnected via the dilution factors to one of the first members with the strongest activity concentration, the so-called master solution. All subsequent calculations and comparisons of activity concentrations are based on this [23].

Uncertainties resulting from diluting and dispensing have been discussed by several authors [307], [42], [23] who show that, with reasonable precautions, these procedures should not introduce a relative uncertainty of more than 0.1% into the final result of an activity concentration measurement. Campion in BIPM ([23], see p. 166) proposed an internal verification procedure using ^{60}Co and several dilutions combined with international comparisons of activity measurements, and suggested that participation should be compulsory for every standards laboratory.

In addition to measurements within a family of dilutions, direct standardization of a particular radionuclide is required from time to time, and a calibration factor for the ionization chamber measuring system is determined within the various solution families. Assuming stable conditions of measurement, the corresponding calibration factors from various measurements on a long-term scale are compared so that their evolution with time can be studied. If these

calibration factors remain constant within a defined uncertainty this confirms that the unit of activity is accurately maintained by the ionization-chamber measurement system [395], [27], [218], [58], [451], NIST SP 250e1989.

9.2. Quality control for activity measurements and intercomparisons in nuclear medicine and industry

The main instrument for activity measurements in the field of nuclear medicine is the radionuclide calibrator, also called the activity meter. It is described in Section 3.2.4 where the technical details and calibration of the instrument are given. These instruments provide a direct reading in units of activity. Here, the aspects of quality control relevant to activity measurements of radiopharmaceuticals and to the corresponding regulations are described. The situation in countries practising nuclear medicine is regulated by laws, standards or recommendations from organizations which have official responsibilities in this field. These regulations apply to the manufacturers of radiopharmaceuticals and measuring instruments (radionuclide calibrators) [429], [430] and to users in hospitals or medical practices. The national standards laboratory, or a laboratory traceable to it, delivers appropriate activity standards for quality assurance of activity measurements for which the user is responsible. Modern regulations specify the accuracy required in measurements of activity and of the dose from radiopharmaceuticals administered to patients, and make it a legal requirement that records are kept. The final responsibility for these procedures in the sense of the radioprotection rests in the hands of the user of a radiopharmaceutical, usually the physician applying it. He is normally assisted by well-trained staff who carry out the necessary activity measurements and have experience in handling activity meters. Their duties include carrying out the checks necessary for daily routine measurements, for field calibration procedures and for the long-term performance of the instrument. There is scientific interest not only in performing correct individual activity measurements for hospital work, but also in obtaining correct results for comparisons on a general research level, and hence to develop new procedures and methods in nuclear medicine.

These requirements for the quality control of activity assays in nuclear medicine can be fulfilled by calibrations made by direct comparisons with standards and by careful application of the regulations. To participate in comparisons of activity measurements organized by national authorities or organizations, for example by the national standards laboratory or a calibration service traceable to it, is strongly recommended [8], [1], [110], [230], [231]. Comparisons are one of the best tools in quality control for field applications, because not only the instrument calibration is checked but also the entire measuring chain, including the personnel operating it. One of the first pilot studies on the quality assurance of activity measurements using radionuclide calibrators was carried out by Garfinkel and Hine ([165], see p. 175), measuring radionuclide sources in US hospitals with different types of calibrator. Since then, many other comparisons have been organized in countries practising nuclear medicine [201], [158], [172], [202], [476], [332], [387], [388], [96], [333].

In such a comparison samples of solution containing a known radionuclide, but with an activity unknown to the participants, are distributed. After careful measurement by the organizer, the participants measure the activity under the usual conditions and report their values to the organizer of the comparison. Later each individual participant is informed of the certified value of the activity of his sample. This procedure serves the purpose of providing a recalibration of the user's instrument. All the results received are treated by statistical methods

and are reported anonymously (Figure 69-1–Figure 69-4 [100], Figure 70-1–Figure 70-4 [477], see p. 195).

In recent years many such comparisons have been organized by national standards laboratories and by calibration services providing traceability. The results have not always been satisfactory [277]. In earlier comparisons deviations by more than 30% from the nominal values were found, far beyond the limits imposed by the regulations [168], [197], [287], [337], [424], [356], [434], [435], [477], [436], [60]. As a result of the continuing attention given to quality assurance, the situation has improved in recent years [81], [60], [486], [351], [100], [162].

The critical radionuclides are those in which the solution to be measured contains radionuclidic impurities or where parts of the radiation are emitted within an energy range with which users are not familiar [275], [202], [331], [477]. This is well known in the metrology of radioactivity, see preceding chapters. A further source of error is that the measuring conditions for calibration and for practical measurement are not the same (e.g. a variation in measurement geometry). In some cases, a systematic trend in an assembly of instruments from a specific manufacturer has also been observed (Figure 69-4 or Figure 70-3–Figure 70-4, see p. 159).

The same concern for quality assurance is necessary in the production of radioactive sources for the nuclear industry and in applications involving radioprotection and environmental surveillance programmes [21], [281], [172], [181]. When, in these fields, ionization chambers are used to measure radioactivity [210], [302], the arguments valid for legal metrology or nuclear medicine obviously apply, and the same measurement conditions must be fulfilled for quality control.

9.3. Half-life measurements

Direct decay measurements using an ionization chamber are the most obvious and least complicated means of determining the half-life of a radionuclide [480]. The equation for this method is given by the law of radioactive decay in Section 2.4, Equation (2). Basically, the method consists in repeated measurements of activity values $A(t)$ of the radionuclide under study as a function of time and a fit to the two parameters, namely the half-life $T_{1/2}$ (or decay constant $\lambda = \ln 2/T_{1/2}$) and an appropriate value for the initial activity $A_0 = A(t_0)$. In the decay method, $A(t) = dN(t)/dt$ is defined as the probability of changing a defined nuclear state where N is the number of nuclides in this state [226].

The half-life is assumed to be an innate parameter of a radionuclide and characteristic of its decay [367], [368]. Its value may be slightly influenced by chemical effects (or interactions) in the case of electron capture nuclides, for which the electron density in the shell plays an important role. These chemical effects are normally of order 10^{-4} of the actual half-life value of the capturing radionuclide. A survey of experimental and theoretical perturbation data of the decay constant ($\Delta\lambda/\lambda$), including many references to historical publications of that problem, from about 1900, is given by Hahn et al. ([194], see p. 177). Special techniques have been developed to measure these effects, for example differential experiments using two ionization chambers with samples of the same radionuclide in different physical or chemical states [132], [32], [301], [243], [33], [15], [321]. Kakiuchi et al. ([243], see p. 180) also reported an application of this differential method for the measurement of a long half-life in a short period of time, e.g. with ^{60}Co in a 10 d run giving $T_{1/2} = (5.27 \pm 0.07)$ a.

Other measuring methods compete with the decay methods and offer the possibility of identifying and counting the different nuclides directly, for example by mass separation of the material containing the decaying radionuclide [101], [102]. These methods are useful for radionuclides with long half-lives, such as ^{233}U [456], or if identification of the radionuclide by radiation discrimination is difficult, as in the case of ^{241}Pu . For this, the half-life was measured by mass spectrometry of the decreasing ratio of $^{241}\text{Pu} / ^{242}\text{Pu}$ [297]. The number of atoms of each nuclide N_i in the sample is determined, and the relation $A(t) = dN(t)/dt = -\lambda N(t)$ for the decaying radionuclide (^{241}Pu), or an equivalent relationship for the ratio of the nuclides ($^{241}\text{Pu} / ^{242}\text{Pu}$) as a function of time, is used.

In other methods for long-lived radionuclides the decay heat is measured by microcalorimetry [292], for example to determine the half-life of ^{210}Pb [343]. At the other extreme, half-lives of less than a minute can be measured by sophisticated electronic methods which involve the time behaviour of scalers and related system properties such as multiscaling or multianalyzing [258], [311], selective sampling [312] and others [150]. Some of these alternative methods are summarized in an early review by Rowlands ([359], see p. 187), which also gives many references to other articles of that period. The direct decay methods with ionization chambers do not give access to very long or very short half-lives.

One difficulty of the direct decay method is that of selecting only the decay from the nuclear state which is to be measured. This requires precise knowledge of all disturbing effects. In an integrating instrument, like an ionization chamber, the detection of radiation from other radionuclides must be avoided and an accurate measurement of the measurand as a function of time is essential. The second point implies the absence of any instrumental fluctuation over both short and long time periods or, more realistically, permanent monitoring of the stability of the instrument response and the application of a correction when necessary. Some of the effects, and their consequences for data fitting, are discussed by Tagesen and Winkler ([439], see p. 192). This is particularly important for measurements of rather long-lived radionuclides like ^{90}Sr with $T_{1/2} = (28.7 \pm 0.3)$ a [184], [490] and, more recently, $T_{1/2} = (28.91 \pm 0.04)$ a [298], and ^{137}Cs with $T_{1/2} = (30.18 \pm 0.15)$ a [480], [225], see Table 10. Considerable effort has been made in a number of standards laboratories to improve the accuracy of half-life values [220], [215], [272], [461], [396], [225], [452]. The determination of accurate half-life values using ionization chambers is discussed in the following subsections which describes the experimental techniques, the fitting procedures for measurement data and the evaluation of existing half-life values from the literature for use in decay corrections to measurement data.

9.3.1. Half-life measurement techniques with ionization chambers

To study the decay of a source for a half-life measurement with good accuracy a mechanically and chemically “stable” source must be used (Chapter 6, see p. 42). Only the decay of interest should be observed, or extreme care must be taken to correct for contributions of radionuclidic impurities which emit photons (Section 6.6, see p. 47). Radiation filters (Section 6.6.3, see p. 51) may be used to reduce an ionization current component from an unwanted impurity. For example at the PTB, to measure ^{154}Eu containing an impurity of ^{155}Eu , a source was permanently mounted in a Pb-Al confinement where it acted as a filter to reduce the contribution of the ^{155}Eu radiation.

The radiation detector preferred for half-life measurements is a pressurized re-entrant ionization chamber integrated, in some cases, into a measuring system which runs with an automated sample changer. The source containing the radionuclide concerned is measured

in cycles which include measurements with a long-lived reference source and with the background. The ionization chamber should show no measurable saturation-current loss in the activity range of interest (Section 2.3, see p. 15). The reference source should contain old ^{226}Ra in near equilibrium with its decay products under a gas-tight seal (Section 2.6, see p. 19). The influence of non-equilibrium ^{226}Ra sources is described by Christmas et al. ([70], see p. 169) and a correction formula is given by Martin and Taylor ([299], see p. 183). During the measurement all raw data, including the accurate time of each measurement, are stored in a computer file for later processing in data-fitting procedures.

Several authors have described measurement techniques and given results of half-lives for various radionuclides. Examples can be found in [173], [176], [174], [421], [68], [166], [462], [393], [445], [220], [369], [463], [370], [371], [461], [161], [485], [242], [389], [396], [299], [487], [177], [298].

9.3.2. Data-fitting procedures for half-lives

The simplest data treatment and fitting procedure for a half-life is to fit the logarithm of the current ratios of sample and reference source, corrected for background and radionuclidic impurities, as a linear function of time (linear regression analysis). In some cases this may give immediate and satisfactory results but a more detailed search for systematic errors is recommended, e.g. by examining the residuals of the fit (Figure 71-1-Figure 71-2, see p. 161). For possible pitfalls, [439] and [313] should be consulted.

Many publications describe data treatment methods of varying degrees of reliability for the calculation of half-lives from measurement data. These begin with simplified graphical diagrams [2], go on to empirical consistency checks [461] and statistical methods, and finally to multi-dimensional non-linear decay-curve fits [138], [185], [199], the latter being necessary for radionuclide mixtures or decay chains.

Some standards laboratories analyse trends by studying the fitted half-life values of subsets from the data set to be analyzed [461], Figure 72-1-Figure 72-4, [298]. Other laboratories use statistical tests.

9.3.3. Half-life evaluations

The half-life is one of the most important characteristics of a radionuclide, and lists can be found in data files, books or compilations [324], [272], [316], [51], [394], [225]. Coordinated research programmes on calibration data formulated by national and international organisations (e.g. ICRM or IAEA) recommend best values for many half-lives. Considerable effort has been made to establish consistent data sets in evaluations [320], and special procedures have been proposed to arrive at recommended values. An example is the half-life evaluation of ^{137}Cs [225], and in more detail Woods ([480], see p. 195). In the articles of the IAEA ([225], see p. 179), groups of radionuclides have been identified as requiring further measurements to resolve discrepancies, and have been classified by the uncertainties of the half-lives. The recommendations and priorities for further measurements depend upon the number of measurement data reported, the inconsistencies and the final uncertainty in the evaluated half-life value. Since 1989, several new measurements have been made. A continuous effort made by the relevant laboratories will improve the prospect to obtain a best set of half-life values. The final report of the IAEA working group on radionuclide data appeared in 1991 [225].

10. Intercomparisons and the International Reference System (SIR)

The International Reference System, in French the “Système International de Référence”, abbreviated SIR, was conceived to complement and extend the international comparisons of activity measurements organized by the BIPM. The growing importance of accurate activity measurements in the 1960s led to the creation of a new section at the BIPM in 1961 which, among other duties, was charged with carrying out radionuclide measurements and intercomparisons. After discussions between the IAEA [219] and the BIPM, and taking advantage of previous experience with international comparisons, an ionization-chamber based measuring system for activity was installed at the BIPM in 1972 [372], [376]. The task of the SIR is to maintain world-wide uniformity in activity measurements, to improve the accuracy of such measurements and to carry out quality control of national activity standards. In this way it ensures traceability to international standards. Since its creation, the SIR has given a most valuable service to the national standards laboratories which participate in its work by submitting solution standards for comparison [384].

The measurement procedures of the SIR, are described in Section 10.2. When applied to a particular sample they provide a value for the equivalent activity A_e of the particular photon-emitting radionuclide relative to a specific radium reference source. It is obvious that all the conditions for reproducibility and stability already discussed must be carefully observed when making measurements in the re-entrant ionization chambers of the SIR. As Houtermans ([219], see p. 178) pointed out: “The essential quantity is A_e , i.e. the activity of the nuclide which gives the same instrument response as the long-lived standard, when measured under standard conditions.” The measured values A_e , together with statements of uncertainty and sample identification, are assembled and distributed annually to participants. The large number of radionuclides compared so far, shows the utility of activity measurements performed at an international level. It also shows the position of each participant with respect to the other. The system may help developing laboratories unable to perform direct activity measurements with particular radionuclides to link their ionization chamber measuring systems to international standards.

10.1. Intercomparisons of activity standards and traceability

When an international comparison of activity measurements is organized for a given radionuclide, a raw solution is carefully selected and checked for suitability (i.e. activity concentration, chemical stability and radionuclidic impurities) by the BIPM or another agreed laboratory. The radioactive solution is then distributed to participants in flame-sealed ampoules of BIPM/NIST standard geometry with a solution mass of about 3.6 g per sample (Figure 50-1, see p. 132). In recent years it has been usual to organize a trial comparison before the main comparison to pick up and resolve any measurement problem that might arise. First, a preliminary ionization-chamber measurement of the radioactivity is required for the original ampoule. Then, the standardization is performed by one or several direct methods, using recommended techniques for source preparation and measurement [23], [316], [294]. A questionnaire is circulated to all participants in the comparison. In this details of techniques, experimental parameters, possible correction factors, uncertainty components and the final activity concentration value at reference time are reported by the participant. The filled-in form is returned to the organizer (BIPM). The results are processed by statistical

methods, illustrated in diagrams, analysed, and published in a report which is distributed to the participants.

International comparisons of this kind have been organized since the early 1960s by the BIPM under the auspices of the Comité Consultatif pour les Étalons de Mesure des Rayonnements Ionisants (CCEMRI), Section II, Mesure des Radionucléides. The first comparison was with ^{32}P in 1961, followed by ^{131}I , ^{198}Au and ^{60}Co in 1961 and 1962 [62], [24] and many others, for example the ^{125}I trial comparison in 1987 [347], the ^{125}I main comparison in 1989 [348], [344], a ^{75}Se trial comparison in 1991 [349], [345], [346] and the ^{75}Se main comparison in 1992. The level of agreement in an international comparison is typically about 2% (1σ) for a single participant [24], with maximum deviations of about 5% for particular cases. In most of the comparisons since the 1960s the number of participants, mainly from national standards laboratories, has averaged around 20. The highest accuracy was obtained in the ^{134}Cs comparison in 1978, with a relative standard deviation of 0.17% (with 24 participants) and a maximum deviation of 0.68% [379], [374], see Figure 73. For some radionuclides, standardizations could not be performed by direct measuring methods like the $4\pi\beta-\gamma$ coincidence technique. Special methods or technique were required: for ^{55}Fe , a tracer or calibrated-detector-response method [381], [419], for $^{93}\text{Nb}^m$ liquid-scintillation counting (LSC, see Section 10.4, see p. 73) or similarly, a calibrated-detector-response method [84], for ^{109}Cd , a calibrated 4π detector, tracer or special coincidence methods [216], [433], for ^{125}I , photon-photon coincidence or sum-peak methods [216], [344], and for ^{137}Cs , coincidence methods with tracer [382], [383] and [377], see Figure 74. The SIR results for a period of five years are included in this diagram.

Consistent results in international comparisons is evidence for the quality of a national standards laboratory on an international level. They establish traceability between the distributors and users of activity standards from different countries (Figure 68-2, see p. 153). International comparisons of a particular radionuclide solution organized by the BIPM, or comparisons of samples measured by the SIR, represent the highest level in a “Traceability Tree” [294] describing the hierarchy of radioactivity-standardization laboratories and organizations [295], [187], [292], [355], [293], [67], [244], [246], [316], [294]. A complete chain of traceability is required linking quality control by users—hospitals, industrial groups [172], universities or government agencies—via regulatory bodies and national standards laboratories to international organisations like the BIPM, the IAEA or the ICRM. Guidelines for the international acceptance of radioactivity calibration sources have been formulated by Hoppes and Hutchinson ([217], see p. 178) in response to a request from the International Committee for Radionuclide (ICRM). Laboratories participating in the traceability system must observe special quality assurance (or quality management) criteria. These include responsibilities for the training of staff, for installations and for measurement procedures. The criteria are set with the aim of proving that the laboratory has the ability to produce certified radioactivity standards or reference materials to agreed standards, so checks in the course of production and calibration must be both carried out and documented. The recommended quality assurance criteria provide a means of bringing the results of the international work on standardization into standards certification procedures and ultimately into user laboratories. They are the basis by which legal, safety and other requirements for the acceptance of standards will be met in an international frame [217].

10.2. Measuring equipment and procedures of the SIR

The SIR is an ionization-chamber measuring system consisting of two re-entrant ionization chambers with current-measuring electronics and data storage [372], [376]. A photograph of this system can be seen in Figure 37-1 [376], [25]. Two identical chambers (20th Century, IG11/N20 [69], see p. 169), filled with nitrogen gas at a pressure of 2 MPa, are set up inside a common lead shielding 5 cm thick. The two chambers are connected alternately to a current-measuring device, based on the Townsend-balance principle with stepwise compensation (Section 4.4, see p. 34), in which the time to charge the capacitor of the balance to a constant voltage level is measured a preset number of times. The background and leakage current of the system is typically about 33 fA. The current of the samples is measured relative to that of a ²²⁶Ra reference source. Five reference sources, with a radium content from about 0.003 mg to 0.3 mg, can be chosen to match the required activity range. The sources were manufactured by Union Minière in Brussels in 1973 from aged radium. They contain radioactive RaSO₄ with an admixture of inactive BaSO₄ in a Pt-Ir sealing. Several tests of this measuring system have been described by Rytz ([376], see p. 188). The sources have been carefully compared, and the ratios are known to about $\pm 2 \cdot 10^{-4}$, at least for the four stronger ones. The absence of leaks is evidenced by the absence of trends in these measurements. To check that the radium daughters in the sources are close to equilibrium, two additional reference sources also containing aged radium were acquired in 1983 and included in the monthly test measurements. The repeatability and reproducibility of the two-chamber system have been tested with the reference sources and the data show that the current ratios are satisfactorily stable. Tests for ampoule geometry and source position dependence have also been carried out. Including an uncertainty component for the ampoule wall thickness as a function of energy, all uncertainty components add up to a combined relative uncertainty (1σ) of 0.1% for photon emitters of about 60 keV (²⁴¹Am), and of 0.05% for emitters of about 1.25 MeV (⁶⁰Co) [294].

The results of the measurements of SIR samples are given in terms of equivalent activity A_e (Section 2.5, see p. 17), which is related to the current (about 330 pA) produced by the strongest reference source (0.308 mg Ra element) according to the formula [376]:

$$A_e = A_s F_i [R + (R - 1)f / (I_s - f)] \exp\{-\lambda_s (t_m - t_s)\} \exp\{\lambda_{Ra} (t_m - t_0)\}, \quad (32)$$

where

A_s is the activity of the source (index s) from the participating laboratory at a stated reference time t_s ,

F_i is the reference source ratio related to the 0.308 mg Ra source,

$R = I_{Ra} / I_s$ is the ratio of the ionization currents of the reference source and of the source from the participating laboratory,

f is the background and leakage current,

λ_s, λ_{Ra} are the decay constants of the submitted radionuclide and of ²²⁶Ra, $T_{1/2} = (1600 \pm 7)$ a [449], respectively,

t_m is the time of the measurement (mid run) at BIPM, and

t_0 is the reference time for the reference sources (1976-01-01).

(These definitions are taken from the original publication and should not be confused with other definitions in this review using the same notation).

The measurements are performed in cycles consisting of a background run, ten readings with the reference source, ten with the sample and again ten with the reference source. The determination of A_e is carried out by a computer programme taking into account the measurement parameters, corrections for decay and radionuclidic impurities. The final result of A_e , expressed in kBq, with its uncertainty components and the sample parameters, is entered into a table. Lower limits of activity and impurity levels acceptable for the SIR are given in a report by Rytz ([375], see p. 188).

10.3. Results of measurements with the SIR

The radionuclide sheets which register equivalent activity values A_e , measured with the SIR, list the results obtained up to date. Until 1993, they gave details on about 570 ampoules containing about 50 radionuclides. Several of the most frequently used radionuclides, such as ^{57}Co , ^{60}Co or ^{133}Ba , have at least about 25 entries per nuclide. Each year about twenty new measurements for various radionuclides are performed and added to the file that is distributed annually to the participants in the SIR. An example of such a sheet for ^{192}Ir is given in Table 11. The standard deviation of the A_e values of an individual radionuclide varies from 0.25% (1σ) for ^{60}Co , in the best case, with 43 measurements from about twenty laboratories, to about 1.1% (1σ), for the unfavourable case of ^{88}Y , with 25 measurements from twelve laboratories.

A graphical representation showing the consistency of the results by establishing the energy-dependent efficiency curve (Figure 63-1, see p. 147), see Section 7.2, has been published by Rytz and Müller ([380], see p. 188), Rytz ([376], see p. 188) and Rytz and Müller ([383], see p. 189) with a supplement by Ratel ([346], see p. 186) for the low-energy part from 30 keV to 250 keV (Figure 63-2, see p. 148). In Figure 63-1 the relative detector response values $f(E_n)$ are displayed, with the definitions from the publication of Rytz ([376], see p. 188), namely

$$f(E_n) = \frac{10^6/A_e - \sum_{i=1}^{n-1} kE_i p_i f_i}{kE_n p_n}. \quad (33)$$

Here E_n and E_i are the photon energies, p_n and p_i the corresponding emission probabilities per decay of the radionuclide, and k is 60, an arbitrarily chosen constant factor, if energies are expressed in mega electron volts (MeV). In this equation, f_i is the relative photon efficiency at energy E_i , as defined in Section 7.4; it should not be confused with the definition of f in Equation (32). The value $f(E_n)$ of a radionuclide is shown at the photon energy E_n for which the emission probability p_n is largest and gives the major contribution to the ionization current.

The value of $f(E_n)$ is calculated from the total reciprocal equivalent activity value $10^6/A_e$, proportional to the efficiency ε_N for the nuclide, by subtracting the weaker components, after interpolation and weighting with the corresponding emission probabilities p_i (Section 7.2, see p. 54). Figure 63-1 shows remarkably large deviations of the individual values from a smooth curve in an energy range from 847 keV (^{56}Co) to 1408 keV (^{152}Eu), for example for ^{56}Co , ^{59}Fe , ^{182}Ta , ^{154}Eu and ^{152}Eu , but also quite large error bars. Radionuclides emitting many photons of different energies and covering a large energy range are also included in the representation, among them ^{133}Ba in the low-energy part, and ^{192}Ir , ^{134}Cs , ^{152}Eu and ^{56}Co , mainly with highenergy photons. A small deviation from the curve for these radionuclides illustrates the consistency of the calibration data.

Another representation (Figure 67, see p. 152) shows the consistency of the results of measurements using the SIR [378]. The deviations Δf as a function of energy, with f as defined in Equation (33), and the relative uncertainty of an activity measurement of the radionuclide with the SIR, $\Delta A/A \sim \Delta A_e/A_e$, are plotted at the energy of the strongest component. The largest deviations from the estimated curve occur for ^{169}Yb , ^{65}Zn , ^{110}Agm , ^{201}Tl , ^{67}Ga , ^{154}Eu , and ^{182}Tl .

Errors in the direct activity measurements or incorrect emission probabilities may be responsible for these deviations. In the publication by Rytz ([378], see p. 188) is included a “wish list” of radionuclides which would improve the calibration points of the SIR at certain energies and fill the gap at higher energies. Among them are ^{124}Sb (1691 keV), ^{206}Bi (1764 keV) and ^{188}Pt (2215 keV).

As explained in Section 7.2, there are no accurate calibration points in the energy range from 1332 keV (^{60}Co) to 1836 keV (^{88}Y). The shape of the energy-dependent efficiency curve in this range can only be described by mathematical expressions derived from a fitting procedure assuming a smooth curve. A suitable procedure may be a polynomial fit, as proposed by Dryak and Dvorak ([122], see p. 172). The cross check published in Dryak’s paper shows deviations of about 1% or less for most of the radionuclides, but larger values for ^{103}Ru (3.0%), ^{109}Cd (2.3%) and ^{65}Zn (1.2%). This shows the method is, in general, feasible at this level of accuracy, and confirms that it is useful when applied to radionuclides where no direct standardization is possible, provided that the emission probabilities are sufficiently well known.

10.4. Extension of the SIR

In metrology it is useful to compare measurement results using different systems so as to detect systematic errors in a system or method. For activity measurements with ionization chambers, alternatives may be found in 4π -NaI detector systems or in liquid-scintillation counting (LSC) systems, as both are capable of measuring photon-emitting radionuclides. However, the LSC systems have the advantage through their sensitivity to α and β particles, and to γ rays with energies below about 20 keV. An LSC system makes it possible to measure radionuclides that emit only these radiations which cannot be measured by ionization chambers. For this reason, an extension of the SIR has been implemented with an LSC system at the BIPM. The LSC system is a commercial instrument using a calibration method developed in collaboration with the CIEMAT and the NIST, using ^3H as an efficiency tracer [180], [179], [82]. Further studies of the energy spectrum from radiations deposited in the scintillator are described by Ortiz et al. ([328], see p. 185). The LSC method shows promising results for radionuclides like ^{14}C , ^{99}Tc [57] and $^{93}\text{Nb}^m$ [84], [192] and successful tests with the BIPM system are reported [346]. The BIPM is developing it as a useful supplement to the ionization-chamber measuring system for radionuclides emitting only α and β particles. Measurements of the activity concentration of a photon-emitting radionuclide solution which can be performed in both systems will provide an interesting check on the quality of activity measurements.

11. Conclusion

The aim of this monograph is to illustrate the usefulness of indirect activity measurements with a calibrated re-entrant ionization chamber measuring system, as they are performed in standards laboratories and for various applications for example in nuclear medicine. Such an indirect measuring system is an essential supplement to direct activity standardizations and extends the capabilities of a radioactivity laboratory. It serves to maintain the unit of activity with good accuracy and ensures quality assurance in all applications of activity standards.

Compact versions of calibrated ionization chambers, with a direct instrument reading in units of activity, are currently used for activity measurements in applications for radiopharmaceuticals.

Calibrated ionization-chamber measuring systems help to establish and maintain uniformity in activity determinations of photon-emitting radionuclides and to improve the accuracy of activity measurements.

12. Tables

Table 1. W values in different gases. Reproduced from [160].

<i>Absolute values, W, and values, R, relative to oxygen, for the average energy required to produce one ion pair in different gases with electrons as primaries.</i>											
Energy	46 keV	0 to 17 and	0 to 1.7 MeV	0 to 1.7 MeV	1 to 34 MeV	Averages*	method	and I.C.	Extrapol. ch.*	Extrapol. ch.*	I.C.*
Hydrogen	1.18	36.3	1.14		36.3	1.17	37.8	1.22	36.9	1.16	
Helium	2.35	42.3	1.37		40.3	1.29	44.5	1.43	41.3		
Nitrogen	1.12	34.7	1.12	34.8	1.12	34.6	1.11	34.8	1.12	34.9	1.12
Oxygen	1.00	(1.00)	30.9	(1.00)	30.9	(1.00)	31.2	(1.00)		31.3	(1.00)
Neon		36.6	1.19		35.3	1.13			35.9	1.16	
Argon	0.86	(26.4)	0.85	25.5	0.82	25.8	0.83		26.3	0.84	
Krypton		24.2	0.78		24.7	0.79			24.4	0.78	
Xenon		22.2	0.72		22.0	0.71			22.1	0.72	
Air 35.0	1.09	33.9	1.10	33.9	1.10	33.9	1.09		34.2	1.09	
Carbon dioxide		32.8	1.06	32.6	1.06				32.7	1.06	
Methane	0.94	27.3	0.89	26.8	0.87				28.1	0.90	
Ethylene				26.3	0.85	26.4	0.85		26.4	0.85	
Acetylene		26.1	0.84								
Pentane		24.6									

Table 2. Characteristic ampoule dimensions of BIPM/NIST (NBS) geometry. Reproduced from [372].

Characteristic dimensions of ampoules (type NBS) with standard deviations and their effect on the ionization current				
$\Delta_I^I (\%)$				
		(mm)	60 keV	1.25 MeV
Side wall thickness		0.642 ± 0.006	0.036	0.002 8
Bottom thickness	max (at center)	0.750 ± 0.025		
	min	0.510 ± 0.025	0.075	0.008 4
Inner diameter		15.16 ± 0.09	0.014	0.001 4
	sum (in quadrature)		0.084	0.008 9

Table 3. Measurement of impurities in a Tl-201 solution.¹ Reproduced from [99].

1

Symbols: $T_{1/2}$ half-life; E photon energy; N number of counts in the peak; p photon emission probability; η full-energy-peak efficiency; T measuring time (8000 s); C correction factor for pile-up and dead-time losses (1.139); activity $A = N \cdot C / (T \cdot p \cdot \eta)$; A_0 ^{201}Tl activity; Detector: Ge(Li), efficiency relative to NaI: 5.5%. (1)

Radio-nuclide	$T_{1/2}$	E keV	$N (10^3$ counts)	p	$\eta (\cdot 10^{-3})$	A (kBq)	A/A_0 (%)
^{201}Tl	73.1 h	68.9	overflow				
		70.8	overflow				
		80.3	overflow				
		135.3	995(2)	0.0272(4)	1.626(16)	3203(57)	100
		167.4	3322(4)	0.1040(10)	1.465(15)	3104(44)	
			(+165.9)				
^{200}Tl	26.1 h	367.9	118.2(4)	0.873(5)	0.636(7)	30.3(10)	1.0
		579.3	11.5(2)	0.138(7)	0.373(4)	31.8(17)	
		828.3	6.1(2)	0.108(7)	0.254(3)	31.7(23)	
		1205.8	11.2(2)	0.299(18)	0.174(2)	30.7(20)	
^{202}Tl	12.33	439.6	1.3(2)	0.914(10)	0.514(5)	0.39(6)	0.012
	d						
^{201}Pb	21.5 h	331.2	3.2(6)	0.80(5)	0.721(8)	0.79(15)	0.025
^{203}Pb	51.9 h	279.2	14.3(2)	0.806(10)	0.884(9)	2.86(6)	0.091

Table 4. Calculation of impurity corrections for ^{201}Tl . (PTB laboratory form).

Nuclide	Half-life in days	Impurity part in per cent at 08.02.1993	Efficiency = $1/k$	^{201}Tl
Tl-201	3.043	-	1/306.00	Solution 880-01
Tl-200	1.088	0.0953	1/43.632	Reference time 08.02.1993
Tl-202	12.23	0.203	1/102.94	0:00
Pb-201	0.392	0.000098	1/71.63	CET
Pb-203	2.1617	0.0398	1/133.85	Instrument IC2
Time t	Δt in days	Impurity part in per cent	Correction factor	(ionization chamber)
		Tl-200 Tl-202 Pb-201 Pb-203		
04.02.93 0:00	-4.	0.4899 0.1024 0.0465 0.0577	0.960885	
05.02.93 0:00	-3.	0.3254 0.1215 0.0099 0.0526	0.972708	
06.02.93 0:00	-2.	0.2161 0.1442 0.0021 0.0479	0.979791	
06.02.93 12:00	-1.5.	0.1761 0.1570 0.0010 0.0457	0.982216	

¹ Symbols: $T_{1/2}$ half-life; E photon energy; N number of counts in the peak; p photon emission probability; η full-energy-peak efficiency; T measuring time (8000 s); C correction factor for pile-up and dead-time losses (1.139); activity $A = N \cdot C / (T \cdot p \cdot \eta)$; A_0 ^{201}Tl activity; Detector: Ge(Li), efficiency relative to NaI: 5.5%.

07.02.93 0:00	-1.	0.1435	0.1711	0.0005	0.0437	0.984090
08.02.93 0:00	0.	0.0953	0.2030	0.0001	0.0398	0.986551
08.02.93 9:00	0.375	0.0817	0.2165	0.0001	0.0384	0.987120
09.02.93 0:00	1.	0.0633	0.2409	0.0000	0.0363	0.987723
10.02.93 0:00	2.	0.0420	0.2858	0.	0.0331	0.987947
12.02.93 0:00	4.	0.0185	0.4025	0.	0.0275	0.986299
15.02.93 0:00	7.	0.0054	0.6725	0.	0.0208	0.979580
18.02.93 0:00	10.	0.0016	1.1236	0.	0.0157	0.967239

Table 5. Calibration nuclides and data for an aluminium well ionization chamber with and without an Fe absorber. Reproduced from [395].

Nuclide	E (keV)	p	ε_N	ε (GBq $^{-1}$)	$\varepsilon_N^{\text{abs}}$	ε^{abs}	Comments
^{60}Co	1252.9	1.999	76.3	38.2	76.3	38.2	(a)
^{54}Mn	834.8	1.000	28.3	28.3	28.3	28.3	-
^{22}Na	511.0	1.798	72.7	19.0	72.7	19.0	1274.5 keV ^(b)
^{85}Sr	514.0	0.984	18.4	18.7	18.4	18.7	868.5 keV ^(b)
^{65}Zn	1115.5	0.504	18.0	34.7	18.0	34.7	511.0 keV ^(b)
^{58}Co	810.8	0.995	33.1	27.1	33.1	27.1	3γ s ^(b)
^{88}Y	1836.1	0.994	78.9	50.8	78.9	50.8	2γ s ^(b)
^{24}Na	2754.1	0.999	111.6	70.9	111.6	70.9	1368.5 keV ^(b)
^{51}Cr	320.1	0.098	1.28	13.0	1.28	13.0	-
^{57}Co	123.6	0.962	11.2	11.6	9.52	9.9	692.0 keV ^{(b)(a)}
^{139}Ce	165.9	0.800	23.9	10.6	7.87	9.6	(c)
^{141}Ce	145.4	0.489	8.95	10.9	4.81	8.6	(c)
^{99m}Tc	140.5	0.890	9.79	11.0	8.73	9.8	-
^{241}Am	59.5	0.360	8.15	21.9	2.47	6.9	(c)
^{210}Pb	46.5	0.042	1.21	27.0	0.17	4.0	(d)
^{207}Bi	76.6	0.752	61.8	16.9	56.0	9.4	X-ray ^{(a)(b)}
^{203}Hg	279.2	0.813	11.8	11.8	10.7	11.7	74.5 keV ^(b)
^{137}Cs	32.9	0.068	21.1	17.9	19.8	0.0	661.7 keV ^{(b)(a)}
^{125}I	28.4	1.465	17.3	11.8	0.0	0.0	(a)(c)
^{113}Sn	24.7	0.967	14.3	4.3	10.1	0.0	^(a) 2γ s ^{(b)(c)}
^{109}Cd	22.6	1.02	3.27	2.7	0.37	0.0	(a)
							88.0 keV ^{(b)(c)}

(a) The weighted average of the γ - or X-ray energies has been used;

(b) One or more $p\varepsilon$ have been subtracted (see text);

(c) X-rays are reduced or absorbed to zero by the absorber;

(d) Corrected for bremsstrahlung.

Table 6. Calibration nuclides and deviations for the ionization chamber of the SIR. Reproduced from [122].

No.	Radionuclide	A	A_{exp}	$100 - (A - A_{\text{exp}})/A$	A_{exp}	$A = 1/R$	is the experimentally measured equivalent activity; is the calculated
1	^{22}Na	7531.1	7525.8	0.07			
2	^{44}Sc	8315.9	8325.9	-0.12			

3	⁴⁷ Sc	165542.4	164691.5	0.52		
4	⁵¹ Cr	486948.4	488199.0	-0.26	$R = \sum_i Y_i r(E_i)$	equivalent activity;
5	⁵⁴ Mn	19228.9	19231.1	-0.01		is the calculated radionuclide response
6	⁵⁸ Co	16284.6	16282.0	0.02		of the SIR chamber;
7	⁶⁵ Zn	29316.1	29671.0	-1.2		
8	⁸⁵ Sr	29771.2	30019.7	-0.83	$r(E) = \sum_{i=0}^3 a_i E^i$	is the energy response
9	⁹⁵ Nb	20697.6	20644.6	0.26		of the SIR chamber;
10	¹¹¹ In	42573.3	42857.0	-0.66		
11	¹¹³ Sn	59071.5	58891.0	0.31		
12	¹³⁹ Ce	132951.8	133620.0	-0.5		
13	²⁴ Na	4962.3	4963.3	-0.02		
14	⁵⁷ Co	169515.3	168685.0	0.5	$a_0 = -0.430 \times$	
15	⁵⁹ Fe	14620.2	14650.6	-0.21	$a_1 = 8.6928 \times 10^{-5}$	
16	⁶⁰ Co	7046.8	7054.7	-0.11	$a_2 = -2.7199 \times$	
17	⁸⁸ Y	6914.2	6900.4	0.20	$a_3 = 0.4647 \times$	
18	¹³³ Ba	44005.0	44033.6	-0.07		
19	⁶⁷ Ga	116399.2	115605.4	0.70		
20	⁷⁵ Se	42997.2	42911.0	0.20		
21	¹⁵⁴ Cs	10119.2	10096.2	0.23		
22	²⁰³ Hg	68071.1	67574.7	0.88		
23	¹⁴¹ Ce	263324.8	265300.0	-0.80		
24	¹⁰⁹ Cd	8356947.5	8162400.0	2.3		
25	¹²³ I	121982.1	119686.6	2.4		
26	¹⁰³ Ru	31255.0	30355.0	3.0		
27	¹³¹ I	40236.0	40420.0	-0.46		

Table 7. Calculation of nuclide efficiency ε from emission probability per decay p_i and photon efficiency ε_i for Ir-192. (PTB laboratory form).

Calculated by the program NUKEF2: 01.07.1993					
Ionization chamber		Files		Nuclide	
IC02	KAMM02	EWGR89	EA02	Ir-192	
index i	Type	Energy/keV	p_i	ε_i	$p_i \cdot \varepsilon_i$
1	L Os	9.87	0.0138	0.	0.
2	L Pt	10.52	0.0383	0.	0.
3	K Os	61.49	0.0115	0.074260	0.000854
4	K Os	63.00	0.0199	0.079192	0.001576
5	K Pt	65.12	0.0256	0.085679	0.002193
6	K Pt	66.83	0.0435	0.090976	0.003957
7	K Os	71.30	0.0068	0.104307	0.000709
8	K Os	73.40	0.00184	0.109677	0.000202
9	K Pt	75.70	0.0148	0.115173	0.001705
10	K Pt	77.90	0.0044	0.119659	0.000526
11		136.34	0.00183	0.147790	0.000270
12		201.31	0.00472	0.169895	0.000802
13		205.80	0.0330	0.171804	0.005670
14		283.27	0.0262	0.208150	0.000545
15		295.96	0.2867	0.214874	0.061604

16	308.46	0.300	0.221569	0.066471
17	316.51	0.8281	0.225918	0.187083
18	374.49	0.00721	0.258258	0.001862
19	416.47	0.00664	0.282453	0.001875
20	468.07	0.4783	0.313576	0.149983
21	484.58	0.03184	0.323830	0.010311
22	489.04	0.00443	0.326622	0.001447
23	588.58	0.04515	0.383647	0.017322
24	604.41	0.0823	0.392334	0.032289
25	612.47	0.05309	0.396644	0.021058
26	average	672.30	0.00180	0.428822
27		884.54	0.00292	0.537449
Calculated:		$k = 37/\varepsilon = 64.6113$	$\varepsilon = \text{sum} (p_i \cdot \varepsilon_i) = 0.572\ 656$	
Experimental:		64.4460		0.574 124
Deviation:		0.26%		

Table 8. Comparison of calculated and measured nuclide efficiencies.
Reproduced from [395].

Comparison of calculated and measured nuclide efficiencies of radionuclides with complex decay scheme

Nuclide	Without absorber			With Fe-absorber		
	ε_N (GBq ⁻¹)	Calculated	Measured	$\varepsilon_N^{\text{abs}}$ (GBq ⁻¹)	Calculated	Measured
^{110m} Ag	90.7	91.3	-0.7	90.7	91.8	-1.2
¹²⁴ Sb	57.5	58.4	-1.5	57.5	57.9	-0.7
¹³¹ I	15.8	15.7	0.6	14.9	14.7	1.1
¹³³ Ba	38.9	39.0	-0.2	17.0	16.7	1.8
¹³⁴ Cs	53.9	54.0	-0.2	53.8	53.7	0.2
¹⁵² Eu	57.6	56.4	2.1	40.3	39.3	2.5
²⁰¹ Tl	18.5	18.6	-0.5	9.71	9.91	-2.0

Table 9. Uncertainty components $\sigma(Q_j)$ for ionization-chamber measurements with an instrument of good quality (relative values in per cent).

Component	Name	Value
Statistics	$\sigma_{\text{star}}(I)$	5.0 + 0.005
charge formation		(from low to high activity)
charge collection		
Current measurements	$\sigma_{\text{meas}}(I)$	-
saturation loss		very large to 0.005 (from high to low activity)
leakage currents		0.005
instable electronics		10.0 to 0.01 (worst case to optimum)
Linearity of instrument (data evaluation with reference source)	$\sigma_{\text{lin}}(I)$	0.05 (if I_{sample}/I_r near to one)

Influence of reference source	$\sigma(I_r)$	0.05
non-equilibrium		(optimum conditions)
half-life		
leakiness		
Background	$\sigma(I_b)$	0.05
shielding		(without statistics and
radon, etc.		varying external sources)
Sample conditions	$\sigma(C_s)$	0.005
chemical stability, plate out		(optimum conditions)
leakiness		
Geometry	$\sigma(C_g)$	3.0 to 0.01
repeatability of position		(worst case to optimum)
filling corrections		
change of form, dimensions, materials		
Radionuclidic impurities	$\sigma(C_i)$	5.0 to 0.3 (depending on radionuclide)
Time measurements	$\sigma(t)$	-
measuring time		0.01
clock accuracy (date)		0.01
time-scale changes and adjustments		5.0 to 0.005 (worst case to optimum)
Half-life	$\sigma(T_{1/2})$ for 0.1% in $T_{1/2}$	→ 0.07% per $T_{1/2}$
Calibration		-
from direct standardization	$\sigma(A_{\text{standard}})$	1.5 to 0.3
indirect from other IC		2.0 to 0.5
by calculated efficiency	$\sigma(p(E_i), \varepsilon(E_i))$	5.0 to 0.5 (worst case to optimum)
(depending on radionuclide and available data)		

Table 10. Cs-137 half-life results. Reproduces from [225].

Measured values		Reference
Value (in days)		
10 968 ± 5	[492]	
11 206 ± 8	[493]	
11 009 ± 11	[220]	
10 906 ± 33	[494]	
11 034 ± 29	[495]	
11 021 ± 5	[496]	
11 023 ± 37	[497]	
11 191 ± 157	[498]	
10 921 ± 17	[499]	

Recommended value:
 $1.102 \times 10^4 \pm 0.006 \times 10^4$ d
Evaluated by K. Debertin
(PTB, Braunschweig, FRG)
and M. J. Woods (NPL,
Teddington, UK)

$11\ 023 \pm 55^{(a)}$ Weighted mean

(a) Uncertainty increased to include lowest uncertainty value.

Table 11. Results of activity measurements for ^{192}Ir with the SIR. Reproduced from the SIR files by BIPM (1993), Sèvres (France).

BIPM, F-92310 SEVRES

International Reference System for the Activity

Measurement of Gamma-Ray Emitting Nuclides (SIR)

Radionuclide: ^{192}Ir Total number of withdrawn results:

Half life adopted:

$$T_{1/2} = (74.02 \pm 0.18) \text{ d}$$

Data reported by laboratory Ionization-chamber measurements
carried out at BIPM

Activity A_e
which would
produce the same
ion current as the
Ra source

Laboratory	Ampoule	Metho	Reference	Activity	Rel. uncert.	Date	Relative	A_e	Combined
	number	of	date	at ref.	Category		uncertainty	uncert. of A_e	
				standardization	date (A (($r_3, \%$)	($A_e(r_1^2 + r_2^2 + r_3^2)^{1/2}$)	
					kBq)	$r_1,$	$r_2,$	kBq)	
						(%)	(%)		
UVVVR	ERX	$4\pi\beta-\gamma$	78-12-13	4 031	0,1	0,6	79-	0,13	19 119
	500-07						01-		163
							23		
LMRI	81	$4\pi\gamma$	81-11-25	3 317	0,07	0,17	81-	0,10	18 39
	84			3 334	0,07	0,17	23	0,10	18 39
								958	
OMH	6627	$4\pi(\beta, \gamma)$	70-01	4 234	0,03	0,38	84-	0,06	18 74
		coincidence					01-		906
							04		
NPL	A113-90	high-pressure	90-05-30	2 661	0,069	0,673	90-	0,069	19 131
	A114-90	ioniz. chamber		2 606	0,069	0,673	29	0,068	241
		calibrated by absolute standardization							19 131
BCMN	9008	$4\pi\beta-\gamma$	90-09-01	3 312	0,040	0,290	90-	0,089	18 58
	9009	coinc.					09-		880
				3 314	0,040	0,290	25	0,092	18 58
		$4\pi\gamma$ -count. and spectrometry						877	

		using							
		an							
		open							
		$4\pi\text{CsI(Tl)}$							
		sandwich							
		detector							
PTB	92-	high-	92-09-01	746	0,048	0,480	92-	0,104	1893
	351A	pressure					09-		934
		ioniz.				21			
		chamber							
		calibrated							
		by							
		$4\pi - \gamma$							
		NaI							
		activity							
		measurements							
		and							
		LSC							
		(CIEMAT-							
		NIST							
		method)							

13. Figures

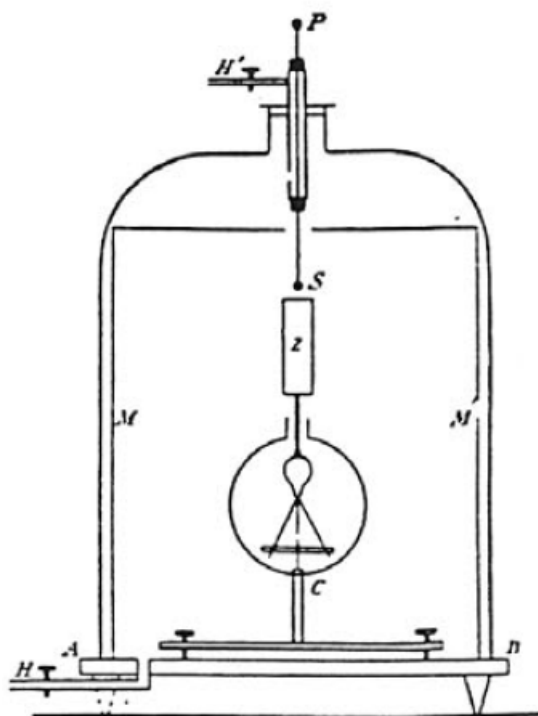


Figure 1-1 — Vessel with electrode (MM') and electroscope (Z) to study the "radioactive emanation" in air. Reproduced from [129].

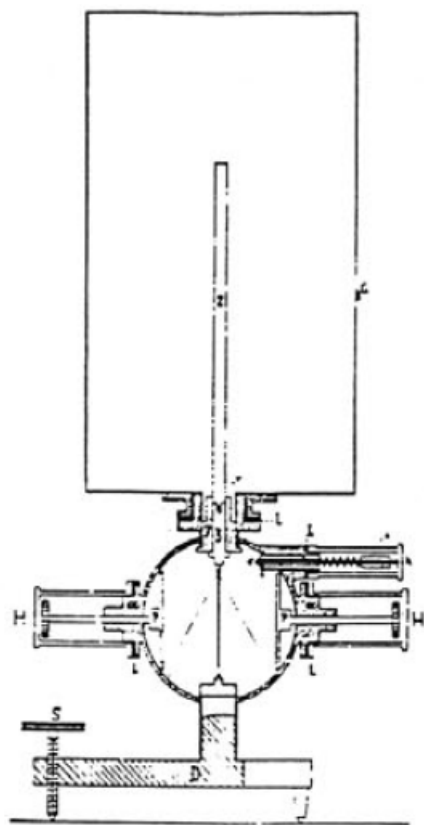


Figure 1-2 — Early ionization chamber (improved model of Figure 1-1 with a closed vessel). Reproduced from [131].

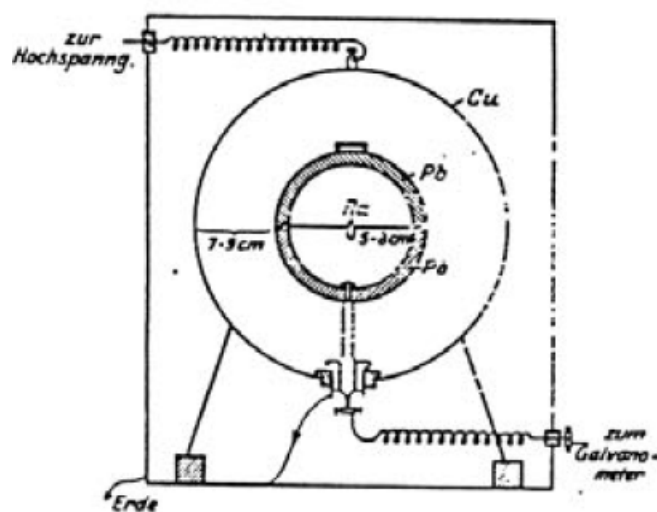


Figure 2-1 — Early spherical ionization chamber with a Ra source inside (zur Hochspannung ⇒ to high-tension, Erde ⇒ earth, ground potential, zum Galvanometer ⇒ to galvanometer). After Meyer and Hess ([308], see p. 184), reproduced from [260].

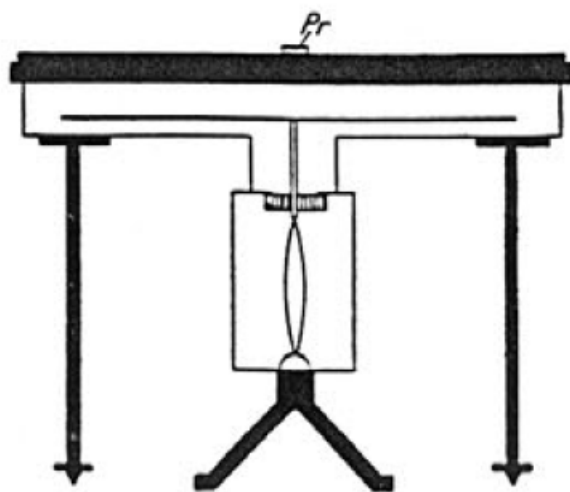


Figure 2-2 — Parallel-plate capacitor with electrometer to compare the activity of γ -ray emitting sources (Pr). After Curie ([87], see p. 170), reproduced from [260].

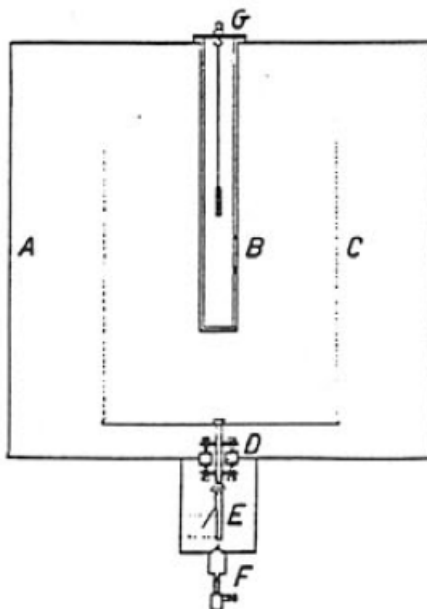


Figure 3-1 — Early re-entrant well ionization chamber with electrodes (A, B, C), amber insulator (D) and gold-leaf electrometer (E, F), source suspended on G, constructed by Bothe at the PTR in 1921. Reproduced from [153].

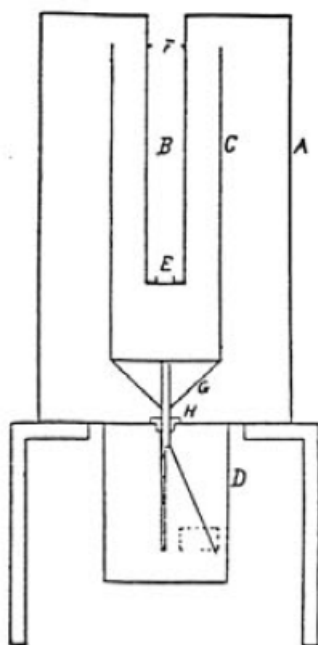


Figure 3-2 — Triple cylinder electroscope to measure sealed radium sources positioned at E within a re-entrant well (B) lined with lead. Reproduced from [117].

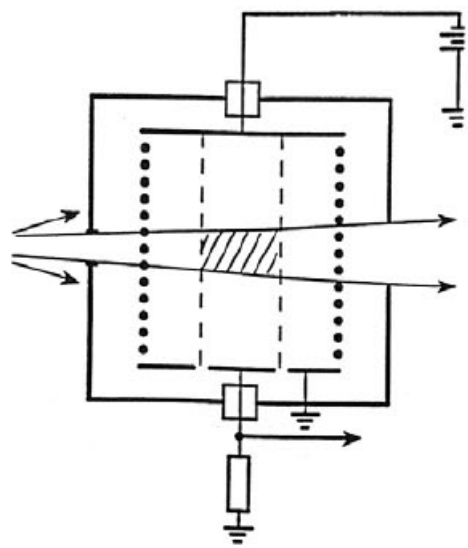


Figure 4-1

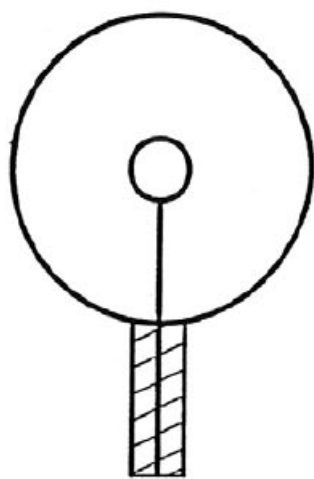


Figure 4-2



Figure 4-3

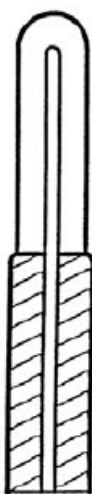


Figure 4-4

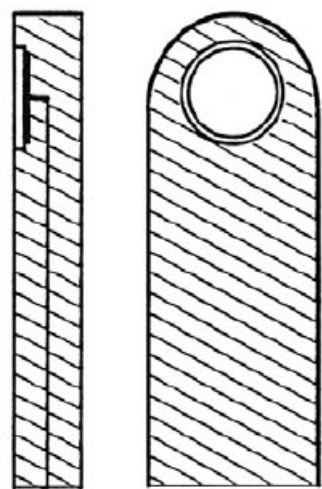


Figure 4-5

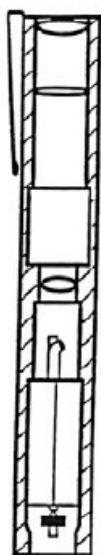


Figure 4-6

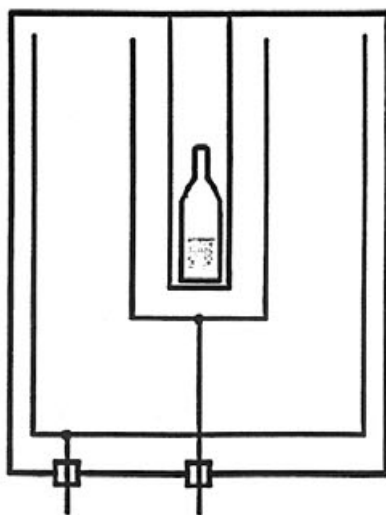


Figure 4-7

Figure 4 — Ionization chamber (IC) designs for various applications. Primary standard measuring systems for dosimetry quantities: a) parallel-plate free air IC, b) spherical IC and c) cylindrical IC. Field instruments for dosimetry measurements: d) compact thimble IC, e) flat IC and f) personal dosimeter. g) Re-entrant well IC for activity measurements. Reproduced from [266].

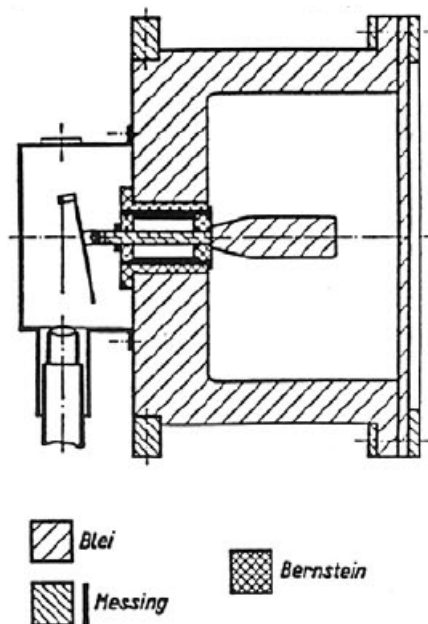


Figure 5 — Ionization chamber for external source positions with lead entrance window (Blei ⇒ lead, Messing ⇒ brass, Bernstein ⇒ amber). Reproduced from [264].

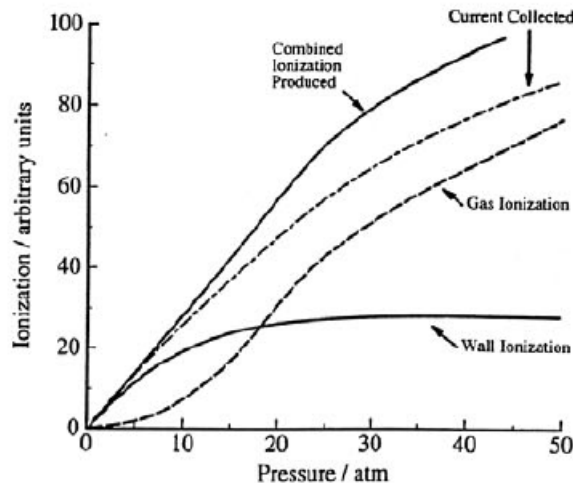


Figure 6 — Charge formation (ionization) and collection, with varying gas pressure in a highpressure ionization chamber with the two main components from the gas and the walls. After Boag ([30], see p. 166).

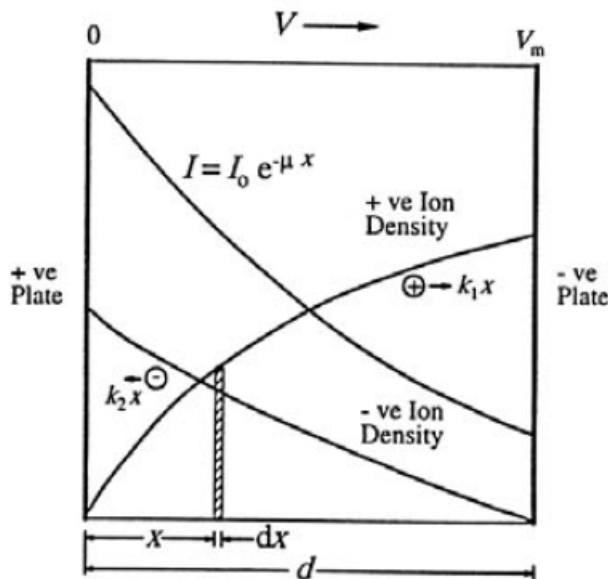


Figure 7 — Charge formation and density in a plane-parallel geometry chamber as a function of distance x measured from the electrode where the beam enters the gas space. I ionization intensity, μ attenuation coefficient, k_1 and k_2 ionic mobilities, V collecting voltage and d distance between plates. After Boag ([31], see p. 167).

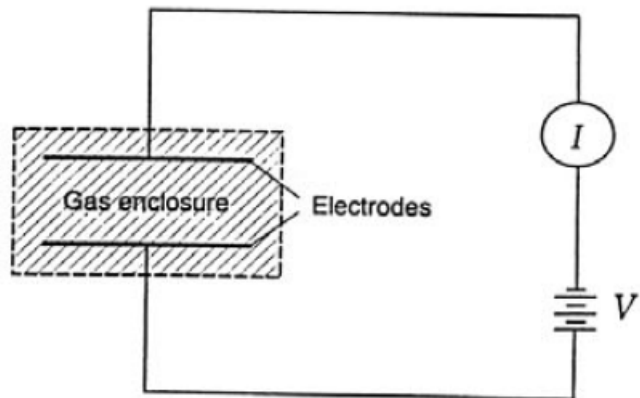


Figure 8-1

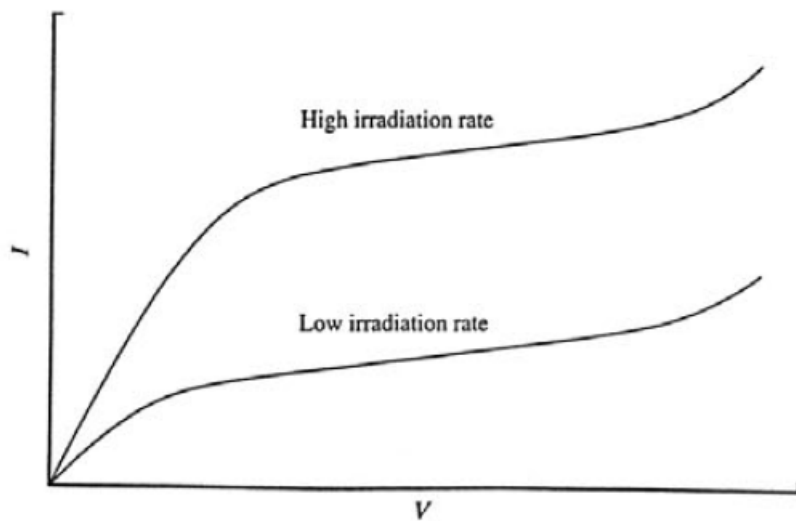


Figure 8-2

Figure 8 — The basic components of an ionization chamber measuring system and the corresponding current-voltage characteristic curve. After Knoll ([258], see p. 181).

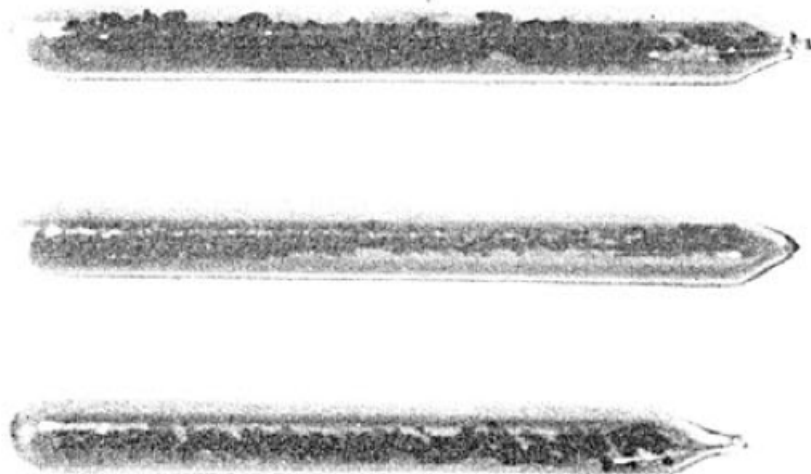


Figure 9 — Three ^{226}Ra standards prepared by Hönigschmid in 1934, from top to bottom no. 5437 (NIST), no. 5440 (NIST) and no. 5426 (PTB), in the chemical form of radium chloride sealed in glass vials. Reproduced from [295].

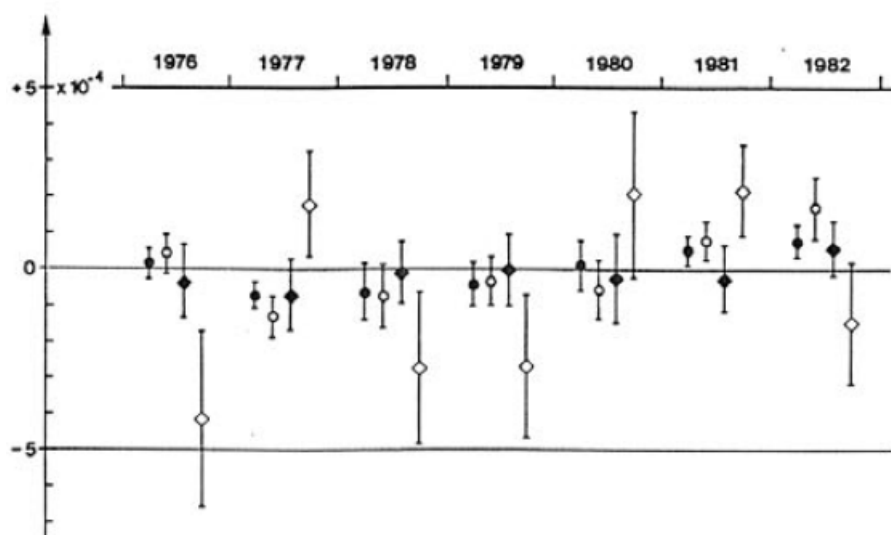


Figure 10-1 — Mean values and their uncertainties derived from periodic measurements of the ratios of reference sources no. 1 to 5, with relative deviations from the general mean for the SIR. • nos. 5/4, o 4/3, ♦ 3/2 and ◇ 2/1, respectively. Reproduced from [376].

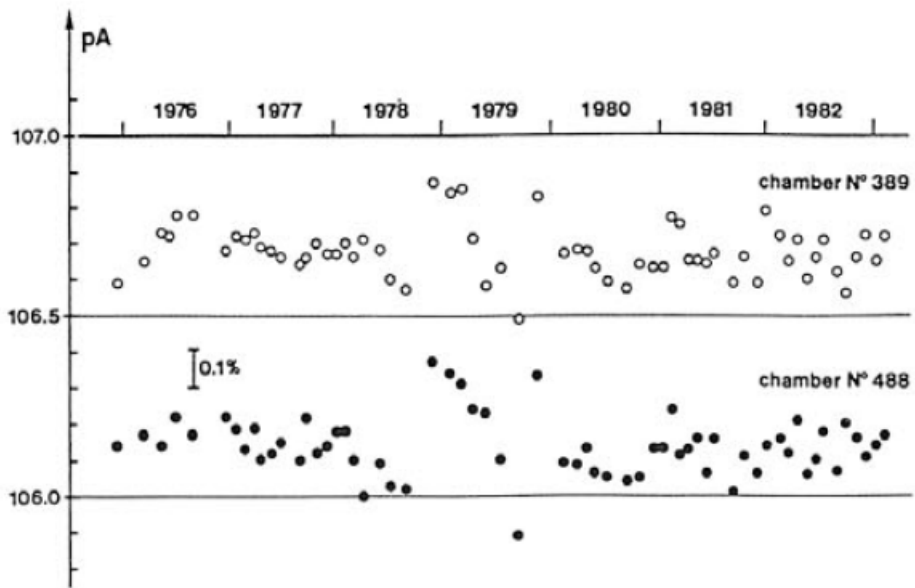


Figure 10-2 — Periodic measurements of the ionization current produced by reference source no. 2, placed in either of the two chambers of the SIR. Reproduced from [376].

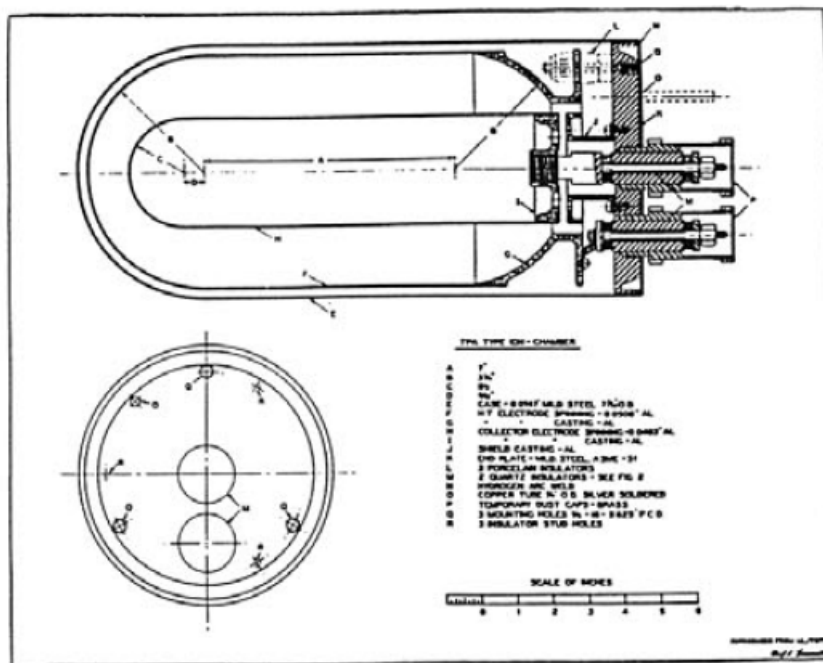


Figure 11 — Scale drawing of the TPA type ionization chamber at AECL (Chalk River). The chamber is tested to be filled with a gas up to a pressure of 20 atmospheres. Reproduced from [65].

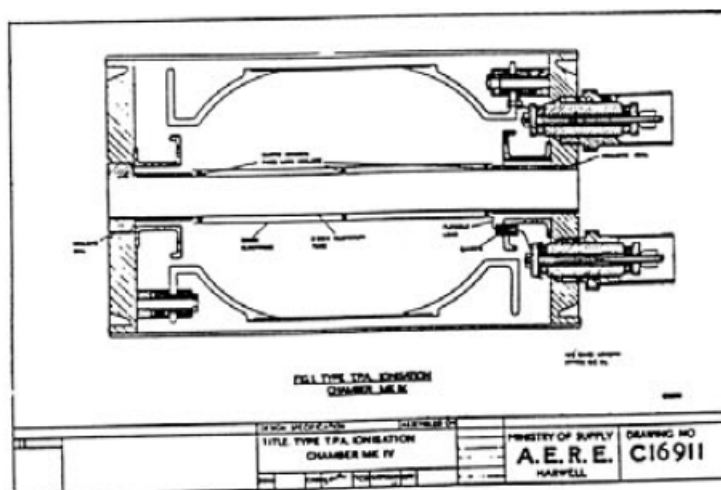


Figure 12 — Drawing of the TPA type Mk IV ionization chamber at AERE, Harwell, UK., constructed with thin aluminium walls and filled with argon to a pressure of one atmosphere. Reproduced from [458].

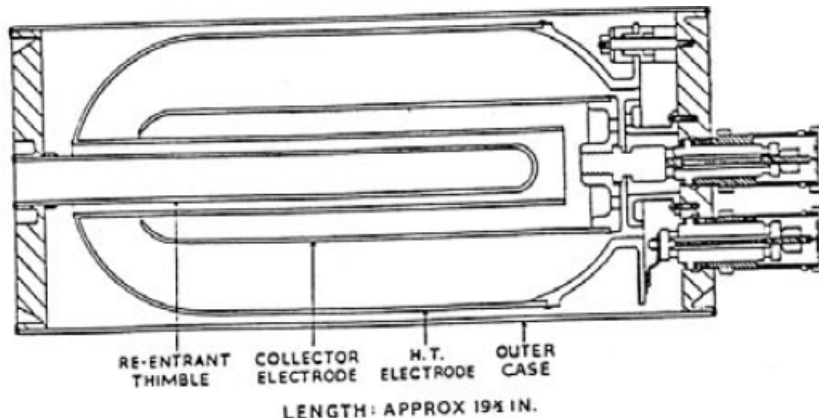


Figure 13 — General arrangement of the redesigned TPA type Mk 2 chamber. The re-entrant thimble for sample insertion and the position of the electrodes can be seen. The chamber is filled with argon of 99.8% purity to a pressure of 20 atmospheres. Reproduced from [406].

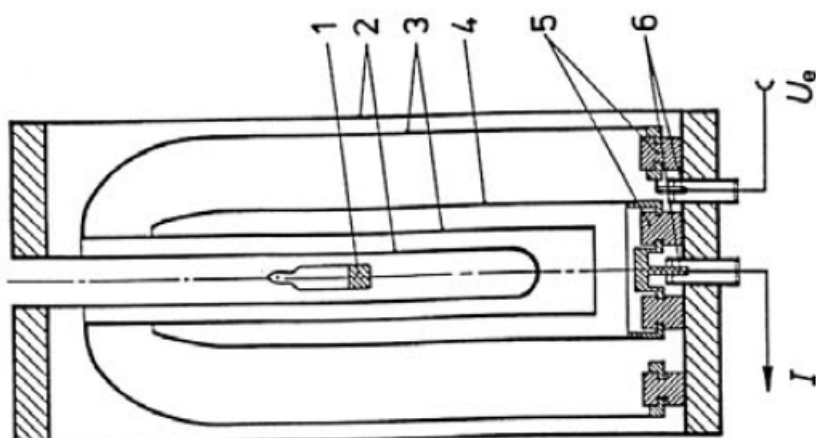


Figure 14 — Ionization chamber type IG 12 of Centronic (20th Century Electronics Ltd., UK.). The construction has steel walls (2), aluminium electrodes (3,

4), a re-entrant tube length of 12.56", an inside diameter of the well of 2.00" and a gas filling of 20 atmospheres (argon). The chamber is tested for an inter-electrode voltage up to 2000 V with the connectors (6) and insulators shown (5), the normal running voltage U_e is 500 V. A typical ampoule position (1) is given. (Schematic drawing from PTB).

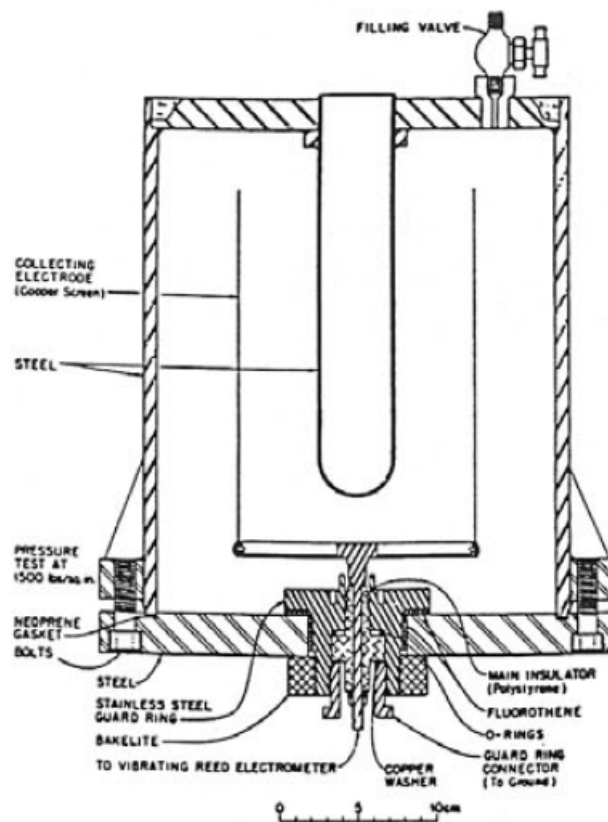


Figure 15 — High-precision, high-pressure ionization chamber by Shonka and Stephenson ([408], see p. 190). The chamber is filled with 40 atmospheres of dry argon. Reproduced from [326].

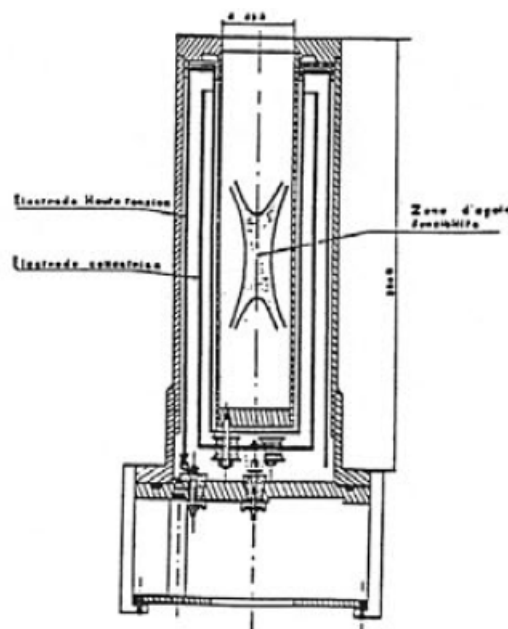


Figure 16 — Pressurized re-entrant ionization chamber filled with argon. The indicated zone in the well represents a cylinder of 4 cm diameter and 11 cm high with nearly constant efficiency values (variation within 1%). Reproduced from [187].

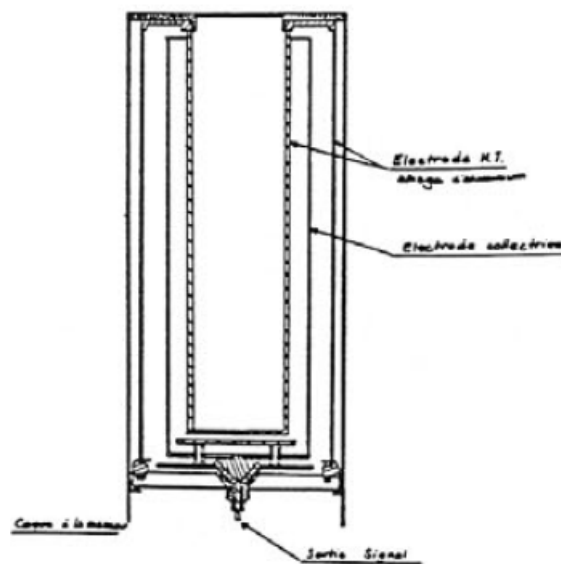


Figure 17-1 — Re-entrant ionization chamber used at LPRI, France.

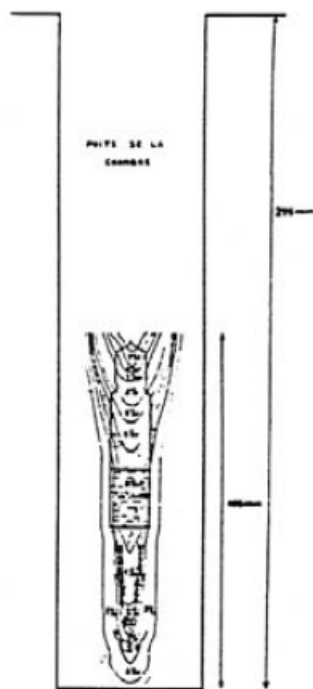


Figure 17-2 — With a map of zones of equal efficiency values. The position of a typical ampoule filled with radioactive solution is marked inside the chamber well. Reproduced from [27].

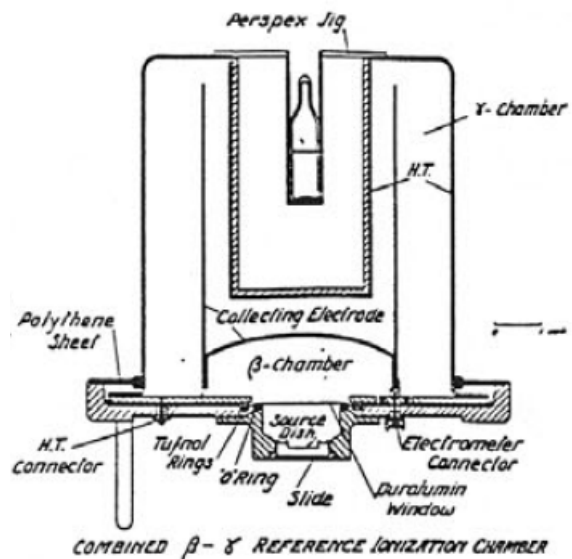


Figure 18 — Combined β - γ reference ionization chamber constructed at NPL. The ampoule position with γ -ray emitting solution is shown in the perspex jig, a β -particle emitting source may be placed on the source dish in the bottom of the chamber below a thin duralumin entrance window [355]. The sensitivity of this chamber was studied in detail by Dale et al. ([91], see p. 170). Reproduced from [316].

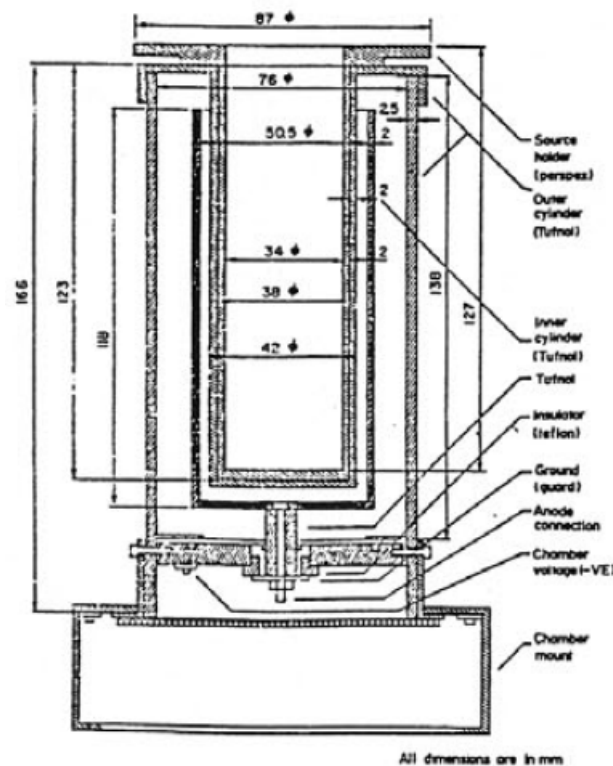


Figure 19 — Drawing of a radionuclide calibrator with a re-entrant air-equivalent chamber constructed from readily available plastic tube materials. A special conductive coating by colloidal graphite has been applied to the electrodes of the chamber. Reproduced from [386].

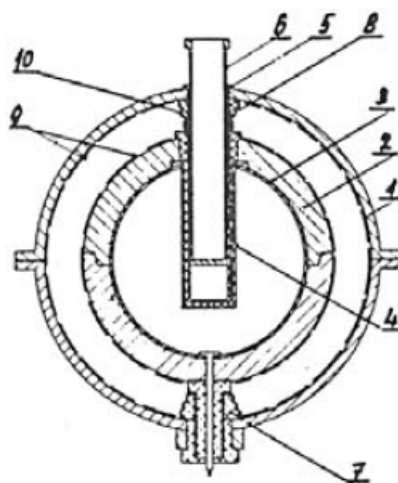


Figure 20 — Spherical $4\pi\gamma$ -ionization chamber constructed from plastic materials (1, 2) coated with graphite varnish and permitting the introduction of lead or aluminium filters (3). The source is positioned inside a thin metal tube (4). Reproduced from [53].

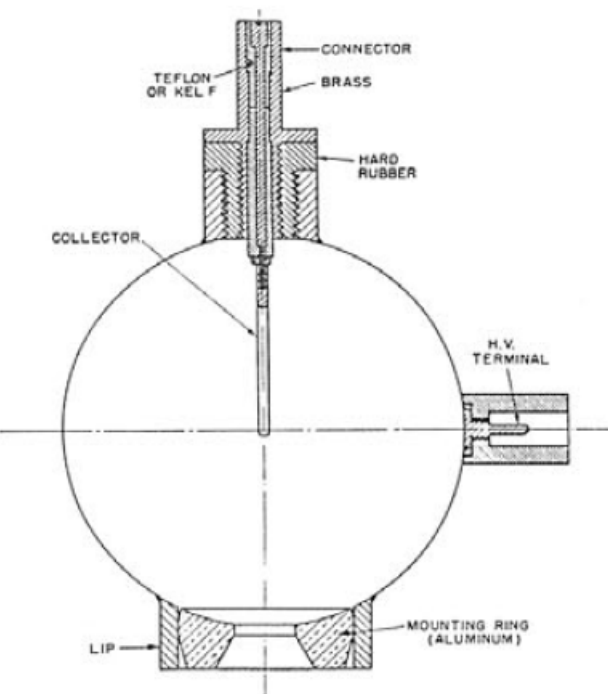


Figure 21 — Schematic drawing showing the construction of the $2\pi\beta$ -ionization chamber at NBS (NIST) with the source mounting at the base of the sphere. Reproduced from [403].

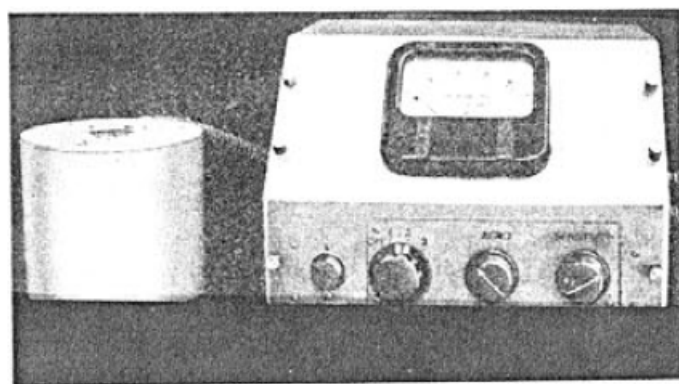


Figure 22-1

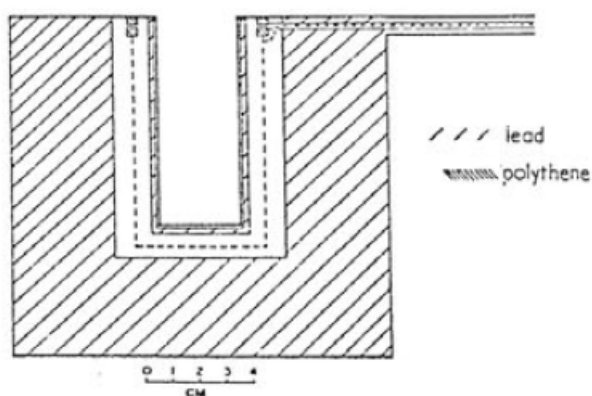


Figure 22-2

Figure 22 — One of the very early radionuclide calibrators with a direct reading for measurements of highly active samples from the field of nuclear medicine.
Reproduced from [414].



Figure 23-1

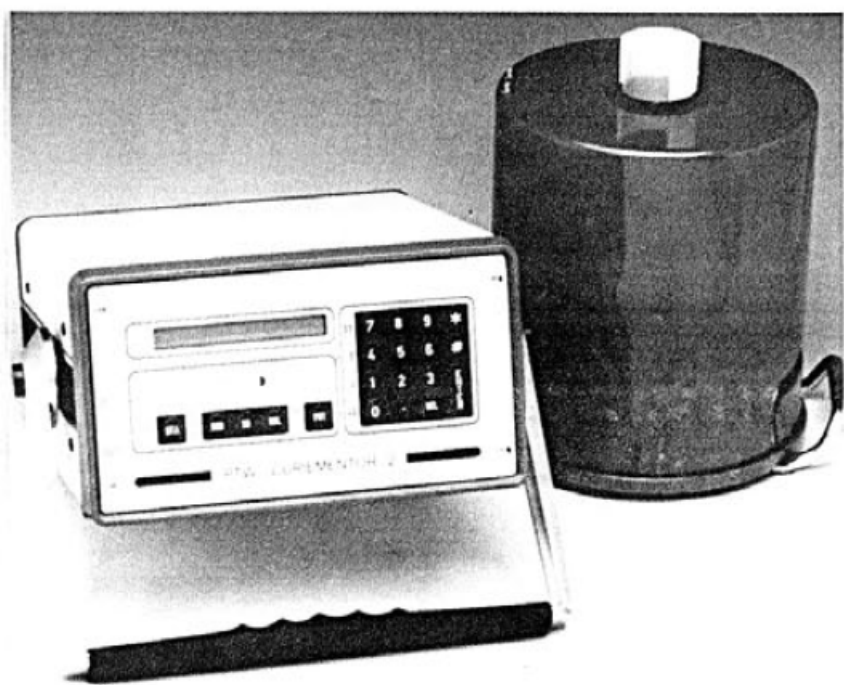


Figure 23-2

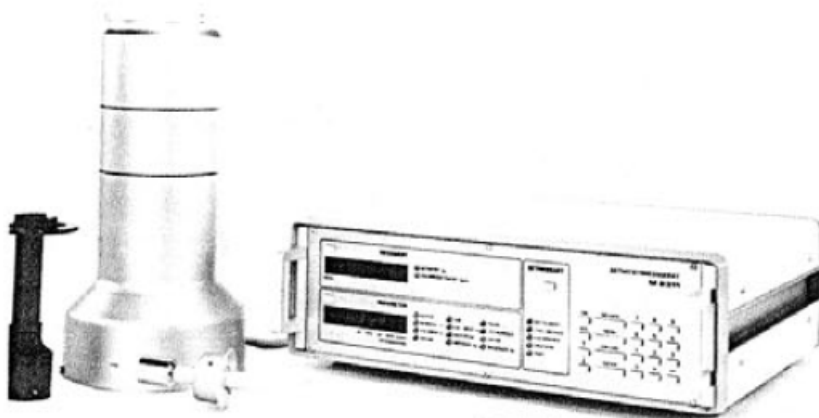


Figure 23-3



Figure 23-4

Figure 23 — Modern designs of radionuclide calibrators from: a) Capintec,
Pittsburgh, USA; b) PTW, Freiburg, Germany; c) Meßelektronik,
Dresden, Germany and d) NE Technology (Vinten), Reading, England.
Reproduced from [398].

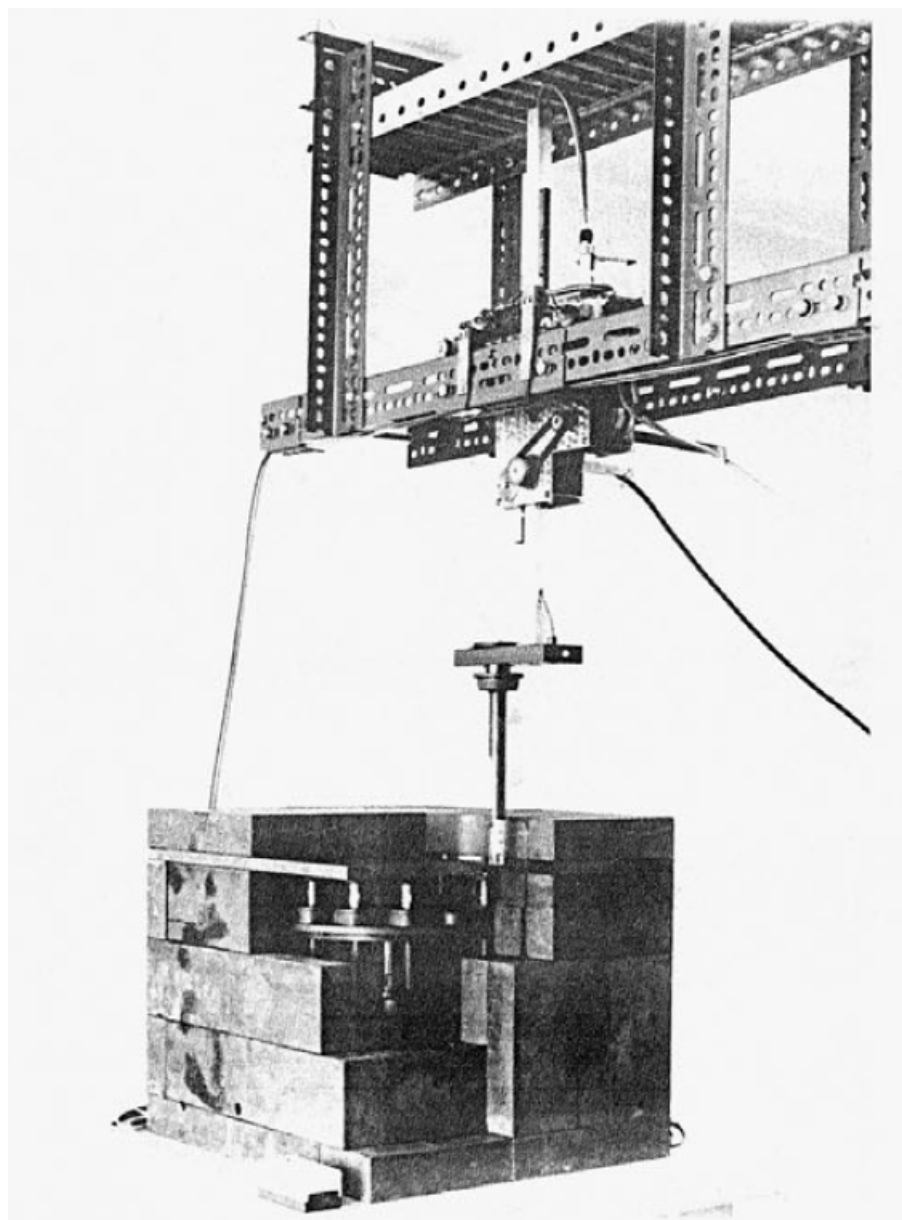


Figure 24-1 — Near the sample reservoir.

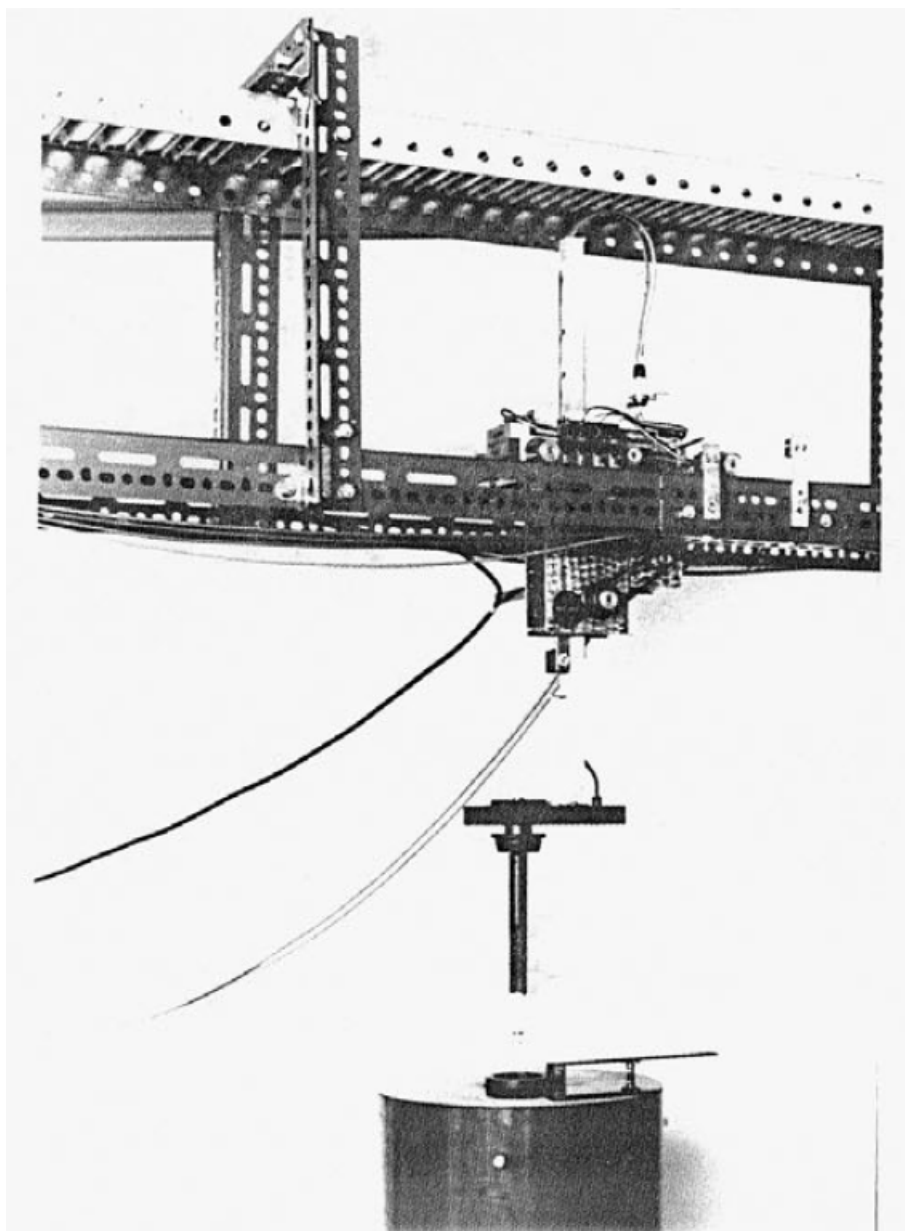


Figure 24-2 — Above the ionization chamber.

Figure 24 — Automatic sample changer with the trolley and source lift moving on rails (photographs, PTB).

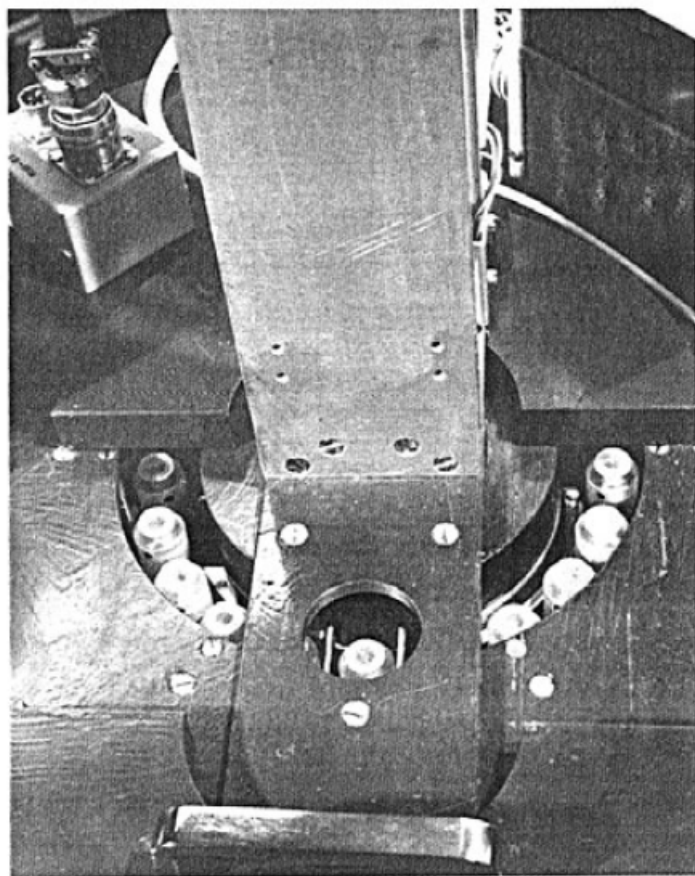


Figure 25-1

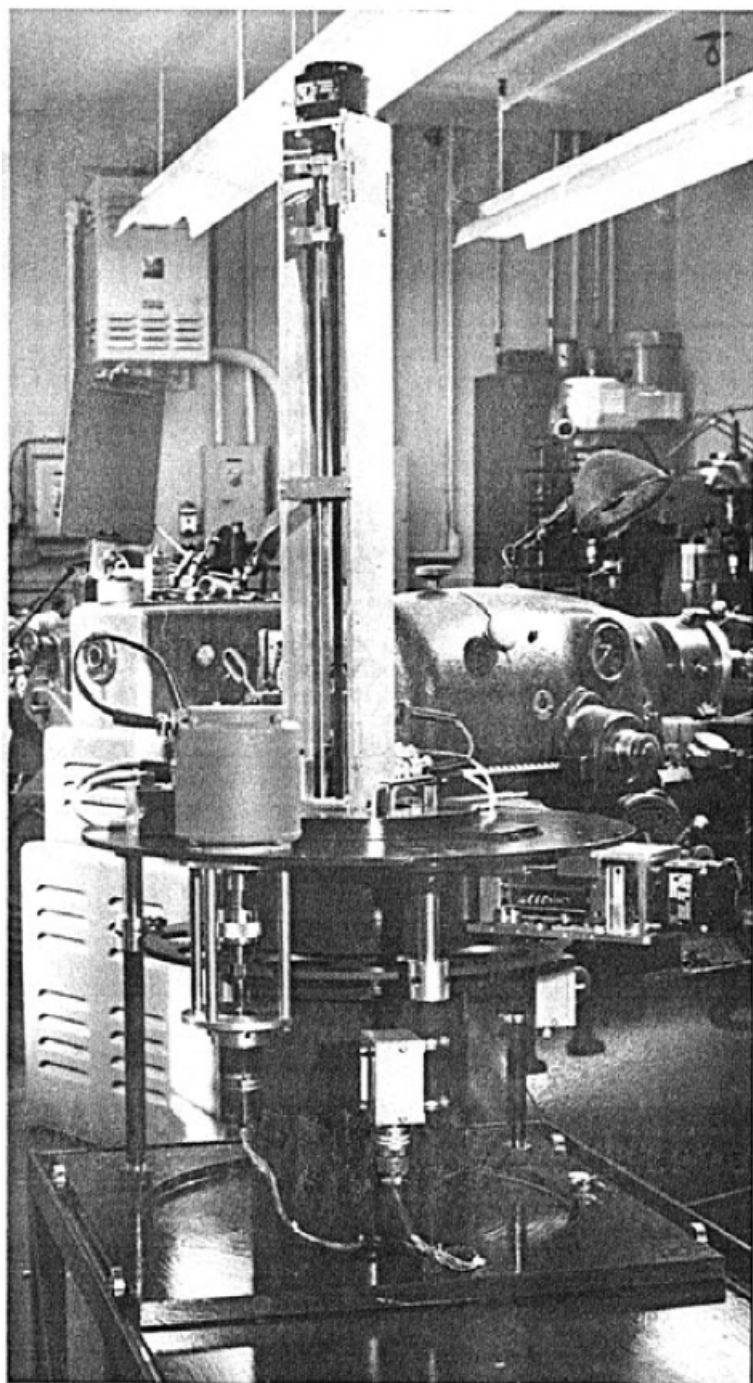


Figure 25-2

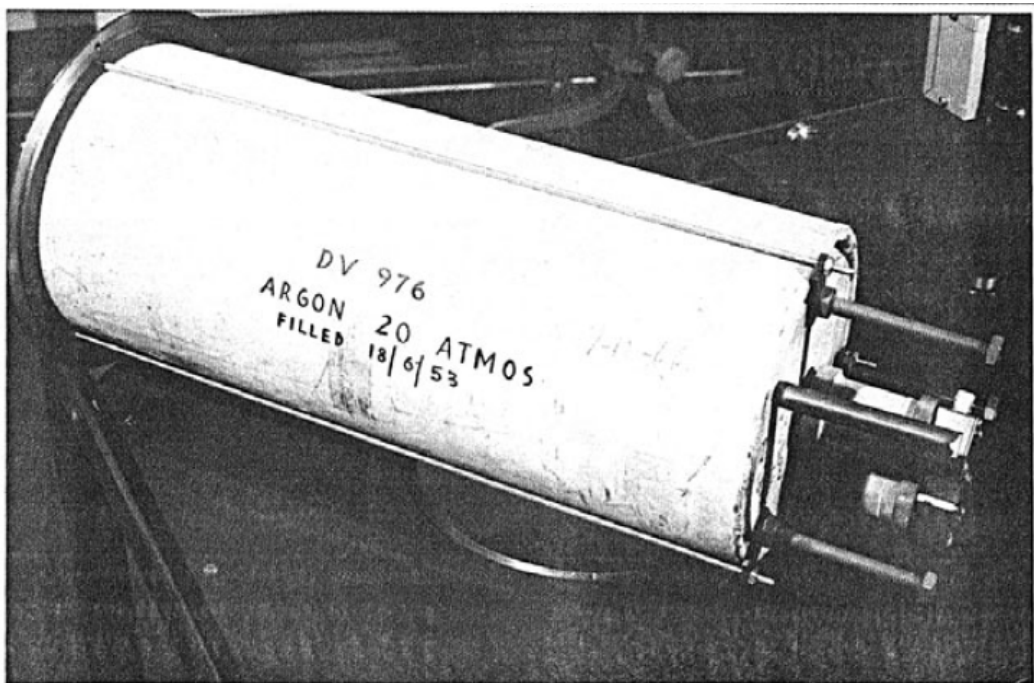
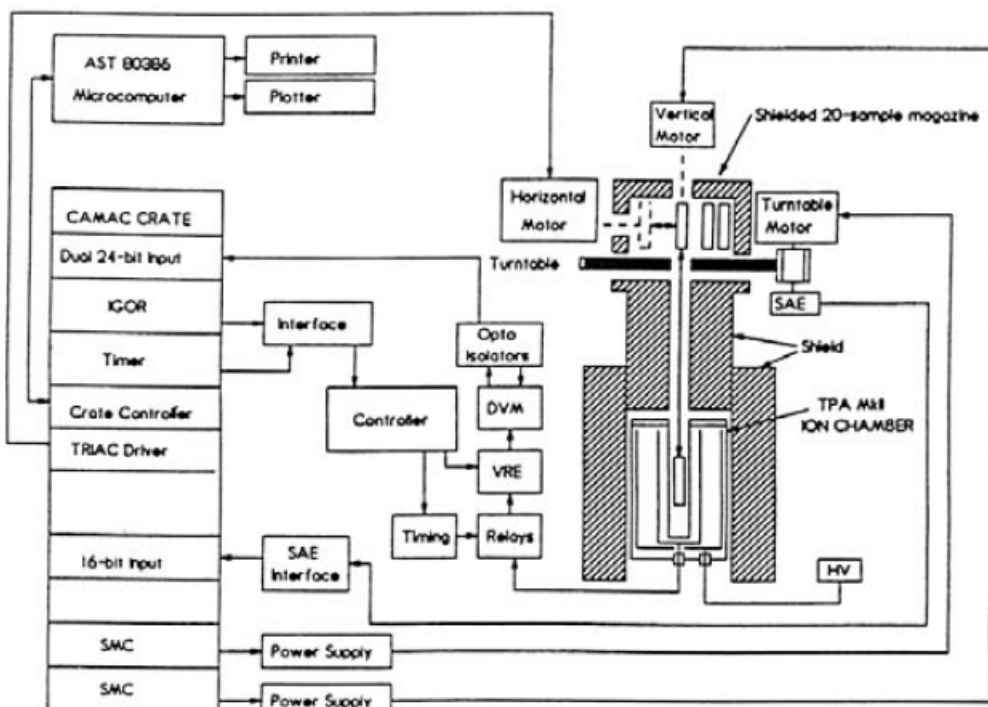


Figure 25-3



1991 Ion Chamber Sample Changer System

Figure 25-4

Figure 25 — Automatic sample-changer system (AECL, Chalk River) with a reservoir a), centered and shielded on top of the ionization chamber c). A general view is given in b) and a schematic drawing with the control electronics in d). Property of AECL Research, used with permission, from [300].

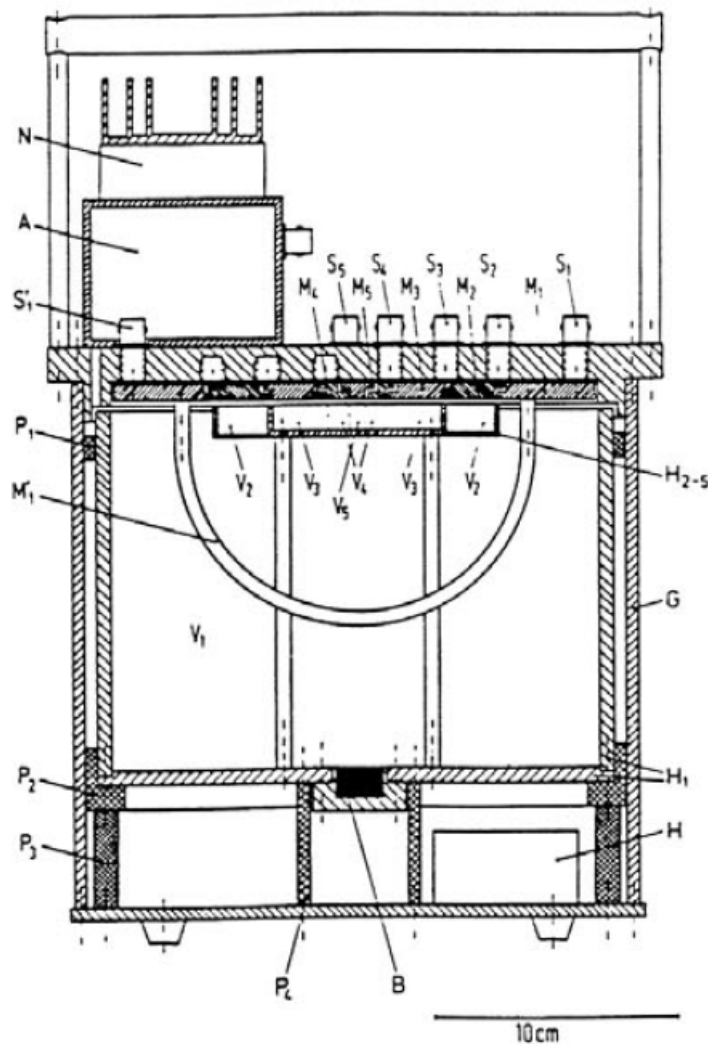


Figure 26 — Sectional drawing of a reference current source using the ionization from β radiation (B) with sensitive volumes V_j and electrodes M_j and H_j (high tension), connected via the plugs S_j to an amplifier A and electronics N. P_j and G are housing materials. Reproduced from [36].

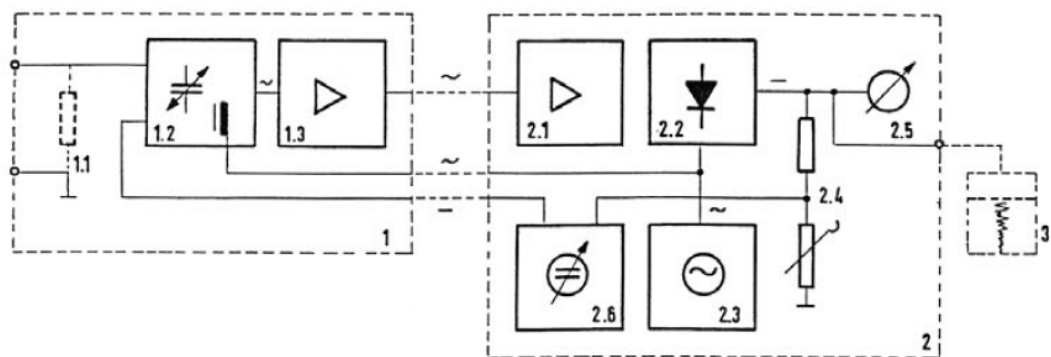


Figure 27 — Diagram of a vibrating-reed electrometer (VRE), with the capacitor modulator (1.2) generating an alternating voltage, a preamplifier (1.3) and amplifier (2.1) connected to a phase-related rectifier (2.2), which is controlled by the oscillator (2.3) driving the capacitor modulator synchronously. At the amplifier output an adjustable (2.4) compensation

voltage (2.6) is created with negative feedback to the capacitor, and the output signal is measured (2.5). Reproduced from [159].

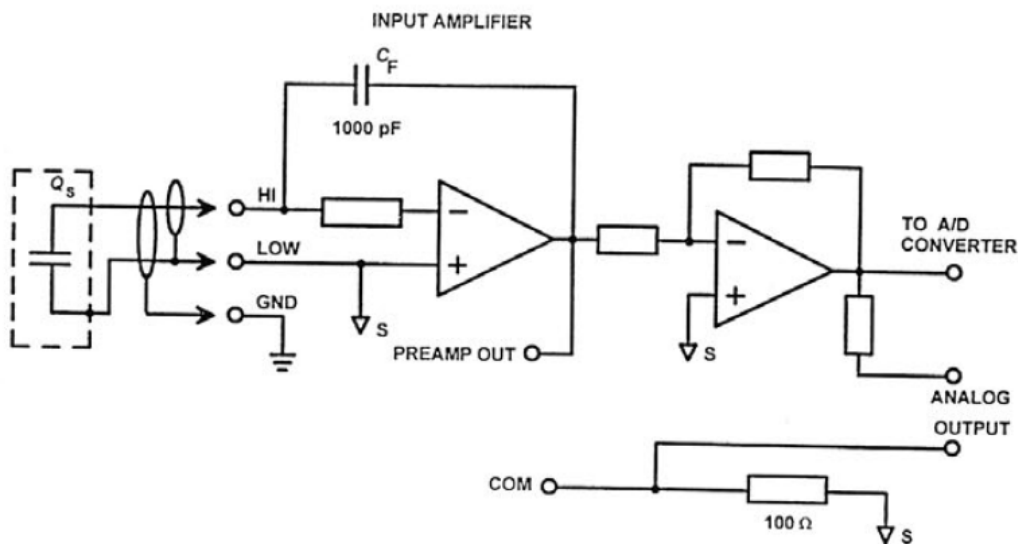


Figure 28 — Diagram of an electrometer with an FET-entrance stage, used for measurement ranges as low as 10^{-14} C. The charge source Q_s is connected by a triax cable to the FET preamplifier, with the feedback capacitor C_F working as an integrator, and via an amplifier to an A/D converter of a voltage instrument with digital display. After Keithley ([249], see p. 180).

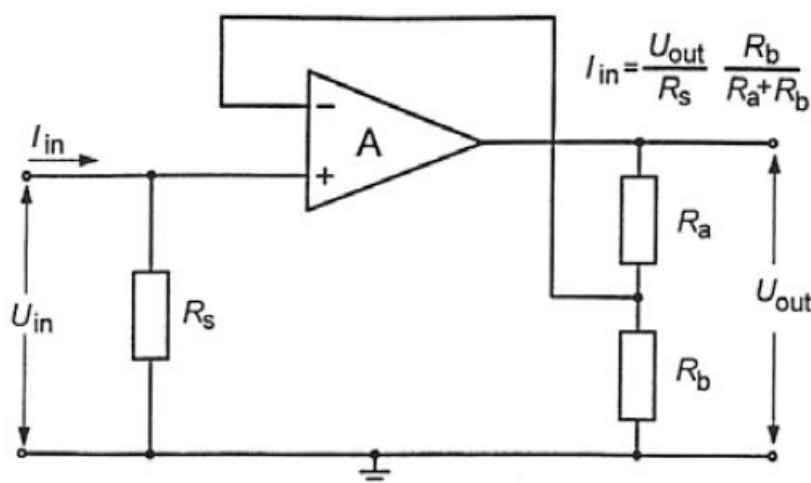
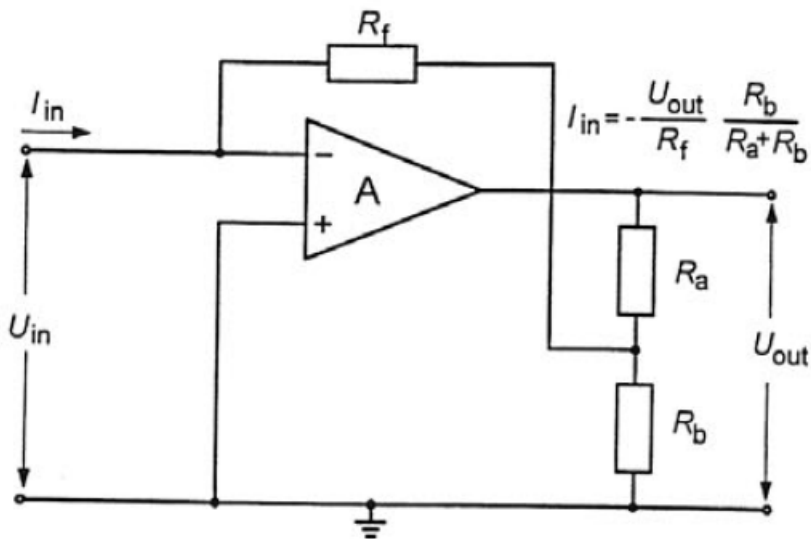
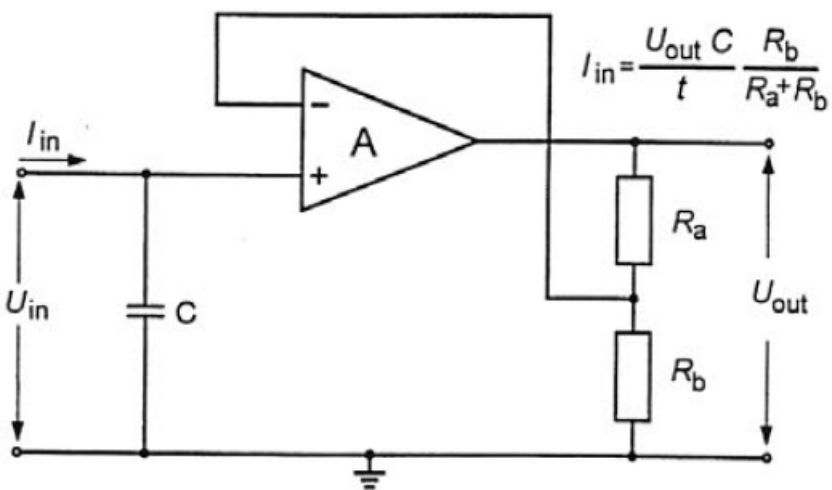


Figure 29-1 — Shunt-type picoamperemeter, with input resistor R_s and output voltage divider R_a, R_b .

Figure 29-2 — Feedback-type picoamperemeter, with feedback resistor R_f .Figure 29-3 — Shunt-type current integrator, with capacitor C and integration time t .

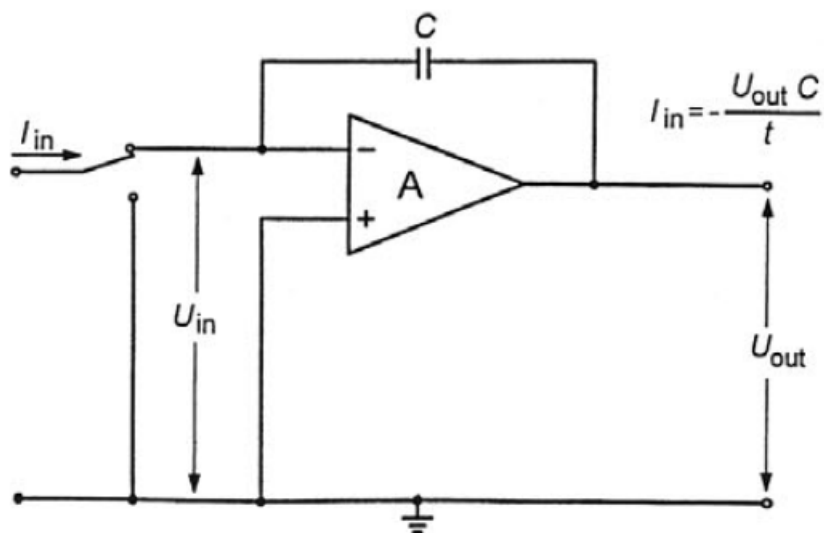


Figure 29-4 — Feedback-type current integrator, with feedback capacitor C .

Figure 29 — Various feedback-amplifier schemes for low-current or -charge measurements with the formulae given for the input current (I_{in}) and the output voltage (U_{out}). After Zsdanszky ([491], see p. 195).

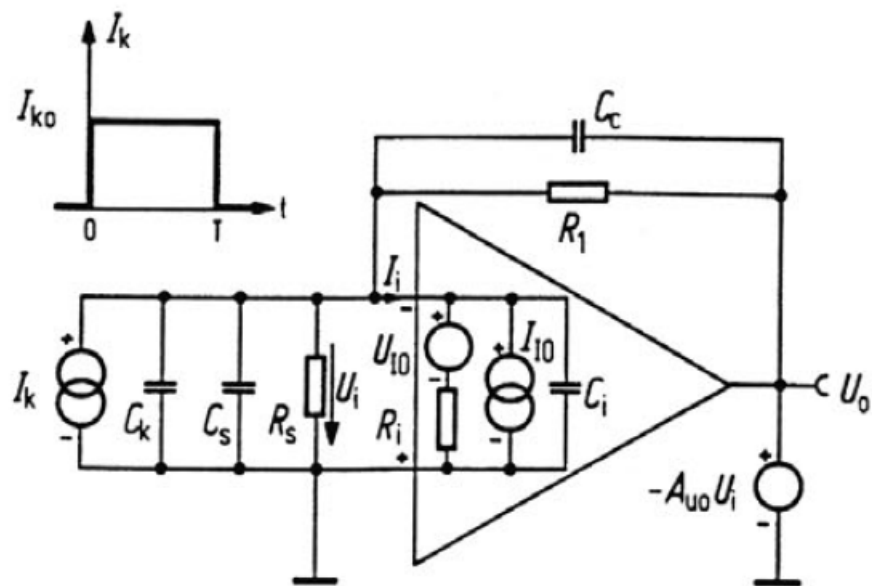


Figure 30 — Current-integrator equivalent-circuit diagram to study the parameters of a measuring system, such as leakage currents or the time dependence of integration for a current pulse of duration T (on top left), with the current to be measured I_k , input current I_i , initial-offset current I_{lo} , input voltage U_i , initial-offset voltage U_{lo} , output voltage U_o , open-loop gain A_{uo} , input resistance R_i , feedback resistance R_1 , stray resistance R_s , stray capacity C_s , capacity of the current source C_k , input capacity C_i and feedback capacity C_c . Reproduced from [34] and [37].

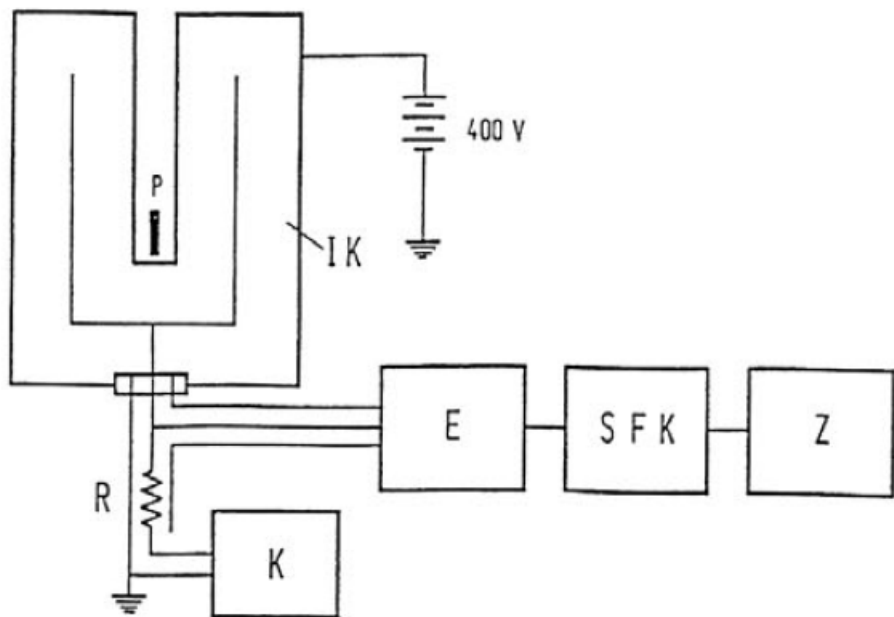


Figure 31 — High-ohmic resistor circuit for ionization current measurements from Walz and Weiss ([459], see p. 193), with radioactive source P, high-ohmic resistor R, vibrating-reed electrometer E, voltage compensator K, voltage-frequency converter SFK and counter chain Z.

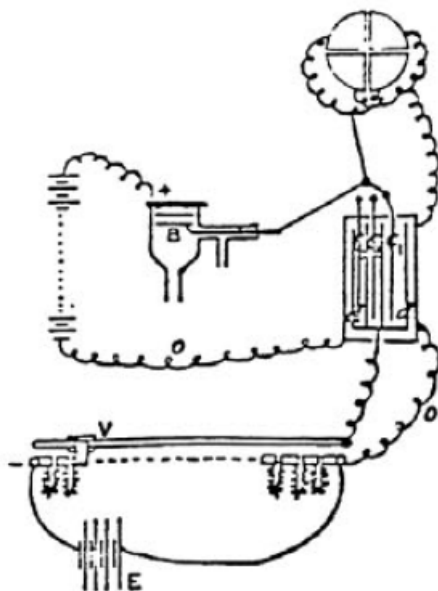


Figure 32 — Early induction balance from Townsend ([450], see p. 193) used for measurements "On the Genesis of Ions by the Motion of Positive Ions in a Gas", with the charge driven by the electric force from a battery (on left) and acquired by the plate B, a parallel plate condenser c_i and d, the control instrument - an electrometer brought to zero by compensation - (on top of the figure), and the required compensation voltage V from a voltage divider of the voltage E, 0 giving the ground connections.

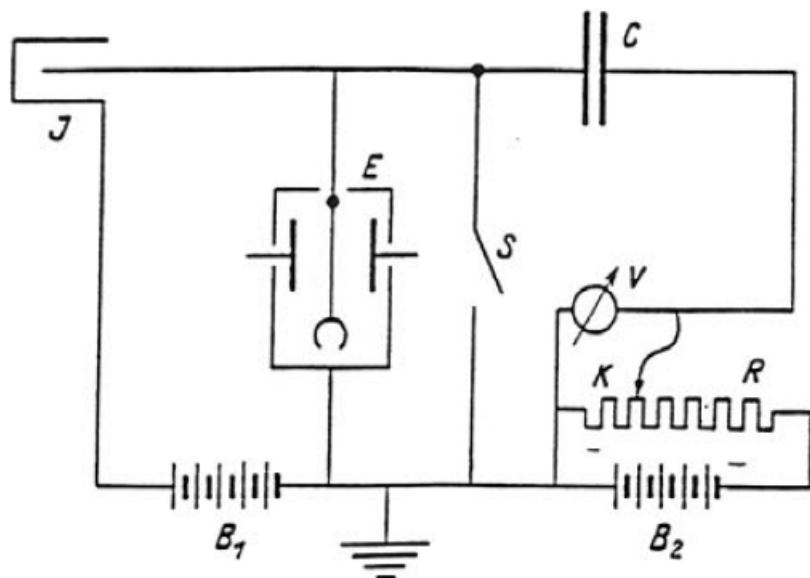


Figure 33-1 — Induction balance after Townsend ([450], see p. 193), with ionization chamber J , electrometer E , high tension on the chamber B_1 , voltage B_2 to create the compensating charge by shifting the contact K on the potentiometer R , precision voltmeter V , charge-collecting precision capacitor C and zero switch S .

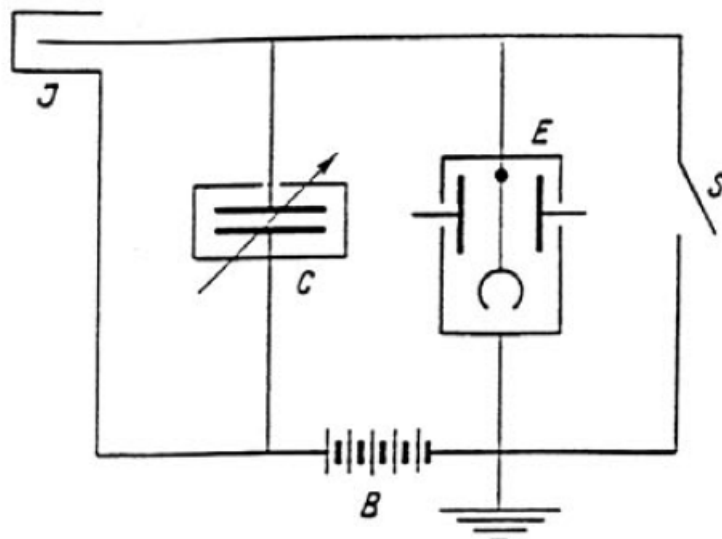


Figure 33-2 — Compensation by varying a calibrated capacitor C with ionization chamber J , electrometer E , high tension B on the chamber and zero switch S .

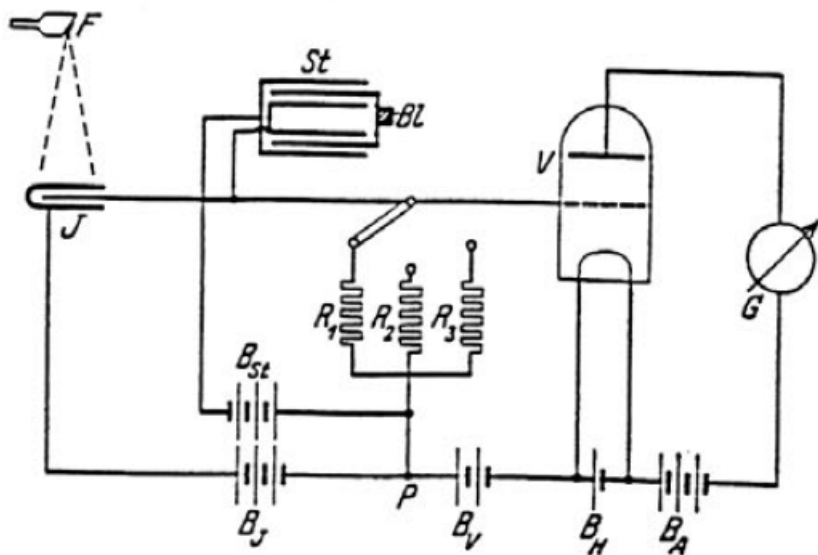


Figure 33-3 — Compensation by an adjustable current source $St(BI)$, with ionization chamber J , vacuum-tube entrance stage V on the measuring instrument G , high tension on the chamber B_J , high-ohmic resistors R_i for range switching and voltage supplies B_i for the various components. This represents an early application of a vacuum tube with an x-ray dosimeter by Siemens.

Figure 33 — Various compensation methods for ionization current measurements after Jaeger ([235] and [236], see p. 179). Reproduced from [235] and [236].

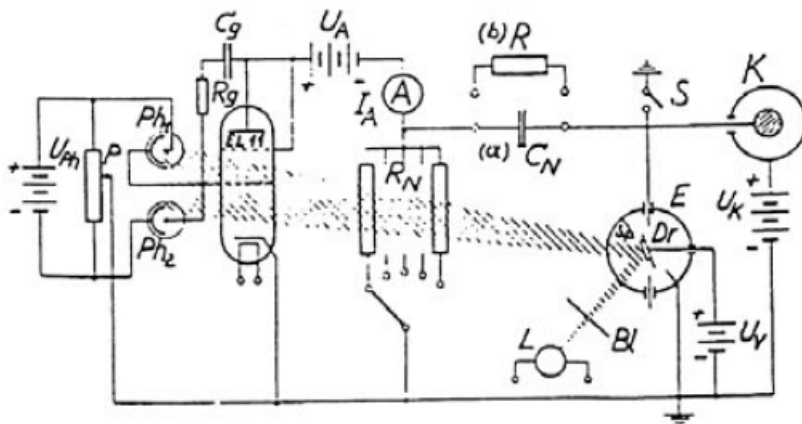


Figure 34 — Electrometer-photocell compensator by Hübner ([222], see p. 178), with ionization chamber K and high tension U_k . The electrometer E with a turning light-mirror system (L , Bl , Dr) initiates variable currents on the photocells Ph_1 and Ph_2 connected to the vacuum tube $EL11$, which itself controls the potential at point (a) by the voltage decrease on the high-ohmic resistor R_N and creating the compensation charge on the collecting capacitor C_N , for zero switch S open. The anode current I_{Ai} of the tube is measured by the instrument A during the time t at the beginning and the end of the compensation giving the ionization current

$I_K = (I_{A2} - I_{A1})R_N C_N / t$. The other voltage supplies U_i are necessary for the instrument components. Reproduced from [222].

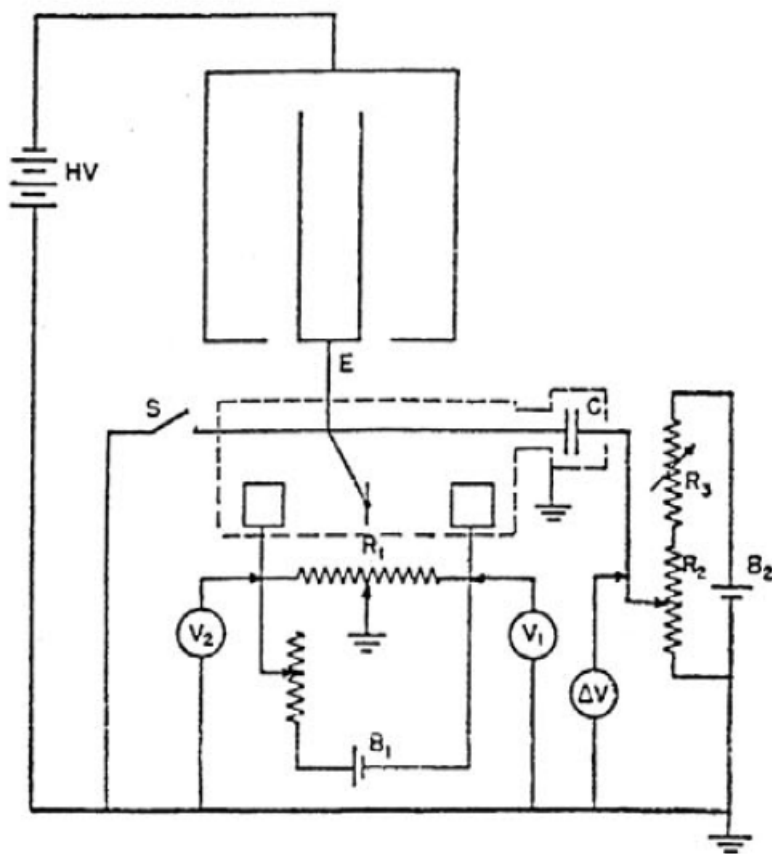


Figure 35-1 — Circuit diagram illustrating the Townsend balance-of-charge system, with semi-automatic compensation: The zero switch is S open, the charge at E is collected and connected to a Lindemann-Ryerson electrometer with quadrant voltages V_1 and V_2 which are adjusted by means of R_1 in the electrical-zero position of the quartz fiber and which corresponds to the mechanical-zero position. The point at E is also connected to the charge-collecting capacitor C and a compensation voltage ΔV is given on its other side from potentiometer R_2 with battery B_2 , driven by an operator. Reproduced from [164].

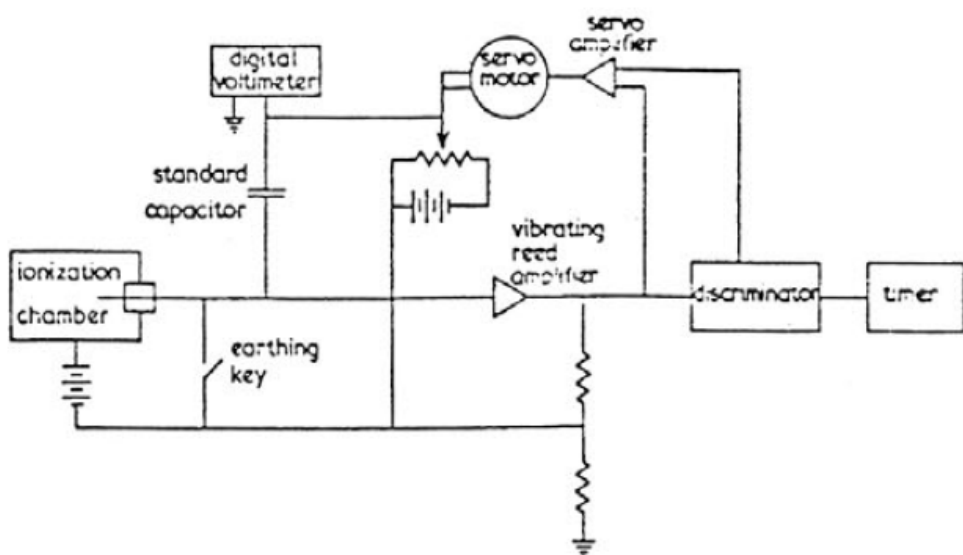


Figure 35-2 — Schematic diagram of an automatic induction balance with a servo-motor driven potentiometer for compensation at a charge-collecting standard capacitor. The control instrument coupled to the ionization chamber is a vibrating-reed amplifier with a discriminator for switching the servo-motor. The time during compensation is measured. Reproduced from [175].

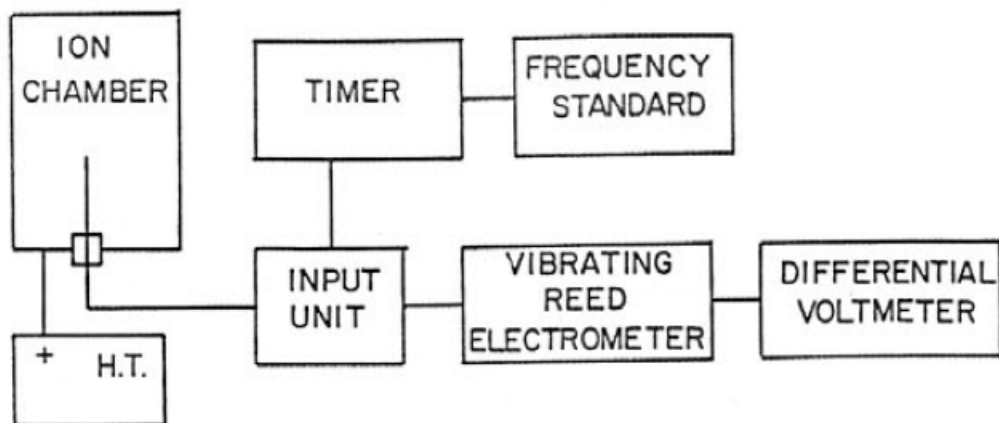


Figure 36-1 — Block diagram of the ionization current measuring system at the AECL, using the induction balance principle. The voltage difference across the capacitor of the input unit is measured by the vibrating-reed electrometer connected to a differential voltmeter during a given time interval.

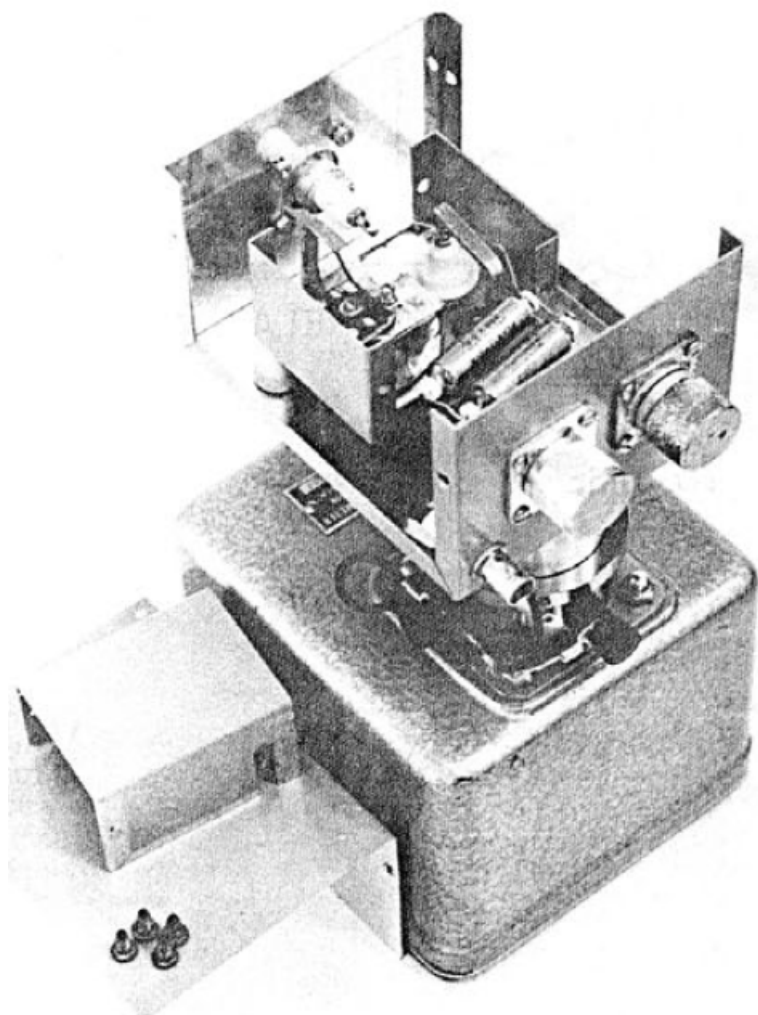


Figure 36-2 — Photograph of the input stage with the capacitor and the timing relay.

Figure 36 — Reproduced from Merritt and Taylor ([307], see p. 184).

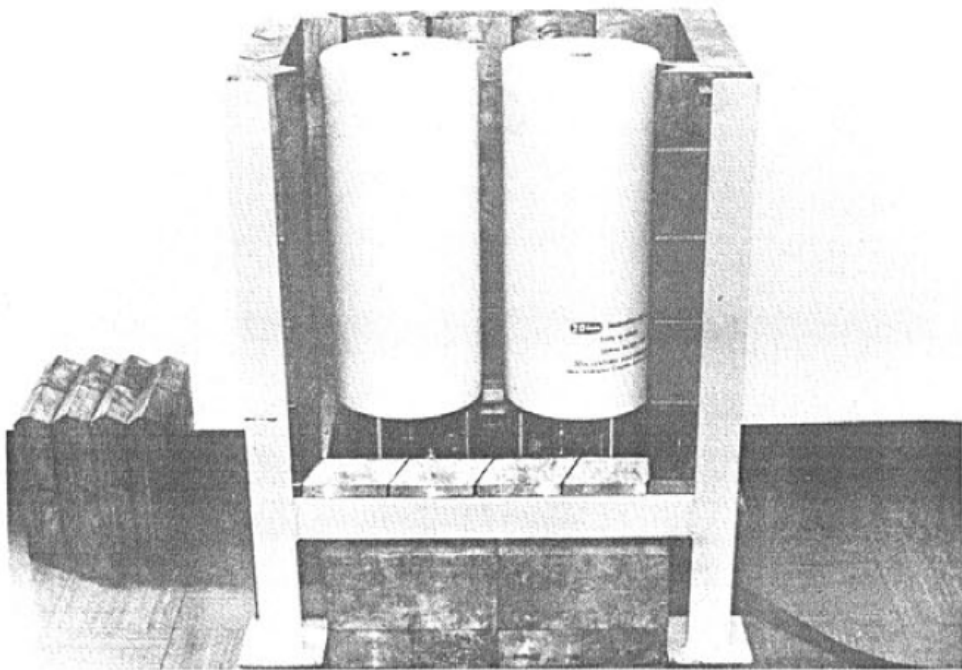


Figure 37-1 — Photograph of the ionization chambers of the SIR (BIPM) mounted in a common lead shield (cover and front wall removed). Reproduced from [376].

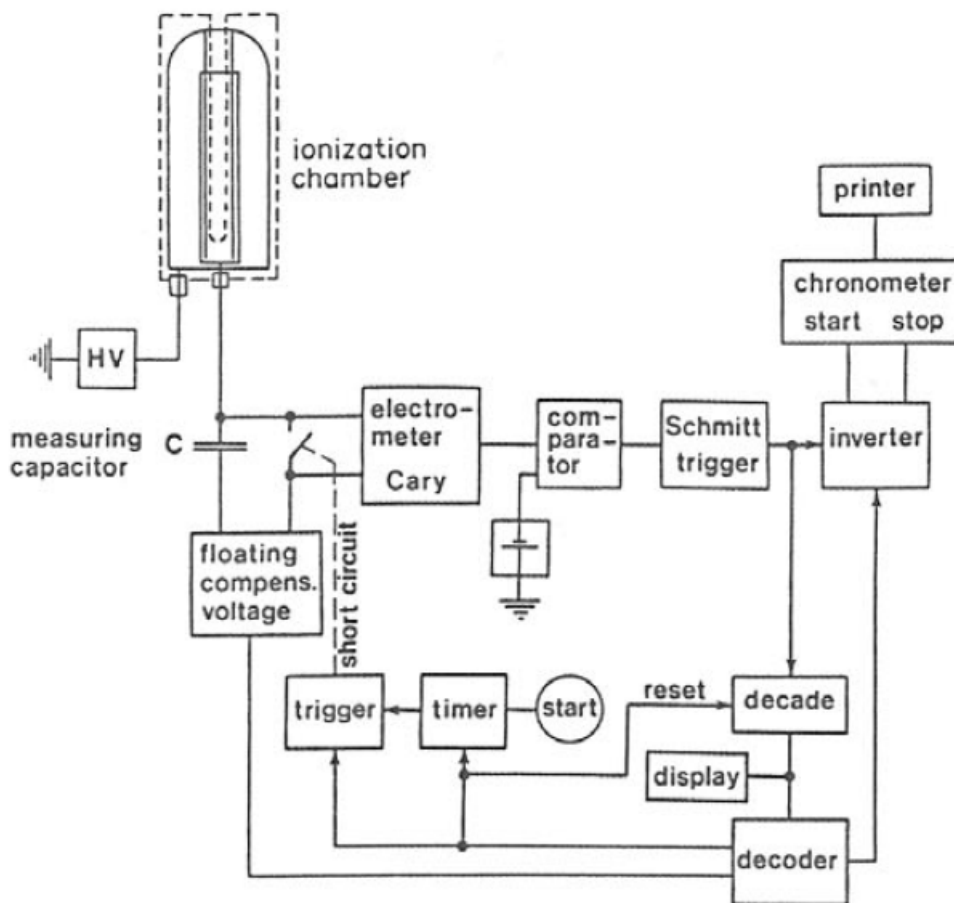


Figure 37-2 — Block diagram of the measuring electronics of the SIR (BIPM), based on the induction balance principle, with stepwise compensation and a preset voltage level. The time is measured for a well-defined number of compensation steps. Reproduced from [376].

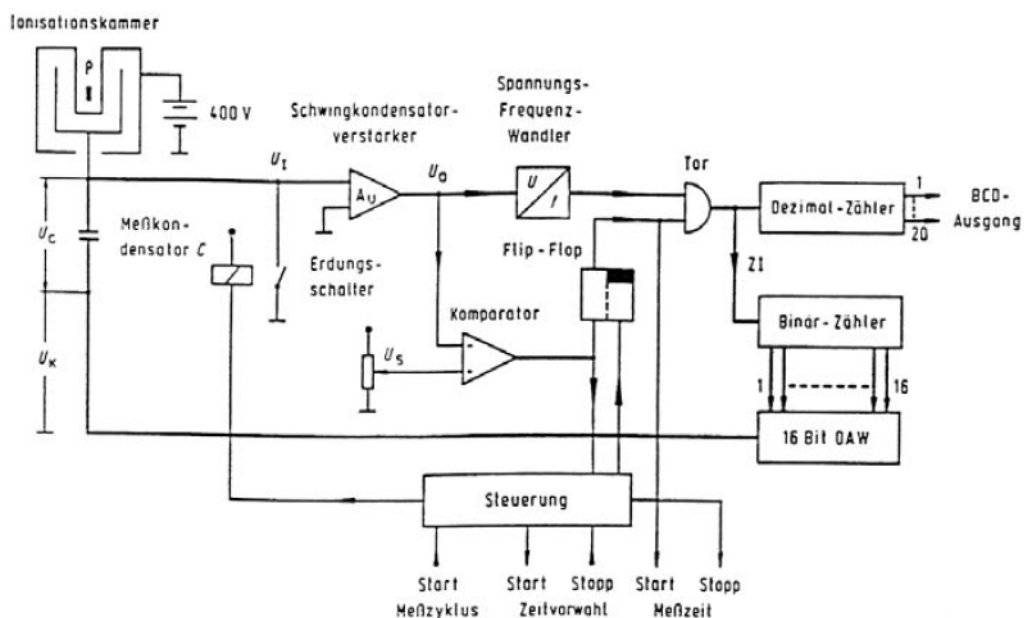


Figure 38-1 — Schematic diagram of an automatic induction balance at the PTB, with a source P and ionization chamber, a collecting capacitor C, a

vibrating-reed amplifier with amplification A_U , a voltage-frequency converter U/f , a gated counter chain at ZI, several control units and the digital-analogue converter DAW of 16 bit resolution which supplies the compensation voltage U_K at the capacitor (Ionisationskammer ⇒ ionization chamber, Schwingkondensatorverstärker ⇒ vibrating-reed amplifier, Spannungs-Frequenz-Wandler ⇒ voltage-frequency converter, Tor ⇒ gate, Dezimal-Zähler ⇒ decimal counter, Meßkondensator ⇒ collecting capacitor, Erdungsschalter ⇒ earth (ground) switch, Flip-Flop ⇒ flip-flop, Komparator ⇒ comparator, Binär-Zähler ⇒ binary counter, Steuerung ⇒ control, Meßzyklus ⇒ measuring cycle, Zeitvorwahl ⇒ time preselection, Meßzeit ⇒ measuring time). Reproduced from [104].

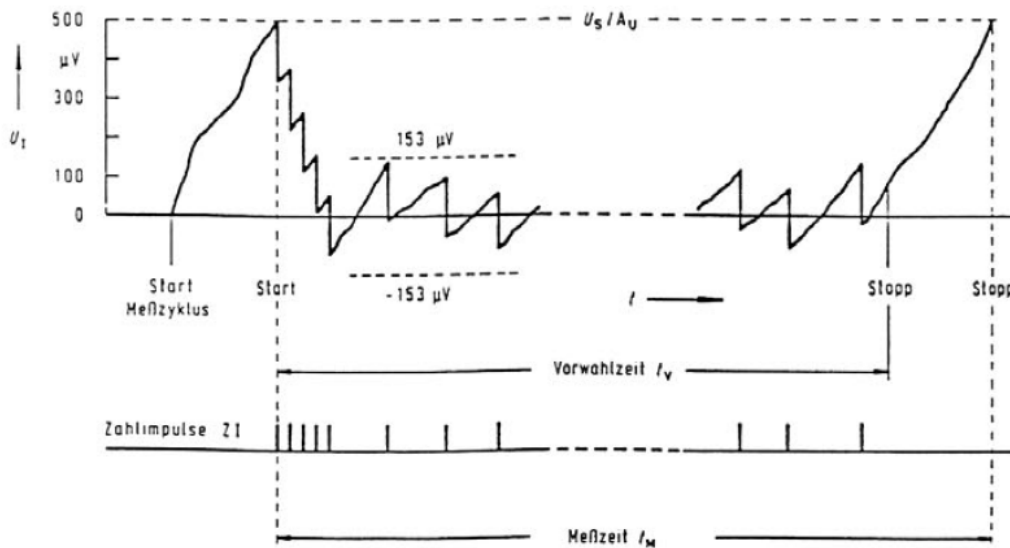


Figure 38-2 — Timing diagram $U_1(t)$ of the PTB induction balance showing a measuring cycle in three parts: The integrated ramp before start up to a voltage level of U_S/A_U , the compensation period between start and stop during which the voltage-frequency converter pulses are counted and the stop ramp to obtain the same voltage level as at start (Meßzyklus ⇒ measuring cycle, Vorwahlzeit ⇒ preselected time, Zählimpulse ⇒ counter pulses, Meßzeit ⇒ measuring time, Start ⇒ start, Stopp ⇒ stop). Reproduced from [104].

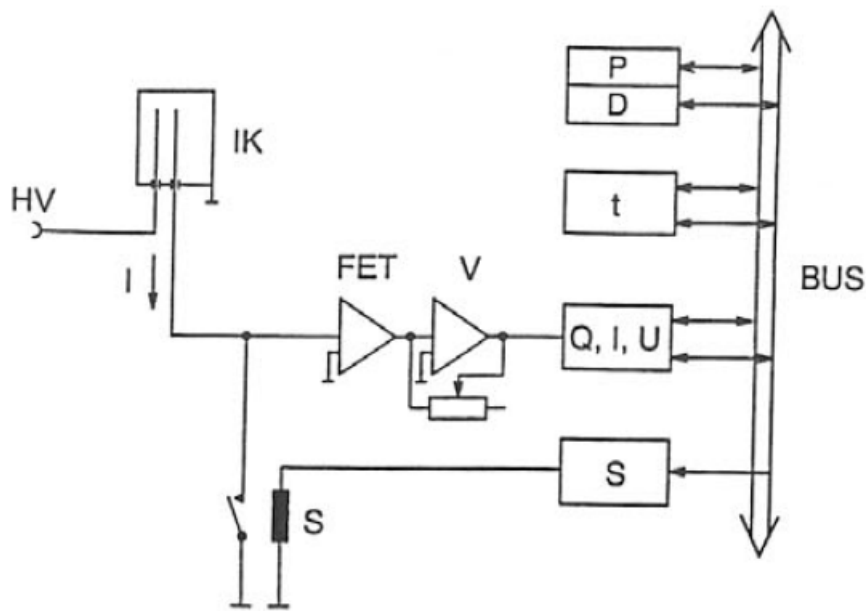


Figure 39-1 — Schematic diagram of a current-measuring system for an ionization chamber IK, with an FET-amplifier input V and programmable components connected to a computer bus: P, D processor and instrument display, t timer, Q, I, U measurement components for charge, current or voltage to be chosen and S switch to ground potential. Reproduced from [398].

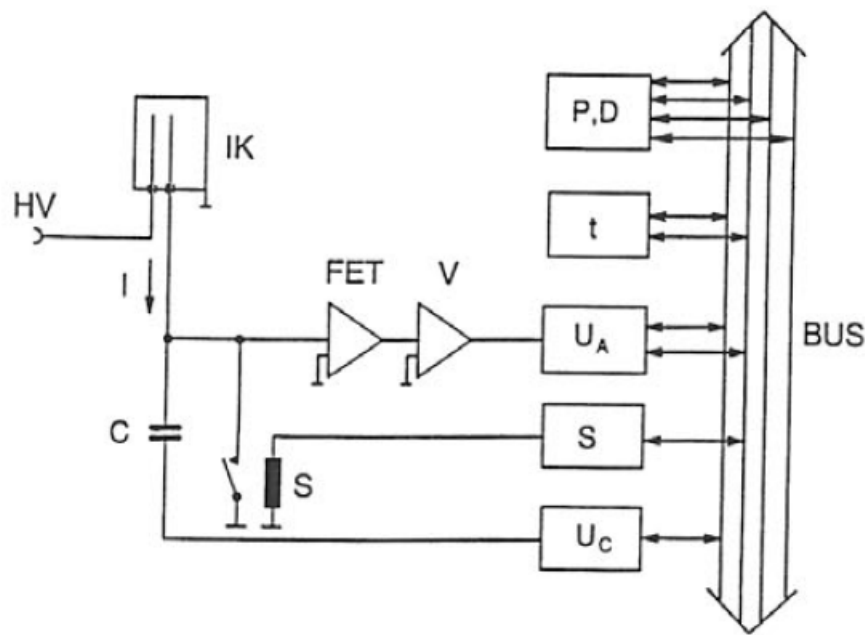


Figure 39-2 — Functional diagram of a current-measuring system by an induction balance, using a modified Townsend method with a capacitor C and a control loop for compensation with a programmable analog-digital (A/D) converter U_A and a digital-analog (D/A) converter U_C of high quality and resolution; other components as in Figure 39-1. Reproduced from [397].

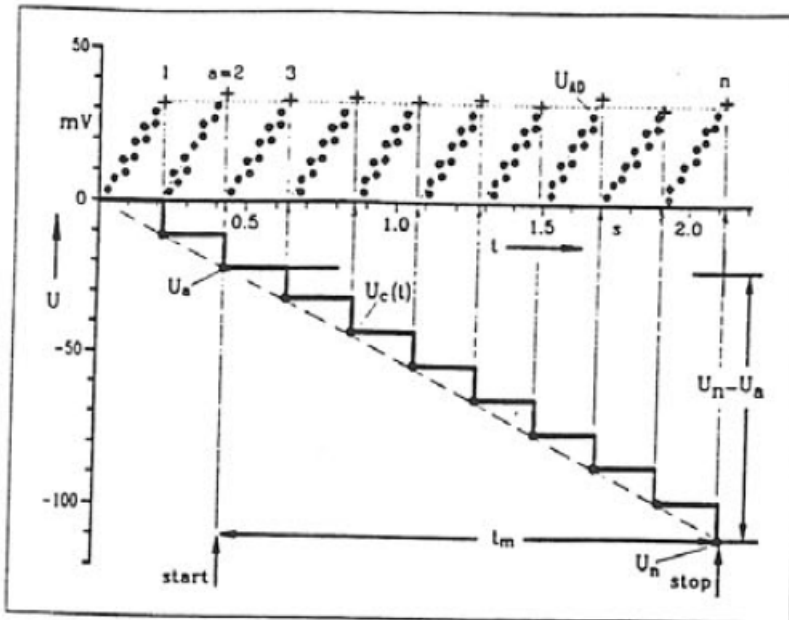


Figure 39-3 — Voltage-time diagram for the induction balance of Figure 39-2 showing n compensation steps during the measuring time t_m . U_{AD} is the voltage at the A/D converter input represented by circles. The crosses show the extrapolated U_{AD} values before a compensation step is transformed in the computer. $U_C(t)$ is the resulting voltage at the D/A converter output which is fed to the capacitor represented by the step function. The measured ionization current is $I = C(U_n - U_a)/t_m$. Reproduced from [397].

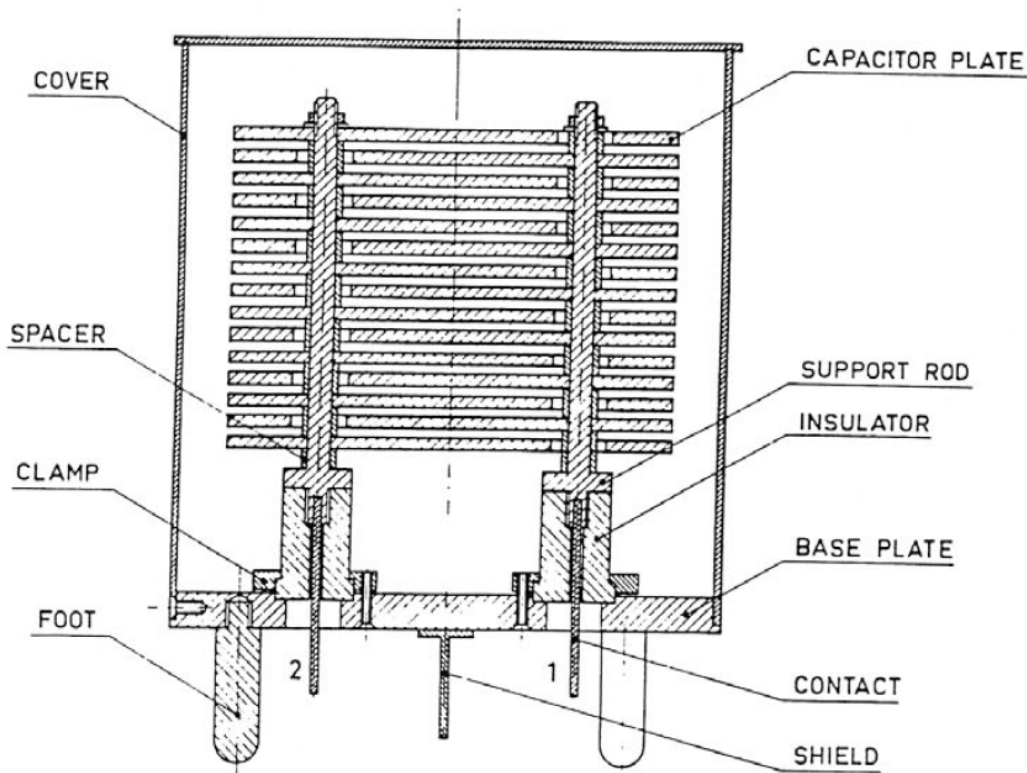


Figure 40 — Schematic view (vertical cut) of the 500 pF air capacitor used at the IRMM (CBNM), Geel. Reproduced from [353].

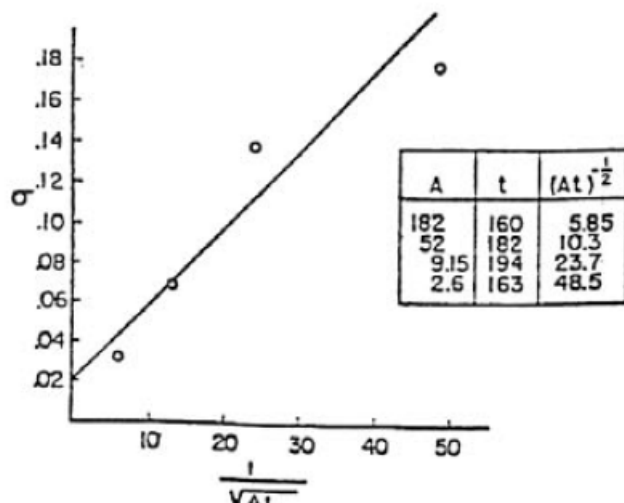


Figure 41-1 — Plot of the relative standard deviation σ of individual current measurements made on four radium sources, with activities from $3 \mu\text{Ci}$ to $200 \mu\text{Ci}$, as a function of the total number of ions collected per radium source. Reproduced from [164].

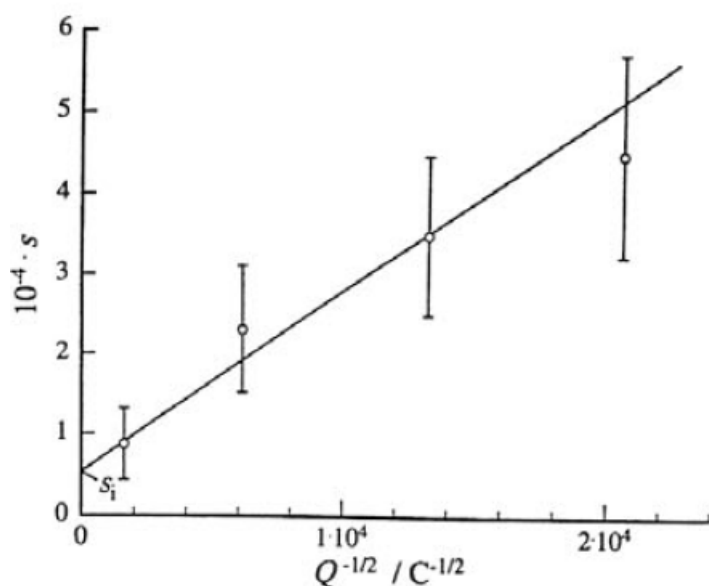


Figure 41-2 — Determination of the "internal" relative standard deviation s of repeated measurements, with sources of different activities, plotted against $Q^{-1/2}$, where Q is the charge collected within the integration time for one measurement. After Weiss ([469], see p. 194).

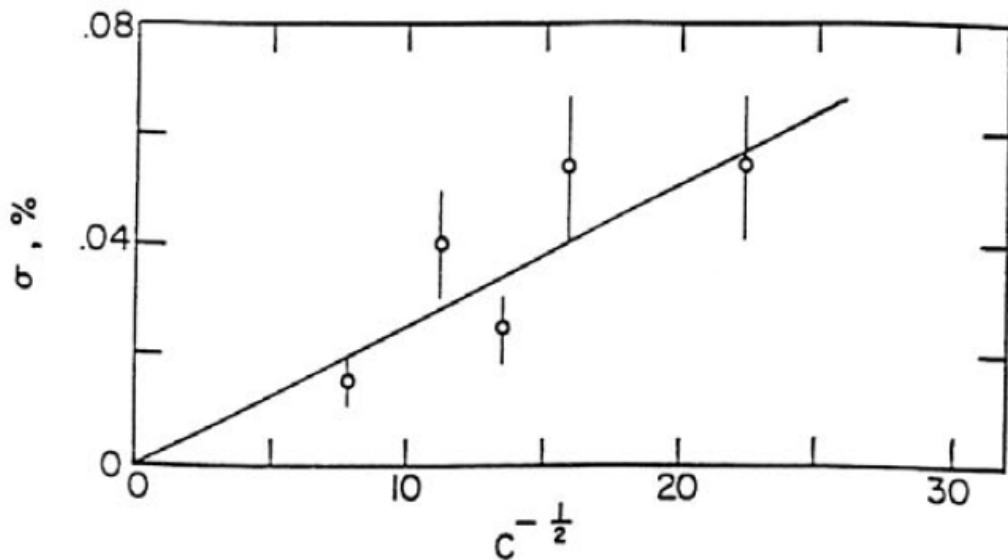


Figure 41-3 — Observed relative standard deviation σ as a function $C^{-1/2}$, where C is the total charge collected per ionization current measurement.
Reproduced from [307].

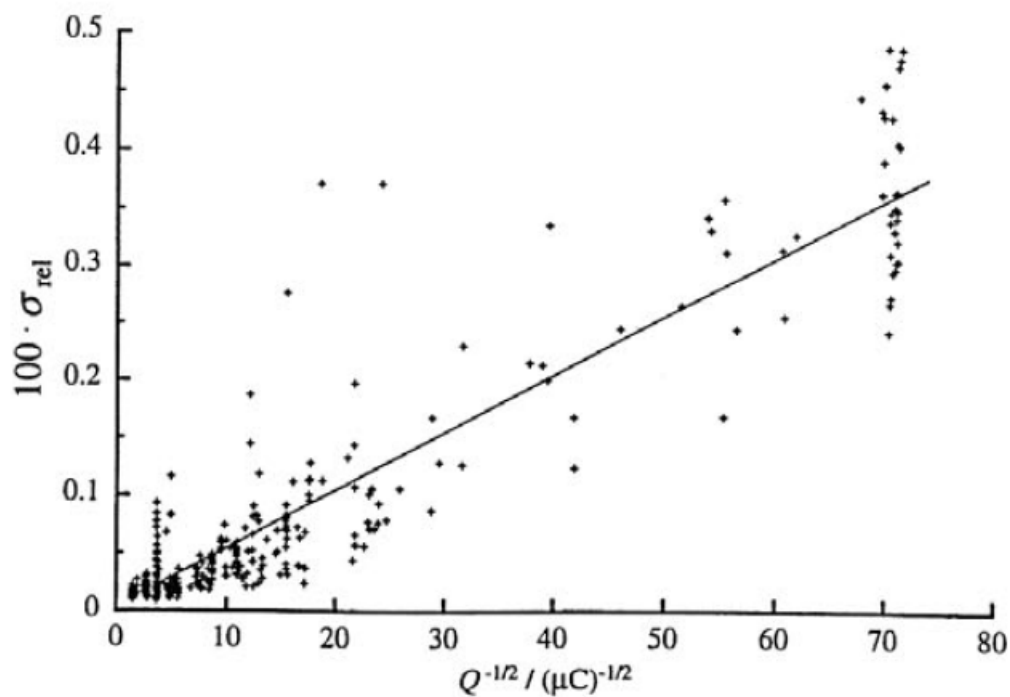


Figure 41-4 — Relative standard deviation σ_{rel} of repeated measurements in a series, with sources of variable activities plotted against $Q^{-1/2}$, where Q is the charge collected within the integration time for one measurement.
Unpublished results from PTB (1992).

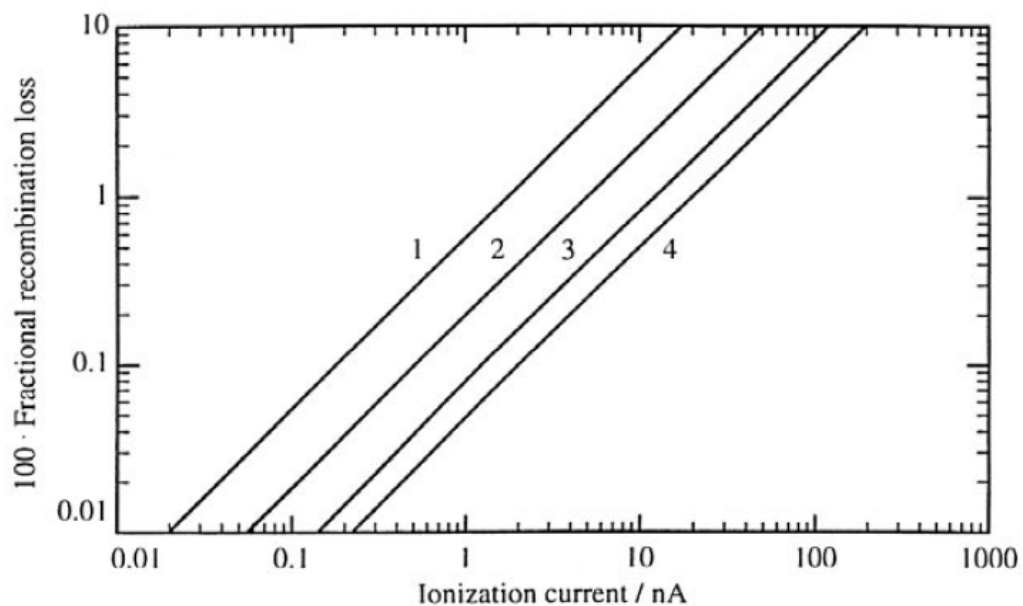


Figure 42 — Recombination loss, expressed as a fraction, in an ionization chamber filled with argon at 1 atm and 23 °C, measured at various collection voltages between the electrodes and plotted versus the ionization current.
After Colmenares ([76], see p. 169).

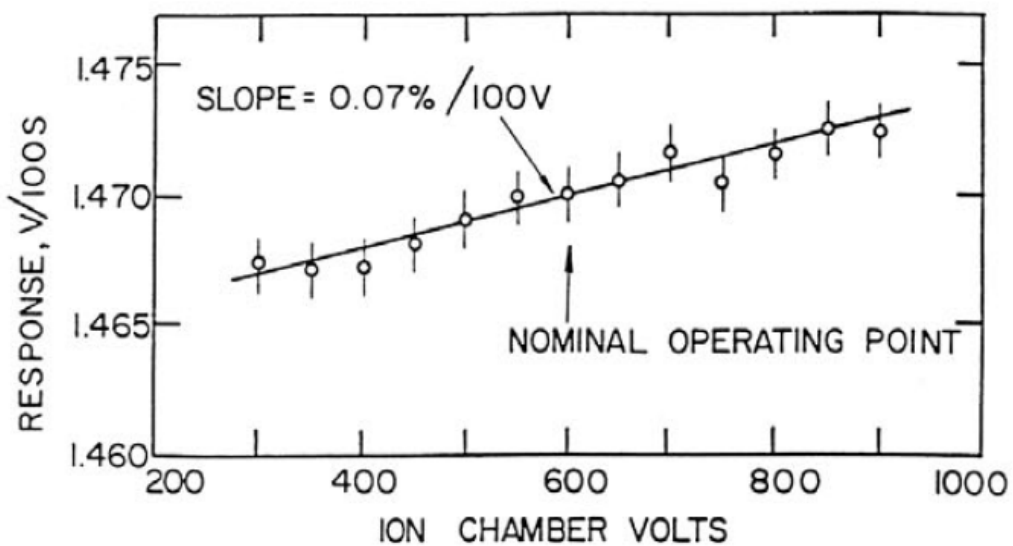


Figure 43-1 — Ionization chamber response for a source measured at various collection voltages applied between the electrodes, showing a slope of 0.07% / 100 V at the nominal operating point of the chamber (AECL, Chalk River). Reproduced from [307].

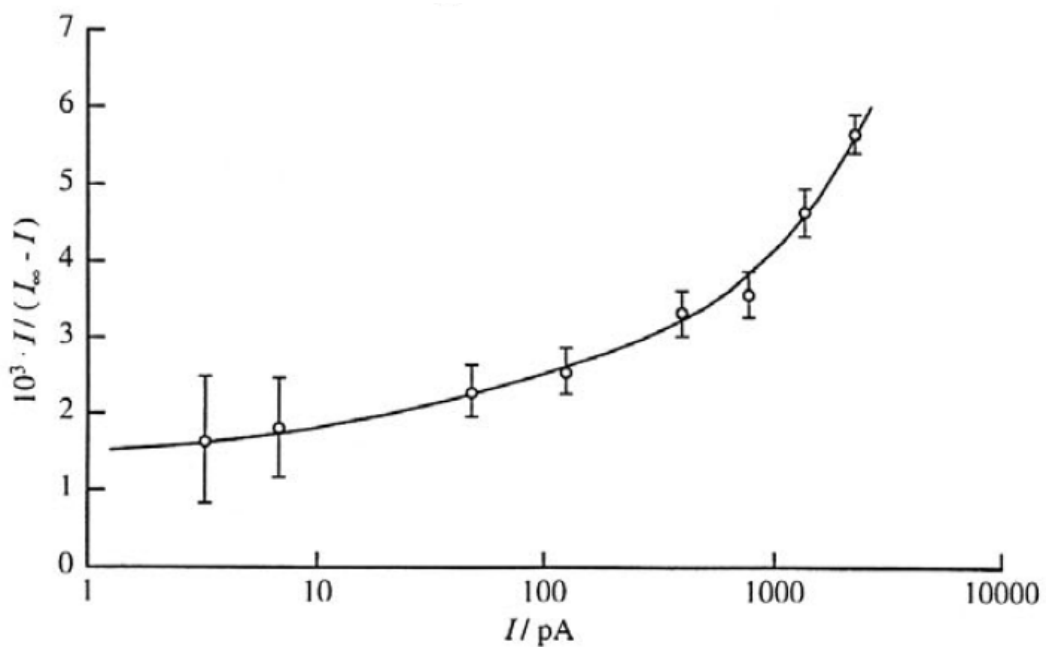


Figure 43-2 — Saturation loss $I/(I_\infty - I)$ as a function of the ionization current I for a chamber at the PTB. After Weiss ([469], see p. 194).

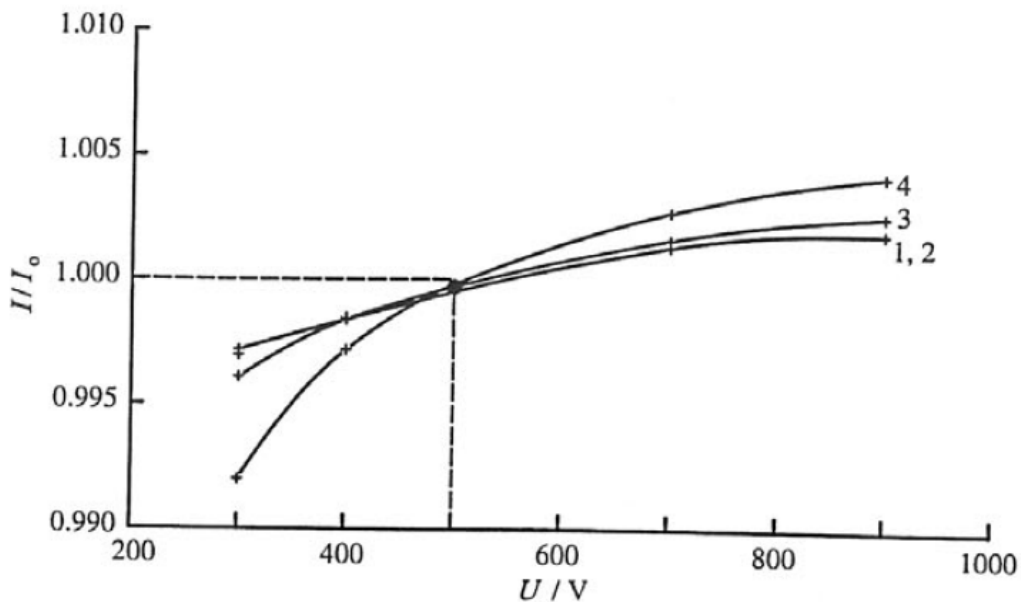


Figure 44-1 — Response characteristics for a chamber of good quality with a slope of $0.08\% / 100 \text{ V}$ at the nominal operating point, similar to the result from AECL in Figure 43-1.

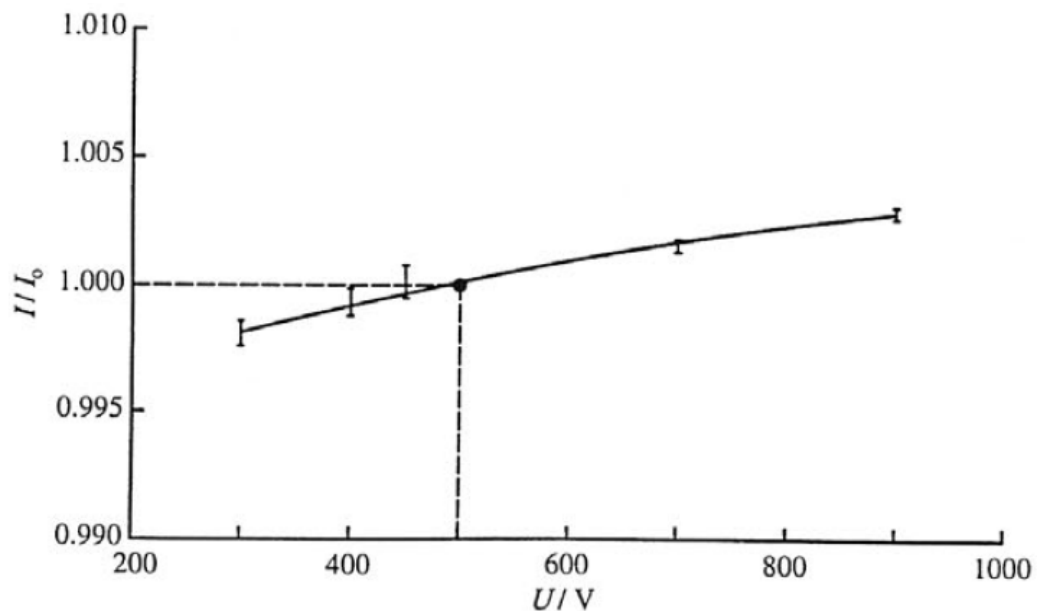


Figure 44-2 — Measurements in an ionization chamber of bad charge collection characteristics with rather large deviations from a flat linear slope for source no. 4. Unpublished results from the PTB (1987).

Figure 44 — Relative ionization current I/I_0 normalized to the current at the nominal operating point (dashed lines) and plotted versus the collection voltage U measured on each of four radium sources.

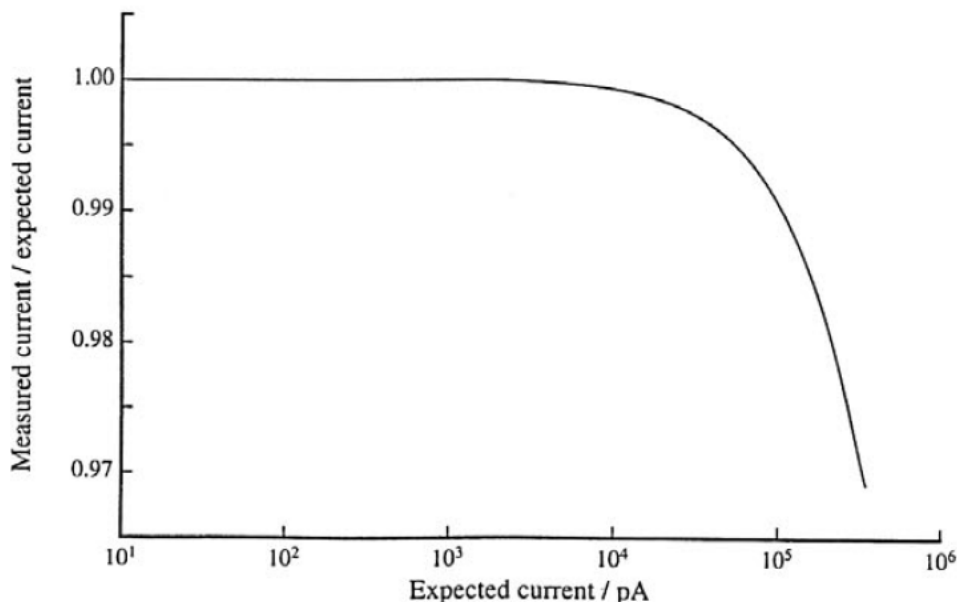


Figure 45 — Saturation loss characteristic for an ionization chamber developed at the NPL showing a break-down at very strong activities or corresponding large currents. After Woods et al. ([482], see p. 195).

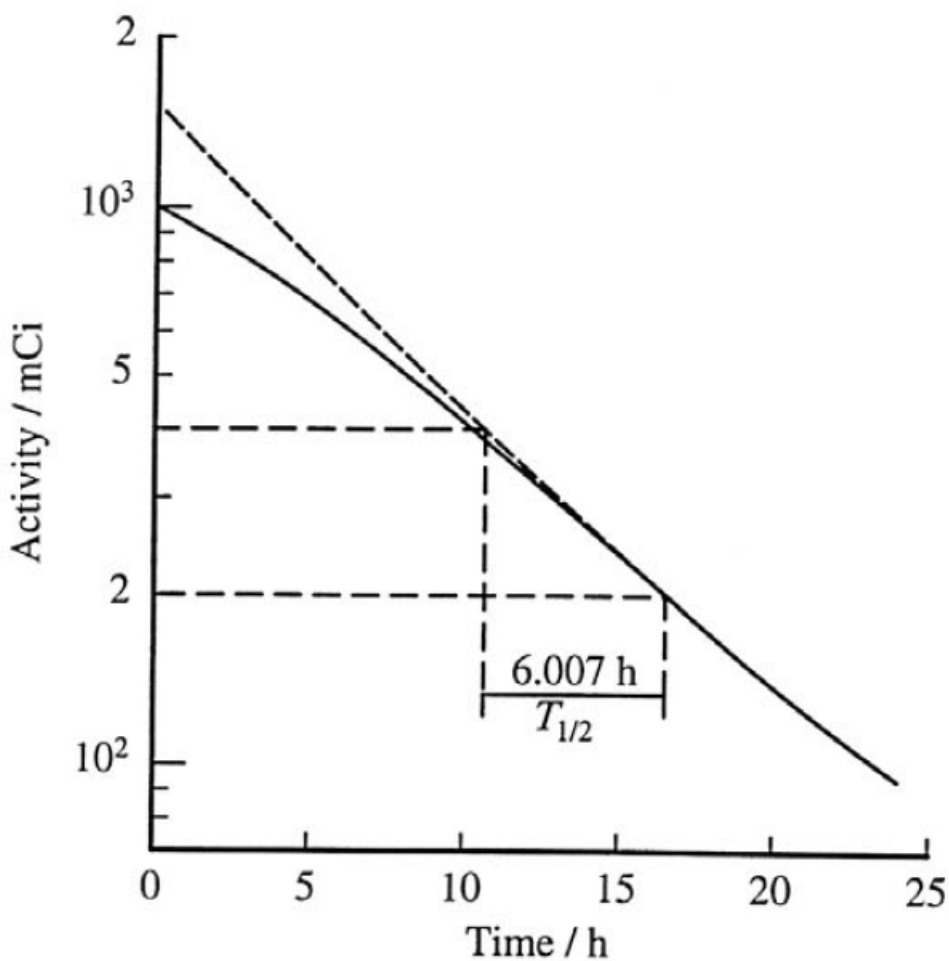


Figure 46-1 — The results for the instrument show smooth deviations from linearity at even low activity values which can only be detected by a half-life analysis for $^{99}\text{Tc}^m$.

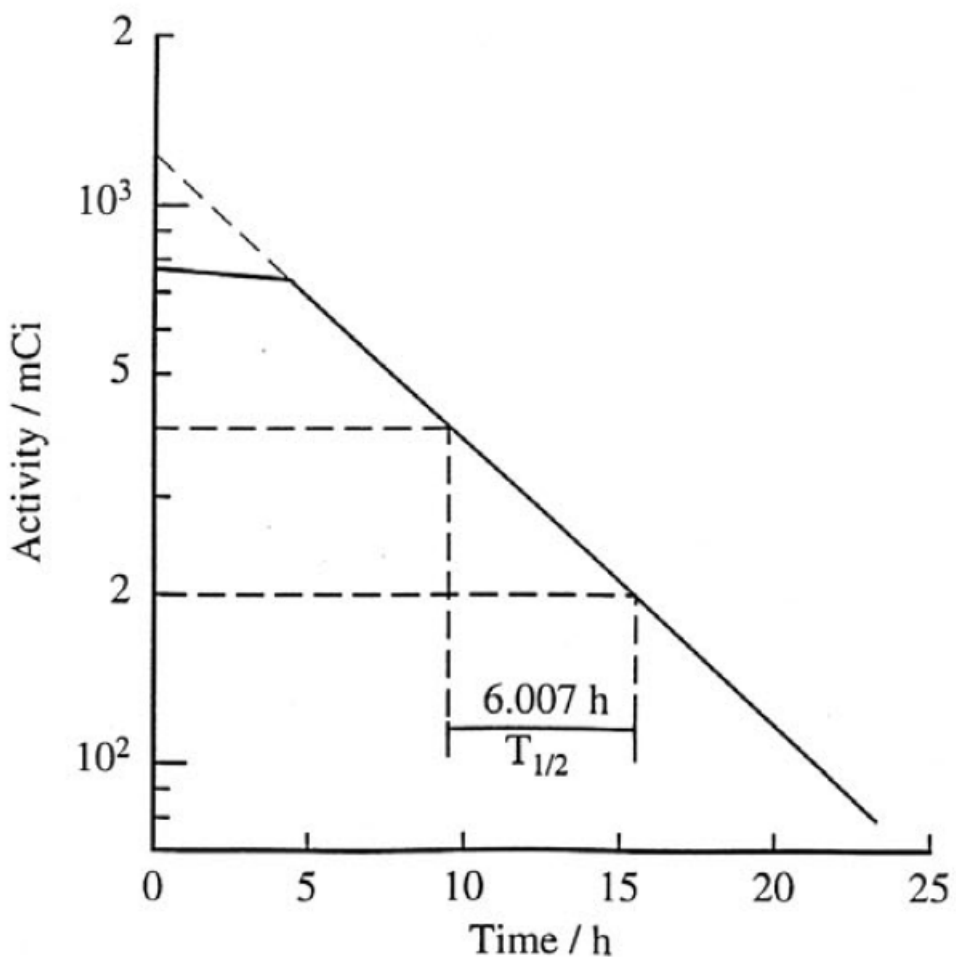


Figure 46-2 — The results for the other instrument show a typical "saturation effect" at high activity values, similar to the instrument of Figure 45.

Figure 46 — Decay curves of $^{99}\text{Tc}^m$ sources with activities in the order of 40 GBq, measured in two types of radionuclide calibrator with different linearity characteristics. The dashed lines indicate an extrapolation to the supposed initial activity values. After Kowalsky et. al. ([270], see p. 181).

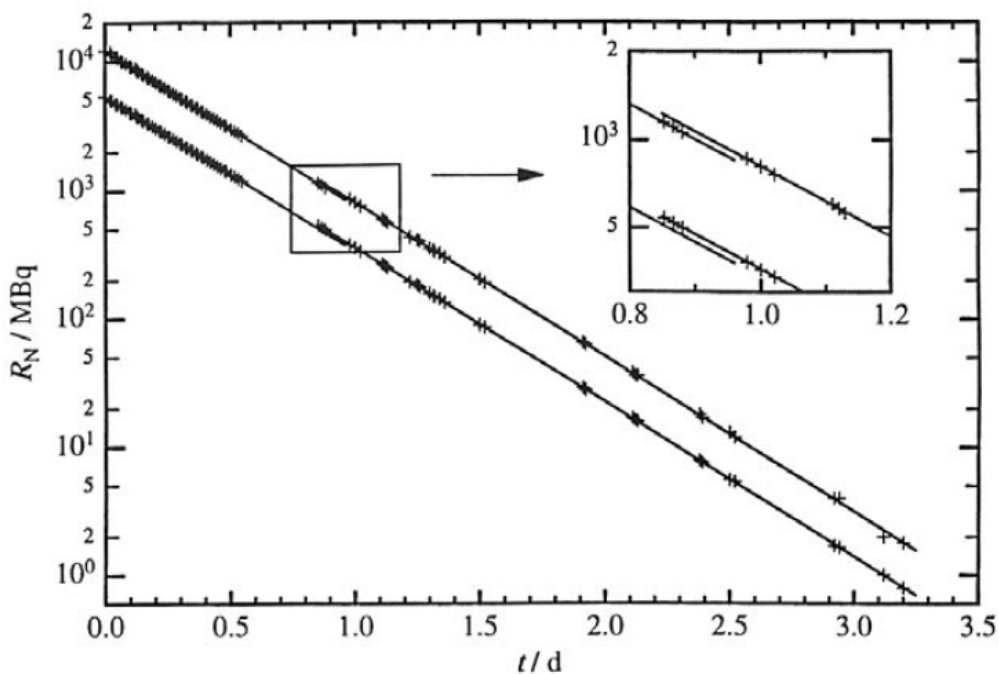


Figure 47-1 — Decay curves of two $^{99}\text{Tc}^m$ sources in a logarithmic plot.

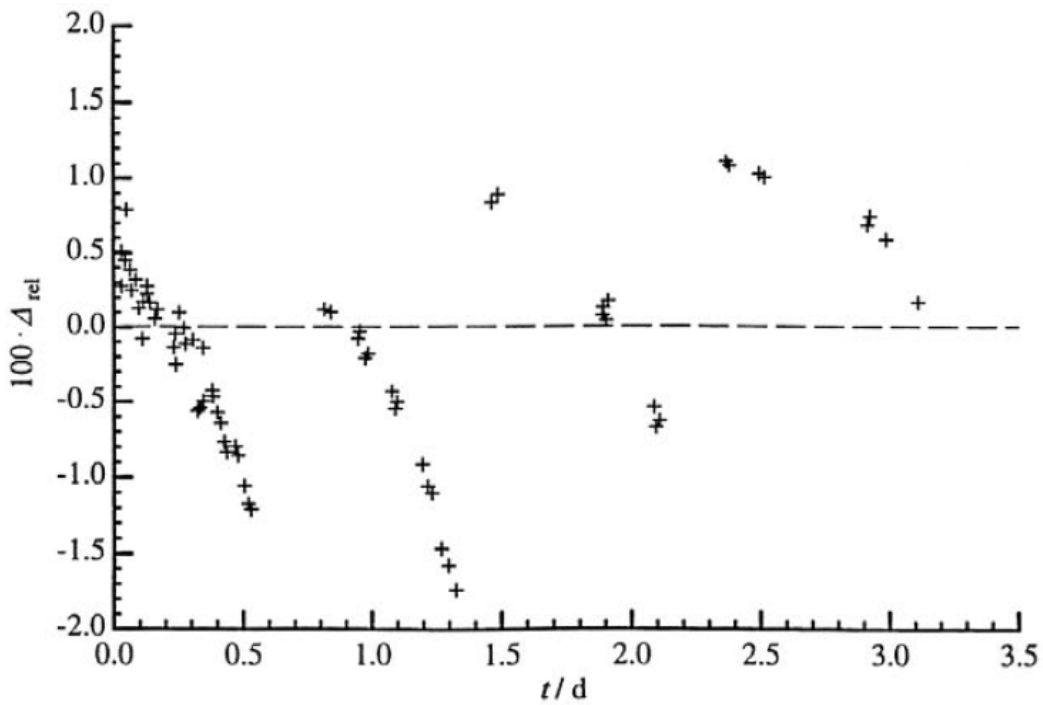


Figure 47-2 — Corresponding residuals from a linear regression analysis. The current measuring electronics of the instrument show switching effects of about 5% around the 1 GBq reading and decade switching effects from the timer in the order of 1%, see values of the pertinent residuals.

Figure 47 — Linearity check for a radionuclide calibrator with two $^{99}\text{Tc}^m$ sources of different activities measured in continuous runs. After Schrader ([398], see p. 190).

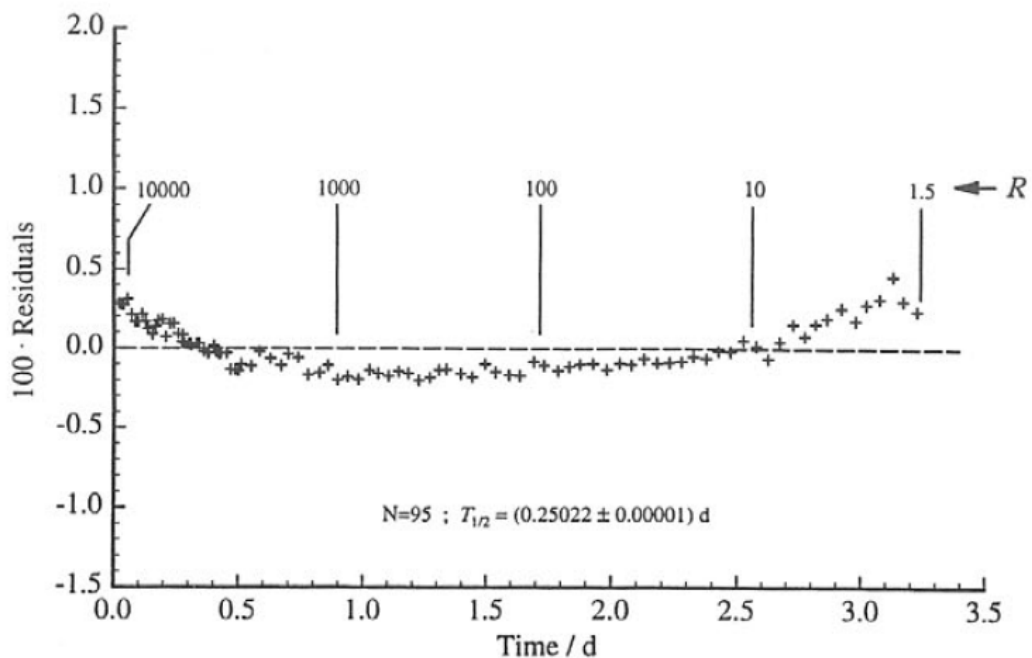


Figure 48-1 — For the full time range of the measurements of longer than twelve times the ^{99}Tcm half-life. The residuals show small deviations from linearity at high activity values in the order of a few per mil due to electronic effects and an increasing contribution from ^{99}Mo at low activity.

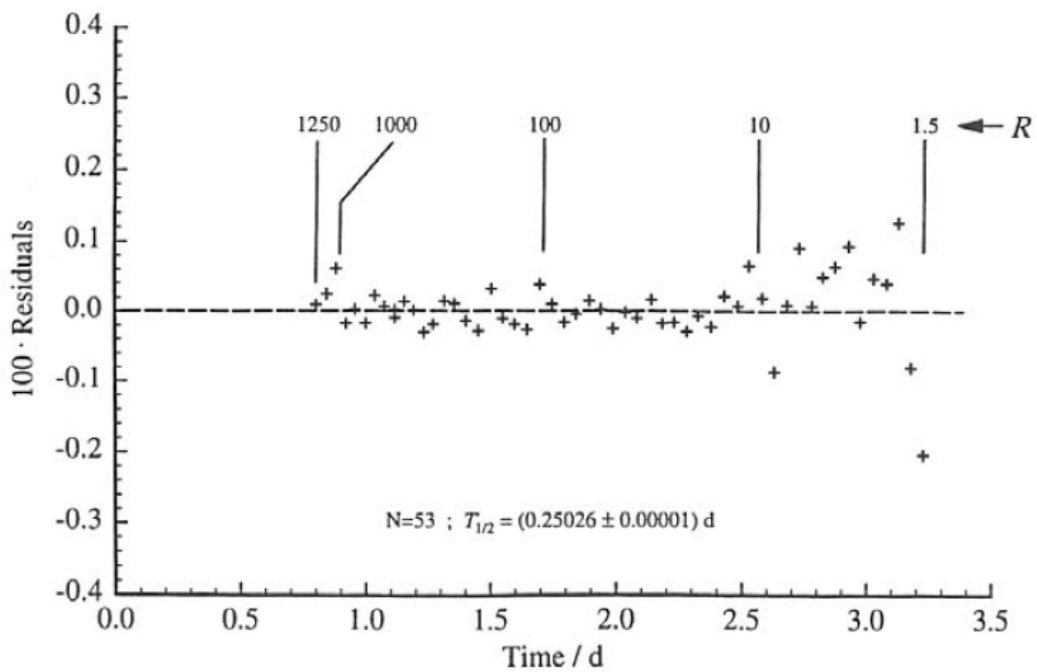


Figure 48-2 — For a reduced range of about eight times the ^{99}Tcm half-life, data corrected for the ^{99}Mo impurity contributions. (Unpublished results, PTB).

Figure 48 — Linearity check and half-life measurement of ^{99}Tcm with an ionization chamber measuring system at the PTB. The residuals of two fits from a

linear regression analysis for the logarithm of the instrument reading R are plotted versus time.

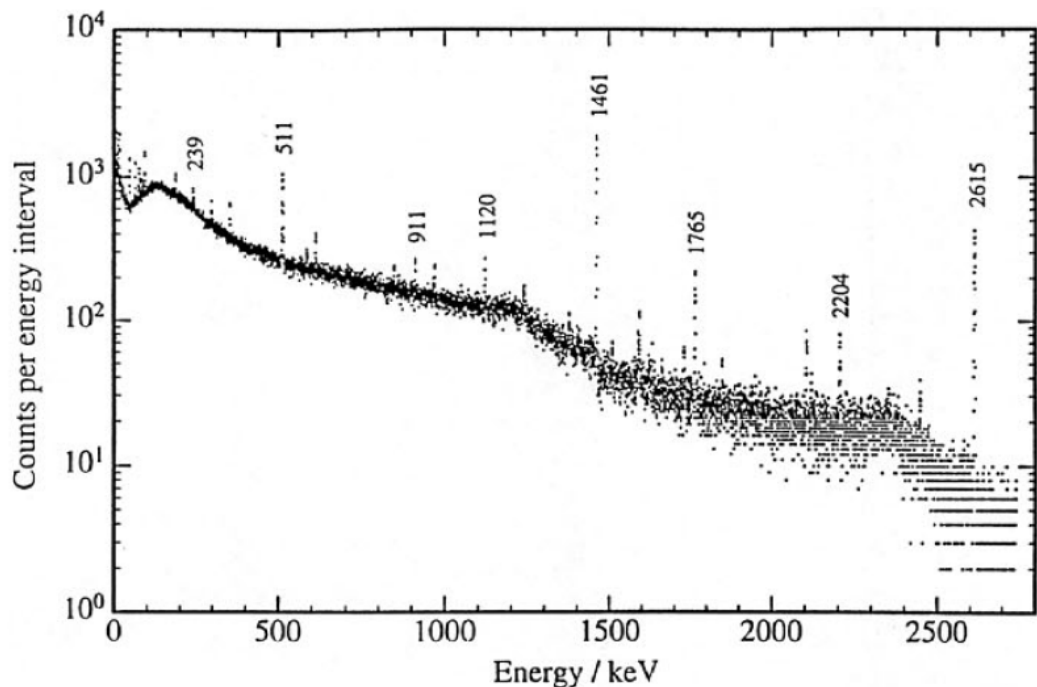


Figure 49 — Pulse-height spectrum of the natural background taken with a Ge-detector spectrometer in a typical environment for ionization chamber measurements. (Unpublished results, PTB).

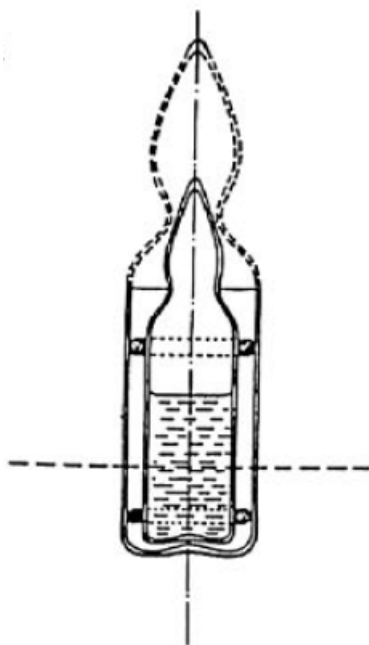


Figure 50-1 — Arrangement for an investigation of the influence of the ampoule walls. The small ampoule of BIPM/NBS(NIST) type contains a strong solution of ^{241}Am . The dashed top of a glass absorber has been cut off. The measurements were done with the SIR at the BIPM. Reproduced from [372].

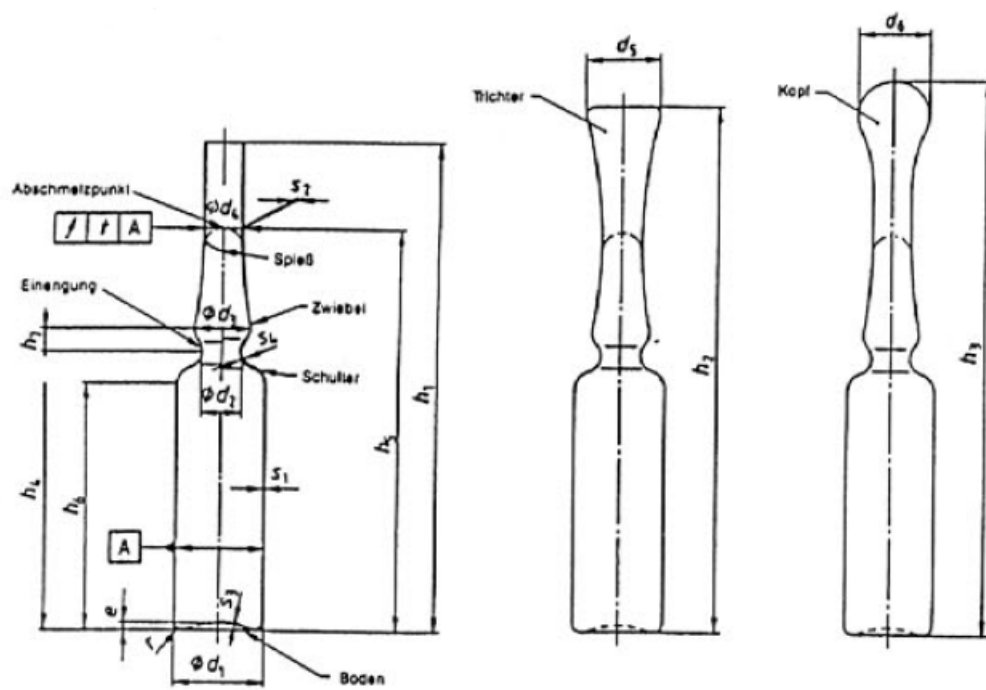


Figure 50-2 — Standard ampoules after ISO 9187-1, Part 1, with dimensions to be standardized. (Abschmelzpunkt ⇒ sealing point, Spieß ⇒ spear, Einengung ⇒ embankment, Zwiebel ⇒ onion (-shape), Schulter ⇒ shoulder, Boden ⇒ bottom). Reproduced from ISO 9187-1.

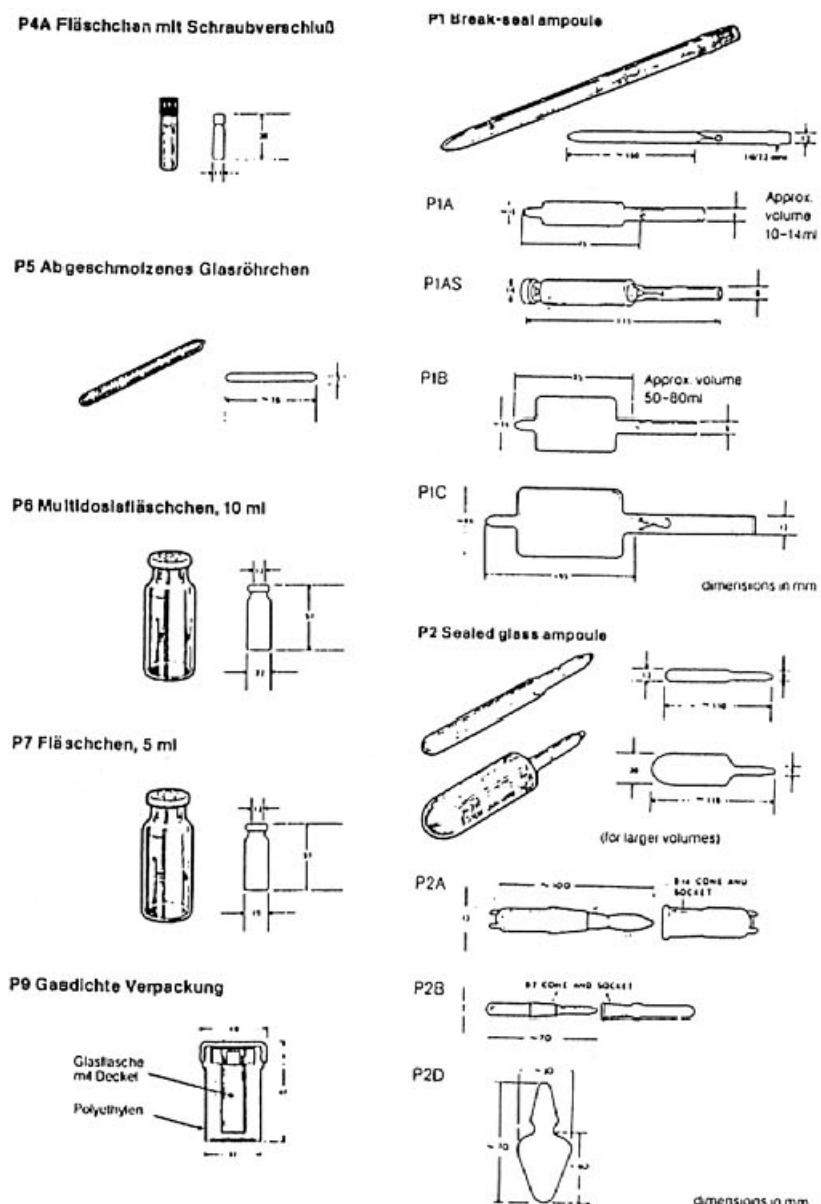


Figure 51 — Various ampoules and vials used by manufacturers of radioactive sources, for example the P6 multidose vial for solutions or P1A for radioactive gases (Fläschchen mit Schraubverschluß ⇒ vial with screw cap, Abgeschmolzenes Glasröhrchen ⇒ sealed glass tube, Multidosisfläschchen ⇒ multidose glass vial, Fläschchen ⇒ vial, Gasdichte Verpackung ⇒ gas tight packaging, Glasflasche mit Deckel ⇒ capped glass vial). Reproduced from [6].

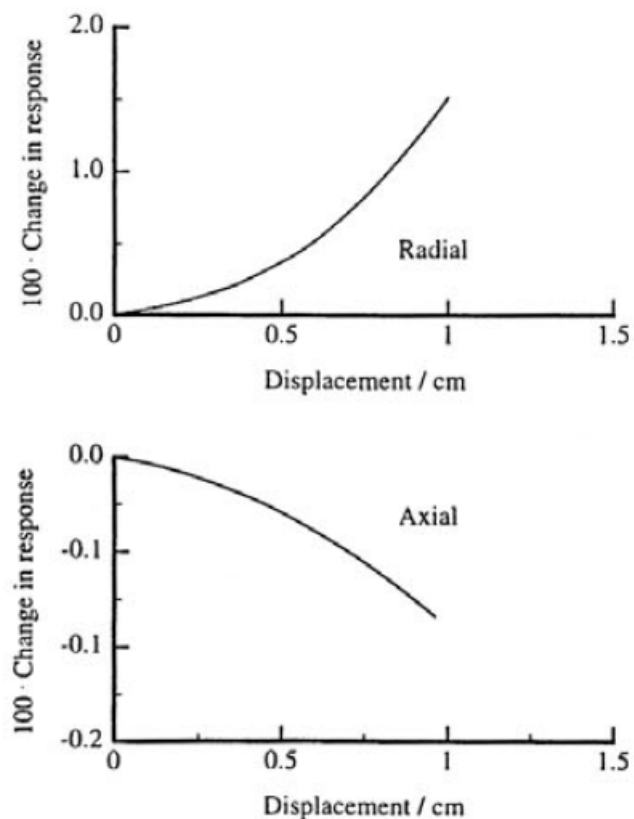


Figure 52-1 — Variation of response with displacement from the centre of an ionization chamber for 3 ml solution in 5 ml ampoule. After Woods et al. ([477], see p. 195).

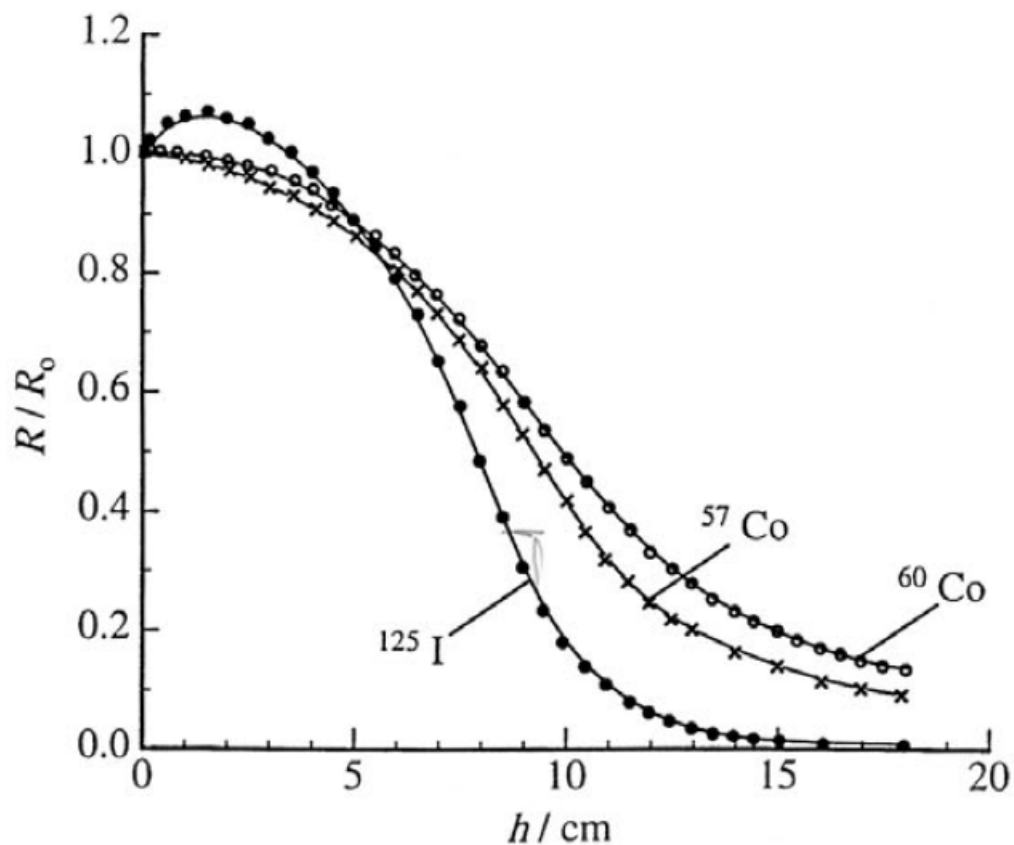


Figure 52-2 — Variation of a radionuclide-calibrator reading R/R_0 , normalized to that of the standard operating position for ^{60}Co , ^{57}Co and ^{125}I . The low-photon energy emitting source of ^{125}I shows a negative characteristic. Vertical displacement in the well. After Schrader ([398], see p. 190).

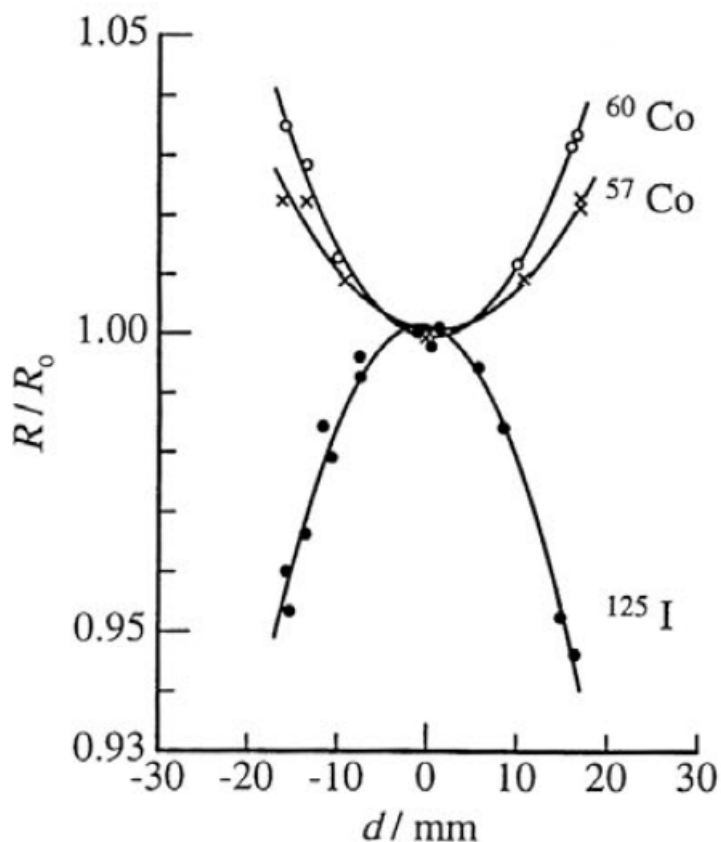


Figure 52-3 — Variation of a radionuclide-calibrator reading R/R_o , normalized to that of the standard operating position for ^{60}Co , ^{57}Co and ^{125}I . The low-photon energy emitting source of ^{125}I shows a negative characteristic. Horizontal displacement. After Schrader ([398], see p. 190).

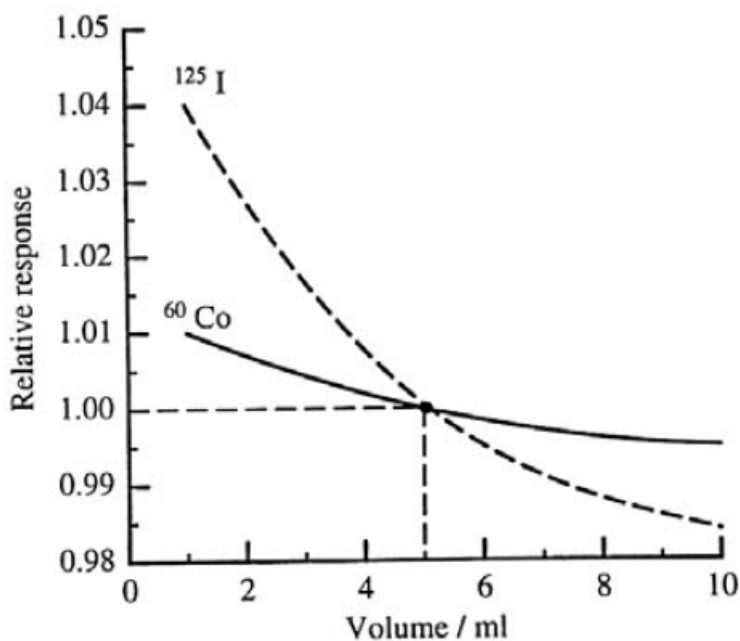


Figure 53-1 — Variation of ionization-chamber response with volume of solution relative to that of 5 ml volume (dashed line) for ^{60}Co and ^{125}I in a 10 ml P6 vial. After Woods et al. ([482], see p. 195).

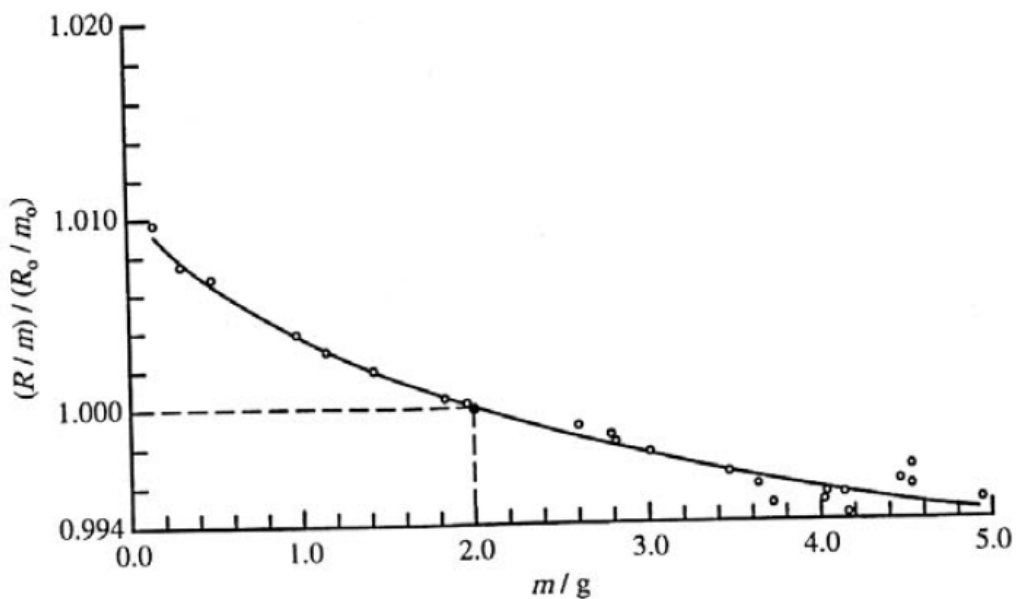


Figure 53-2 — Variation of instrument reading per solution mass $(R/m)/(R_0/m_0)$, normalized to that of a standard filling of $m_0 = 2 \text{ g}$ in a PTB ampoule: For a radionuclidecalibrator and ^{60}Co , ^{57}Co and ^{125}I . From Schrader ([398], see p. 190).

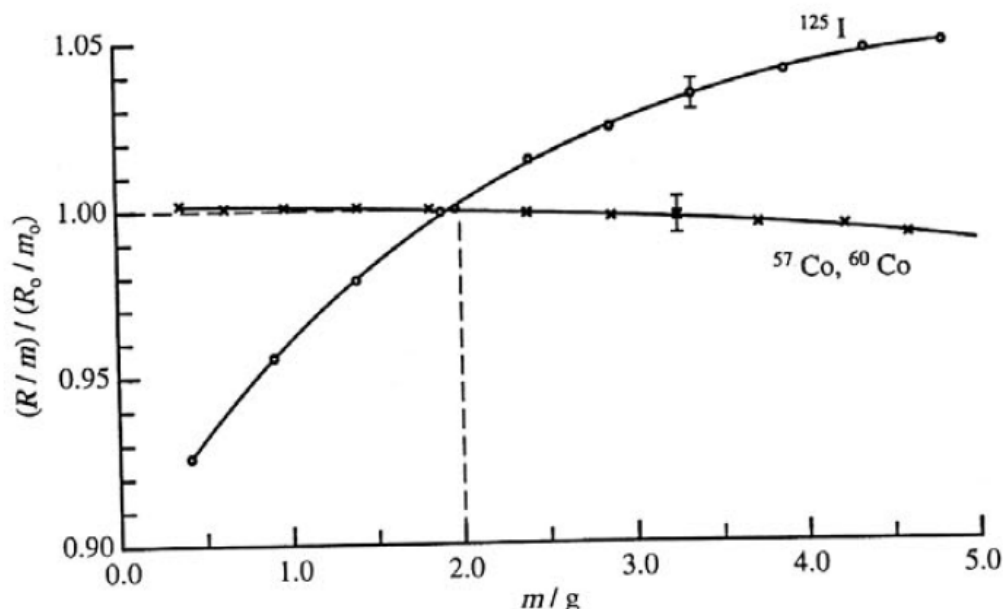


Figure 53-3 — Variation of instrument reading per solution mass $\frac{R/m}{R_0/m_0}$, normalized to that of a standard filling of $m_0 = 2 \text{ g}$ in a PTB ampoule: For the PTB ionization chamber, type IG 12 of Centronic (see Figure 14, see p. 94) with $m_0 = 2 \text{ g}$ (dashed line) and various photon-emitting radionuclides with energies above 120 keV . (Unpublished results, PTB).

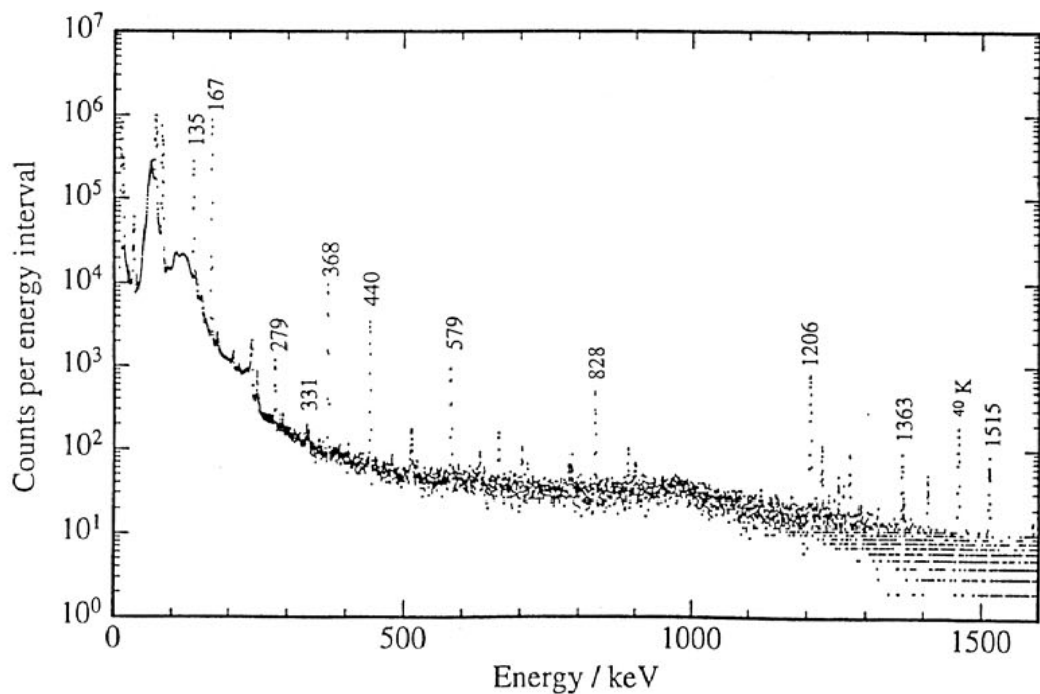


Figure 54 — Pulse-height spectrum of a ^{201}Tl solution source measured with a Ge-detector spectrometer to determine the activity parts of radionuclidic impurities such as in Table 3. (Ge-detector spectrum by PTB).

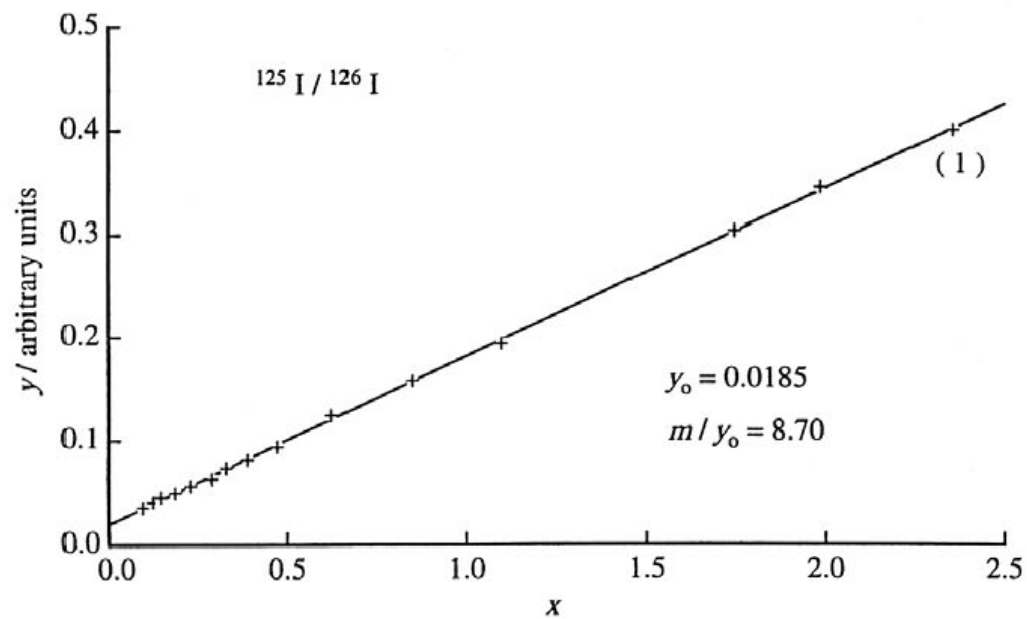


Figure 55-1 — For a ^{125}I source with a radionuclidic impurity of ^{126}I .

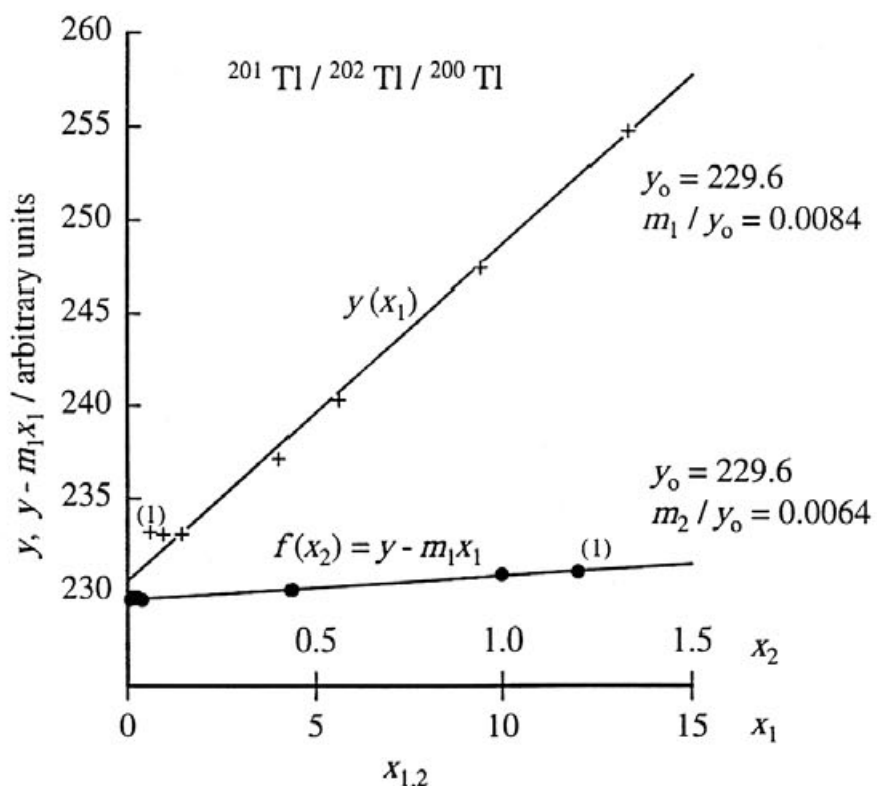


Figure 55-2 — For a ^{201}Tl source with two radionuclidic impurities; the admixture of ^{202}Tl is first analysed in the presentation of $y(x_1)$, indicated by crosses, and then, ^{200}Tl in $y - m_1 x_1$, indicated by dots. The x_1 and the x_2 scale differ by a factor of 10.

Figure 55 — Data of the decay-constant difference method by Schrader and Walz ([399], see p. 190). The first measuring point is marked by (1). The given values of y_0 and m/y_0 and the straight lines result from linear regression analysis

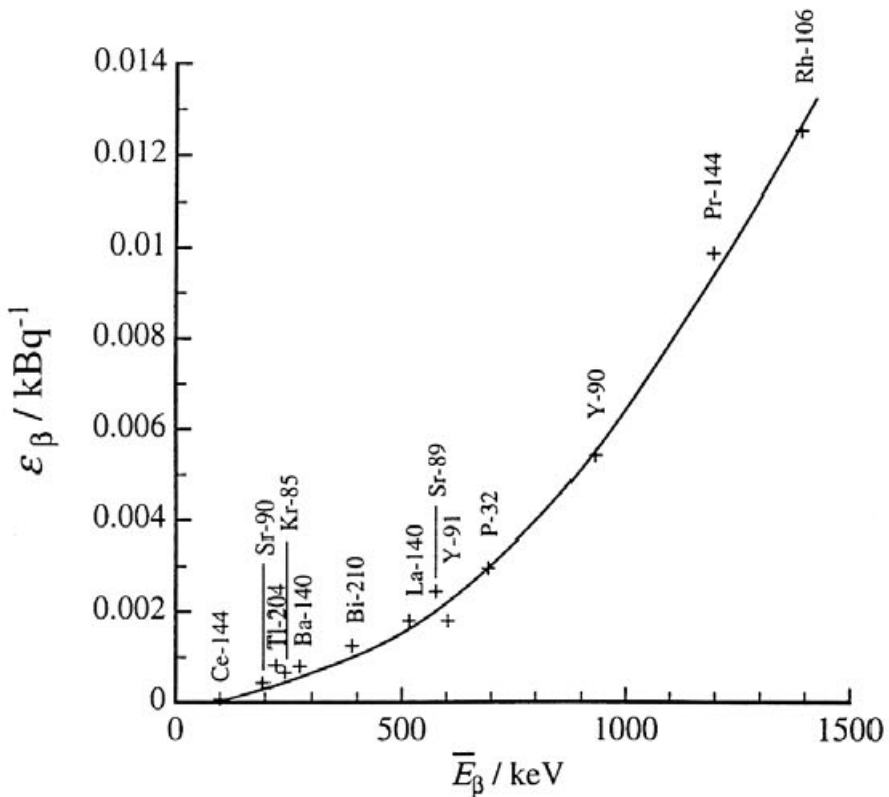


Figure 56-1 — For an ionization chamber, type IG 12 of Centronic, see drawing in Figure 14. (Unpublished data from PTB).

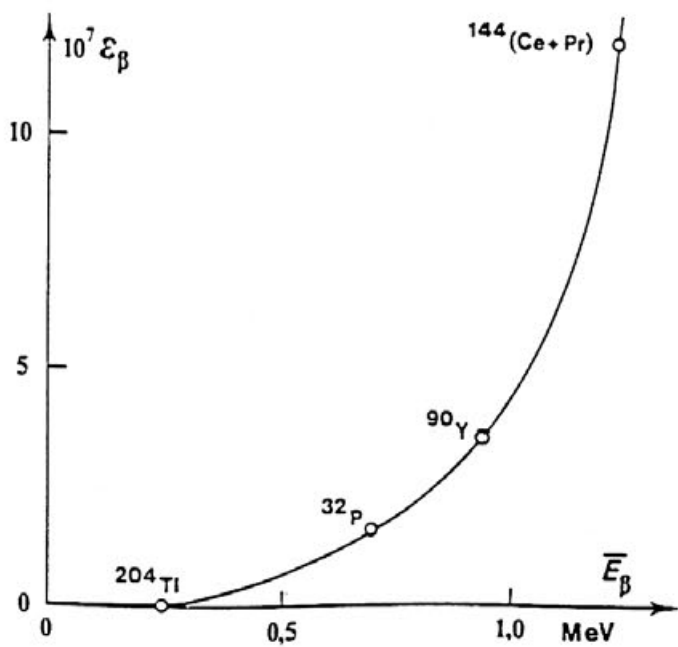


Figure 56-2 — For the ionization chamber of the SIR (BIPM). Reproduced from [384].

Figure 56 — β efficiency of an ionization chamber by bremsstrahlung photons versus average energy of the primary emitted β particles from various radionuclides. In case of further γ rays emitted by a nucleus their

contributions to the ionization current have been subtracted in the data treatment. The results are normalized to the pertinent current values of a reference source.

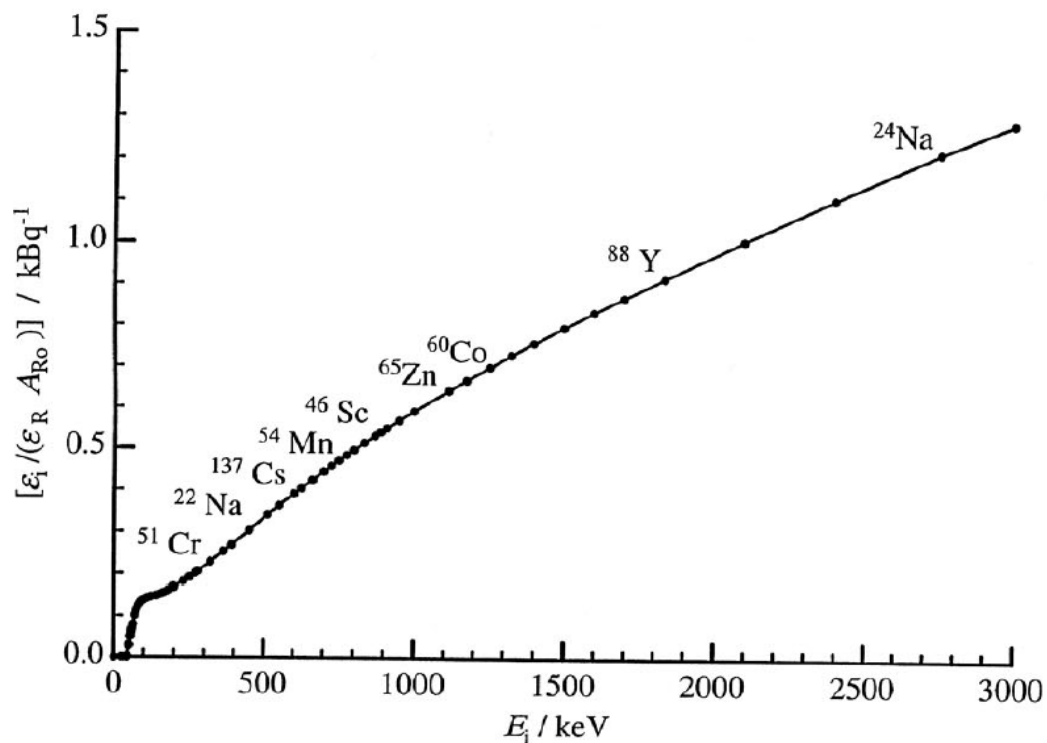


Figure 57 — Photon efficiency ε versus photon energy E for the PTB ionization chamber, type IG 12 of Centronic (see Figure 14, see p. 94), with various radionuclides. (Unpublished data from PTB).

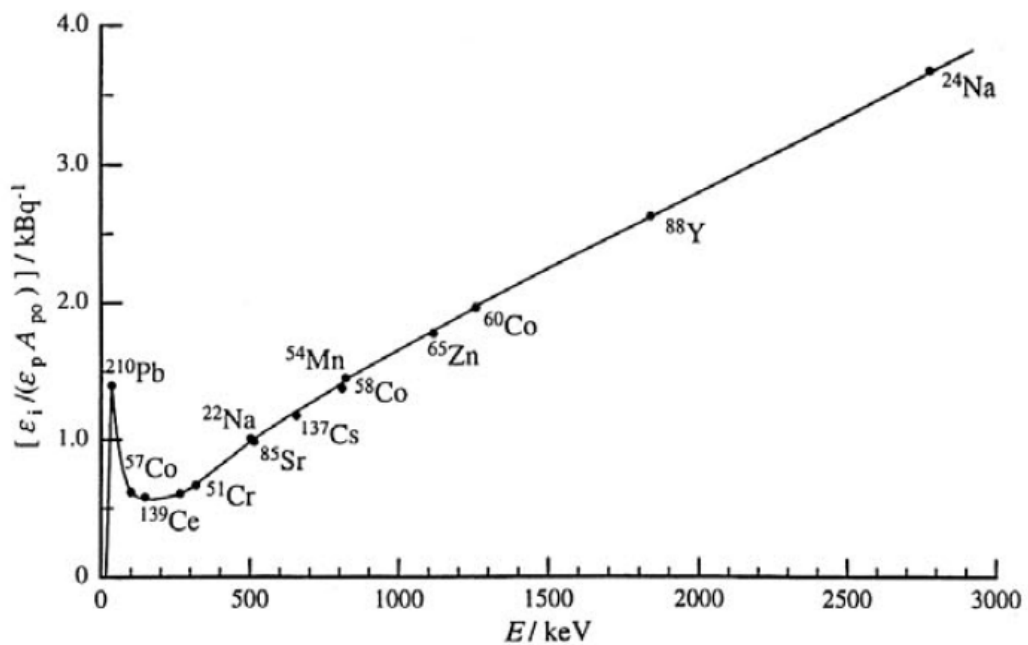


Figure 58-1 — Without filter up to a photon energy of 2754 keV.

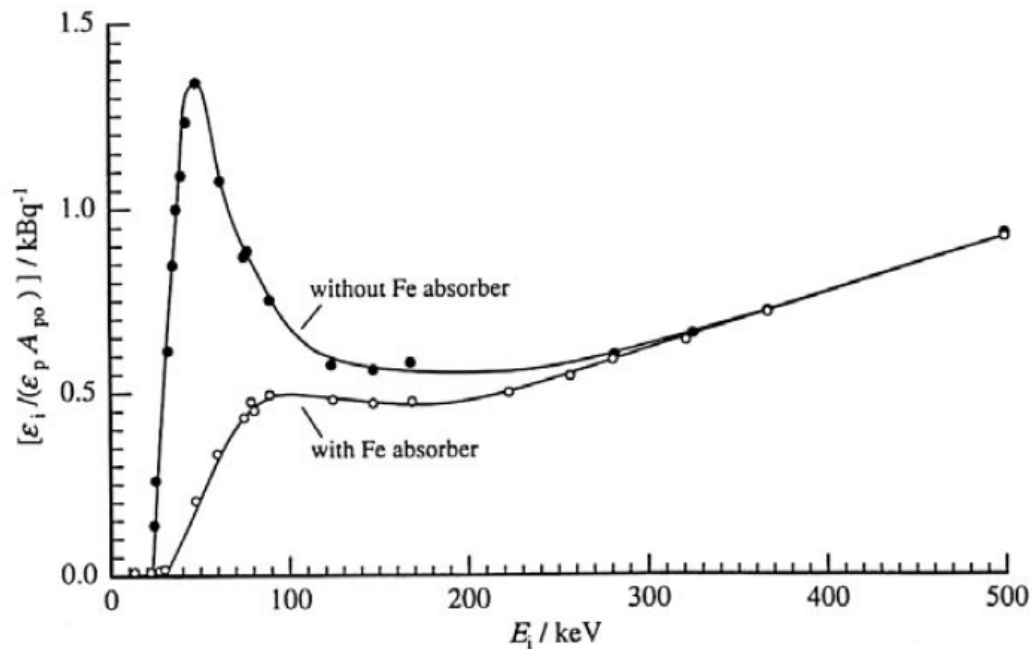


Figure 58-2 — Without and with Fe filter 1 mm thick and for photon energies from about 15 keV to 550 keV.

Figure 58 — Photon efficiencies ε versus photon energy E with various radionuclides for a radionuclide calibrator without and with filter (absorber) around the source. Reproduced from [401].

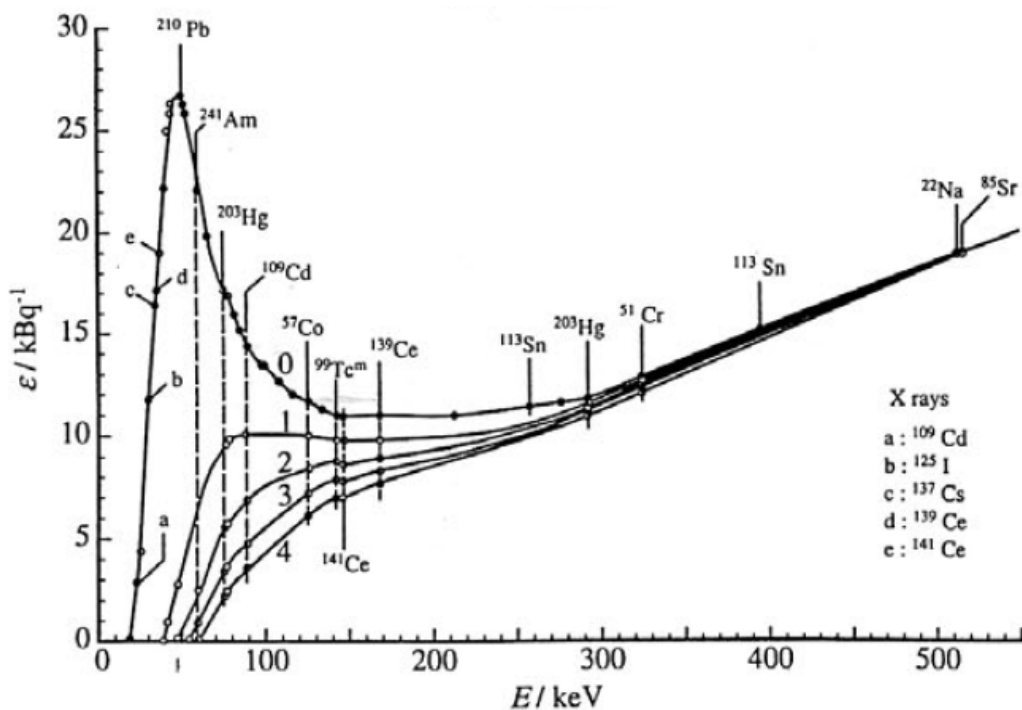


Figure 59 — Photon efficiencies ε versus photon energy E with various radionuclides for a radionuclide calibrator without and with Fe filters of various thickness around the source for photon energies from about 15 keV to 550 keV, without filter, marked by (0), and with Fe filter from 1 mm to 4 mm thick, marked by (1) to (4). (Unpublished data from PTB).

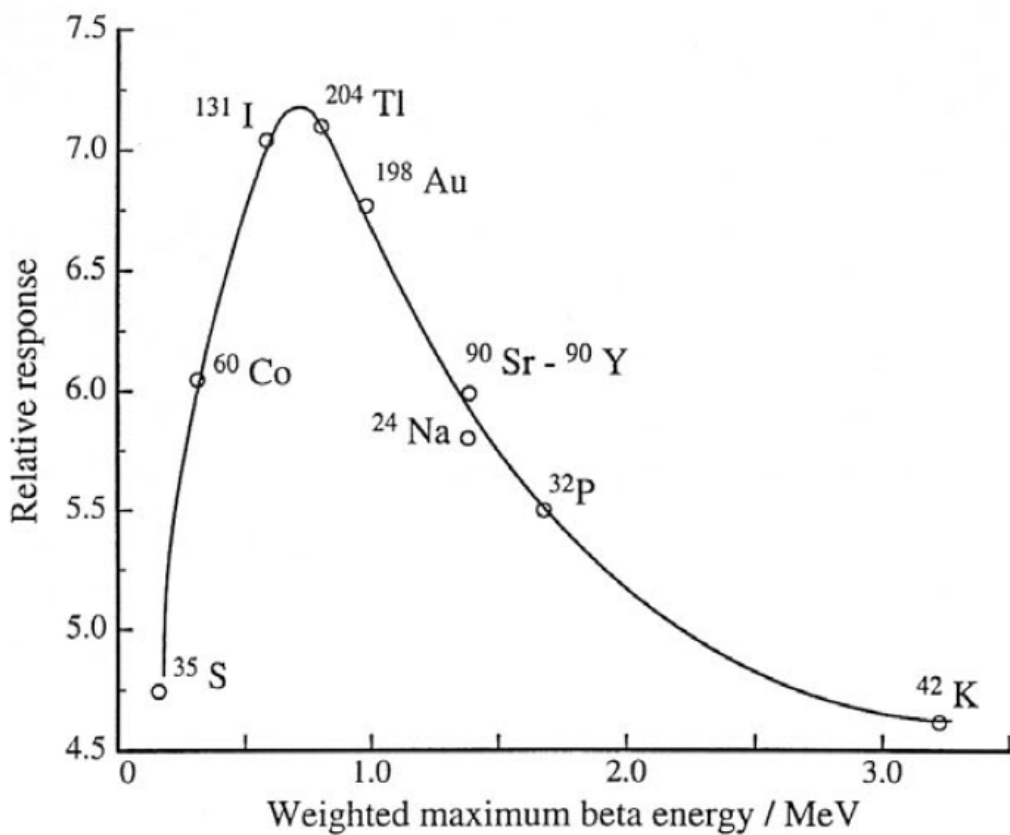


Figure 60-1 — Energy response of the NBS $2\pi\beta$ -ionization chamber. The current per unit activity has been plotted as a function of the maximum β -particle energy. The energy value is the weighted average of the energies of the branches when there is β -particle branching. The response curve appears to be a smooth curve on both sides of a peak at a maximum energy of approximately 0.7 MeV. The decrease above the peak is due to the finite dimensions of the chamber. Early data after Mann and Seliger ([295], see p. 183).

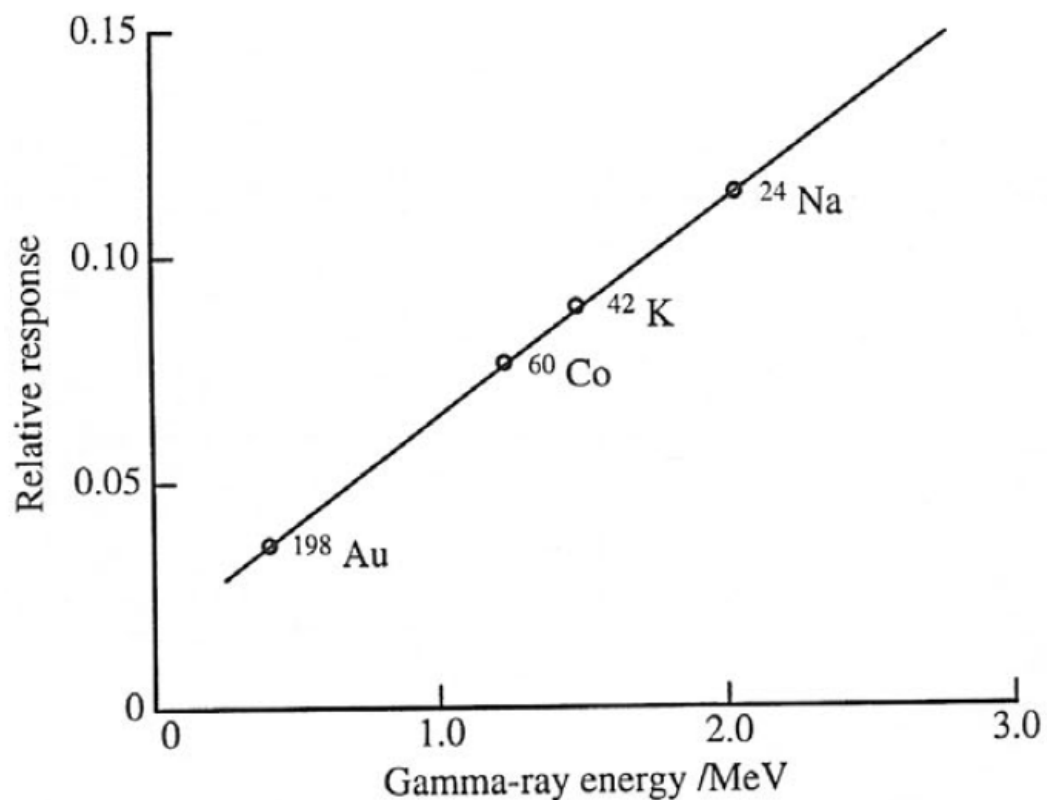


Figure 60-2 — Energy response of the NBS $4\pi\gamma$ -ionization chamber. The current per unit activity has been plotted as a function of the γ -ray energy. Where two γ rays appear in cascade, the energy values have been averaged. It should be possible, knowing the decay scheme of a particular radionuclide, to interpolate and to standardize the disintegration rate of a sample of the nuclide by measurement of the current only. Early data after Mann and Seliger ([295], see p. 183).

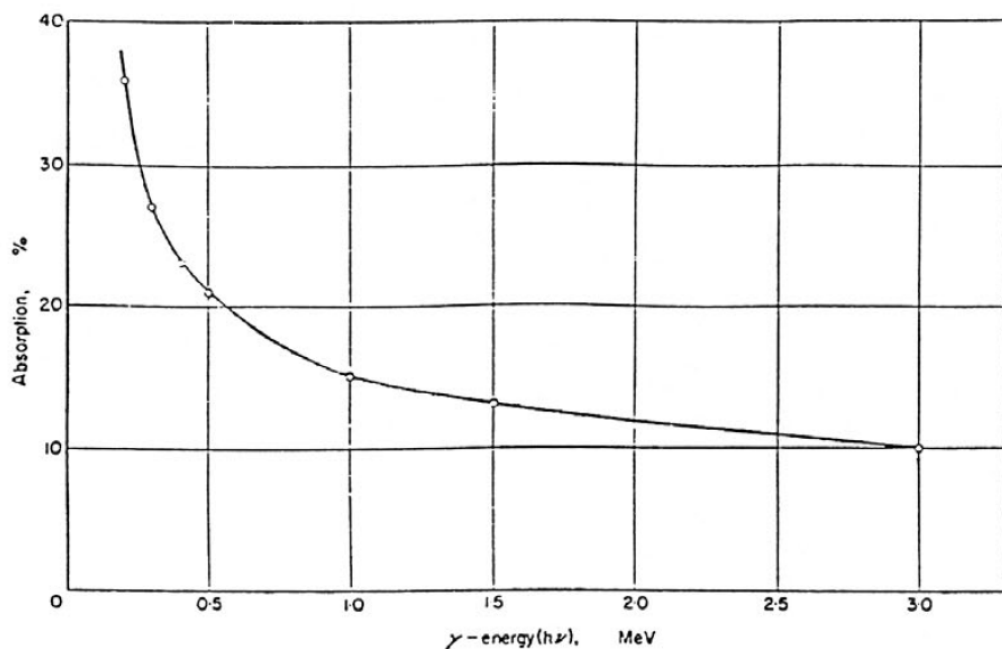


Figure 61-1 — Absorption of γ radiation in a brass liner of an ionization chamber cavity. Reproduced from [90].

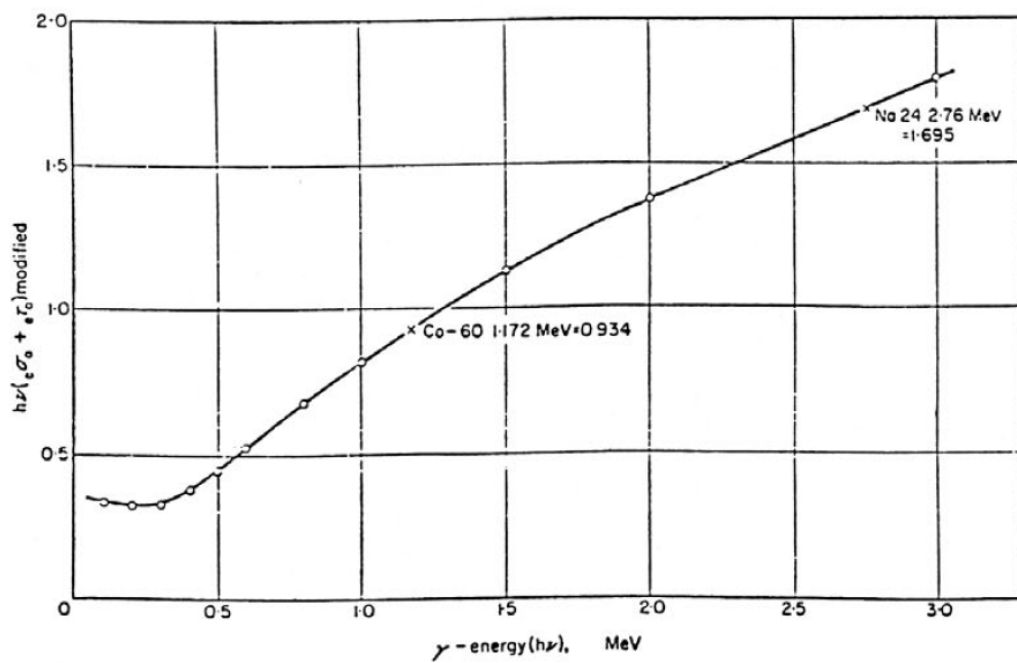


Figure 61-2 — Secondary electron production in brass against γ energy (modified for absorption in a brass liner of an ionization chamber cavity). Two radionuclides were selected, namely, ^{60}Co and ^{24}Na , from which it was hoped to normalize the curve so as to read directly in current I per γ -ray quantum against γ energy, and to calculate a response by simple summing of the contributions of the constituent γ rays of a radionuclide. Reproduced from [90].

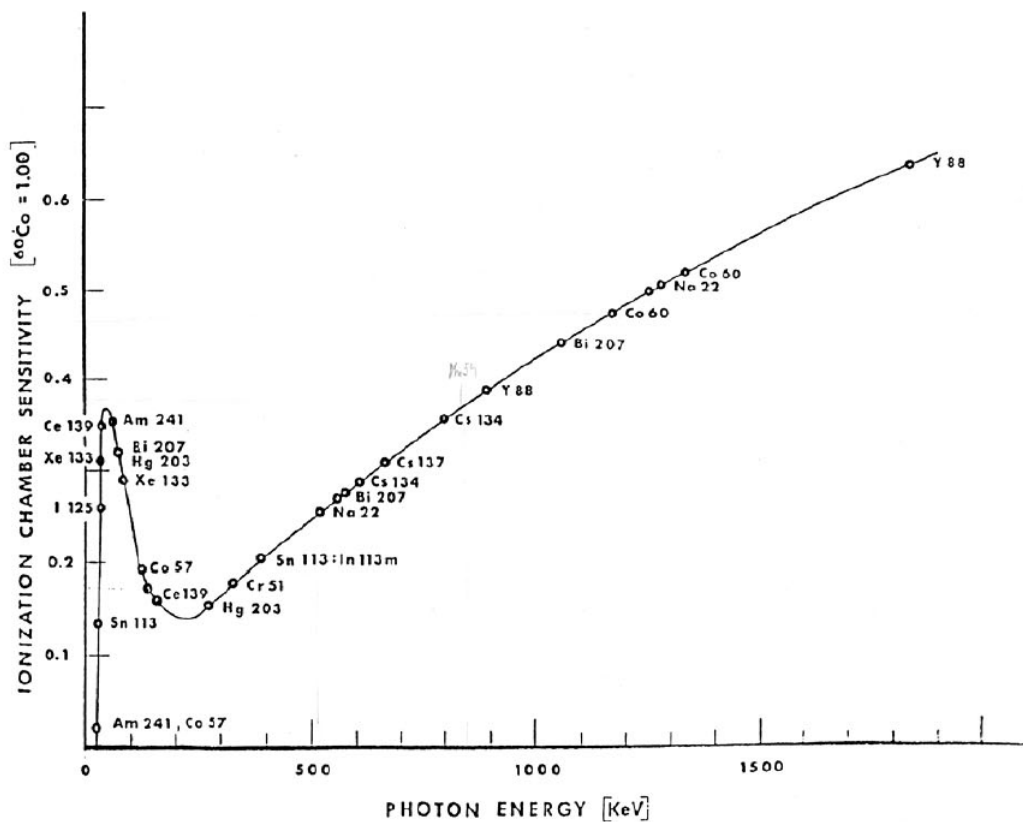


Figure 62 — Sensitivity of typical ionization chamber of calibrator as a function of photon energy. Sensitivity is normalized by chamber response to ^{60}Co radiations. Reproduced from [431].

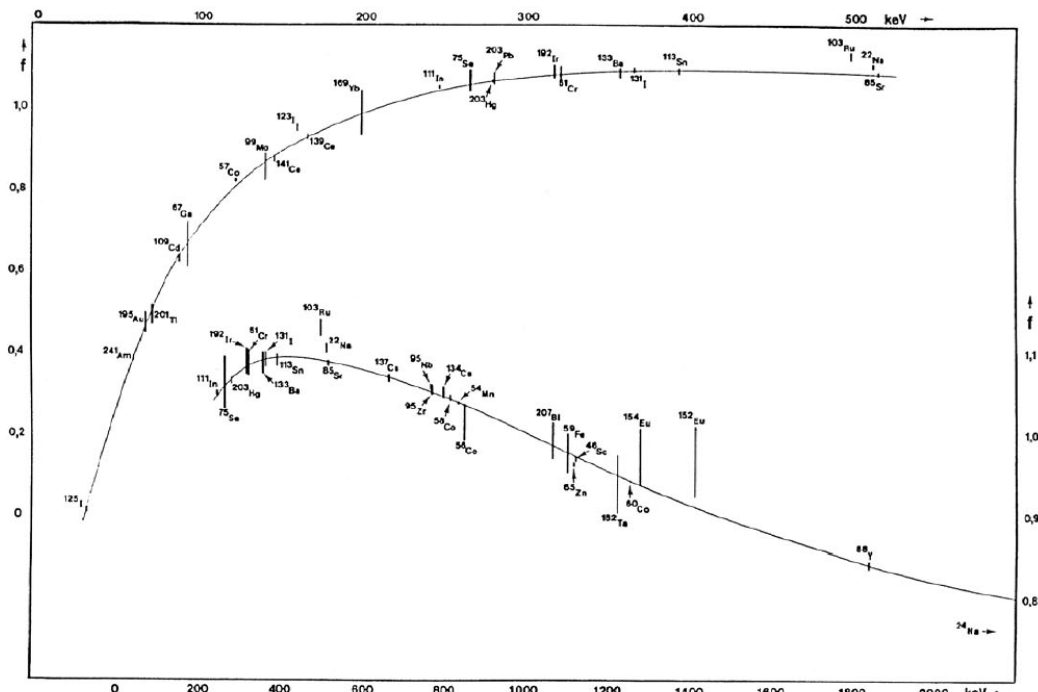


Figure 63-1 — Relative photon efficiency f of the ionization chamber of the SIR (BIPM) versus photon energy. The ordinate f is calculated relative to an arbitrarily chosen efficiency function which increases linearly with energy. The curve on the right gives the high energy part of the relative efficiency

(different energy scales on left (top) and right (bottom) of the figure!). The value of a radionuclides is plotted at the photon energy with the highest emission probability. Reproduced from [376] and [383].

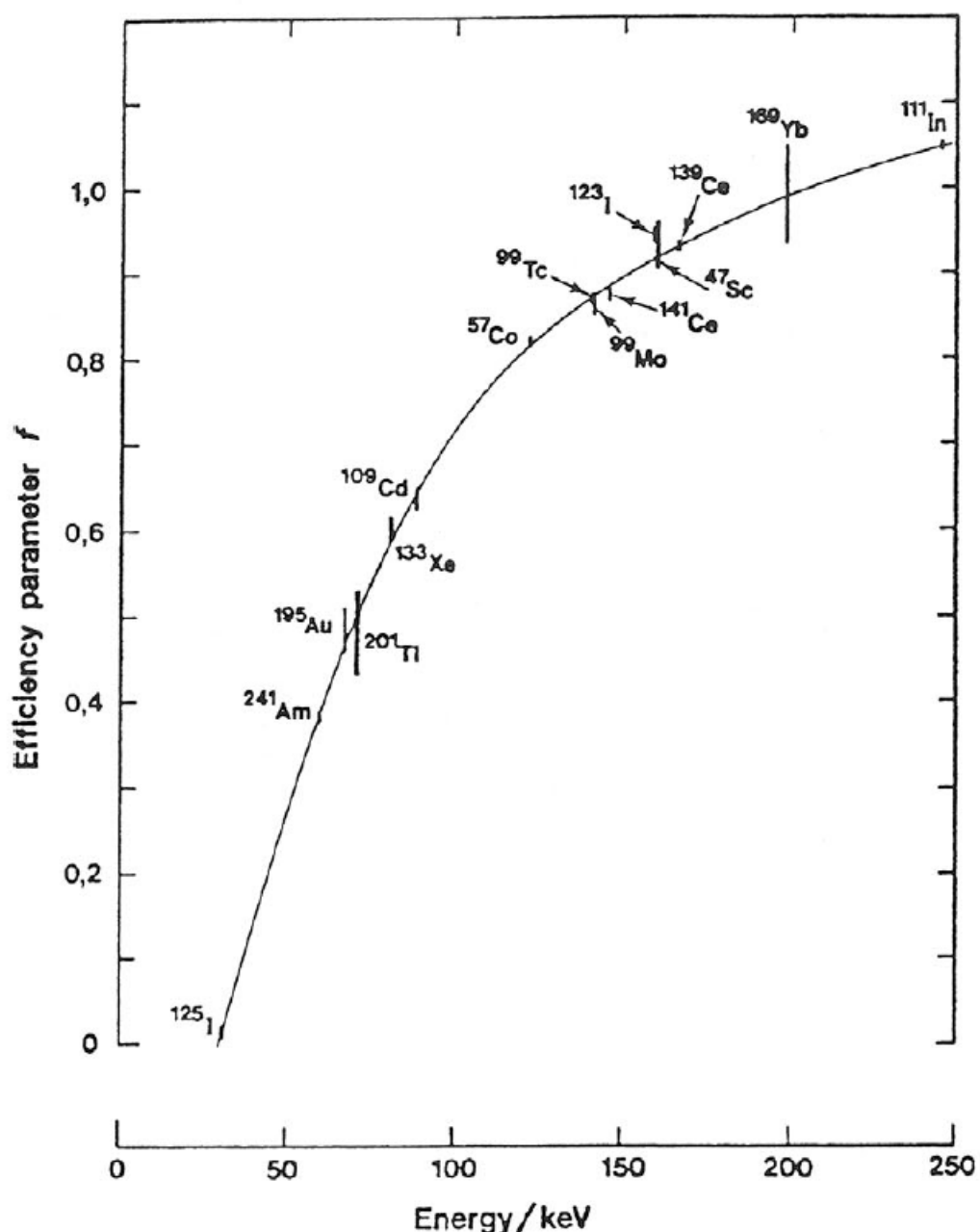


Figure 63-2 — Efficiency as a function of photon energy - updated low energy part of the curve of Figure 63-1 - for the SIR ionization chamber at the BIPM.
Reproduced from [346].

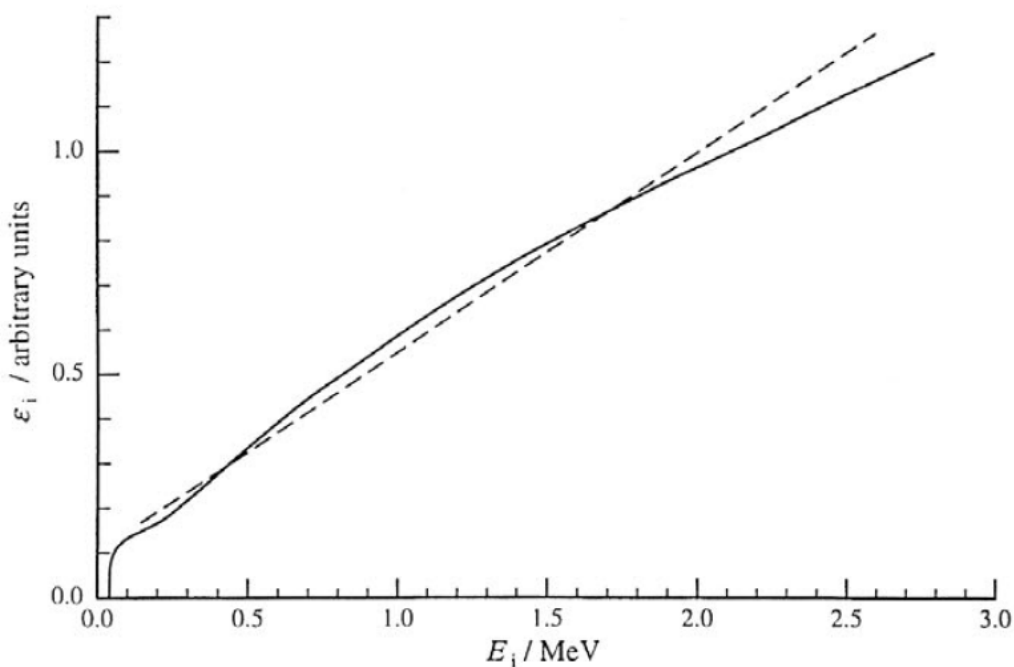


Figure 64-1 — Photon efficiency ε_i versus photon energy for the PTB ionization chamber, type IG 12 of Centronic (see Figure 14, see p. 94). The dashed line shows the chosen linear efficiency function $\varepsilon = 0.45 E + 0.1$ for reduction (energy E in MeV). After Weiss ([470], see p. 194).

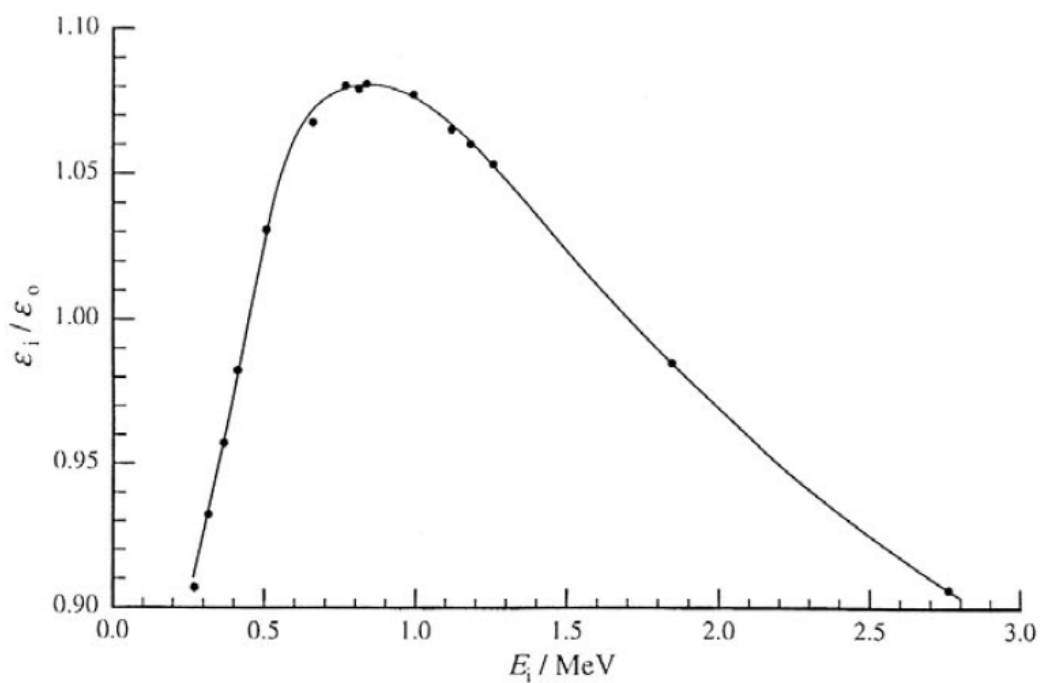


Figure 64-2 — Reduced efficiency curve. After Weiss ([470], see p. 194).

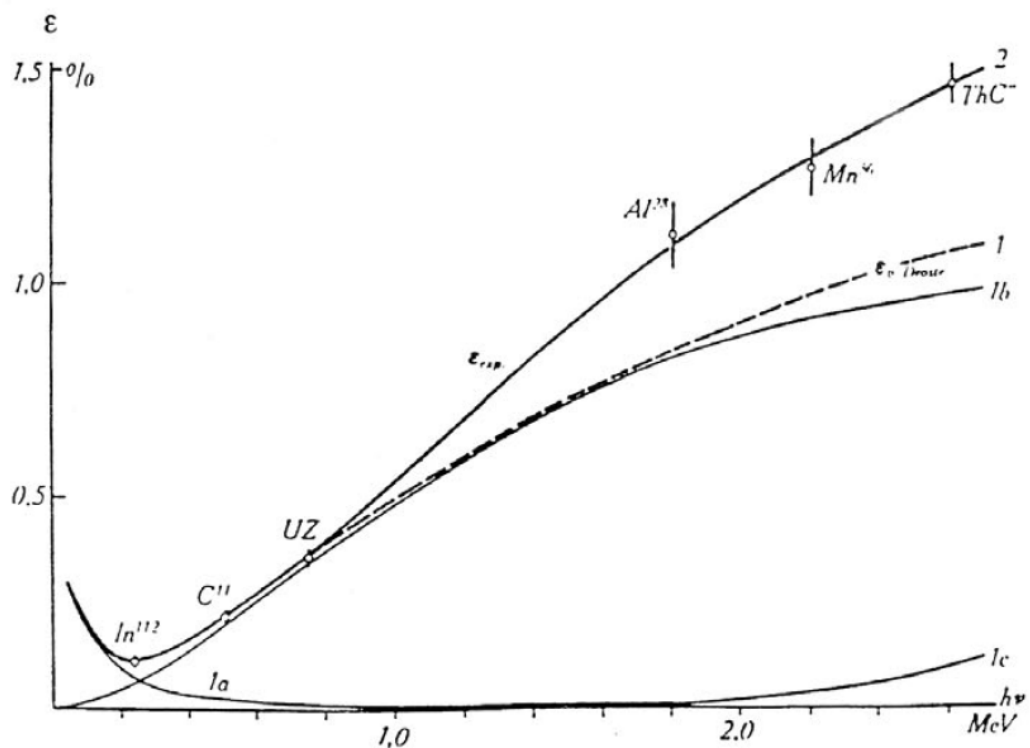
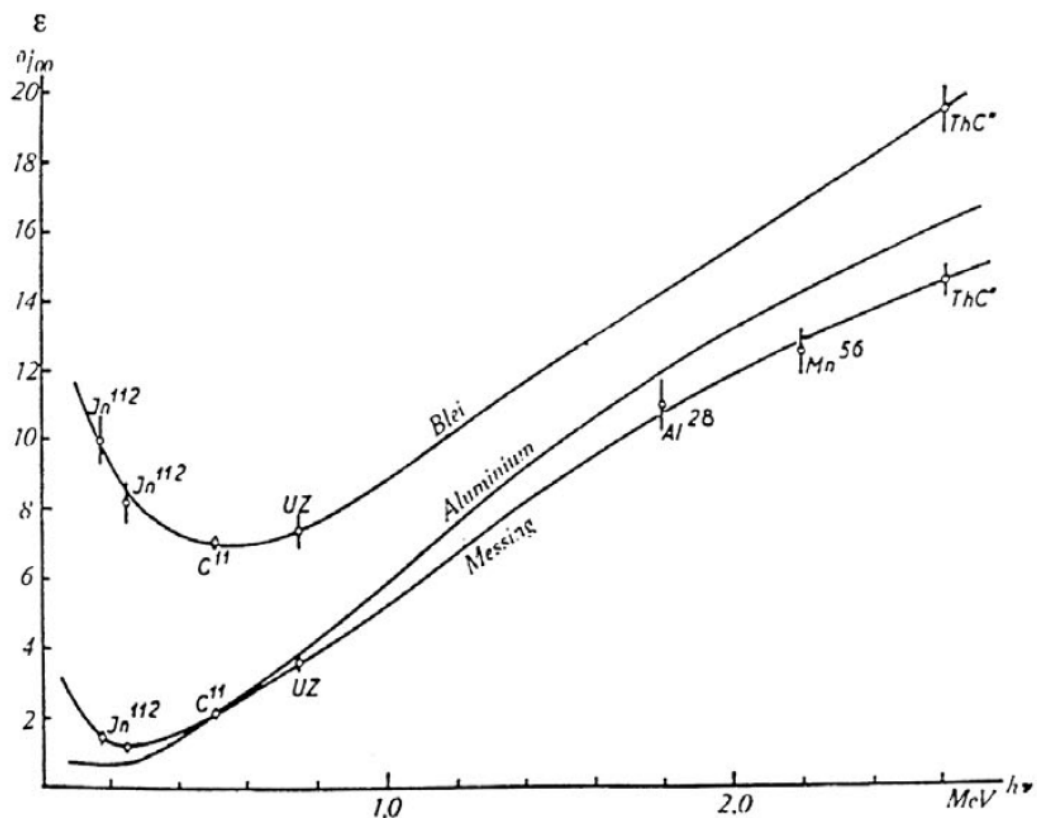


Figure 65-1 — Curve 1 is calculated for copper by the model of v. Droste ([118], see p. 172) using photon interaction with parts from photo effect (a), Compton effect (b) and pair creation (c), curve 2 is experimentally determined.



**Figure 65-2 — Curves for tube materials such as lead, aluminium and brass
(Aluminium \Rightarrow aluminium, Blei \Rightarrow lead, Messing \Rightarrow brass).**

Figure 65 — Sensitivity of counter tubes for various materials and photon energies $h\nu$.
Reproduced from [43].

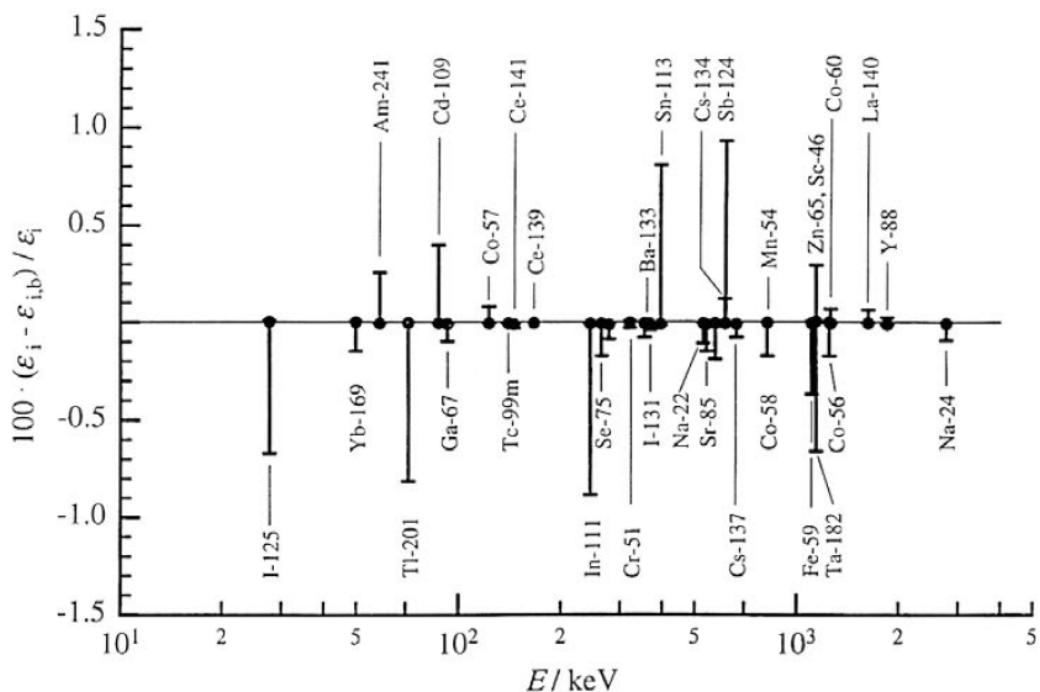


Figure 66 — Consistency check for the photon efficiency curve of the PTB ionization chamber. The radionuclide efficiency values were calculated in term of the weighted average of the corresponding photon efficiencies from the

curve of Figure 57. The relative deviation of a measured and a calculated radionuclide efficiency is represented by a bar. This is plotted versus the photon energy with the highest emission probability for the relevant radionuclide. (Unpublished data from PTB).

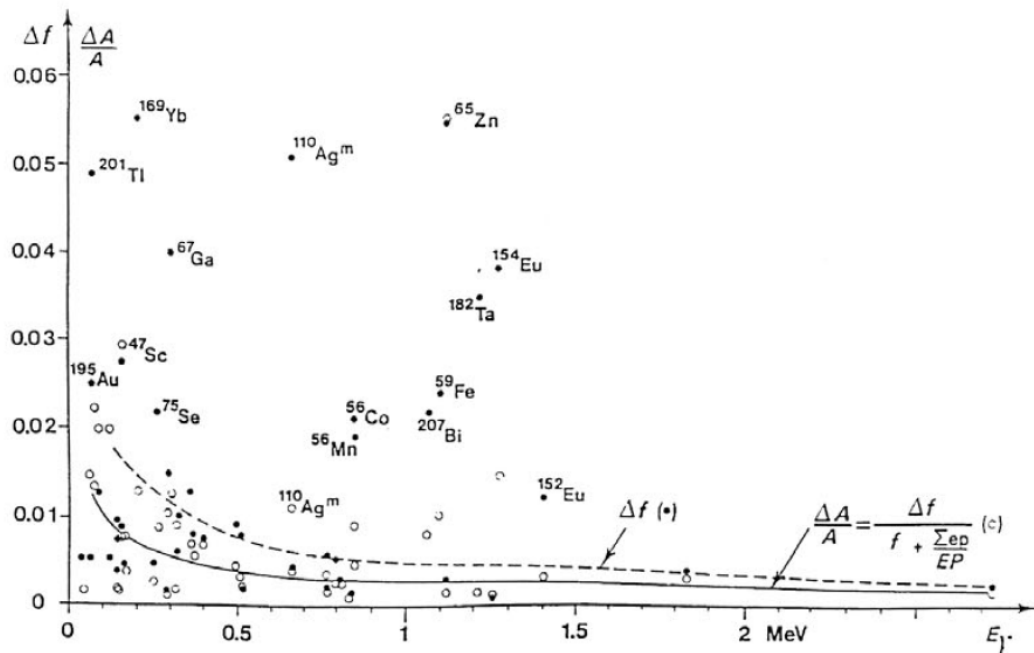


Figure 67 — Uncertainty of the measurements with the ionization chamber of the SIR (BIPM). The values of the deviation Δf (full dots and dashed line) calculated by the error propagation law from the uncertainty components of the reduced efficiency function f and the relative uncertainty of an activity measurement $\Delta A/A$ (circles and full line) estimated from f are plotted versus photon energy E . Radionuclides showing larger deviations are referred. Reproduced from [378].

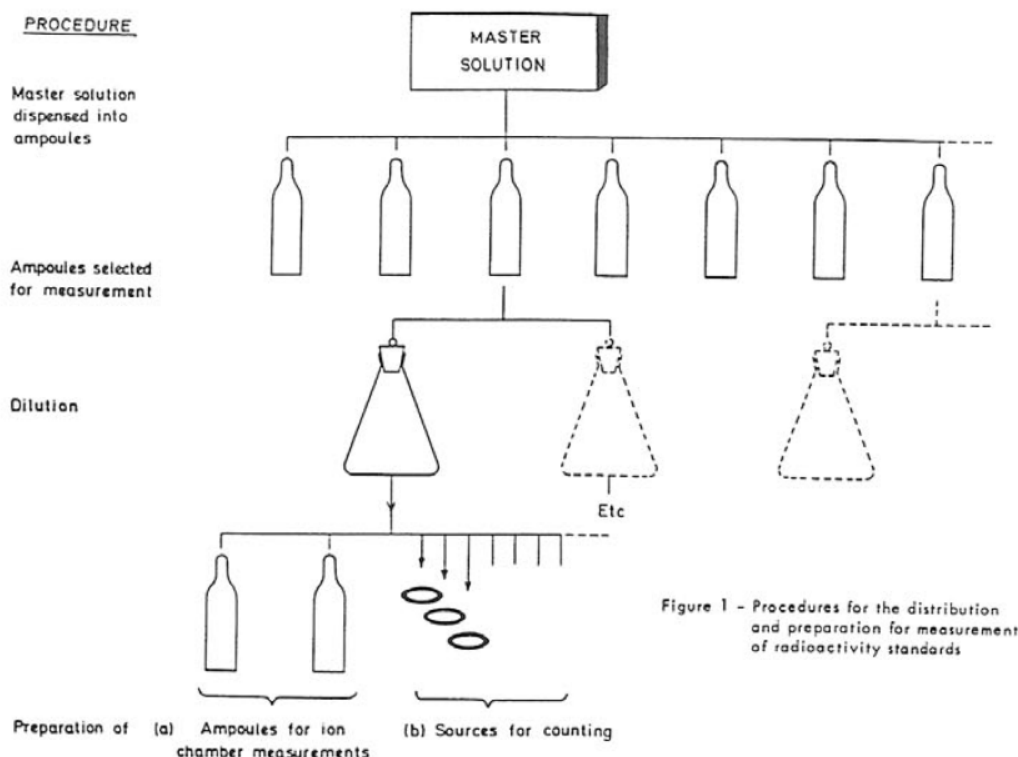


Figure 1 - Procedures for the distribution and preparation for measurement of radioactivity standards

Figure 68-1 — Procedures for the distribution and preparation for measurement of radioactivity standards. The dilution steps are shown in a family of solutions dispensed into ampoules or dripped on foils for solid sources. Each step is followed by weighing procedures and controlled by measurements. Reproduced from the monograph of Campion, BIPM ([63], see p. 168).

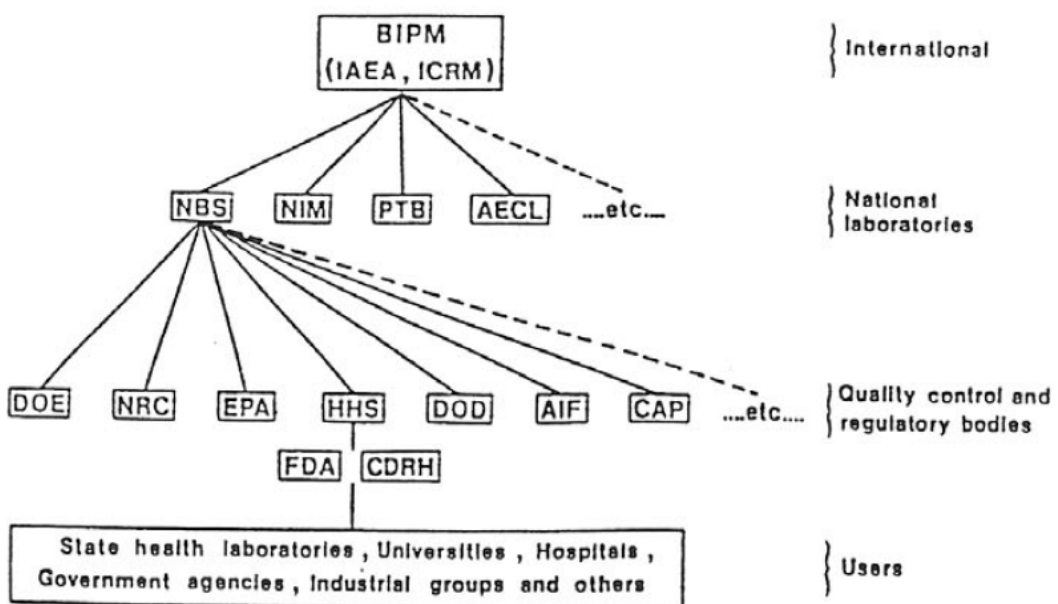


Figure 68-2 — Hierarchy of radioactivity-standardization laboratories and organizations ("Traceability tree"). Reproduced from [294].

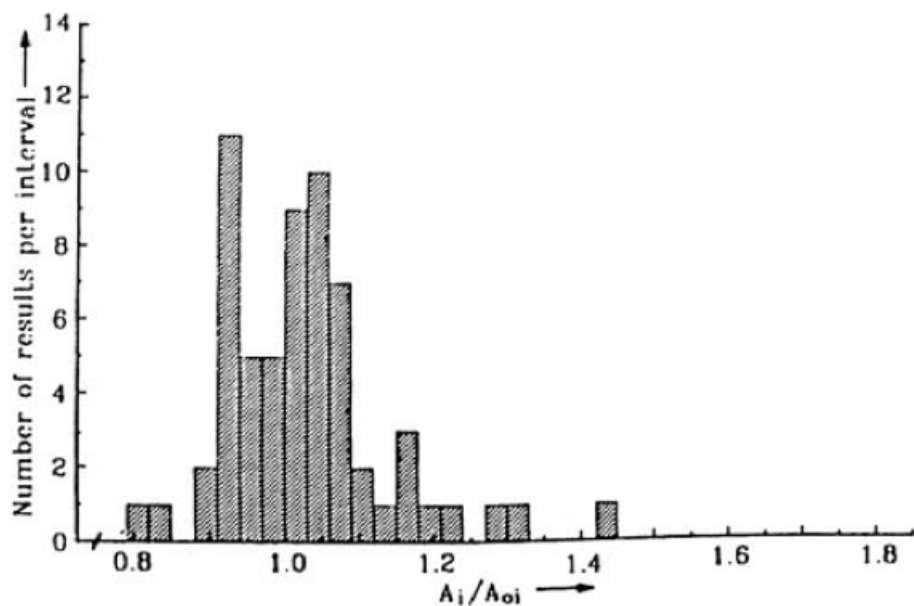


Figure 69-1 — Interval distribution for $^{99}\text{Tc}^m$ solution measured in glass vials.

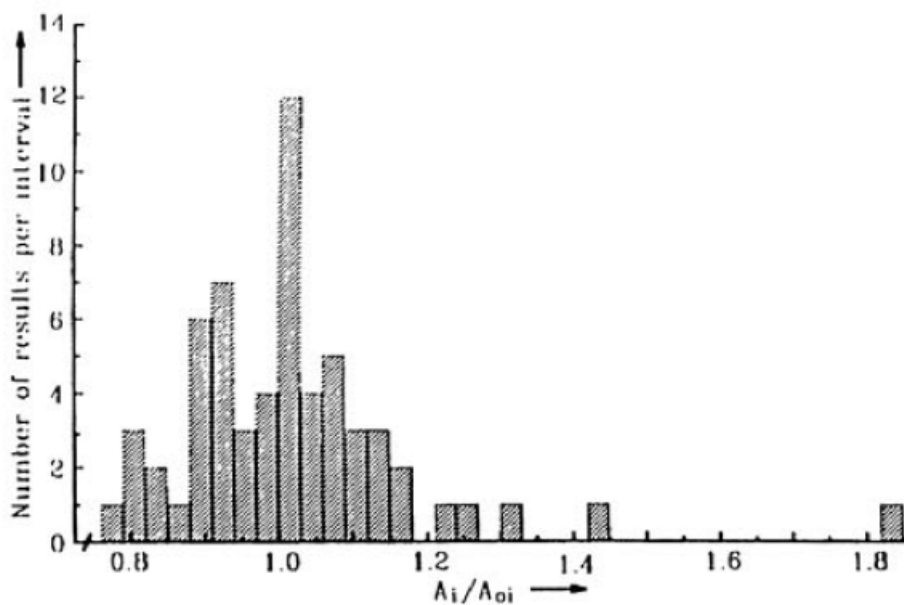


Figure 69-2 — The same solution filled by a participant in a syringe and measured again (the reported activity values corrected for the residual activity in the "empty" glass vial).

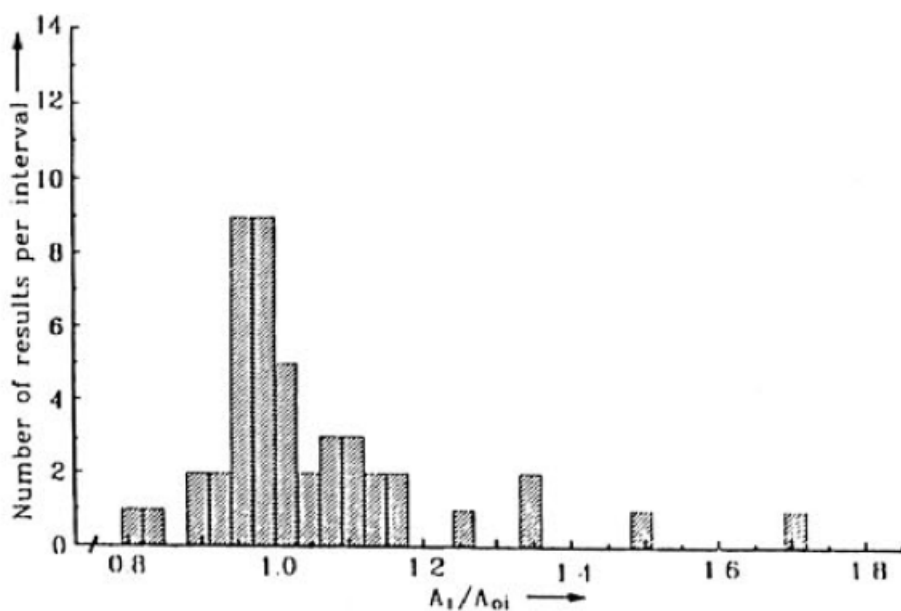


Figure 69-3 — Interval distribution for a ^{123}I solution in glass vials.

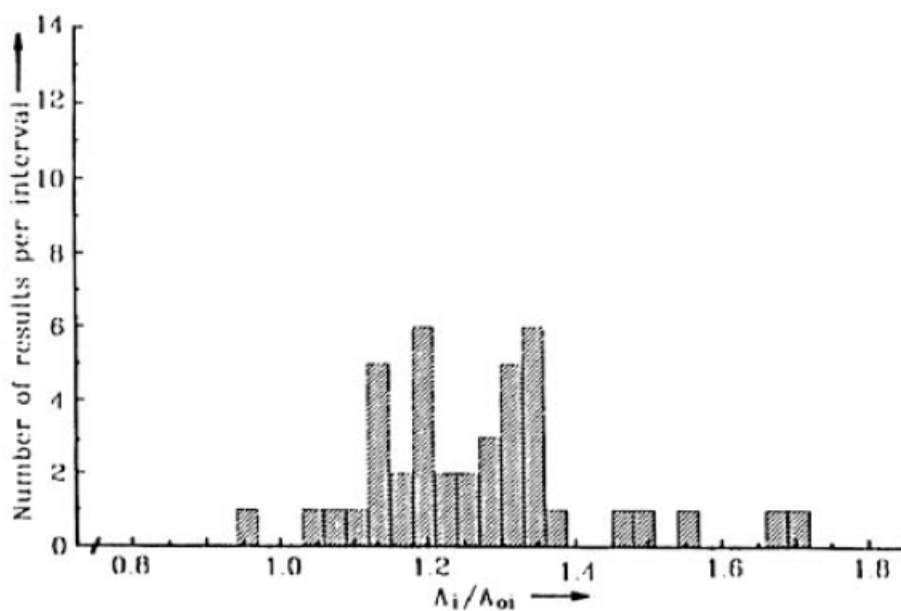


Figure 69-4 — Interval distribution of the same ^{123}I solution measured in a syringe and corrected for the residual activity.

Figure 69 — Distribution of results from comparisons in nuclear medicine. A_i activity measured by participant. A_{oi} activity measured by PTB. Reproduced from [100].

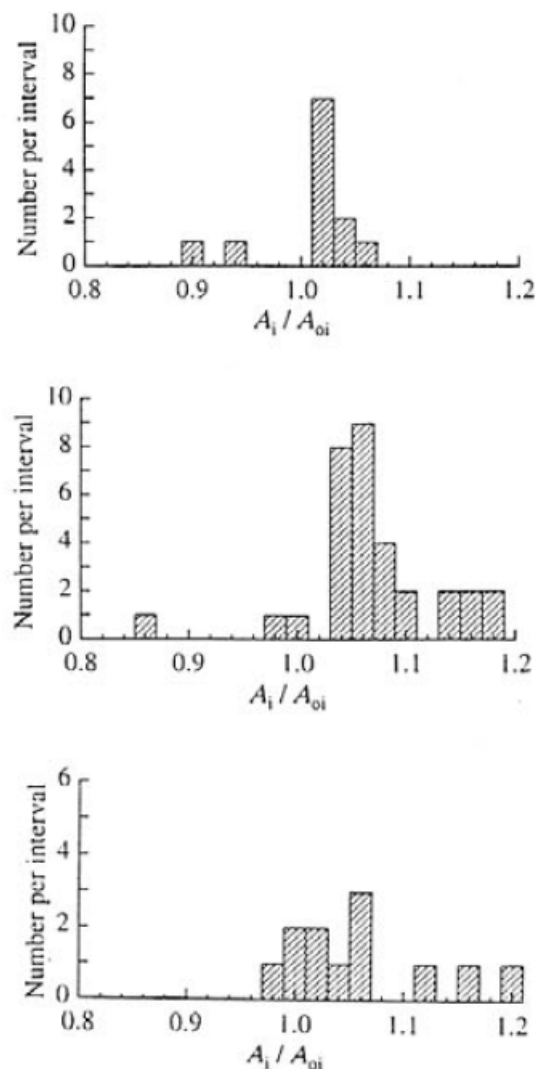


Figure 70-1 — For ^{57}Co solution measured in BS ampoules.

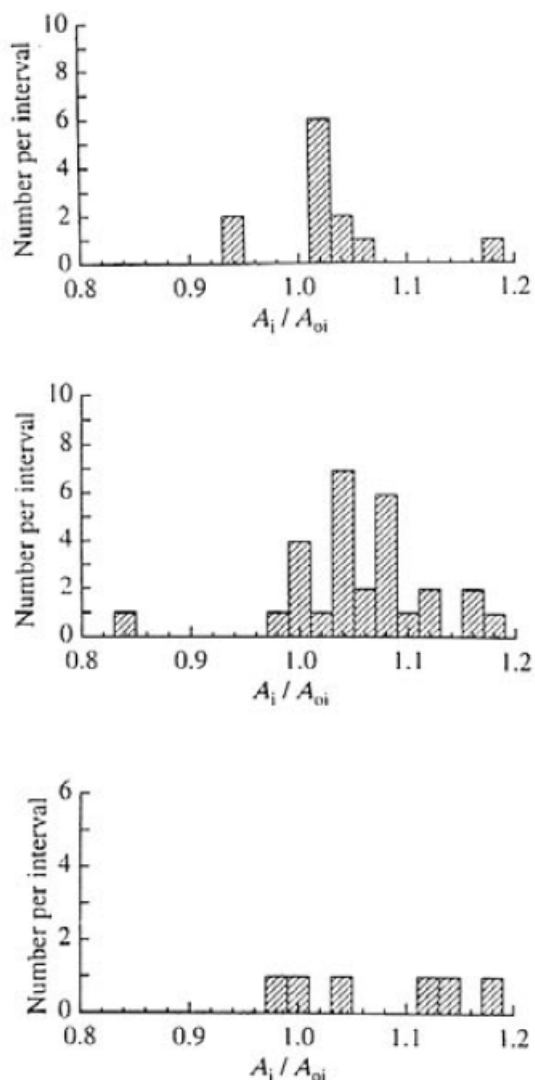


Figure 70-2 — For the same ^{57}Co solution measured in routine containers.

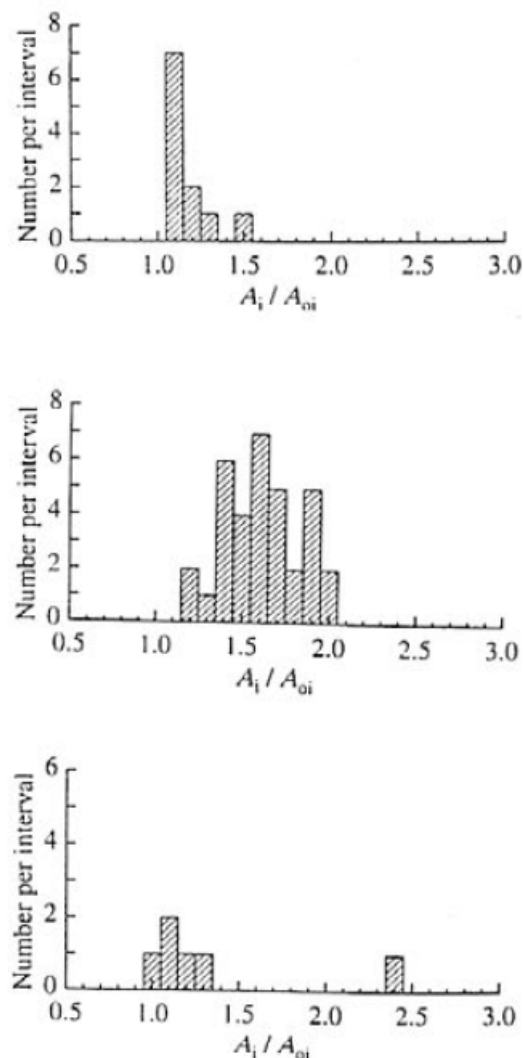


Figure 70-3 — For ^{125}I solution measured in BS ampoules.

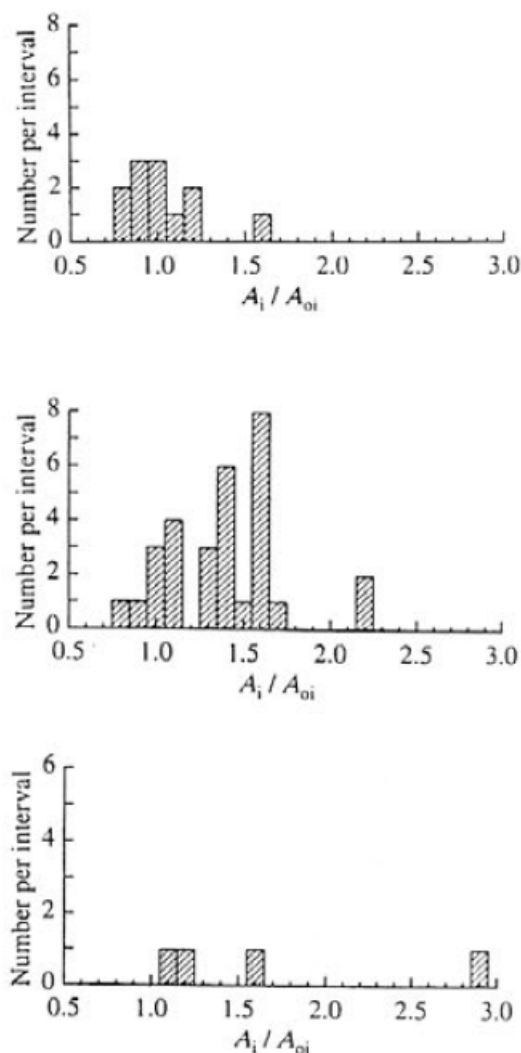


Figure 70-4 — For the same ^{125}I solution measured in routine containers.

Figure 70 — Interval distribution of reported activity / NPL activity A_i/A_o from a comparison in the UK. The results of various radionuclide calibrators are separated; calibrator type A on top, calibrator type B in the middle and others on bottom of each figure. After Woods ([477], see p. 195).

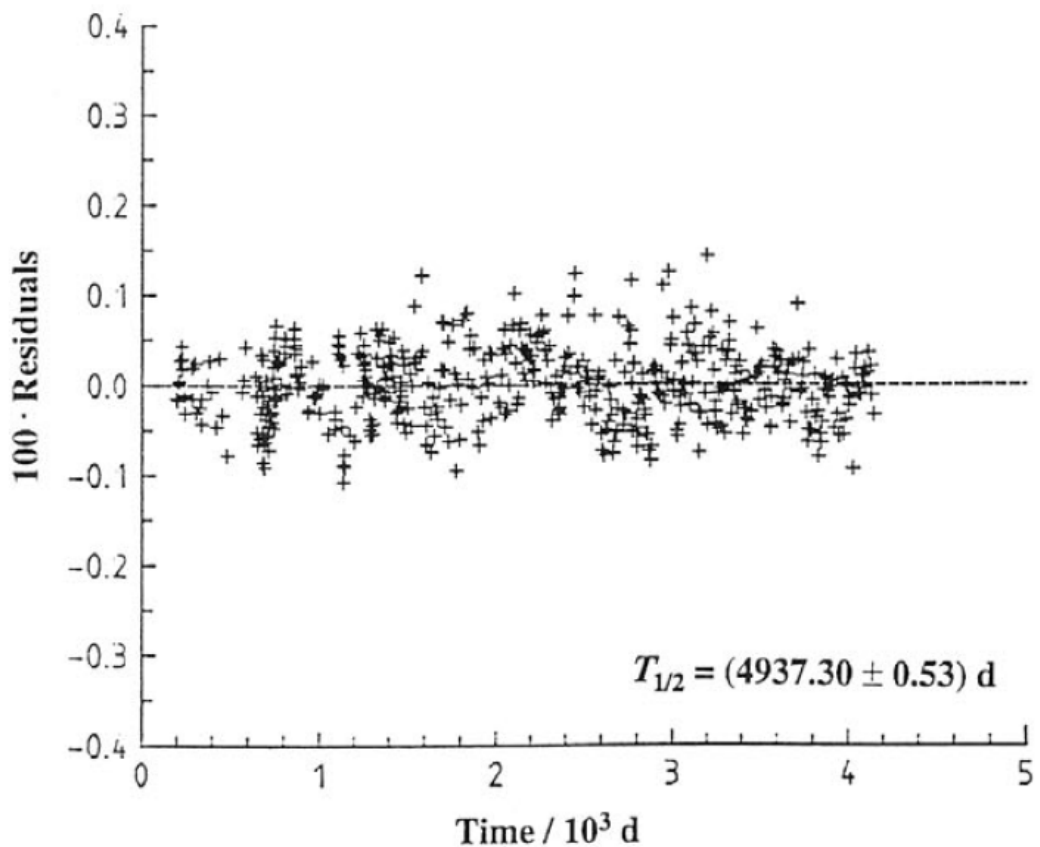


Figure 71-1 — Residuals for 557 data points measured during 3950 d giving a half-life value of (4937.30 ± 0.53) d.

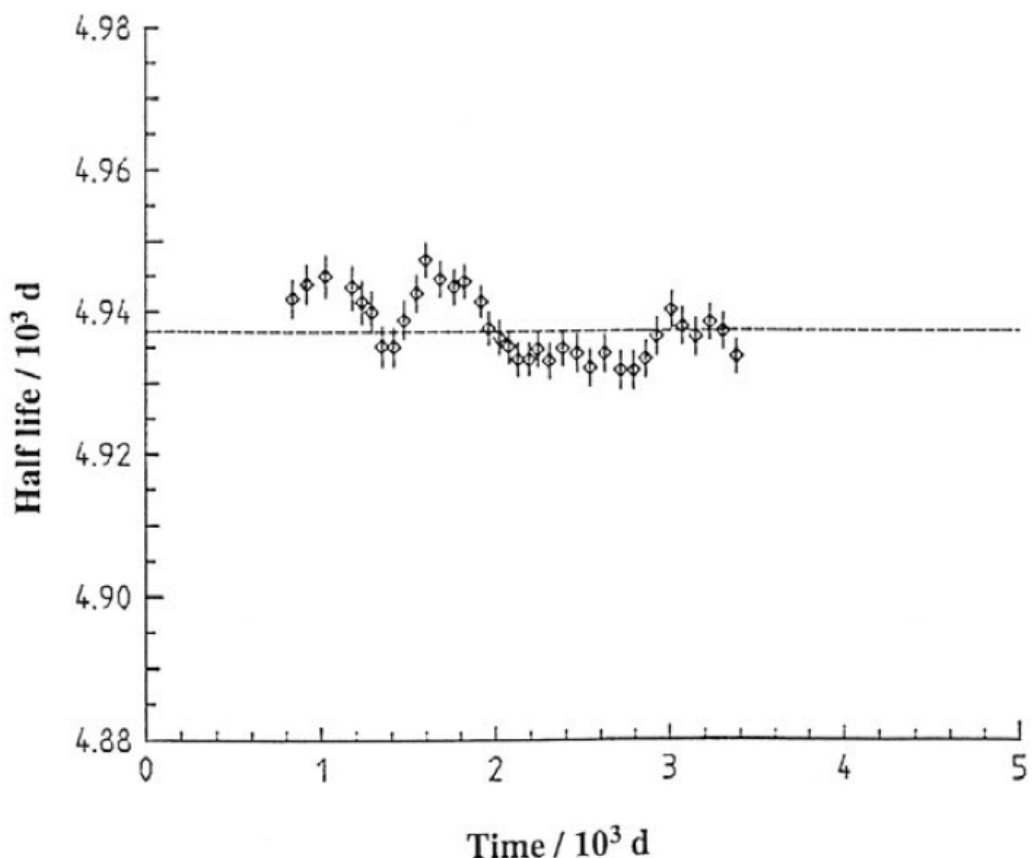


Figure 71-2 — Half-life values are plotted from fits of various data subsets with lower number of data points and shorter time period versus an average time for each subset.

Figure 71 — Results of ^{152}Eu half-life measurements and data analysis by linear regression analysis on the logarithm of ionization chamber current reading. (Unpublished data from PTB).

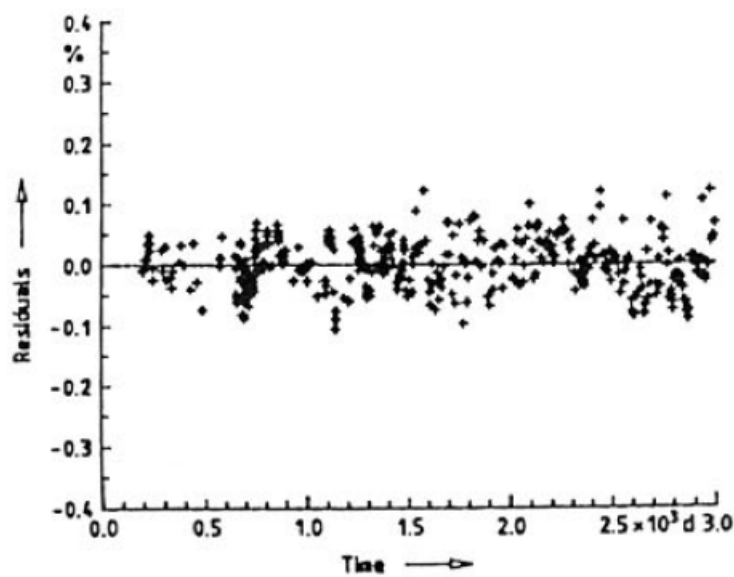


Figure 72-1 — Residuals for 384 data points measured during 2700 d giving a fitted half-life value of (4938.31 ± 0.98) d.

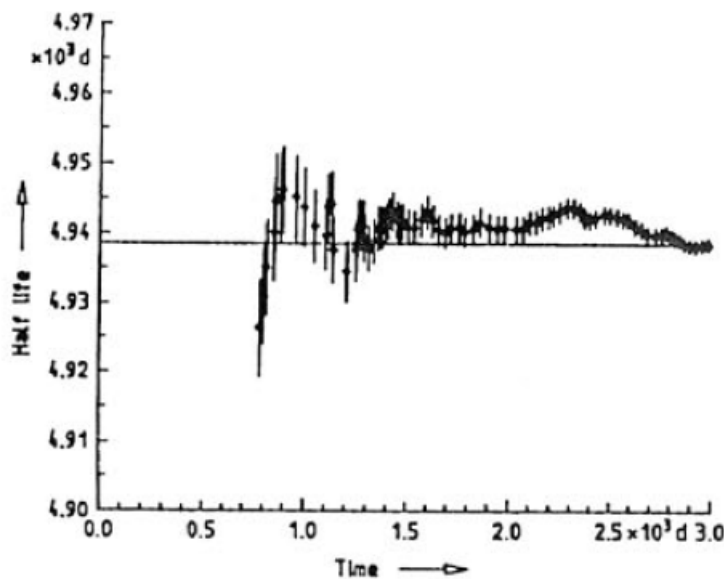


Figure 72-2 — Half-life values obtained from the 384 data points starting with a data subset covering the first 600 d and then, increasing the number of data points in the subset successively (from left to right).

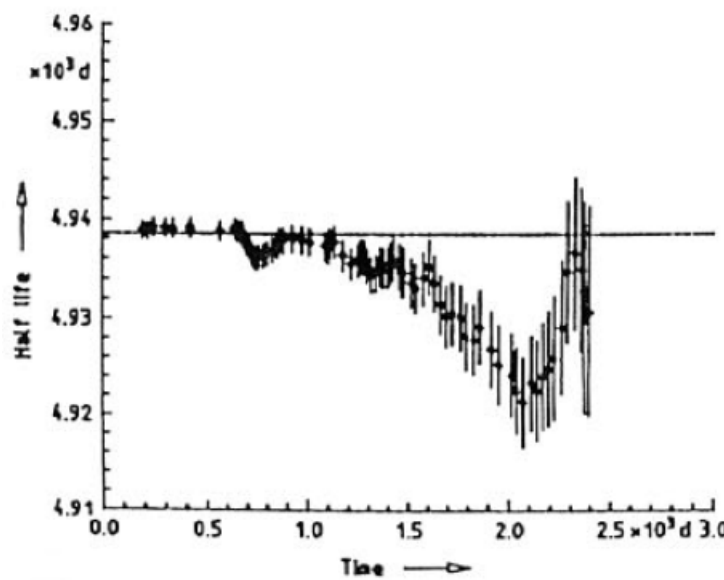


Figure 72-3 — Half-life values obtained starting from a data subset within the last 600 d and then, increasing the number in the subset by preceding data points successively (from right to left).

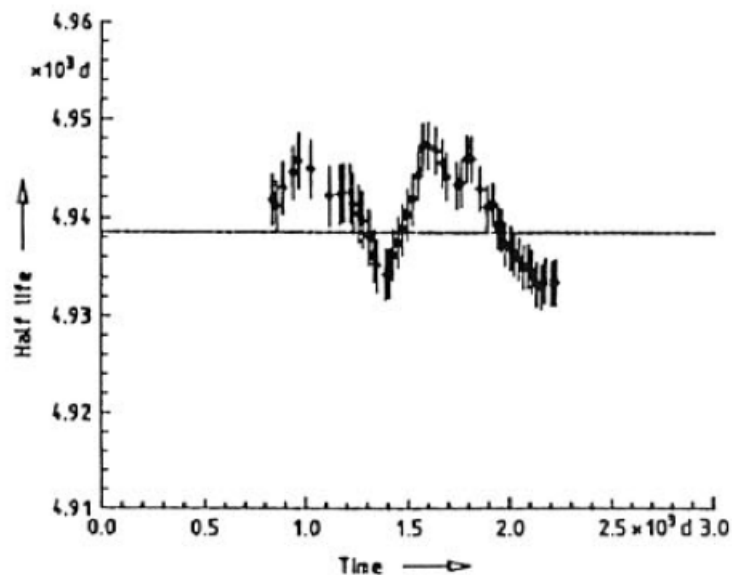


Figure 72-4 — Half-life values obtained from subsets of 200 points which were formed by a shift in the total set with steps of 5 data points each.

Figure 72 — Results of ^{152}Eu half-life measurements and data analysis. Reproduced from [461].

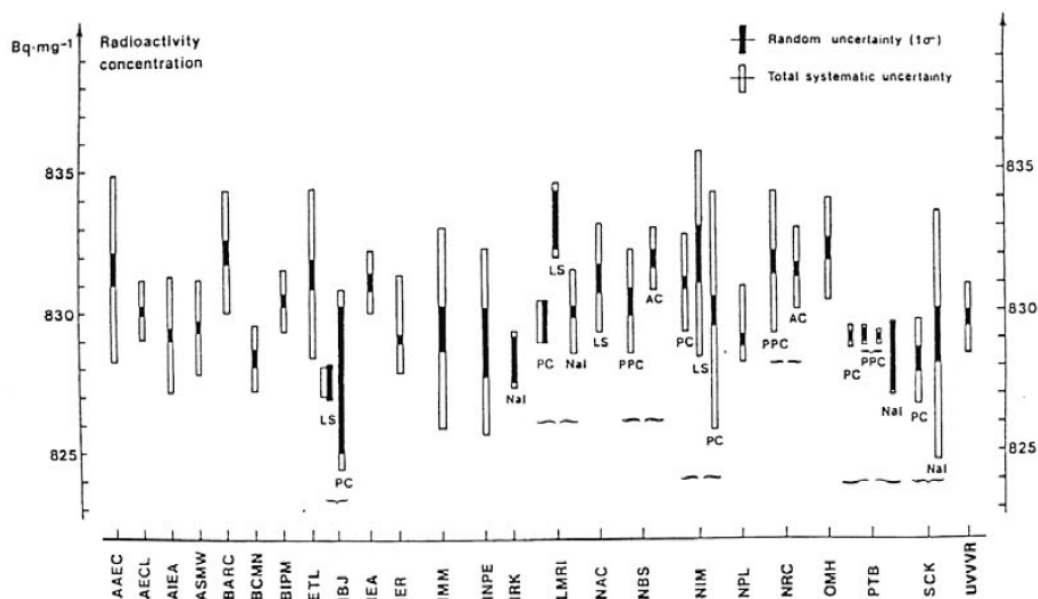


Figure 73 — Graphical representation of the results and their combined uncertainties (random and systematic effects) from a comparison of activity-concentration measurements with ^{134}Cs . The type of detector is indicated if a laboratory has submitted several results. Reproduced from [374].

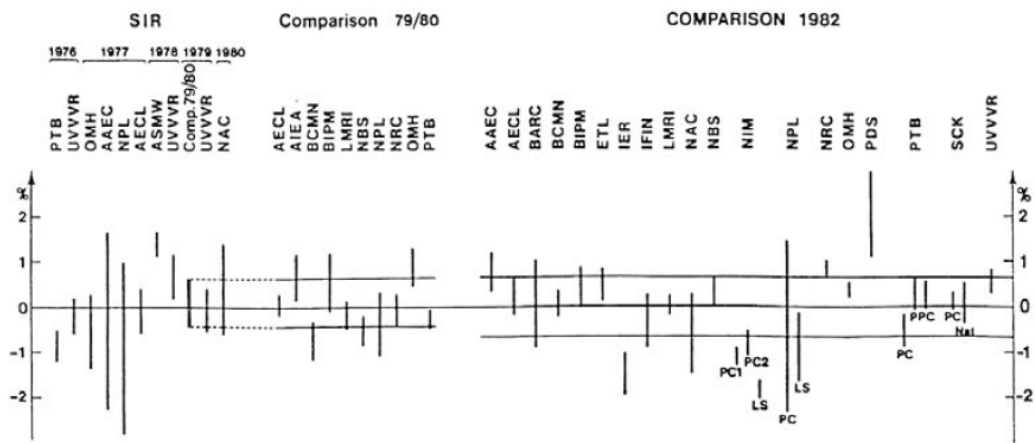


Figure 74 — Graphical representation of the results and their combined uncertainties from comparisons of activity-concentration measurements with ^{137}Cs . The type of detector is indicated if a laboratory has submitted several results. The mean values of the two comparisons are aligned by means of the corresponding ionization chamber results from the SIR. Their respective standard deviations are represented by pairs of horizontal lines.

Reproduced from [377].

References

- [1] ACNP (1984). American College of Nuclear Physicians. Initial testing and quality control for radionuclide dose calibrators. Committee report prepared by members of the Committee on Standardization of Nuclear Medicine Instrumentation (Weber K., Chairman), 19 p.
- [2] AHAFIA A. K. (1989). Ahagraphs: a new method for the accurate determination of half-lives. *Appl. Radiat. Isot.* 40, 407-411.
- [3] AHLUWALIA B. (1985). Dose calibrator linearity—A regulatory requirement. *Health Phys.* 49, 967-969.
- [4] ALLEN R. A. (1966). Ionization chamber measurements. Chap. 5.3. in Alpha-, Beta- and Gamma-Ray Spectroscopy, Vol. 1 (Siegbahn K., Ed.), Amsterdam, North-Holland, 462-465.
- [5] ALLISY A., CARNET D. (1964). Measurements of small ionization currents. *BIPM Proc.-Verb. Com. Int. Poids et Mesures* 32, Sèvres, BIPM, 54-55.
- [6] AMERSHAM (1994). Packaging. In Catalogue: Life science. Little Chalfont, Buckinghamshire, Amersham International plc, 204-207.
- [7] ANDRESEN E. G. (1967). Statistische Schwankung, Anzeigeträgheit, Nachweisgrenze (Statistical fluctuation, time lag of indication, least instrument reading). *Kerntechnik* 9, 163-165.
- [8] ANSI (1978). Calibration and usage of “dose calibrator” ionization chambers for the assay of radionuclides.
- [9] ANSI N42.13-1978, New York, Institute of Electrical and Electronics Engineers, Inc., 10 p.
- [10] ANSI (1986). Calibration and usage of “dose calibrator” ionization chambers for the assay of radionuclides.
- [11] ANSI N42.13-1986, re-edition of ANSI N42.13-1978, New York, Institute of Electrical and Electronics Engineers, Inc.
- [12] ARSAC (1988). Administration of Radioactive Substances Advisory Committee. Notes for guidance on the administration of radioactive substances to persons for purpose of diagnostics, treatment or research. London, NRPB, Health and Safety Executive (HMSO), 32 p.
- [13] ARTHUR R. J., REEVES J. H., MILEY H. S. (1988). Use of low-background germanium detectors to preselect high-radiopurity materials for constructing advanced ultralow-level detectors. *IEEE Transact. Nucl. Sci.* 35, 582-585.
- [14] ATTIX F. H., GORBICS S. G. (1968). Guard ring shielding to eliminate instability of collecting volume in ionization chambers. *Rev. Sci. Instr.* 39, 1766-1767.
- [15] AUMANN D. C., NIRSCHL E. (1979). A differential ionization chamber for the determination of small differences in decay rates of beta emitters. *Nucl. Instr. Meth.* 163, 135-139.

- [16] BEARDEN J. A. (1933). Radioactive contamination of ionization chamber materials. *Rev. Sci. Instr.* 4, 271-275.
- [17] BECQUEREL H. (1896). Sur quelques propriétés nouvelles des radiations invisibles émises par divers corps phosphorescents. *C. R. Acad. Sci.* 122, 559-564; idem 123, 855-858 (German abstract in *Fortschr. der Phys.* 1896, II, 77-79).
- [18] BECQUEREL H. (1897a). Sur la loi de la décharge dans l'air de l'uranium électrisé. *C. R. Acad. Sci.* 124, 800-803 (German abstract in *Fortschr. der Phys.* 1897, II, 466).
- [19] BECQUEREL H. (1897b). Expériences sur la décharge de corps électrisés sous l'influence des radiations émises par l'uranium. *Soc. franc. de phys.* [96] 3-4, idem Séances soc. franc. de phys. 1897, Rés. 38-40. (German abstract in *Fortschr. der Phys.* 1897, II, 466).
- [20] BEHNKEN H. (1924). Die Vereinheitlichung der Röntgenstrahlen-Dosismessung und die Eichung von Dosismessern. *Zeitschr. f. techn. Phys.* 5, 3-16.
- [21] BENNSCH F., LEDERMANN H. (1969). Rapid determination of radionuclide activities by a well-type gammaionization chamber. *Nucl. Instr. Meth.* 72, 56-60.
- [22] BILLINGHURST M. W., PALSER R. F. (1983). Some factors affecting the calibration of radionuclide calibrators—I. Tc-99m. *Int. J. Nucl. Med. Biol.* 10, 117-119.
- [23] BIPM (1975a). Bureau International des Poids et Mesures. Procedures for accurately diluting and dispensing radioactive solutions. Monographie BIPM-1 (Campion P. J., Ed.), Sèvres, BIPM, 32 p.
- [24] BIPM (1975b). Bureau International des Poids et Mesures. Mesures de la radioactivité. Chap. IX, in Le Bureau International des Poids et Mesures, 1875-1975. Sèvres, BIPM, 166-181.
- [25] BIPM (1987). Bureau International des Poids et Mesures. Étalons du domaine des rayonnements ionisants. In Le BIPM et la Convention du Mètre, Sèvres, BIPM, 32.
- [26] BIPM (1991). Bureau International des Poids et Mesures. Le système international d'unités (SI), 6th edition, Sèvres, BIPM.
- [27] BLANCHIS P. (1985). Caractéristiques et utilisations d'une chambre d'ionisation au Laboratoire Primaire du LMRI. *Bulletin BNM* 59, 33-40.
- [28] BMU (1992). Bundesminister für Umwelt, Naturschutz und Reaktorsicherheit. Richtlinie für den Strahlenschutz bei der Verwendung radioaktiver Stoffe und beim Betrieb von Anlagen zur Erzeugung ionisierender Strahlen und Bestrahlungseinrichtungen mit radioaktiven Quellen in der Medizin. (Richtlinie Strahlenschutz in der Medizin). Bonn, BMU, 103 p.
- [29] BOAG J. W. (1956). Ionization chambers. Chap. 4. in *Radiation Dosimetry* (Hine G. J., Brownell G. L., Eds.), New York, Academic Press.
- [30] BOAG J. W. (1966). Ionization chambers. Chap. 9. in *Radiation Dosimetry*, Vol. II (Attix F. H., Roesch W. C., Eds.), New York, Academic Press, 1-72.

- [31] BOAG J. W. (1975). General recombination in ionization chambers with spatially non-uniform ionization intensity—two special cases. *Int. J. Radiat. Phys. Chem.* 7, 243-249.
- [32] BOGE M. (1974). Mise au point de chambres d'ionisation différentielles pour la mesure de variation de période radioactive. Rapport d'activité. Bulletin semestriel no.6, CEA-N-1784, Grenoble, CEA, Centre d'Etudes Nucléaires de Grenoble, 158-160.
- [33] BOGE M., MEYKENS A. (1976). Chambres d'ionisation différentielles pour la mesure de variation de période radioactive. *Rev. Phys. Appl.* 11, 167-174.
- [34] BÖHM J. (1976a). A measuring and calibration system for currents down to 10E-17 A. *Atomkernenergie (ATKE)* 27, 139-143.
- [35] BÖHM J. (1976b). Saturation corrections for plane-parallel ionization chambers. *Phys. Med. Biol.* 21, 754-759.
- [36] BÖHM J. (1979). Eine Referenzstromquelle zur Kalibrierung von Strommeßsystemen in der Dosimetrie mit Ionisationskammern. *PTB-Mitteilungen* 89, 237-241.
- [37] BÖHM J. (1980). Measurements of low ionization currents. In *Ion chambers for neutron dosimetry*. Report EUR 6782 EN, Harwood Academic Publishers, 167-179.
- [38] BORTELS G. (1975). Pressurized $4\pi\gamma$ ionization chamber for radionuclide metrology. Report CBNM/RN/8/75, Geel, CBNM, 16 p.
- [39] BORTNER T. E. (1951). An extrapolation chamber: construction and use. *Nucleonics* 9, no. 3, 40-43 and 94. 81
- [40] BOTHE W. (1915). Die Gehaltsbestimmung schwach radiumhaltiger Substanzen durch Gammastrahlen-Messung. *Physikalische Zeitschrift* 16, 33-36.
- [41] BOTHE W. (1924). Die Unterscheidung von Radium, Mesothor und Radiothor durch Gammastrahlenmessung. *Z. Physik* 24, 10-19.
- [42] BOWES G. C., BAERG A. P. (1970). Sampling and storage of radioactive solutions. Report NRC-11513, Ottawa, National Research Council of Canada (NRCC).
- [43] BRADT H., GUGELOT P. C., HUBER O., MEDICUS H., PREISWERK P., SCHERRER P. (1946). Empfindlichkeit von Zählrohren mit Blei-, Messing- und Aluminiumkathode für Gamma-Strahlung im Energieintervall 0.1 MeV bis 3 MeV. *Helv. Phys. Acta* 19, 77-90.
- [44] BRAGG W. L., JAMES R. W., BOSANQUET C. H. (1921). The intensity of reflexion of X-rays by rock-salt. *Phil. Mag.* 41, 309-337.
- [45] BRETHON J.-P., REDON P. (1973). Patent; Availability Note: FR 2251911 A, 15 Nov 1973, CEA, Paris, 18 p.
- [46] BRODA R. (1980). The method of activity determination of Tc-99m in ionization chambers. Report INR-1870/I/A, Warsaw, Institute of Nuclear Research, 17 p.

- [47] BROJ K., GREGOR J. (1979). Metric aktivity (Activity meter). Jad. Energ. 25, 146-149.
- [48] BRONSON H. L. (1906). Current measurements. Phil. Mag. 6th series, 11, 143.
- [49] BROSE J. (1992). Entwicklung einer Methode zur Messung von Ionisationsströmen im fA-Bereich nach dem Prinzip der digitalen Filterung. Thesis Fachhochschule für Technik und Wirtschaft, Berlin, 38 p.
- [50] BROWN P. (1983). Testing reed relays for electronic applications. Electronic Engineering, May 1983, 57-60.
- [51] BROWNE E., FIRESTONE R. B. (1986). Table of Radioactive Isotopes (Shirley V. S., Ed.), New York, John Wiley & Sons, Inc.
- [52] BROWNELL G. L., LOCKHART H. S. (1952). CO₂ ion-chamber techniques for radiocarbon measurements. Nucleonics 10, no. 2, 26-32.
- [53] BUCINA I., ZALESKY K., KUCERA P. (1967). Precision 4π gamma ionization chamber with minimal position dependence. Report IAEA/STI/PUB/139 SM-79/35, Vienna, IAEA, 431-441.
- [54] BÜERMANN L., KRAMER H.-M., SCHRADER H., SELBACH H.-J. (1994). Activity determination of ¹⁹²Ir solid sources by ionization chamber measurements using calculated corrections for self-absorption. Nucl. Instr. Meth. A339, 369-376
- [55] BULLEN M. A. (1953). Ionization-chamber device for clinical gamma-ray use. Nucleonics 11, no.12, 15-17.
- [56] CALDAS L. V. E., ALBUQUERQUE P., XAVIER M. (1994). Calibration techniques for components of clinical dosimeters. Appl. Radioat. Isot. 45, 31-33.
- [57] CALHOUN J. M., CESSNA J. T., COURSEY B. M. (1992). A system for intercomparing standard solutions of beta-particle emitting radionuclides. Nucl. Instr. Meth. A312, 114-120.
- [58] CALHOUN J. M. (1986a). Radioactivity calibration with the NBS “ 4π ” gamma ionization chamber. NBS Internal Report, Gaithersburg, MD, Center for Radiation Research, National Bureau of Standards, 1-45.
- [59] CALHOUN J. M. (1986b). NBS measurements of sample geometry effects on ionization chamber calibrations. Trans. Amer. Nucl. Soc. 53, 21.
- [60] CALHOUN J. M., GOLAS D. B., HARRIS S. G. (1987). Effects of varying geometry on dose calibrator response: Cobalt-57 and Technetium-99m. J. Nucl. Med. 28, 1478-1483.
- [61] CAMP D. C., GATROUSIS C., MAYNARD L. A. (1974). Low-background Ge(Li) detector systems for radioenvironmental studies. Nucl. Instr. Meth. 117, 189-211.
- [62] CAMPION P. J. (1973). The work of the BIPM consultative committee for measurement standards of ionizing radiations, Section II: Radionuclide measurements. Nucl. Instr. Meth. 112, 41-45.
- [63] CAMPION P. J. (1975). See [23].

- [64] CARMICHAEL H. (1945). Ion-chamber data. Report AECL-290, Chalk River Nuclear Laboratories, 19 p.
- [65] CARMICHAEL H. (1946). Design of the Chalk River ion-chambers types TPA, TPJ and TPD. Report AECL-293, Chalk River Nuclear Laboratories, 21 p.
- [66] CARY (1966). Vibrating reed electrometer, model 31cv (Instruction Manual). Applied Physics Corporation, Monrovia, California.
- [67] CAVALLO L. M., COURSEY B. M., GARFINKEL S. B., HUTCHINSON J. M. R., MANN W. B. (1973). Needs for radioactivity standards and measurements in different fields. Nucl. Instr. Meth. 112, 5-18.
- [68] CAVALLO L. M., SCHIMA E. J., UNTERWEGER M. P. (1974). Decay of ^{133}Xe . Phys. Rev. C 10, 2631-2632.
- [69] CENTRONIC (1965). Ionization chamber, Type IG 12 (Product information). Private communication by Centronic, Twentieth Century Ltd., New Addington, Croydon CR9 0BG, Surrey, England, 1 p.
- [70] CHRISTMAS P., MERCER R. A., WOODS M. J., JUDGE S. M. (1983). ^{210}Bi and the apparent half-life of a sealed ^{226}Ra source. Int. J. Appl. Radiat. Isot. 34, 1555.
- [71] CLOOS O., HEIGWER G. (1970). An automatic compensating instrument for measuring low electric direct current. Nucl. Instr. Meth. 91, 633-635.
- [72] COBB P. D., CHEN T. S., KASE K. R. (1981). Calibration of brachytherapy iridium-192 sources. Int. J. Radiat. Oncology Biol. Phys. 7, 259-262.
- [73] COCKROFT, A. L., CURRAN S. C. (1951). The elimination of end effects in counters. Rev. Sci. Instr. 22, 37-42.
- [74] COHEN E. R., GIACOMO, P. (1987). Symbols, units, nomenclature and fundamental constants in Physics. Document I.U.P.A.P.—25 (SUNAMCO 87-1), Sèvres, BIPM, 80 p.
- [75] COHEN J., ONCESCU M., REBIGHAN F. (1964). Apparatus for relative measurements of gamma activities, provided with 4π ionization chamber (well type). Rev. Roum. Phys. 9, 479-486.
- [76] COLMENARES C. A. (1974). Bakeable ionization chamber for low-level tritium counting. Nucl. Instr. Meth. 114, 269-275.
- [77] COMPTON A. H., HOPFIELD J. J. (1932). Use of Argon in the ionization method of measuring cosmic rays. Phys. Rev. 41, 539.
- [78] COMPTON A. H., WOLLAN E. O., BENNETT R. D. (1934). A precision recording cosmic-ray meter. Rev. Sci. Instr. 5, 415-422.
- [79] CONNOR W. S., YOUND W. J. (1954). Comparison of four national radium standards, Part 2. Statistical Procedures and Survey. J. Research NBS 53, no. 5 (RP2544), Washington, D.C., NBS, 273-275.
- [80] COURSEY B. M., HOPPES D. D., UNTERWEGER M. P., GRAU MALONDA A., MARGOLIN R. A., KESSLER R. M., MANNING R. (1983). Standardization

- of ^{18}F for use in positron-emission tomography. Int. J. Appl. Radiat. Isot. 34, 1181-1189.
- [81] COURSEY B. M., CALHOUN J. M. (1986). Distributions of calibrated samples by commercial pharmaceutical laboratories in FDA-organized quality-assurance exercises. Report NBSIR 86-3441, Washington, D.C., Center for Radiation Research, NBS, 211-212.
- [82] COURSEY B. M., MANN W. B., GRAU MALONDA A., GARCIA-TORAÑO E., LOS ARCOS J. M., GIBSON J. A. B., REHER D. F. G. (1986). Standardization of carbon-14 by 4-pi-beta-liquid scintillation efficiency tracing with hydrogen-3. Appl. Radiat. Isot. 37, 403-408.
- [83] COURSEY B. M., GOODMAN L. J., HOPPES D. D., LOEVINGER R., MCLAUGHLIN W. L., SOARES C. G., WEAVER J. T. (1992). The needs for brachytherapy source calibrations in the United States. Nucl. Instr. Meth. A312, 246-250.
- [84] COURSEY B. M., VANINBROUKX R., REHER D. F. G., HUTCHINSON J. M. R., MULLEN P. A., DEBERTIN K., GEHRKE R. J., ROGERS J. W., KOEPPEN L. D., SMITH D. (1990). The standardization of ^{93}Nb for use as a reference material for reactor neutron dosimetry. Nucl. Instr. Meth. A290, 537-550.
- [85] COURSOL N., LAGOUTINE F. (1983a). Evaluation of non-neutron nuclear data for the ^{226}Ra decay-chain. Int. J. Appl. Radiat. Isot. 34, 1269-1275.
- [86] COURSOL N., LAGOUTINE F. (1983b). Table de radionucléides. Ra-226 et descendants. Gif-sur-Yvette, CEN-Saclay, CEA-LMRI, 1-10.
- [87] CURIE M. (1912). Les mesures en radioactivité et l'étalon du radium. Journ. de Phys. (5) 2, 795-826.
- [88] CURIE M., DEBIERNE A., EVE A. S., GEIGER H., HAHN O., LIND S. C., MEYER ST., RUTHERFORD E., SCHWEIDLER E. (1931). The radioactive constants as of 1930. Report of the International Radium-Standards Commission. Rev. Mod. Phys. 3, 427-445.
- [89] CURTISS L. F. (1928). A projection electroscope for standardizing radium preparations. Rev. Sci. Instr. 16, 363.
- [90] DALE J. W. G. (1961). A beta-gamma ionization chamber for substandards of radioactivity—II. Int. J. Appl. Radiat. Isot. 10, 72-78.
- [91] DALE J. W. G., PERRY W. E., PULFER R. F. (1961). A beta-gamma ionization chamber for substandards of radioactivity—I. Int. J. Appl. Radiat. Isot. 10, 65-71.
- [92] DALE J. W. G., WILLIAMS A. (1964). Calibration factors for the type 1383A beta-gamma ionization chamber. Int. J. Appl. Radiat. Isot. 15, 567-568.
- [93] DALMAZZONE J. (1966). Contribution à la mesure précise de l'activité de sources non ponctuelles au moyen de la chambre d'ionisation à puits (Thèse d'ingénieur C.N.A.M.). Report CEA-R3071, Gif-sur-Yvette, CEA, CEN-Saclay.
- [94] DALMAZZONE J. (1972). Générateurs de courants faibles. Nucl. Instr. Meth. 105, 237-244.

- [95] DALMAZZONE J., GUIHO J.-P. (1968). Utilisation des chambres d'ionisation à puits en metrologie radioactive. Rapport CEA-R3438, Gif-sur-Yvette, CEA, CEN-Saclay, 23 p.
- [96] DA SILVA C. J., IWAHARA A. (1991). Calibraçao et manutençao de soluções radioactivas e rastreamento à rede internacional de metrologia. Revista Argentina de Radioprotección no. 5, 15 p.
- [97] DAVENPORT T. I., MANN W. B., McCRAVEN C. C., SMITH C. C. (1954). Comparison of four national radium standards, Part 1. Experimental procedures and results. J. Research NBS 53, no. 5 (RP2544), Washington, D.C., NBS, 267-272.
- [98] DEBERTIN K. (1991). Radioactivity. Chap. 2.3.4.1, in Landolt-Börnstein: Units and Fundamental Constants in Physics and Chemistry, subvolume a: Units in Physics and Chemistry (Madelung O., Bortfeld J., Kramer B., Eds.). Berlin, Springer-Verlag, 302-309.
- [99] DEBERTIN K., HELMER R. G. (1988). Gamma- and X-ray spectrometry with semiconductor detectors. Amsterdam, North-Holland.
- [100] DEBERTIN K., SCHRADER H. (1992). Intercomparisons for quality assurance of activity measurements with radionuclide calibrators. Nucl. Instr. Meth. A312, 241-245.
- [101] DE BIEVRE P. (1978). Accurate isotope ratio mass spectrometry: Some problems and possibilities. In Advances in Mass Spectrometry, Vol. 7A (Daly N. R., Ed.), London, Heyden and Son Ltd. on behalf of The Institute of Petroleum, 395-430.
- [102] DE BIEVRE P., GALLET M., WERZ R. (1982). Determination of the ^{241}Pu half-life by isotope mass spectrometry. Report CBNM/MS/124/82, Geel, CBNM, 3-22.
- [103] DE WAARD H., LAZARUS, D. (1966). Modern electronics—A practical guide for scientists and engineers. Chap. 5: Feedback amplifiers. Reading, Massachusetts, Addison-Wesley Publishing Company, 164-185.
- [104] DEIKE S., WALZ K. F. (1975). Automatik zur Messung von Ionisationsströmen. PTB-Jahresbericht, Braunschweig, PTB, 232-233.
- [105] DEM'YANOV V. A., SHCHERBAKOV V. M., EPSHTEIN A. M. (1978). Portable gas radiometer. Instrum. & Exp. Tech. 21, 1444-1445. (Transl. from: Prib. Tekh. Eksp. (USSR, 1978), 21, 261-262).
- [106] DHALIWAL A. S., POWAR M. S., SINGH M. (1991). Attenuation of ^{204}Tl and ^{32}P beta ray bremsstrahlung in thick targets of Al, Cu, Sn and Pb. Appl. Radiat. Isot. 42, 427-430.
- [107] DIAS M. S. (1978). Calibracao de um sistema de camara de ionizacao de poco 4pi-gamma para medidas de atividade de radionuclideos. Report IEA-DT-87 (Thesis, M. Sc.), Sao Paulo, Instituto de Energia Atomica, 106 p.
- [108] DIAS M. S. (1982). Activity determination by a 4pi-gamma well-type ionization chamber. Report IPEN-PUB-40, Instituto de Pesquisas Energeticas e Nucleares, Sao Paulo, 16 p.

- [109] DIN (1985). Deutsches Institut für Normung. Technetium-Generatoren. DIN 6854, Berlin, Beuth Verlag GmbH, 7 p.
- [110] DIN (1987). Deutsches Institut für Normung. Aktivimeter. DIN 6852, Berlin, Beuth Verlag GmbH, 7 p.
- [111] DIN (1990). Deutsches Institut für Normung. Begriffe und Benennungen in der radiologischen Technik.
- [112] DIN 6814, Teil 4, Radioaktivität. Berlin, Beuth Verlag GmbH, 7 p.
- [113] ISO 9187-1 *Injection equipment for medical use—Part 1: Ampoules for injectables*
- [114] DÖRFEL G. (1967). Statistische Fehler und Zeitverhalten bei der Impulsdichte- und Ionisationsstrommessung. Isotopenpraxis 3, 8-11.
- [115] DOLEZALEK F. (1901). Über ein einfaches und empfindliches Quadrantenelektrometer. Zeitschr. f. Instrumentenkunde 21, 345-350.
- [116] DORN E. (1910). Radioaktivität; H. Becquerel 1896. II. Hilfsmittel, C. Die elektrischen Methoden. In Lehrbuch der Praktischen Physik, 11. Auflage (Kohlrausch F., Ed.), Leipzig, B. G. Teubner, 634-638.
- [117] DORSEY N. E. (1922). An instrument for the gamma-ray measurement of the radium content of weakly active materials. Journ. Opt. Soc. Amer. 6, 633-638.
- [118] DROSTE G. Frh. v. (1936). Über die Anzahl der Ausschläge eines Zählrohres bei Bestrahlung mit Gamma-Strahlen verschiedener Wellenlänge. Z. Physik 100, 529-533.
- [119] DRYAK P., NOVOTNA P., KOKTA L., KOVAR P. (1981). Idem 2nd ed. (1989). Impurities in radionuclide materials. UVVVR-Report No. 8, Prague, Institute for Research, Production and Application of Radioisotopes, 101 p.
- [120] DRYAK P. (1982). Stanoveni koeficientu samoabsorpce pri mereni aktivity pevných vzorku 4pi ionizacní komorou. Determination of self-absorption coefficient in measurement of solid sample activity using a 4pi ionization chamber, Prague, Ceske Vysoke Uceni Technicke, Fakulta Jaderna a Fysikalne Inzenyrska, 28-32.
- [121] DRYAK P., CHOC M., KITS J., LATAL F., ZIDEK V., KOKTA L. (1982). The UVVVR $4\pi\gamma$ ionization chambers. Jaderna Energie 28, 381.
- [122] DRYAK P., DVORAK L. (1986). Measurement of the energy response function of the UVVVR and SIR $4\pi\gamma$ ionization chambers. Appl. Radiat. Isot. 37, 1071-1073.
- [123] DUBUQUE G. L., GRANT R. J., KEREIAKES J. G., TUINER R. J. van (1976). Measuring mixed energy gamma radionuclides using a radionuclide calibrator. Int. J. Nucl. Med. Biol. 3, 145-147.
- [124] DYE R. E. A., REECE B. L. (1984). Use of two ionization chambers with a commercial isotope assay calibrator. Phys. Med. Biol. 29, 1571-1573.
- [125] EEC (1980). European Economic Community. COUNCIL DIRECTIVE of 20. Dec. 1979 (80/181/EEC) on the approximation of the laws of the Member States relating to units of measurement. ANNEX, chap. 1.2.3: Derived SI units having names and

- symbols. Official Journal of the European Communities No. 1.39. Brussels, Council of the European Communities, 40-50.
- [126] EIJK W. van der, VANINBROUKX R. (1972). Sampling and dilution problems in radioactivity measurements. Nucl. Instr. Meth. 102, 581-587.
 - [127] ELSTER J., GEITEL H. (1897). Versuche über Hyperphosphorescenz. Abstract in Fortschr. der Phys. 1897, II, 67.
 - [128] ELSTER J., GEITEL H. (1899). Über einen Apparat zur Messung der Elektricitätszerstreuung in der Luft. Physikalische Zeitschrift 1, no. 1 and 2, 11-14.
 - [129] ELSTER J., GEITEL H. (1902). Über die Radioaktivität der im Erdboden enthaltenen Luft. Physikalische Zeitschrift 3, no. 24, 574-577.
 - [130] ELSTER J., GEITEL H. (1904). Über Radioaktivität von Erdarten und Quellsedimenten. Physikalische Zeitschrift 5, no. 12, 321-325.
 - [131] ELSTER J., GEITEL H. (1905). Versuche über die Schirmwirkung des Steinsalzes gegen die allgemein auf der Erde verbreitete Becquerelstrahlung. Physikalische Zeitschrift 6, no. 22, 733-737.
 - [132] EMERY G. T. (1972). Perturbation of nuclear decay rates. Ann. Rev. Nucl. Sci. 22, 165-197.
 - [133] ENGELMANN J. J. (1960). Etude des performances d'une chambre d'ionisation $4\pi\gamma$. Report CEA-1539, Gif-sur-Yvette, CEA, CEN-Saclay.
 - [134] ENGELMANN J. J. (1962). Mesure des émetteurs gamma par chambres d'ionisation. Détermination du coefficient spécifique d'émission gamma de quelques radioéléments (Thèse). Report CEA-2036, Gif-sur-Yvette, CEA, CEN-Saclay.
 - [135] ERDÉLYVARY I., FEHÉR I. (1967). $4\pi\gamma$ -ionization chamber for measurement of low energy gamma-emitters. Nucl. Instr. Meth. 54, 163-164.
 - [136] ERIKSON H. A. (1908). The ionization of gases at high pressures. Phys. Rev. 27, 473-491.
 - [137] EUROPEAN PHARMACOPEIA (1986). European Pharmacopeia. Strasbourg, Commission of the European Communities, Section of Health.
 - [138] EVANS L. E., OKAZAKI E. A. (1983). Nonlinear multiparameter fitting. Report AECL-6076 (Rev. D), Routine 1-11-20. Chalk River, AECL Research.
 - [139] EVANS R. D. (1933a). Direct fusion method for determining the radium content of rocks. Rev. Sci. Instr. 4, 223-230.
 - [140] EVANS R. D. (1933b). Techniques for the determination of the radioactive content of liquids. Rev. Sci. Instr. 4, 216-222.
 - [141] EVANS R. D. (1935). Apparatus for the determination of minute quantities of radium, radon and thoron in solids, liquids and gases. Rev. Sci. Instr. 6, 99-112.
 - [142] EVANS R. D., EVANS R. O. (1948). Studies of self-absorption in gamma-ray sources. Rev. Mod. Phys. 20, 305-326.

- [143] EVANS R. D. (1955). Ionization chambers. In *The Atomic Nucleus*. New York, McGraw-Hill Book Company, Inc., 811-818.
- [144] EVE A. S. (1906). Gamma rays from radium. *Phil. Mag.* (6) 12, 189.
- [145] EVE A. S. (1911). On the number of ions produced by the beta rays and by the gamma rays from radium C. *Phil. Mag.* (6) 22, 551-562.
- [146] EVE A. S. (1917). Gamma rays from radium. *Phil. Mag.* (6) 27, 39.
- [147] FANO U. (1947). Ionization yield of radiations. II. The fluctuations of the number of ions. *Phys. Rev.* 72, 26-29.
- [148] FANO U. (1954). Note on the Bragg-Gray cavity principle for measuring energy dissipation. *Radiation Res.* 1, 237-240.
- [149] FASSBENDER H. (1958). Einführung in die Meßtechnik der Kernstrahlung und die Anwendung der Radioisotope. Ionisationskammergerät mit Meßverstärker, chap. 7. Stuttgart, Georg Thieme Verlag, 75-80.
- [150] FAVRET D. (1969). Recherches sur la mesure précise de durées de vie des niveaux isomères. Villeurbanne, Inst. Phys. Nucl., Université de Lyon, 71 p.
- [151] FINCK R. R., LIDEN K., PERSSON R. B. R. (1976). In situ measurements of environmental gamma radiation by the use of a Ge(Li)-spectrometer. *Nucl. Instr. Meth.* 135, 559.
- [152] FLIEGEL H. F., FLANDERN T. C. van (1968). A machine algorithm for processing calendar dates. *Communications of the ACM* 11, no. 10, 657.
- [153] FRÄNZ H. , WEISS C.-F. (1935). Die Ermittlung der Eigenabsorption bei der Gehaltsbestimmung schwach radiumhaltiger Substanzen nach der γ -Strahlenmethode. *Physikalische Zeitschrift* 36, 486-489.
- [154] FRIEDLANDER G., KENNEDY J. W. (1949). *Introduction to Radiochemistry*. New York, John Wiley & Sons, Inc.
- [155] FRIEDLANDER G., KENNEDY J. W. (1960). *Nuclear and Radiochemistry*. 4th ed., New York, John Wiley & Sons, Inc.
- [156] FRIEDMANN H. (1983). A portable radonmeter. *Radiat. Prot. Dosim.* 4, 119-122.
- [157] FRIEDMANN H. (1990). An electrometer amplifier for ionization chamber measurements. Progress Report, Vienna, Inst. für Radiumforschung und Kernphysik der Universität Wien, 37-38.
- [158] FRIER M., HESSLEWOOD S. R., Eds. (1980). Quality assurance of radiopharmaceuticals. A guide to hospital practice. *Nucl. Med. Commun.*, Special issue, 58 p.
- [159] FRIESEKE, HOEPFNER (1963). Schwingkondensator-Meßverstärker FHT 408A. Service-Unterlagen. Erlangen-Bruck, Friesike und Hoepfner GmbH.
- [160] FULBRIGHT H. W. (1958). Nuclear Instrumentation II. Ionization Chambers in Nuclear Physics. In *Handbuch der Physik, Encyclopedia of Physics*, Vol. XLV (Flügge S., Ed.), Berlin, Springer-Verlag, 1-51.

- [161] FUNCK E., SCHÖTZIG U., WALZ K. F. (1983). Standardization and decay of ^{169}Yb . Int. J. Appl. Radiat. Isot. 34, 1215-1224.
- [162] FURNARI J. C., DE CABREJAS M. L., ROTTA M. del C., IGLICKI F. A., MILA M. I., MAGNAVACCA C., DIMA J. C., RODRIGUEZ PASQUÉS R. H. (1992). Impact of dose calibrators quality control programme in Argentina. Nucl. Instr. Meth. A312, 269-271.
- [163] FURNARI J. C., MILA M. I., ROTTA M. del C., DE CABREJAS M. L. (1994). ^{141}Ce source as mock standard for $^{99\text{m}}\text{Tc}$. Nucl. Instr. Meth. A339, 61-63.
- [164] GARFINKEL S. B. (1959). Semiautomatic Townsend balance system. Rev. Sci. Instr. 30, 439-442.
- [165] GARFINKEL S. B., HINE G. J. (1973). Dose calibrator pilot study. NBS Technical Note 791, Washington, D.C., NBS, 1-4.
- [166] GARFINKEL S. B., SCHIMA F. J. (1975). Ionization chamber half-life measurement of the 99-minute ^{113}In isomer. Int. J. Appl. Radiat. Isot. 26, 314-316.
- [167] GEIGER K. W., CAMPION P. J. (1960). Routine methods of standardization in Canada (National Research Council of Canada). Report IAEA/STI/PUB/6, Part II, Vienna, IAEA, 13-20.
- [168] GENNA S., WEBSTER E. W., BRANTLEY J. C., BROWNELL G. L., CARDARELLI J. A., CASTRONOVO F. P., CHANDLER H. L., MASSE F. X. (1972). A nuclear medicine quality control program. J. Nucl. Med. 13, 285-286.
- [169] GLASS F. M., COURTNEY C. C., KENNEDY E. J., WILSON H. N. (1967). A new approach to direct current integration. IEEE Trans. on Nucl. Sci. 2, 143-147.
- [170] GOETSCH S. J., ATTIX F. H., PEARSON D. W., THOMADSEN B. R. (1991). Calibration of ^{192}Ir high-doserate afterloading systems. Med. Phys. 18, 462-467.
- [171] GOGOLAK C. V. (1982). In situ methods for quantifying gamma-radiation levels and radionuclide concentrations. IEEE Trans. Nucl. Sci. 29, 1216-1224.
- [172] GOLAS D. B., CALHOUN J. M. (1983). U.S. National Bureau of Standards/Atomic Industrial Forum Radioactivity Measurements Assurance Program. Int. J. Nucl. Med. Biol. 10, 163-168.
- [173] GOODIER I. W. (1968). The half-lives of ^{56}Mn and ^{198}Au . Int. J. Appl. Radiat. Isot. 19, 823.
- [174] GOODIER I. W., HUGHES F. H. (1968). Calibration of the 1383A ionization chamber for iodine-132. Int. J. Appl. Radiat. Isot. 19, 889-890.
- [175] GOODIER I. W., HUGHES F. H., WILLIAMS A. (1965). Precise measurement of the activity of low-energy beta-emitters with calibrated ionization chambers. Report IAEA/STI/PUB/106, Vienna, IAEA, 613-623.
- [176] GOODIER I. W., HUGHES F. H., WOODS M. J. (1968). The calibration of the 1383A ionization chamber for $^{87\text{m}}\text{Sr}$. Int. J. Appl. Radiat. Isot. 19, 795-797.

- [177] GOSTELY J.-J. (1992). A determination of the half-life of ^{137}Cs . *Appl. Radiat. Isot.* 43, 949-951.
- [178] GRAEME J. G., TOBEY G. E. (1971). Operational amplifiers—Design and applications. New York, McGraw-Hill Book Company, Inc. (Copyright Burr-Brown Research C.), 213-235.
- [179] GRAU MALONDA A. (1982). Counting efficiency for electron-capturing nuclides in liquid scintillator solutions. *Int. J. Appl. Radiat. Isot.* 33, 371-375.
- [180] GRAU MALONDA A., GARCIA-TORAÑO E. (1982). Evaluation of counting efficiency in liquid scintillation counting of pure beta-ray emitters. *Int. J. Appl. Radiat. Isot.* 33, 249-253.
- [181] GRAY D. H., GOLAS D. B., CALHOUN J. M. (1991). Review of the USCEA/NIST measurement assurance program for the nuclear power industry. *Radioactivity & Radiochemistry*, 30-41.
- [182] GRAY L. H. (1936). An ionization method for the absolute measurement of γ -ray energy. *Proc. Roy. Soc. A* 156, 578-596.
- [183] GRAY L. H. (1949). The experimental determinations by ionization methods of the rate of emission of beta- and gamma-ray energy by radioactive substances. *Br. J. Radiol.* 22, 677.
- [184] GRAY P. W., MACMAHON T. D. (1985). Strontium-90 half-life evaluation. Report Document ICRC/85/2, Ascot, Imperial College Reactor Centre.
- [185] GREGORICH K. E. (1991). Maximum likelihood decay curve fits by the simplex method. *Nucl. Instr. Meth. A* 302, 135-142.
- [186] GREUPNER H., GROCHE K. (1979). Über die Anwendung einer 2-Detektor-Methode für relative Aktivitätsmessungen mittels Zylinderionisationskammern. *Isotopenpraxis* 15, 214-215.
- [187] GRINBERG B. (1960). L'étalonnage des radioéléments en France. Report IAEA/STI/PUB/6, Vienna, IAEA, 21-31.
- [188] GRINBERG B., LE GALLIC Y. (1961). Caractéristiques fondamentales d'un laboratoire de mesure de très faibles activités. *Int. J. Appl. Radiat. Isot.* 12, 104-117.
- [189] GROSSWENDT B., WAIBEL E. (1978). Transport of low energy electrons in nitrogen and air. *Nucl. Instr. Meth.* 155, 145-156.
- [190] GUBKIN E. S., DRICHKO A. F., KARAVAEV F. M., SLUSHNEVA R. M. (1980). Sfericheskaya 4pi-ionisationnaya kamera s kolodtsem. Transl. from Izmer. Tekh.: Spheric 4pi-ionization chamber with a well. *Measurement Techniques (USA)* 7, 67-68.
- [191] GÜHNE F., RODLOFF G. (1973). Automatisierung von Strommessungen mit dem Schwingkondensatorverstärker VA-J-51. *Isotopenpraxis* 9, 121-123.
- [192] GÜNTHER E., SCHÖTZIG U. (1992). Activity determination of ^{93}mNb . *Nucl. Instr. Meth. A* 312, 132-135.

- [193] GUIHO J.-P., OSTROWSKY A., SIMOEN J.-P., HILLION P. (1974). Mesure des courants faibles au laboratoire de métrologie des rayonnements ionisants. Rapport CEA-R-4637, Gif-sur-Yvette, CEA, CEN-Saclay, 15 p.
- [194] HAHN H. P., BORN H. J., KIM J. I. (1976). Survey on the rate perturbation of nuclear decay. *Radiochim. Acta* 23, 23-37.
- [195] HALBIG J. K., CAINE J. C. (1985). ION-1 technical manual. Report LA-10433-M (ISPO-240), available from NTIS, PC A03/MF A01; 1 as DE85017955, Los Alamos National Lab., 41 p.
- [196] HALLEDAUER G. (1925). Über eine Methode zur Messung kleinster Emanationsmengen und ihre Anwendung zur Bestimmung des Radiumgehaltes einiger Meteorite. *Mitt. d. Inst. f. Radiumf.* Nr. 175, Wien. Ber., Math.-naturw. Klasse, Abt. IIa 134, 39-44.
- [197] HARE D. L., HENDEE W. R., WHITNEY W. P., CHANEY E. L. (1974). Accuracy of well ionization chamber isotope calibrators. *J. Nucl. Med.* 15, 1138-1141.
- [198] HARRIS C. C., JASZCZAK R. J., GREER K. L., BRINER W. H., COLEMAN R. E. (1984). Effects of characteristic X-rays on assay of I-123 by dose calibrators. *J. Nucl. Med.* 25, 1367-1370.
- [199] HARTLEY B. M. (1991). The real-time fitting of radioactive decay curves. *Nucl. Instr. Meth.* A308, 599-608.
- [200] HARTSHORN L. (1926). A convenient arrangement for the measurement of very small currents. *J. Sci. Instr.* 3, 297-301.
- [201] HAUSER W. (1974). The 1972 nuclear medicine survey—radionuclide identification and activity measurement. *Am. J. Clin. Pathol.* 61, 943.
- [202] HERRERA N. E., PARAS P. (1983). Q-Series. The College of American Pathologists surveillance of activity (dose) calibrators. *Int. J. Nucl. Med. Biol.* 10, 107-110.
- [203] HERTZ G. (1958). Beobachtung von Ionisationsströmen. In section B., chap. V. *Lehrbuch der Kernphysik, Experimentelle Verfahren*, vol. 1, Leipzig, B. G. Teubner, 104-120.
- [204] HESS V. F. (1913). Über Neuerungen und Erfahrungen an den Radiummessungen nach der γ -Strahlenmethode. *Physikalische Zeitschrift* 16, 1135-1141.
- [205] HESS V. F., DAMON E. E. (1922a). Improvement in the determination of the Radium content of low-grade Radium-Barium salts. *Phys. Rev.* 19, 530-531.
- [206] HESS V. F., DAMON E. E. (1922b). Improvement in the determination of the Radium content of low-grade Radium-Barium salts. *Phys. Rev.* 20, 59-64.
- [207] HEUSSER G. (1986). The background components of germanium low-level spectrometers. *Nucl. Instr. Meth.* B17, 418-422.
- [208] HEUSSER G. (1993a). Cosmic ray-induced background in Ge-spectrometry. *Nucl. Instr. Meth.* B83, 223-228.

- [209] HEUSSER G. (1993b). Background in ionizing radiation detection illustrated by Ge-spectrometry. Proc. 3rd. Int. Summer School on “Low-level measurements of radioactivity in the environment”: Techniques and Applications” (García-León M., Madurga G., Eds.) in Huelva, Spain. Report MPI H-V26-93, Heidelberg, Max-Planck-Institut für Kernphysik, 44 p.
- [210] HEYDORN K. (1967). Geometrical effects on the response of the National Physical Laboratory ionization chamber type 1383A. *Int. J. Appl. Radiat. Isot.* 18, 479-483.
- [211] HEYDORN K. (1970). Determination of radionuclide activities by a well-type gamma-ionization chamber. *Nucl. Instr. Meth.* 78, 177-178.
- [212] HEYDORN K. (1972). Use of the National Physical Laboratory ionization chamber type 1383A in neutron activation analysis. *J. Radioanal. Chem.* 10, 245-256.
- [213] HÖGBERG S. A. C., GUSTAVSSON J. E. (1973). An ionization chamber for ^{222}Rn measurements. *Nucl. Instr. Meth.* 113, 583-588.
- [214] HOPFIELD J. J. (1933). Use of Argon in the ionization method of measuring cosmic rays and gamma-rays. *Phys. Rev.* 43, 675-686.
- [215] HOPPES D. D., SCHIMA F. J. (1982). Nuclear data for the efficiency calibration of germanium spectrometer systems: Measurements from the laboratories of the International Committee for Radionuclide Metrology, α -, β -, and γ -Ray Spectrometry Group. NBS Special Publication 626, Washington, D.C., NBS, 146 p.
- [216] HOPPES D. D. (1988). Rapport du Comité Consultatif pour les Étalons de Mesure des Rayonnements Ionisants (CCEMRI), Section II. Mesure des radionuclides. 9e réunion (juin 1987), Sèvres, BIPM, 20-27.
- [217] HOPPES D. D., HUTCHINSON J. M. R. (1991). International Committee for Radionuclide Metrology: Guidelines for International Acceptance of Radioactivity Calibration Sources. *Appl. Radiat. Isot.* 42, 893-897.
- [218] HORVATH G., SZÖRENYI A., ZSINKA A. (1985). Ujabb eredmények a 4 PI aknás ionizációs kamrás mérések területén. New results of measurements with 4 PI ionization chambers. *Mérésügyi Közlemények* 26, 73-75.
- [219] HOUTERMANS H. (1970). Aspects of Radionuclide Standardization in the IAEA. NBS Special Publication 331 (Mann W. B., Garfinkel S. B., Eds.), Washington, D.C., NBS, 5-12.
- [220] HOUTERMANS H., MILOSEVIC O., REICHEL F. (1980). Half-lives of 35 radionuclides. *Int. J. Appl. Radiat. Isot.* 31, 1L53-154.
- [221] HÜBNER W. (1954). Der elektrometrische Photozellenkomparator. *ETZ-A* 75, 529-534.
- [222] HÜBNER W. (1955). Der elektrometrische Photozellenkompensator, ein neues Gerät zur Messung der Dosis und Dosisleistung ionisierender Strahlung. *Strahlentherapie* 96, 461-468.
- [223] HÜBNER W. (1958). Ein Diagramm zur Ermittlung der Sättigungsverluste bei Standard-Ionisationskammern. *Fortschritte auf dem Gebiet der Röntgenstrahlen und der Nuklearmedizin* 89, 764-767.

- [224] HUSAK V., KLEINBAUER K. (1980). Zkouseni a hodnoceni merice aktivity Tesla NNG 601 na pracovisti nuklearni mediciny. Performance testing of Tesla NNG 601 activity meter in nuclear medicine department. *Cesk. Radiol.* 34, 202-210.
- [225] IAEA (1991). International Atomic Energy Agency. X-ray and gamma-ray standards for detector calibration. Report IAEA-TECDOC-619, Vienna, IAEA, 157 p.
- [226] ICRU (1980). International Commission on Radiation Units and Measurements. *Radiation Quantities and Units*.
- [227] ICRU Report 33, Washington, D.C, ICRU, 15 p.
- [228] IEC (1977). International Electrotechnical Commission. Dimensions of test tubes made of glass or plastics for radioactivity measurements.
- [229] IEC 583, (Publication 583A, First supplement, 1981). Geneva, Bureau Central de la Commission Electrotechnique Internationale, 7 p.
- [230] IEC (1992a). International Electrotechnical Commission. Calibration and usage of ionization chamber systems for assay of radionuclides. IEC 1145, Geneva, Bureau Central de la Commission Electrotechnique Internationale, 21 p.
- [231] IEC (1992b). International Electrotechnical Commission. Medical electrical equipment: Particular methods for declaring the performance of radionuclide calibrators. In preparation as project number 62C.38.1 by IEC 62C (Secretariat) 85, Geneva, Bureau Central de la Commission Electrotechnique Internationale.
- [232] ISO (1993a). International Organisation for Standardization. International vocabulary of basic and general terms in metrology (VIM). Geneva, ISO.
- [233] ISO/IEC 98-3:1993 *ISO (1993b). International Organisation for Standardization. Guide to the expression of uncertainty in measurement*. Geneva, ISO, 101 p.
- [234] JACOBSEN J. C. (1934). Eine Vorrichtung zur Messung schwacher Ionisierungsströme. *Z. Physik* 91, 167-168.
- [235] JAEGER R. (1929). Eine Kompensationsmethode zur Messung schwacher Ströme. *Z. Physik* 52, 627-636.
- [236] JAEGER R. (1940). Elektrometrische Messung von Ionisierungsströmen. Archiv für Technisches Messen (ATM) V 3211-1, T6-T7.
- [237] JAFFÉ G. (1913). Zur Theorie der Ionisation in Kolonnen. *Ann. d. Phys.* 42, 303-344.
- [238] JAIN A. N., REHMAN M. AB. (1981). Quality control of dose calibrators. *Nuklearmedizin* 20, 247-250.
- [239] JANSZEN H. (1994). BSPLINE—Ein Dialogprogramm für lineare Ausgleichsrechnung mit Spline-Funktionen (And: Cubic spline fit. Private communication, 1986). Report PTB-6.31-94-4, Braunschweig, PTB, 46 p.
- [240] JEDLOVSZKY R., SZÖRÉNYI A. (1983). Detection of radionuclidic impurities. *Int. J. Nucl. Med. Biol.* 10, 65-68.

- [241] JOHNSTON A. S., COLOMBETTI L. G., BAKER S. I., PINSKY S. M. (1980). Dose calibrator readings due to radionuclidic impurities found in radiopharmaceuticals. *Nuklearmedizin* 19, 1-6.
- [242] JUDGE S. M., GRANT C., LUCAS S. E. M., MERCER R. A., MUNSTER A., PRIVITERA A. M., WOODS M. J. (1987). Decay-scheme data for ^{65}Ni . *Appl. Radiat. Isot.* 38, 907-910.
- [243] KAKIUCHI S., MAZAKI H., KATANO R., SHIMIZU S., SELLAM R. (1975). A double ionization chamber for the differential method. *Nucl. Instr. Meth.* 158, 435-441.
- [244] KARAVAEV F. M., DRICHKO A. F., GREUPNER H., SUCKER K.-H. (1975). Zur Methodik der Messung der Aktivität von umschlossenen Gamma-Strahlungsquellen mittels Ionisationskammern. *Isotopenpraxis* 11, 396-399.
- [245] KATANO R., KAKIUCHI S., MAZAKI H. (1976). Measurements of ion currents by a conventional sampling method. *Bull. Inst. Chem. Res., Kyoto Univ.* 54, 30-35.
- [246] KAWADA Y., YURA O. (1983). Present status of radioactivity standardization and its future problems. *Densi Gijutsu Sogo Kenkyusho Iho* (Bull. Electrotech. Lab.) 47, 797-814.
- [247] KEITHLEY (1977). Electrometer measurements. Keithley Instruments, Inc., Cleveland, Ohio.
- [248] KEITHLEY (1983). Model 642 electrometer. Manual and product information. Keithley Instruments, Inc., Cleveland, Ohio.
- [249] KEITHLEY (1984). Model 617 programmable electrometer. Instruction manual. Keithley Instruments, Inc., Cleveland, Ohio, 140 p.
- [250] KEITHLEY (1992). Low level measurements. Precision DC current, voltage and resistance measurements. 4th ed., Keithley Instruments, Inc., Cleveland, Ohio, 200 p.
- [251] KEITHLEY J. F., YEAGER J. R., ERDMAN R. J. (1984). Low level measurements: For effective low current, low voltage and high impedance measurements. Keithley Instruments, Inc., Cleveland, Ohio, 127 p.
- [252] KEMP L. A. W. (1945). A new circuit with special applications in gamma-ray and x-ray dosimetry. *Brit. J. Radiol.* 18, 107.
- [253] KEMP L. A. W. (1951). A method of calibrating an ionization current comparator without reference to radiation. *Brit. J. Radiol.* 24, 211.
- [254] KEMP L. A. W., WOODALL J. E. (1968). Evaluation of a high-insulation dry-reed switch for electrometer applications. *Electronic Engineering* 40, 236-239.
- [255] KLEEVEN W. J. G. M. (1983). Calibratie van een re-entrant ionisatiekamer. Experimentele en theoretische bepaling van de gevoeligheidscurve. Report maart 1983/VDF/NK 83.48, Eindhoven, Technische Hogeschool Eindhoven, Technische Natuurkunde, 88 p.

- [256] KLEEVEN W. J. G. M., WIJNHOVEN P. J. (1985). Effect of electrode coating on the response curve of dose calibrators for nuclear medicine: A computer simulation study. *Nucl. Instr. Meth.* A237, 604-609.
- [257] KMENT V., KUHN A. (1960). Ionisationkammern. Chap. 12.1, in *Technik des Messens radioaktiver Strahlung*. Leipzig, Akademische Verlagsgesellschaft Geest & Portig K.G., 53-90.
- [258] KNOLL G. F. (1989). Ionization Chambers. Chap. 5. in *Radiation Detection and Measurement*, 2nd ed., New York, John Wiley & Sons, Inc., 131-159.
- [259] KOBAYASHI K., ISHIKAWA I. (1977). Absolute measurement of Cu-64. Report JAERI-M-7402, Tokyo, Japan Atomic Energy Research Inst., 25 p.
- [260] KOHLHÖRSTER W. (1928). Registrierapparate für Fadenelektrometer. *Zs. f. Phys.* 47, 449.
- [261] KOHLRAUSCH F. (1910). Lehrbuch der Praktischen Physik. 11. Auflage, Leipzig, B. G. Teubner, 700 p.
- [262] KOHLRAUSCH F. (1928). Meßmethoden der Radioaktivität, chap. VIII. 2. Aktivitätsmessungen. In *Handbuch der Experimentalphysik*, Bd. 15 (Wien W., Harms F., Eds.), Leipzig, Akademische Verlagsgesellschaft m.b.H., 694-720.
- [263] KOHLRAUSCH F. (1935). D. Stromstärke. d) Kompensationsmethoden. In *Praktische Physik*, 17. Auflage, Leipzig, B. G. Teubner, 649-651.
- [264] KOHLRAUSCH F. (1956). *Praktische Physik*, Vol. 2, 20. Auflage. Mengenbestimmung radioaktiver Stoffe, chap. 7.67 (by Fränz H.). Stuttgart, B. G. Teubner, 579-591.
- [265] KOHLRAUSCH F. (1968). *Praktische Physik*, Vol. 2, 22. Auflage. Relative Aktivitätsbestimmung, chap. 7.1.4.4., Stuttgart, B. G. Teubner, 507-517.
- [266] KOHLRAUSCH F. (1985). *Praktische Physik*. Vol. 2, 23. Auflage. Stromstärke und Ladung, chap. 6.1.4, 74-82. And: Relativbestimmung der Aktivität, chap. 9.5.6, Stuttgart, B. G. Teubner, 588-590.
- [267] KOLB W. A. (1968). Die Eigenaktivität von Blei. In Proc. 1st Int. Congr. Radiation Protection (Rome 1966), Oxford, Pergamon Press, 1385-1391.
- [268] KORN G. A., KORN T. M. (1964). Electronic Analog and Hybrid Computers. New York, McGraw-Hill Book Company, Inc., 213-235.
- [269] KOSTYLEVA YU. G., MYSEV I. P., YUR'EV A. V. (1977). Ionizatsionnaya kamera dlya izmereniya aktivnosti radioaktivnykh istochnikov (Ionization chamber for radioactive source activity measuring). Patent SU 673076 A 5 Jul 1977, 6 p.
- [270] KOWALSKY R. J., JOHNSTON R. E., CHAN F. H. (1977). Dose calibrator performance and quality control. *J. Nucl. Med. Technol.* 5, 35-40.
- [271] KROPF F. (1939). Methodische Fragen zur Bestimmung kleinster Emanations- und Radiummengen und der Radiumgehalt von Kalkstein. *Mitt. d. Inst f. Radiumf.* Nr. 429, Wien-Ber., Math.-naturw. Klasse, Abt. IIa 148, 163-177.

- [272] LAGOUTINE F., COURSOL N., LEGRAND J. (1982). Table de radionucléides. Gif-sur-Yvette, CEN-Saclay, CEA-LMRI.
- [273] LAURITSEN C. C., LAURITSEN T. (1937). A simple quartz fiber electrometer. Rev. Sci. Instr. 8, 438-439.
- [274] LEA D. E. (1937). An instrument for measuring ionization currents. J. Sci. Instr. 14, 89-94.
- [275] LEGRAND J., MOREL J., VATIN R., GOENVEC H. (1978). La radioactivité au service de la médecine nucléaire. La métrologie des rayonnements ionisants et la médecine nucléaire. Chapitre 1: Les méthodes de mesure et d'analyse radioactive. Bull. Inf. Sci. Tech. (Paris) 228-229, 141-147.
- [276] LEO W., HÜBNER W. (1950). Zur Strahlungsmessung mittels Thermoelementen und hochempfindlicher Photozellenkompensation. Z. angewandte Phys. 2, 454-461.
- [277] LEVINE G., MALHI B., STRUTTMAN L. (1984). Discrepancies in dose calibrator assays for various forms of therapeutic iodine-131. J. Nucl. Med. Technol. 25, 84-86.
- [278] LEWIS V. E., WOODS M. J., GOODIER I. W. (1972). The calibration of the 1383A ionization chamber for ^{67}Ga . Int. J. Appl. Radiat. Isot. 23, 279-283.
- [279] LINDEMANN F. A., KEELEY T. C. (1924). A new form of electrometer. Phil. Mag. 47, 577-583.
- [280] LOEVINGER R. (1966). Precision measurement with the total-feedback electrometer. Phys. Med. Biol. 11, 267-279.
- [281] LOFTUS T. P. (1975). Relation of activity measurements to free-air ionization chamber measurements. Health Phys. 29, 355.
- [282] LOFTUS T. P. (1980). Standardization of iridium-192 gamma-ray sources in terms of exposure. J. Research NBS 85, no. 1, Washington, D.C., NBS, 19-25.
- [283] LOFTUS T. P., MANN W. B., PAOLELLA L. F., STOCKMANN L. L., YOUDEN W. J. (1957). Comparisons of national radium standards. J. Research NBS 58, no. 4 (RP2749), Washington, D.C., NBS, 169-174.
- [284] LOWENTHAL G. C. (1969). Secondary standard instruments for the activity measurement of pure β emitters. A review. Int. J. Appl. Radiat. Isot. 20, 559-568.
- [285] LOWENTHAL G. C. (1981). Automated sample changers—Their costs and their benefits. Report on ICRM Action 80/7. Lucas Heights, Australia, AAEC Research Laboratory, 21 p.
- [286] LUCAS L. L. (1986). Uncertainties associated with the calibration and use of NBS pressurized $4\pi\gamma$ ionization chamber “A”. Trans. Amer. Nucl. Soc. 53, 23.
- [287] LUNDEHN I. (1974). Testing of Isotope Calibrators. Proc. 1st World Congr. Nucl. Medicine, Tokyo, Japan, in: Advances in Nucl. Medicine, 1287-1289.
- [288] MACARTHUR D. W., ALLANDER K. S., BOUNDS J. A., BUTTERFIELD K. B., MCATEE J. L. (1992). Long-range alpha detector. Health Physics 63, 324-330.

- [289] MAIER-LEIBNITZ H. (1957). Statistische Schwankungen und optimale Übergangsfunktionen beim Zählhäufigkeitsmesser (Counting Rate Meter). Zeitschr. f. angewandte Phys., einschl. Nukleonik 9, 57-60.
- [290] MAKOWER W., GEIGER H. (1912). Practical measurements in radio-activity. London, Longmans, Green, and Co, 150 p.
- [291] MALMSTADT H. V., ENKE C. G. (1969). Digital electronics for scientists. New York, Benjamin Inc.
- [292] MANN W. B. (1960). Routine methods of radioactivity standardization at the National Bureau of Standards (USA). Report IAEA/STI/PUB/6, Vienna, IAEA, 89-102.
- [293] MANN W. B., GARFINKEL S. B. (1970). Radioactivity calibration standards. NBS Technical Note TN-331, Washington, D.C., NBS, 118 p.
- [294] MANN W. B., RYTZ A., SPERNOL A. (1991). Radioactivity Measurements: Principles and Practice. (Chap. 5.4.6. 4π ionization chambers). First published in Appl. Radiat. Isot. 39 (1988). Oxford, Pergamon Press, 202 p.
- [295] MANN W. B., SELIGER H. H. (1958). Preparation, maintenance, and application of standards of radioactivity. NBS Circular 594, Washington, D.C., NBS.
- [296] MANN W. B., STOCKMANN L. L., YOUNDEN W. J., SCHWEBEL A., MULLEN P. A., GARFINKEL S. B. (1959). Preparation of new solution standards of radium. J. Research NBS 62, no. 1 (RP2924), Washington, D.C., NBS, 21-26.
- [297] MARSH S. F., ABERNATHEY R. M., BECKMAN R. J., REIN J. E. (1980). ^{241}Pu half-life determined by mass-spectrometric measurements of decreasing $^{241}\text{Pu}/^{242}\text{Pu}$ ratios. Int. J. Appl. Radiat. Isot. 31, 629-631.
- [298] MARTIN R. H., BURNS K. I. W., TAYLOR J. G. V. (1994). A measurement of the half-life of ^{90}Sr . Nucl. Instr. Meth. A339, 158-163.
- [299] MARTIN R. H., TAYLOR J. G. V. (1990). A measurement of the half-life of ^{137}Cs . Nucl. Instr. Meth. A286, 507-513.
- [300] MARTIN R. H., TAYLOR J. G. V. (1991). Ion chamber sample changer system. Private communication, Chalk River, AECL Research, 1 p.
- [301] MAZAKI H., KAKIUCHI S., YOSHIOKA E. (1975). A double ionization chamber for the differential method. Bull. Inst. Chem. Res. (Kyoto Univ.) 53, 1-10.
- [302] MAZKAROV S. A. (1979). 4pi-ionization chambers in the radioactive isotope production. Yadrena Energ. (Bulgaria) 8, 40-44.
- [303] MERRITT J. S., GIBSON F. H. (1977a). Measurement of a ^{141}Ce standard with dose calibrators. Report AECL-5909, Chalk River Nuclear Laboratories, 22 p.
- [304] MERRITT J. S., GIBSON F. H. (1977b). Standardization of Cs-134 (1977). Report AECL-5834, Chalk River Nuclear Laboratories, 15 p.

- [305] MERRITT J. S., GIBSON F. H. (1978). Standardization of Cs-137 by the 4pi(PC)-gamma efficiency-tracing method with Cs-134 as tracer. Report AECL-6203, Chalk River Nuclear Laboratories, 18 p.
- [306] MERRITT J. S., MERRITT W. F., SMITH L. V., RUTLEDGE A. R. (1981). Noble-gas standards for calibration of stack-effluent monitoring systems. 4 pi gamma ionization chamber measurements, chap. 4., Report AECL-7427, Chalk River Nuclear Laboratories, 7-15.
- [307] MERRITT J. S., TAYLOR J. G. V. (1967). Gravimetric sampling in the standardization of solutions of radionuclides. Precision activity measurements with a “ $4\pi\gamma$ ” ion chamber. Report AECL-2679, Chalk River Nuclear Laboratories, 28-36.
- [308] MEYER S., HESS V. F. (1912). Zur Definition der Wiener Radiumstandardpräparate. Mitt. d. Inst. f. Radiumf. Nr. 17, Wien-Ber., Math.-naturw. Klasse, Abt. IIa 121, 603-631.
- [309] MEYER S., SCHWEIDLER E. (1927). Messungen der Ionisation. In Radioaktivität. 2. Aufl., Leipzig, B. G. Teubner, 278-301.
- [310] MILLIKAN R. A. (1932). Cosmic-ray ionization and electroscope-constants as a function of pressure. Phys. Rev. 39, 397.
- [311] MÜLLER J. W. (1981a). Counting statistics of short-lived nuclides. J. Radioanal. Chem. 61, 345-359.
- [312] MÜLLER J. W. (1981b). Selective sampling—an alternative to coincidence counting. Nucl. Instr. Meth. 189, 449-452.
- [313] MÜLLER, J. W. (1994). Some mathematical problems in counting statistics. In Advanced Mathematical Tools in Metrology, World Scientific, Singapore, 197-203
- [314] MUSTAFA S. M., MAHESH K. (1978). Criterion for determining saturation current in parallel plate ionization chambers. Nucl. Instr. Meth. 150, 549-553.
- [315] MUTH H. (1956). Zur physikalischen Dosimetrie radioaktiver Isotope. Atompraxis 2, 79-85.
- [316] NCRP (1985). National Council on Radiation Protection and Measurement. Ionization Chambers, chap. 4.4, and Assay of Radiopharmaceuticals, chap. 6.4. In A Handbook of Radioactivity Measurements Procedures. Report NCRP No. 58, Bethesda, MD, NCRP.
- [317] NEGRO V. C., CASSIDY M. E., GRAVESON R. T. (1967). A guarded insulated gate field effect electrometer. IEEE Trans. on Nucl. Sci. 135-142.
- [318] NELSON W. R., HIRAYAMA H., ROGERS D. W. O. (1985). The EGS4 code system. Report SLAC-265, Electron-Gamma Shower (EGS). Stanford Linear Accelerator Center.
- [319] NE TECHNOLOGY (1993). Instruction manual for ISOCAL IV, model 288, Radionuclide assay calibrator with pressurized ion chamber. Beenham, Reading, Berkshire, NE Technology Ltd. (former Vinten Instruments Ltd.), 20 p.

- [320] NICHOLS A. L. (1990). X- and gamma-ray standards for detector efficiency calibration. Nucl. Instr. Meth. A286, 467-473.
- [321] NIRSCHL E., AUMANN D. C. (1981). Influence of the chemical environment on the beta decay of As-77. Phys. Rev. C 23, 2377-2379.
- [322] NIST SP 250e1989 Simmons, Joe D. (1989) *NIST calibration services users guide*. NIST SP 250e1989.
- [323] NRPB (1988). National Radiological Protection Board. Guidance notes for the protection of persons against ionising radiations arising from medical and dental use. London, NRPB, Health and Safety Executive (HMSO), 82 p.
- [324] NUCLEAR DATA SHEETS (1994). Cumulated index to A-chains. In Nuclear Data Sheets 72 (Edited by National Nuclear Data Center, Tuli J. K., Martin M. J., Eds.), San Diego, Academic Press, p. ii.
- [325] OKABE S., NISHIKAWA T., AOKI M., YAMADA M. (1987). Looping variation observed in environmental gamma-ray measurement due to atmospheric radon daughters. Nucl. Instr. Meth. A255, 371.
- [326] O'KELLEY G. D. (1962). Detection and measurement of nuclear radiation. Report NAS-NS 3105, Springfield, Virginia, National Technical Information Service.
- [327] ONCESCU M., REBIGAN F. (1968). Calibration of a $4\pi\gamma$ ionization chamber. Rev. Roum. Phys. 13, 837-845.
- [328] ORTIZ F., LOS ARCOS J. M., RODRIGUEZ L., FERNANDEZ-VAREA J. M., SALVAT F. (1992). Evaluation of beta-particle emitter spectra in liquid scintillation counting systems. Nucl. Instr. Meth. A312, 136-140.
- [329] OWENS R. B. (1899). Thorium radiation. Phil. Mag. (5) 48, 360-387. (German abstract in Fortschr. der Phys. 1899, II, 104).
- [330] PALEVSKY H., SWANK R. K., GRENCHIK R. (1947). Design of dynamic condenser electrometers. Rev. Sci. Instr. 18, 298-314.
- [331] PARAS P., HAMILTON D. R., EVANS C., HERRERA N. E., LAGUNAS-SOLAR M. C. (1983). Iodine-123 assay using a radionuclide calibrator. Int. J. Nucl. Med. Biol. 10, 111-115.
- [332] PARAS P., COMER F. M., DEMEIS F., COURSEY B. M., CALHOUN J. M., GOLAS, D. B. (1986). Evaluation of radionuclide dose-calibrator measurements. Trans. Amer. Nucl. Soc. 53, 18.
- [333] PARKIN A., SEPHTON J. P., AIRD E. G. A., HANNAN J., SIMPSON A. E., WOODS M. J. (1992). Protocol for establishing and maintaining the calibration of medical radionuclide calibrators, and their quality control. Teddington, NPL, 27 p.
- [334] PARTHASARATHY K. S. (1976). Influence of the decay products of ^{222}Rn on the background counting rate of a sensitive whole-body radioactivity monitor. Nucl. Instr. Meth. 136, 585-597.
- [335] PASCOLINI A. (1991). GRAN SASSO, Roman lead for physics experiments. CERN Courier (September 1991), 17-21.

- [336] PATSTONE W. (1972). Designing femtoampere circuits requires special considerations. Application note; AN-3, July 1, 1972, Dedham, Massachusetts, Teledyne Philbrick, 3 p.
- [337] PAYNE J. T., LOKEN M. K., PONTO R. A. (1974). Comparison of dose calibrators for radioactivity assay. *J. Nucl. Med. (Chicago)* 15, 522.
- [338] PEABODY C. O. (1946). Apparatus and methods used for the calibration of the Chalk River ion-chambers types TPA, TPJ and TPD. Report AECL-294, Chalk River Nuclear Laboratories, 1-9.
- [339] PERTZ H. (1937). Über die Radioaktivität von Quellwässern. *Mitt. d. Inst. f. Radiumf. Nr. 408*, Wien-Ber., Math.-naturw. Klasse, Abt. IIa 146, 611-621.
- [340] PRAGLIN J. (1967). Elektrometertechnik. *Z. f. Instrumentenkunde* 75, 10-15.
- [341] PRICE W. J. (1958). Idem 2nd ed. (1964). Ionization chambers. Chap. 4. in Nuclear Radiation Detection. New York, McGraw-Hill Book Company, Inc., 70-114.
- [342] RAMANUJA RAO K. (1970). A re-entrant ionization chamber for measuring activities of gamma ray emitting isotopes. *Indian J. Radiol.* 24, 270-272.
- [343] RAMTHUN H. (1964). Kalorimetrische Neubestimmung der Halbwertszeit von RaD (Pb-210). *Z. Naturforschg.* 19a, 1064-1069.
- [344] RATEL G. (1990). International comparison of activity measurements of a solution of I-125. Rapport BIPM-90/3, Sèvres, BIPM, 80 p.
- [345] RATEL G. (1992a). Trial comparison of the measurement of the activity of Se-75. *Nucl. Instr. Meth. A* 312, 201-205.
- [346] RATEL G. (1992b). Activity measurements. i) International comparison of ^{75}Se activity measurements. ii) International reference system for measuring the activity of gamma-ray emitting radionuclides (SIR). iii) Extension of the SIR to α - and β -ray emitting radionuclides. In BIPM Proc.-Verb. Com. Int. Poids et Mesures 60, Sèvres, BIPM, 198-201.
- [347] RATEL G., MÜLLER J. W. (1988). Mesures d'activité, Comparaisons internationales de mesures d'activité. In BIPM Proc.-Verb. Com. Int. Poids et Mesures 56, Sèvres, BIPM, 92.
- [348] RATEL G., MÜLLER J. W. (1989). Activity measurements, International comparisons of activity measurements. In BIPM Proc.-Verb. Com. Int. Poids et Mesures 57, Sèvres, BIPM, 149.
- [349] RATEL G., MÜLLER J. W. (1991). Activity measurements, International comparisons of activity measurements. In BIPM Proc.-Verb. Com. Int. Poids et Mesures 58, Sèvres, BIPM, 139.
- [350] REHER D. F. G., BALLAUX C., CELEN E. (1986a). Ionization chamber. Annual progress report on nuclear data. NEANDC(E) 282 "U", Vol. III Euratom, Geel, CBNM, 48-50.
- [351] REHER D. F. G., MERLO P. (1990). A quality control exercise of radionuclide calibrators among Belgian hospitals. *Eur. J. Nucl. Med.* 17, 103-105.

- [352] REHER D. F. G., SIBBENS G. (1993). Efficiency curve for the CBNM radionuclide calibrator. Private communication, in CBNM (now IRMM) Group Report, for the Comité Consultatif pour les Étalons de Mesure des Rayonnements Ionisants (CCEMRI), Section II, Sèvres, BIPM.
- [353] REHER D. F. G., WOODS M. J., BALLAUX C., NIJS R., CELEN E. (1986b). Construction of a stable air capacitor for use with standard ionization chambers. CBNM Internal Report, GE/R/RN/18/86, Geel, CBNM, 16 p.
- [354] RICHARDS P., O'BRIEN M. J. (1969). Rapid determination of Mo-99. *J. Nucl. Med.* 10, 517.
- [355] ROBINSON B. M. W. (1960). Routine standardization of radionuclides in the UK. Report IAEA/STI/PUB/6, Vienna, IAEA, 41-51.
- [356] RODRIGUEZ PASQUES R. H., ROTTA M. C., DE CABREJAS M. L. (1983). Experience on radionuclide calibrators at the National Atomic Energy Commission of Argentina. *Int. J. Nucl. Med. Biol.* 10, 97-101.
- [357] ROSSI B. B., STAUB H. H. (1949). Ionization chambers and counters. New York, McGraw-Hill Book Company, Inc.
- [358] ROTHE H., WILLUHN K. (1972). Der elektrometrische Fotozellenkompensator und sein Einsatz in der Strahlungsmeßtechnik. *Isotopenpraxis* 8, 121-129.
- [359] ROWLANDS S. (1948). Methods of measuring very long and very short half-lives. *Nucleonics*, September 1948, 2-13.
- [360] RUTHERFORD E. (1897). On the electrification of gases exposed to Röntgen rays and the absorption of Röntgen radiation by gases and vapours. *Phil. Mag.* (5) 43, 241-255. (German abstract in *Fortschr. der Phys.* 1897, II, 738).
- [361] RUTHERFORD E. (1899). Uranium radiation and the electrical conduction produced by it. *Phil. Mag.* (5) 47, 109-163. (German abstract in *Fortschr. der Phys.* 1899, II, 98).
- [362] RUTHERFORD E. (1902). Übertragung erregter Radioaktivität (translat. from English). *Physikalische Zeitschrift* 3, no. 10, 210-214.
- [363] RUTHERFORD E. (1904). Radioactivity. Montreal, McGill University.
- [364] RUTHERFORD E. (1907). Radioaktivität (Aschkinass E., Ed.). Berlin, Verlag Julius Springer, 600 p.
- [365] RUTHERFORD E., CHADWICK J., ELLIS C. D. (1930). Idem 2nd ed. (1951). Radiations from Radioactive Substances. Cambridge, University Press.
- [366] RUTHERFORD E., McCLUNG R. K. (1901). Über die Energie der Becquerel- und Röntgenstrahlen und über die zur Erzeugung von Ionen in Gasen nötige Energie. *Physikalische Zeitschrift* 2, no. 4, 53-55. (transl. from English, *Proc. Roy. Soc.* 67 (1900) 245-250).
- [367] RUTHERFORD E., SODDY F. (1902). Radioactivity: Growth and decay. *Phil. Mag.* (6) 4, 370.

- [368] RUTHERFORD E., SODDY F. (1903). Radioactive change (Review). Phil. Mag. (6) 5, 576-591.
- [369] RUTLEDGE A. R., SMITH L. V., MERRITT J. S. (1980). Decay data for radionuclides used for the calibration of x- and γ -ray spectrometers. Report AECL-6692, Chalk River Nuclear Laboratories, 26 p.
- [370] RUTLEDGE A. R., SMITH L. V., MERRITT J. S. (1983). Experimental study of half-life determinations using ^{60}Co . Nucl. Instr. Meth. 206, 211-217.
- [371] RUTLEDGE A. R., SMITH L. V., MERRITT J. S. (1986). The half-lives of ^{41}Ar and ^{111}In . Appl. Radiat. Isot. 37, 1029-1031.
- [372] RYTZ A. (1978a). International coherence of activity measurements. Environment International 1, 15-18.
- [373] RYTZ A. (1978b). Contribution of the Bi-210 bremsstrahlung to the ion current produced by the radium reference source. Private communication, Sèvres, BIPM, 1 p.
- [374] RYTZ A. (1982). Activity measurements of a solution of ^{134}Cs : Report on an international comparison. Nucl. Instr. Meth. 192, 427-431.
- [375] RYTZ A. (1983a). Minimum activity and maximum impurity rates for SIR samples. Rapport BIPM-83/9, Sèvres, BIPM, 9 p.
- [376] RYTZ A. (1983b). The international reference system for activity measurements of gamma-ray emitting nuclides. Int. J. Appl. Radiat. Isot. 34, 1047-1056.
- [377] RYTZ A. (1985). Activity concentration of a solution of ^{137}Cs : An international comparison. Int. J. Appl. Radiat. Isot. A228, 506-511.
- [378] RYTZ A. (1986). Complementary information concerning the International Reference System (SIR). Rapport BIPM-86/11, Sèvres, BIPM, 3 p.
- [379] RYTZ A., MÜLLER J. W. (1980). Mesures d'activité. Comparaisons internationales de mesures d'activité. In BIPM Proc.-Verb. Com. Int. Poids et Mesures 48, Sèvres, BIPM, 68-71.
- [380] RYTZ A., MÜLLER J. W. (1981). Mesures d'activité. Mesures relatives au moyen d'une chambre d'ionisation à puits pressurisé (Contrôles des sources de référence. Fonctions d'efficacité de la chambre d'ionisation). In BIPM Proc.-Verb. Com. Int. Poids et Mesures 49, Sèvres, BIPM, 68-69.
- [381] RYTZ A., MÜLLER J. W. (1982). Mesures d'activité. Comparaisons internationales de mesures d'activité. In BIPM Proc.-Verb. Com. Int. Poids et Mesures 50, Sèvres, BIPM, 56-57.
- [382] RYTZ A., MÜLLER J. W. (1983). Mesures d'activité. Comparaison internationale de mesures d'activité d'une solution de Cs-137. In BIPM Proc.-Verb. Com. Int. Poids et Mesures 51, Sèvres, BIPM, 67-69.

- [383] RYTZ A., MÜLLER J. W. (1984). Mesures d'activité. Mesures relatives au moyen d'une chambre d'ionisation à puits pressurisée (Courbe d'efficacité). In BIPM Proc.-Verb. Com. Int. Poids et Mesures 52, Sèvres, BIPM, 74-76.
- [384] RYTZ A., MÜLLER J. W. (1985). Mesures d'activité. Mesures relatives au moyen d'une chambre d'ionisation à puits pressurisée (Réponse de la chambre d'ionisation au rayonnement de freinage produit par de rayons β). In BIPM Proc.-Verb. Com. Int. Poids et Mesures 53, Sèvres, BIPM, 99-101.
- [385] SAMUELSON G., BENGTSSON L. G. (1973). Precise and rapid measurements of small currents from high impedance sources. Rev. Sci. Instr. 44, 920-921.
- [386] SANKARAN A., GOKARN R. S. (1982). A compact wide range radioisotope calibrator with digital display using an air-equivalent re-entrant chamber. Int. J. Appl. Radiat. Isot. 33, 341-347.
- [387] SANTRY D. C. (1986). The calibration of radionuclide calibrators in Canadian hospitals. Trans. Amer. Nucl. Soc. 53, 17.
- [388] SANTRY D. C., BOWES G. C. (1987). The NRCC calibration service for radionuclide calibrators in Canadian hospitals. Report NRCC PIRS-0089, Ottawa, Ontario, NRCC, 9 p.
- [389] SANTRY D. C., BOWES G. C. (1989). Half-life of ^{99m}Tc in linearity testing of radionuclide calibrators. Health Phys. 57, 673-675.
- [390] SANTRY D. C., BOWES G. C., MUNZENMAYER K. (1987). Precision electronics for ionization chamber measurements. Appl. Radiat. Isot. 38, 879-883.
- [391] SCHAEKEN B., VANNESTE F., BOUILLER A., HOORNAERT M. T., VANDENBROECK S., HERMANS J., PIRON A. (1992). ^{192}Ir brachytherapy sources in Belgian hospitals. Nucl. Instr. Meth. A312, 251-256.
- [392] SCHIFF L. I., EVANS R. D. (1936). Statistical analysis of the counting rate meter. Rev. Sci. Instr. 7, 456-462.
- [393] SCHÖTZIG U., DEBERTIN K., WALZ K.F. (1977). Standardization and decay data of ^{133}Ba . Int. J. Appl. Radiat. Isot. 28, 503-507.
- [394] SCHÖTZIG U., SCHRADER H. (1993). Halbwertszeiten und Photonen-Emissionswahrscheinlichkeiten von häufig verwendeten Radionukliden. Report PTB-Ra-16/4, Braunschweig, PTB, 66 p.
- [395] SCHRADER H. (1983). Sekundärmethoden zur Aktivitätsbestimmung. In Radioaktive Standards und ihre Anwendung im Bereich der Kerntechnik und Umgebungsüberwachung (Debertin K., Ed.). Report PTB-Ra-13, Braunschweig, PTB, 13-18.
- [396] SCHRADER H. (1989). Measurement of the half-lives of ^{18}F , ^{56}Co , ^{125}I , ^{195}Au and ^{201}Tl . Appl. Radiat. Isot. 40, 381-383.
- [397] SCHRADER H. (1992a). Measurements of small currents using a modified Townsend method with fast, programmable A/D and D/A converters. Nucl. Instr. Meth. A312, 34-38.

- [398] SCHRADER H. (1992b). Aktivimeter. In Qualitätssicherung von Aktivitätsmessungen in Nuklearmedizin und Strahlenschutz (Rodloff G., Debertin K., Eds.). Report PTB-Ra-28, Braunschweig, PTB, 16-38.
- [399] SCHRADER H., WALZ K. F. (1986). Determination of radioactive impurities in activity measurements with non-discriminating detectors. *Appl. Radiat. Isot.* 37, 115-120.
- [400] SCHRADER H., WEISS H. M. (1981). Bestimmung des Ansprechvermögens einer $4\pi\gamma$ -Ionisationskammer für die Nuklearmedizin. PTB-Jahresbericht, Braunschweig, PTB, 179.
- [401] SCHRADER H., WEISS H. M. (1983). Calibration of radionuclide calibrators. *Int. J. Nucl. Med. Biol.* 10, 121-124.
- [402] SCHÜTZE D. (1980). Aktivitätsmeßgerät 27013. *Medizintechnik* 20, 83-84.
- [403] SELIGER H. H., SCHWEBEL A. (1954). Standardization of beta-emitting nuclides. *Nucleonics* 12, no. 7, 54-63.
- [404] SHAMOS M. H., LIBOFF A. R. (1968). New ionization chamber technique for the measurement of environmental radiation. *Rev. Sci. Instr.* 39, 223-229.
- [405] SHARPE J., WADE F. (1951). T.P.A. Mk II ionization chamber. Report AERE EL/R806, Harwell, AERE.
- [406] SHARPE J., WADE F. (1953). A re-entrant thimble ionisation chamber. *Atomics* 4, 32-33.
- [407] SHARPE J. (1955). Ionization devices, chap. VI, D.C. ionization chambers. In Nuclear Radiation Detectors. London, Methuen & Co, Ltd., and New York, John Wiley & Sons, Inc., 131-137.
- [408] SHONKA F. R., STEPHENSON R. J. (1949). Chicago pressure ionization chamber for gamma ray measurement. Univ. Chicago Metallurgical Lab., Report MUC-RJS-2, AECD-2463, Springfield, Virginia, National Technical Information Service.
- [409] SIBBENS G. (1991). A comparison of NIST/SIR-, NPL-, and CBNM-5ml ampoules. Report CBNM/GE/R/RN/14/91, Geel, CEC-JRC, IRMM (former CBNM), 17 p.
- [410] SIEMENS (1992). Styroflex capacitors. Product information. Erlangen, Siemens AG.
- [411] SIEVERT R. M. (1932a). Ionisation at high gas pressures. *Nature* 129, 792-793.
- [412] SIEVERT R. M. (1932b). Eine Methode zur Messung von Röntgen-, Radium- und Ultrastrahlung. *Acta Radiol. Suppl.* 14, 1.
- [413] SINCLAIR W. K. (1950). Comparison of Geiger-counter and ion-chamber methods of measuring gamma radiation. *Nucleonics* 7, no. 6, 21-26.
- [414] SINCLAIR W. K., NEWBERY S. P. (1951). A direct reading meter for the measurement of highly active samples of gamma-emitting radioisotopes. *J. Sci. Instr.* 28, 234-236.

- [415] SINCLAIR W. K., TROTT N. G., BELCHER E. H. (1954). The measurement of radioactive samples for clinical use. *Brit. J. Rad.* 27, 565-574.
- [416] SIRI W. E. (1949). Ionization chambers. Chap. 12 in Isotopic Tracers and Nuclear Radiations. New York, McGraw-Hill Book Company, Inc., 344-357.
- [417] SMITH B. S., PEABODY C. O., CRAIG D. S. (1946). Characteristics of Chalk River ion-chambers types TPA, TPD and TPJ. Report AECL-291, Chalk River Nuclear Laboratories, 8 p.
- [418] SMITH C. C., SELIGER H. H. (1953). Improvement in response of 4π gamma-ionization chambers. *Rev. Sci. Instr.* 24, 474.
- [419] SMITH D. (1982). International comparison of activity measurements of a solution of ^{55}Fe . *Nucl. Instr. Meth.* 200, 383-387.
- [420] SMITH D. (1993). New robots for ion-chamber measurement. Privat communication, in NPL Radioactivity Group Report 1991-1993 for the Comité Consultatif pour les Étalons de Mesure des Rayonnements Ionisants (CCEMRI), Section II, Sèvres, BIPM.
- [421] SMITH D., WILLIAMS A. (1971). A 4π beta-gamma coincidence method for mixed electron-capture/ positron emitters: the absolute measurement of ^{68}Ga . *Int. J. Appl. Radiat. Isot.* 22, 615-623.
- [422] SMITH L. V., MERRITT J. S. (1980). Instrumentation for $4\pi\gamma$ ionization chamber. Report AECL-7055, Chalk River Nuclear Laboratories, 42-43.
- [423] SPRINKLE E. A., TATE P. A. (1966). The saturation curve in cylindrical and spherical ionization chambers. *Phys. Med. Biol.* 11, 31-46.
- [424] SRIVASTAVA P. K., KAMBOJ S. (1982). National intercomparison of activity measurements with iodine-131. Report BARC-1149, Bombay, BARC, 27 p.
- [425] STAUB H. H. (1953). Detection Methods. In Experimental Nuclear Physics (Segré E., Ed.), Vol. I, Part I. New York, John Wiley & Sons, Inc.
- [426] STEINKE E. G. (1933). Die kosmische Ultrastrahlung, chap. 5, A. Meßmethoden und Apparaturen, 2. Die Entwicklung der Ionisationskammermethoden. In Handbuch der Physik, Bd. XXIII, 2. (Geiger H., Scheel K., Eds.). Berlin, Verlag Julius Springer, 479-489.
- [427] STELJES J. F. (1946). Manufacture of the Chalk River ion-chambers types TPA, TPJ and TPD. Report AECL-292, Chalk River Nuclear Laboratories, 16 p.
- [428] STRAUSS K. H. (1936). Über die Verwendungsmöglichkeit einer Urankompensation zur exakten Messung der Ultrastrahlung. *Z. Physik* 100, 237-249.
- [429] SUNDE P. B., DICKINSON P. (1986). Ion chamber measurement assurance: A manufacturer's perspective. *Trans. Amer. Nucl. Soc.* 53, 20.
- [430] SUZUKI A., SUZUKI M. N. (1986). Calibration factors for radionuclide calibrators. *Trans. Amer. Nucl. Soc.* 53, 22.

- [431] SUZUKI A., SUZUKI M. N., WEIS A. M. (1976). Analysis of a radioisotope calibrator. *J. Nucl. Med. Technol.* 4, 193-198.
- [432] SWANN W. F. G. (1921). A compensation scheme for electrostatic measurements. *Phys. Rev.* 17, 240-242.
- [433] SZÖRÉNYI A. (1985). Report on a trial comparison of activity measurements of a solution of ^{109}Cd . Rapport BIPM-85/10, Sèvres, BIPM, 15 p.
- [434] SZÖRÉNYI A., VAGVÖLGYI J. (1983a). Experiences of the metrological supervision of radionuclide calibrators in Hungary. *Int. J. Nucl. Med. Biol.* 10, 91-96.
- [435] SZÖRÉNYI A., VAGVÖLGYI J. (1983b). A nukleáris orvosi gyakorlatban használt ionizációs kamrás aktivitásmérő készülékek mérésügyi ellenőrzése. (Metrological supervision of radionuclide calibrators with ionization chamber used in nuclear medical practice.) *Izotópteknika* 26, 1-10.
- [436] SZÖRÉNYI A., VAGVÖLGYI J. (1984). A nukleáris orvosi gyakorlatban használt aktivitásmérők metrológiai ellenőrzése Tc-99m és Co-57 radioaktív hiteles anyagmintával. (Calibration inspection of radioactivity measuring instruments used in nuclear medicine with Tc-99m and Co-57 calibrated radioactive samples.) *Izotópteknika* 27, 275-278.
- [437] SZÖRÉNYI A., ZSINKA A. (1980). A 4 PI aknás ionizációs kamrás mérések szerepe a hiteles radioaktív anyagminták készítésénél. (Role of measurements made by 4 PI well-type ionization chambers in the preparation of radioactive certified reference materials.) OMH-Report 7839 (in Russian), 9 p., and Mérésügyi Közleményik 21, 73-75.
- [438] SZÖRÉNYI A., ZSINKA A., HORVATH G. (1984). New results of measurements with a 4 pi gamma ionization chamber (in Russian). Proc. of Symposium on "Production and Application of Radioactivity Standards" in Csopak (Hungary), September 1984, Budapest, OMH, 67-76.
- [439] TAGESEN S., WINKLER G. (1993). Troubles, traps and tricks in fitting exponential decay data. Proc. Int. Symp. on "Nuclear Data Evaluation Methodology" (Dunford C. L., Ed.) at Brookhaven National Lab., Upton, NY, 12-16 Oct. 1992. Singapore, World Scientific, 267-272.
- [440] TANIGUCHI K., MIYAKAWA T., DOINOBU I., SUNAYASHIKI T. (1979). Correction factor of radioisotope calibrator for radioisotope volume and the vessel (in Japanese). *Nippon Hoshisen Gijutsu Gakkai Zasshi*. 35, 352-357.
- [441] TAPP G. A. (1987). An ion-chamber control system for high precision measurements of gamma radiation. Report CRNL-4158, Chalk River Nuclear Laboratories, 29 p.
- [442] TAYLOR D., SHARPE J. (1951). Nuclear particle and radiation detectors, Part 1. Ion chambers and ionchamber instruments. Symposium on "Radiation Monitoring Apparatus", session I, in Proceedings of the Institution of Electrical Engineers, Vol 98 (II), #62, 1951 April, 174-190.

- [443] TAYLOR J. G. V., SPENCELEY H. C., SLATER W. F., MILANI L., MERRITT J. S., SMITH L. V. (1980). Ion-chamber sample changer. Report AECL-6956, Chalk River Nuclear Laboratories, 61.
- [444] THOMANN J., KASCH G., FOTTNER J., STIEF D. (1990). Handbuch der Datenwandlung. Einführung in die Technik der A/D-D/A-Umsetzung und ihre praktische Anwendung, 2. erweiterte Auflage, München, Datel GmbH, 175 p.
- [445] THOMAS D. J. (1978). The electron capture decay of ^{85}Sr ; measurements of the K x-ray emission probability, half-life, and decay scheme. Z. Phys. A 289, 51-58.
- [446] THOMSON J. J., RUTHERFORD E. (1896). On the passage of electricity through gases exposed to Röntgen rays. Phil. Mag. (5) 42, 392-407. (German abstract in Fortschr. der Phys. 1896, II, 652).
- [447] THOR A. J. (1993/94). New international standards for quantities and units. Metrologia 30, 517-522.
- [448] TIETZE U., SCHENK C. (1974). Integratoren, chap. 10.9. In Halbleiter-Schaltungstechnik, 3rd ed., Berlin, Springer-Verlag, 238-248.
- [449] TOTH K. S. (1977). Nuclear Data Sheets for A=226. Nuclear Data Sheets 20, 119-137.
- [450] TOWNSEND J. S. (1903). The genesis of ions by the motion of positive ions in a gas, and a theory of sparking potential. Phil. Mag., 6th series 6, 598-618.
- [451] UNTERWEGER M. P. (1986). Ionization chambers in the National Bureau of Standards Radioactivity Group. Trans. Amer. Nucl. Soc. 53, 18.
- [452] UNTERWEGER M. P., HOPPES D. D., SCHIMA F. J. (1992). New and revised half-life measurements results. Nucl. Instr. Meth. A312, 349-352.
- [453] URITANI A., GENKA T., MORI C., REHER D. F. G. (1994). Analytical calculations on radiactivity measurements of ^{192}Ir metallic sources with a calibrated ionization chamber. Nucl. Instr. Meth. A339, 377-380.
- [454] US PHARMACOPEIA (1985). United States Pharmacopeia XXI. Washington, D.C., Pharmacopeial Convention, Inc.
- [455] VALKONEN M., KANTELE J. (1972). A simple two-detector method for precision intercomparisons of source strengths. Nucl. Instr. Meth. 99, 25-27.
- [456] VANINBROUKX R., DE BIEVRE P., LE DUIGOU Y., SPERNOL A., EIJK W. van der, VERDINGH V. (1976). New determination of the half-life of ^{233}U . Phys. Rev. C 13, 315-320.
- [457] VICTOREEN (1980). Product information: Hi-Meg resistor, type RX-15 Megamite. Cleveland, Ohio, Victoreen Instrument Company, 2 p.
- [458] WADE F. (1951). T.P.A. Ionization chamber Mk IV. Report AERE EL/R807, Harwell, AERE, 5 p.
- [459] WALZ K. F., WEISS H. M. (1970). Messung der Halbwertszeiten von Co-60, Cs-137 und Ba-133. Z. Naturforsch. 25a, 921-927.

- [460] WALZ K. F. (1977). Messung der Aktivität von I-123 mit Ionisationskammern. PTB-Jahresbericht, Braunschweig, PTB, 180-181.
- [461] WALZ K. F., DEBERTIN K., SCHRADER H. (1983). Half-life measurements at the PTB. Int. J. Appl. Radiat. Isot. 34, 1191-1199.
- [462] WATERS S. L., WOODS M. J. (1975). The half-life of ^{77}Br . Int. J. Appl. Radiat. Isot. 26, 484-485.
- [463] WATERS S. L., FORSE G. R., HORLOCK P. L., WOODS M. J. (1981). The half-life of ^{68}Ge . Int. J. Appl. Radiat. Isot. 32, 757.
- [464] WEBER K.-H. (1966). Statistische Schwankungen bei Strommessungen an Detektoren für ionisierende Strahlung. Isotopenpraxis 2, 349-354.
- [465] WEIGEL F. (1977). Nuclear properties of ^{226}Ra . Chap. 8.2.15, in Handbuch der Anorganischen Chemie (Gmelin L., Ed.), Radium-Syst. Nr. 31 Ra, Erg. Bd. 2 (8. Auflage), Berlin, Springer-Verlag, 307.
- [466] WEISE L. (1971). Statistische Auswertung von Kernstrahlungsmessungen. Der statistische Fehler bei Impulsdichte- und Ionisationsstrommessungen, chap. 2.5, München, Verlag Oldenbourg, 37-39.
- [467] WEISS C.-F. (1943). Zur Frage der als Normale festgelegten Radiumstandards. Z. Physik 120, 652-672.
- [468] WEISS H. M. (1960). Absolute measurement of radioactive materials at the Physikalisch-Technische Bundesanstalt. Report IAEA/STI/PUB/6, Vienna, IAEA, 53-60.
- [469] WEISS H. M. (1973). $4\pi\gamma$ -ionization chamber measurements. Nucl. Instr. Meth. 112, 291-297.
- [470] WEISS H. M. (1982). Aktivitätsbestimmungen mit einer kalibrierten $4\pi\gamma$ -Ionisationskammer. PTB-Jahresbericht, Braunschweig, PTB, 186.
- [471] WILKINSON D. H. (1950). The Ionization Chamber. Chap. 5, in Ionization Chambers and Counters. Cambridge, University Press, 105-142.
- [472] WILLIAMS A., BIRDSEYE R. A. (1967). Calibration factors for the type 1383A $\beta\text{-}\gamma$ ionization chamber for low energy γ -emitters. Int. J. Appl. Radiat. Isot. 18, 202-203.
- [473] WILLIAMS R. W. (1961). Ionization Chambers. Chap. 1.2, in Nuclear Physics, Vol. 5, Part A (Yuan L. C. L., Chien-Shiung Wu, Eds.), New York, Academic Press, 89-110.
- [474] WILSON C. T. R. (1900). On the leakage of electricity through dust-free air. Nature 63, 195. (German abstract in Fortschr. der Phys. 1900, II, 431).
- [475] WOODS M. J. (1970). Calibration figures for the type 1383A ionization chamber. Int. J. Appl. Radiat. Isot. 21, 752-753.

- [476] WOODS M. J. (1983a). Quality control of nuclear medicine instrumentation. In Quality control of radionuclide calibrators, Report CRS-38, London, Hospital Physicists Association, 111-124.
- [477] WOODS M. J. (1983b). Intercomparison of radionuclide calibrator measurements in UK hospitals. Int. J. Nucl. Med. Biol. 10, 103-105.
- [478] WOODS M. J. (1986a). A feasibility study of the use of radionuclide calibrators for the assay of pure betaemitters. Report NPL-RS(INT) 85, Teddington, NPL, 10 p.
- [479] WOODS M. J. (1986b). Design considerations for the UK secondary standard radionuclide calibrator—Type 271+671. Trans. Amer. Nucl. Soc. 53, 17.
- [480] WOODS M. J. (1990) The half-life of ^{137}Cs —A critical review. Nucl. Instr. Meth. A286, 576-583.
- [481] WOODS M. J. (1994). Quality assurance of medical brachytherapy sources. NPL News 374, 33-35.
- [482] WOODS M. J., CALLOW W. J., CHRISTMAS P. (1983). The NPL radionuclide calibrator—Type 271. Int. J. Nucl. Med. Biol. 10, 127-132.
- [483] WOODS M. J., GOODIER I. W., LUCAS S. E. M. (1975). The half-life of ^{133}Xe and its calibration factor for the 1383A ionization chamber. Int. J. Appl. Radiat. Isot. 26, 485-487.
- [484] WOODS M. J., LUCAS S. E. M. (1975). Calibration of the 1383A ionization chamber for ^{125}I . Int. J. Appl. Radiat. Isot. 26, 488-490.
- [485] WOODS M. J., LUCAS S. E. M. (1986). The half-life of ^{152}Eu and ^{154}Eu . Int. J. Appl. Radiat. Isot. 37, 1157-1158.
- [486] WOODS M. J., LUCAS S. E. M. (1987). Intercomparison of $^{99\text{m}}\text{Tc}$ and ^{131}I by radionuclide calibrators in UK hospitals. Report NPL-RS(EXT) 88, Teddington, NPL, 26 p.
- [487] WOODS M. J., LUCAS S. E. M. (1990). The half-life of ^{125}I . Nucl. Instr. Meth. A286, 517-518.
- [488] WOODS M. J., ROSSITER M. J., SEPHTON J. P., WILLIAMS T. T., LUCAS S. E. M., REHER D. F. G, DENECKE B., AALBERS A., THIERENS H. (1992). ^{192}Ir brachytherapy sources: Calibration of the NPL secondary standard radionuclide calibrator. Nucl. Instr. Meth. A312, 257-262.
- [489] YAIR R. (1974). Charge sampling method for low current measurement. Rev. Sci. Instr. 45, 395-399.
- [490] ZIJP W. L. (1985). On the statistical evaluation of inconsistent measurement results illustrated on the example of the ^{90}Sr half-life. Report ECN-179, Petten, Netherlands Energy Research Foundation ECN, 1-28.
- [491] ZSDANSZKY K. (1973). Precise measurement of small currents. Nucl. Instr. Meth. 112, 299-303.

- [492] Martin, R.H., Taylor, J.G.V., Nucl. Instr. Meth. To be published
- [493] Hoppes, D.D., Hutchinson, J.M.R., Schima, F.J., Unterweger, M.P., NBS Special publication 626 (1982) 85
- [494] Gries, W.H., Steyn, J., Nucl. Instr. Meth. 152 (1978) 459
- [495] Corbett, J.A., Nucl. Eng. Int. 18 (1973) 1769
- [496] Dietz, L.A., Pachucki, C.F., J. Inorg. Nucl. Chem. 35 (1973) 1769
- [497] Emery, J.F., Reynolds, S.A., Wyatt, E.I., Gleason, G.I., Nucl. Sci. Eng. 48 (1972) 319
- [498] Harbottle, G., Radiochim. Acta 13 (1970) 132
- [499] Walz, K.F., Weiss, H.M., Z. Naturforsch. 25A (1970) 921



